ON ALGEBRAIZATION IN LOW-DIMENSIONAL TOPOLOGY

ANNA BELIAKOVA, IVELINA BOBTCHEVA, MARCO DE RENZI, AND RICCARDO PIERGALLINI

Abstract. In this paper, we give a new direct proof of a result by Bobtcheva and Piergallini that provides finite algebraic presentations of two categories, denoted 3Cob and 4HB, whose morphisms are manifolds of dimension 3 and 4, respectively. More precisely, 3Cob is the category of connected oriented 3-dimensional cobordisms between connected surfaces with connected boundary, while 4HB is the category of connected oriented 4-dimensional 2-handlebodies up to 2-deformations. For this purpose, we explicitly construct the inverse of the functor $\Phi : 4\mathrm{Alg} \to 4\mathrm{HB}$, where 4Alg denotes the free monoidal category generated by a Bobtcheva–Piergallini Hopf algebra. As an application, we deduce an algebraic presentation of 3Cob and show that it is equivalent to the one conjectured by Habiro.

Contents

1. Introduction	2
1.1. Strategy of the proof of Theorem A	4
1.2. Organization	6
1.3. Acknowledgments	7
2. Algebraic categories	8
2.1. Monoidal categories	8
2.2. Braided Hopf algebras and the category Alg	11
2.3. Adjoint action	13
2.4. BP Hopf algebras and the category 4Alg	17
2.5. Frobenius structure and braided cocommutativity in 4Alg	22
2.6. Factorizable BP Hopf algebras and the categories 3Alg and $3\mathrm{Alg}^{\mathrm{H}}$	26
3. Topological categories	34
3.1. The category KT of Kirby tangles	34
3.2. 4-dimensional relative 2-handlebodies	37
3.3. The categories 4HB and 4KT	39
3.4. 3-dimensional relative cobordisms	40
3.5. The quotient categories 3Cob and 3KT	42
4. Algebraic presentation of 4HB and 3Cob	45
4.1. The functor $\Phi : 4\mathrm{Alg} \to 4\mathrm{KT}$	45
4.2. The subcategory TAlg of 4Alg	47
4.3. Bi-ascending states of link diagrams	55
4.4. Definition of the inverse functor $\bar{\Phi} : 4\mathrm{KT} \to 4\mathrm{Alg}$	57
4.5. The category MAlg	62
4.6. Invariance of $\bar{\Phi}(T)$	69
4.7. Proof of Theorem A	79
Appendix A. Tables.	84
Appendix B. Proofs.	90
B.1. Consequences of the braided Hopf algebra axioms in Table A.2	90
B.2. Consequences of the integral axioms in Table A.4	90
B.3. Properties of the ribbon structure of a BP Hopf algebra in Table A.5	91
B.4. Properties of a factorizable anomaly free BP Hopf algebra in Table A.7	93
References	95

2020 *Mathematics Subject Classification.* 57K16, 57K40, 57R56, 57R65, 16T05, 18C40, 18M15.
Key words and phrases. 3-Manifolds, 4-Manifolds, Handlebodies, Kirby Calculus, Hopf Algebras.

1. Introduction

Categories of n-dimensional cobordisms play a central role in low-dimensional topology, and have been the subject of extensive study. The category 2Cob of 2-dimensional cobordisms is known to be freely generated, as a symmetric monoidal category, by a commutative *Frobenius* algebra: the circle. This algebraic presentation yields the classification of all *Topological Quantum Field Theories* (*TQFTs*) in dimension 2. This paper focuses on an extension of this result to dimensions 3 and 4. More precisely, we discuss complete algebraic presentations (with finitely many generators and relations) of certain topological categories generated, as braided monoidal categories, by a single object: the punctured torus, in dimension 3, and the solid torus, in dimension 4. In both cases, these objects admit structures of braided *Hopf* algebras that can be further enriched, thus leading to the notion of Bobtcheva–Piergallini Hopf algebras, or simply BP Hopf algebras, see Subsections 2.4 and 2.6 for a definition.

A nice and simple algebraic presentation, such as the one for 2Cob, cannot be expected for the standard categories of cobordisms in dimension 3 and 4, since both admit infinitely many non-isomorphic connected objects. Indeed, a complete algebraic presentation of the standard category of n-dimensional cobordisms was given, for every $n \geqslant 3$, by Juhász in terms of surgery operations [Ju14], but his lists of generating objects, generating morphisms, and relations between morphisms are all infinite. There is, however, a natural category of 3-dimensional cobordisms that admits a single generating object: it is the category 3Cob of connected oriented (relative) 3-dimensional cobordisms between connected surfaces with connected boundary, whose tensor product is given by boundary connected sum. This category is a PROB, meaning that it is a braided monoidal category whose set of objects can be identified with $\mathbb{N}$, and whose tensor product adds up natural numbers. Hence, 3Cob is monoidally generated by a single object, the once-punctured torus. The fact that the punctured torus admits the structure of a braided Hopf algebra in 3Cob was first discovered by Crane and Yetter [CY94].

Building on this observation, Kerler provided a finite set of generating morphisms for 3Cob, and exhibited a finite list of beautiful and conceptual relations between them [Ke01], although he was not able to prove that his list was complete, and that he had an algebraic presentation. Since finding one would also yield a classification of all TQFTs with source 3Cob, this was recognized as one of the central problems in quantum topology, and included in Ohtsuki's list [Oh02, Problem 8.16.(1)]. A few years later, Habiro announced a solution to the problem, and his presentation appeared in [As11]. Unfortunately, a proof of his claim was never written down.

Kerler's question was answered by two of the authors of the present paper, who first gave a complete algebraic presentation of 3Cob in [BP11]. Surprisingly, the solution follows from an algebraic presentation of a category whose morphisms are manifolds one dimension higher.

In order to explain this, we need to turn our attention to 4-dimensional 2-handlebodies, which are smooth manifolds obtained from the 4-ball by attaching finitely many 1-handles and 2-handles. Up to considering a natural equivalence relation on them, discussed here below, connected oriented 4-dimensional 2-handlebodies can be organized as the morphisms of a category 4HB whose objects are connected oriented 3-dimensional 1-handlebodies[1]. As for 3Cob, this is a close relative of the standard category of (smooth) connected oriented 4-dimensional cobordisms, whose objects have boundary, and whose tensor product is induced by boundary connected sum. By contrast with 3Cob, however, or with any other category of cobordisms, the vertical boundary of morphisms in 4HB is not required to be trivial, in the sense that it is not necessarily the cylinder over a surface.

The natural equivalence relation appearing in the definition of morphisms in 4HB is called 2-equivalence, and it is induced by 2-deformations, which are diffeomorphisms that can be implemented by finite sequences of handle moves that never step outside of the class of 4-dimensional 2-handlebodies. In other words, when considering 4-dimensional 2-handlebodies up to 2-deformations, creation and removal of canceling pairs of handles of index 2/3 and 3/4 is forbidden. Whether 2-deformations form a proper subclass of diffeomorphisms is still an open question, which is closely related to a fundamental open problem in combinatorial group theory: the Andrews–Curtis conjecture.

A standard way of representing 4-dimensional 2-handlebodies is through Kirby tangles, which are obtained by drawing the attaching maps of 2-handles on the boundary of a single 0-handle with 1-handles glued to it, and then considering a generic planar projection. It is convenient to represent 1-handles as dotted unknots bounding Seifert disks in the plane. Under this convention, a 2-handle running over a 1-handle will appear as a knot that pierces the corresponding Seifert disk. Such tangles, modulo

[1] For the sake of simplicity, in the rest of the paper we will write 4-dimensional 2-handlebodies to mean connected oriented ones, and 3-dimensional handlebodies to mean connected oriented 3-dimensional 1-handlebodies.

isotopy, 2-handle slides, and 1/2-handle cancellations, form a category 4KT which is equivalent to 4HB [Ki89, GS99, Ke98, BP11].

The algebraic counterpart of 4HB is the category 4Alg, which is a PROB that is freely generated by a Bobtcheva–Piergallini (or BP) Hopf algebra. The approach of [BP11] consists in defining a functor $\Phi : 4\mathrm{Alg} \to 4\mathrm{KT}$ and showing that it is an equivalence by factoring it through an equivalence functor from the category of labeled ribbon surfaces to 4Alg. A labeled ribbon surface serves as a branching set in the description of a 4-dimensional 2-handlebody as a branched cover of the 4-ball.

In the present paper we provide a simpler direct proof of the same result.

Theorem A. *The functor* $\Phi : 4\mathrm{Alg} \to 4\mathrm{HB}$ *sending the generating BP Hopf algebra of* 4Alg *to the solid torus is an equivalence of braided monoidal categories.*

The idea of our new proof is to construct the inverse functor $\bar{\Phi} : 4\mathrm{KT} \to 4\mathrm{Alg}$ directly and explicitly, without any reference to branched coverings. The assignment of a morphism in 4Alg to a Kirby tangle depends, in our approach, on many auxiliary choices. The main body of the proof deals with the independence on these choices.

An immediate application of Theorem A is the following detection result. If T and T' are Kirby tangles such that $\bar{\Phi}(T) = \bar{\Phi}(T')$, then T is isomorphic to T' in 4KT and the corresponding 4-dimensional 2-handlebodies in 4HB can be 2-deformed into each other.

A further important consequence of Theorem A is an algebraic presentation of 3Cob. Indeed, there exists a natural boundary functor $\partial_+ : 4\mathrm{HB} \to 3\mathrm{Cob}$ making the diagram

$$\begin{tikzcd} 4\mathrm{Alg} \arrow[r, "\pi"] \arrow[d, "\Phi"'] & 3\mathrm{Alg} \arrow[d, "\partial_+\Phi"] \\ 4\mathrm{HB} \arrow[r, "\partial_+"'] & 3\mathrm{Cob} \end{tikzcd}$$

into a commutative one. Here, 3Alg is a certain quotient of 4Alg obtained by adding two additional relations (which make the generating object into a factorizable and anomaly-free BP Hopf algebra). In order to represent morphisms in 3Cob, we use top tangles in handlebodies, which are an adaptation to our conventions of Habiro's bottom tangles in handlebodies (since Habiro reads diagrams from top to bottom, while we do the opposite). Thus, we can deduce the following.

Corollary B. *The functor* $\partial_+\Phi : 3\mathrm{Alg} \to 3\mathrm{Cob}$ *sending the generating factorizable and anomaly-free BP Hopf algebra of* 3Alg *to the punctured torus is an equivalence of braided monoidal categories.*

Proof (*assuming Theorem A*). We will show in Section 3 that $3\mathrm{Cob} \cong 3\mathrm{KT}$ is the quotient of $4\mathrm{HB} \cong 4\mathrm{KT}$ by the two relations depicted in Table 3.5.1. Written algebraically, these relations correspond exactly to relations (f) and (n) introduced in Subsection 2.6. Moreover, 3Alg is defined precisely as the quotient of 4Alg by these relations. The claim follows now from Theorem A and Proposition 3.5.7. □

This algebraic presentation, first appeared in [BP11], does not coincide with the one announced by Habiro (see [As11]). Indeed, the latter identifies 3Cob with the free monoidal category $3\mathrm{Alg}^{\mathrm{H}}$ generated by a Habiro Hopf algebra, which features a different set of generating morphisms, and a different list of relations (see Subsection 2.6 for a definition). However, we prove that 3Alg and $3\mathrm{Alg}^{\mathrm{H}}$ are equivalent as braided monoidal categories, thus establishing the Kerler–Habiro conjecture.

Theorem C (Kerler–Habiro Conjecture). *The functor* $\Gamma : 3\mathrm{Alg}^{\mathrm{H}} \to 3\mathrm{Alg}$ *sending the generating Habiro Hopf algebra of* $3\mathrm{Alg}^{\mathrm{H}}$ *to the generating factorizable anomaly-free BP Hopf algebra of* 3Alg *is an equivalence of braided monoidal categories. Hence, the functor* $\partial_+\Phi \circ \Gamma : 3\mathrm{Alg}^{\mathrm{H}} \to 3\mathrm{Cob}$ *sending the generating Habiro Hopf algebra of* $3\mathrm{Alg}^{\mathrm{H}}$ *to the punctured torus is an equivalence of braided monoidal categories.*

The braided monoidal functor $\Gamma : 3\mathrm{Alg}^{\mathrm{H}} \to 3\mathrm{Alg}$ was first constructed by the second author in [Bo20]. In this paper, we define its inverse, thus proving that the algebraic presentations of 3Cob given in [BP11] and [As11] are equivalent. In addition, we provide a third algebraic presentation $3\mathrm{Alg}^{\mathrm{K}}$ by adding to Kerler's original list of axioms the braided cocommutativity relation for the adjoint action (a crucial relation appearing in Habiro's presentation), and show that $3\mathrm{Alg}^{\mathrm{K}}$ is equivalent to $3\mathrm{Alg}^{\mathrm{H}}$. Clearly, also in dimension 3 the equality $\pi(\overline{\Phi}(T)) = \pi(\overline{\Phi}(T'))$ implies an isomorphism between T and T' in 3KT, and an equivalence of the corresponding cobordisms in 3Cob.

Besides giving a complete algebraic presentation of 4HB and 3Cob, Theorems A and C also classify braided monoidal functors on them. For what concerns existence of examples, in [BD21] it is shown that every unimodular ribbon Hopf algebra, and more generally every unimodular ribbon category,[2] gives rise to such a functor (a TQFT) on the category of 4-dimensional 2-handlebodies up to 2-deformations. We point out that the notion of 2-deformation between 4-dimensional 2-handlebodies is conjectured by Gompf in [Go91] to be different from the one of diffeomorpism, which in this context is equivalent to 3-deformation. In order to prove Gompf's conjecture, we can look for a unimodular ribbon Hopf algebra whose corresponding quantum invariant distinguishes diffeomorphic handlebodies that are not 2-equivalent. The search for such Hopf algebras is a non-trivial challenge, since they have to combine several properties: at the very least, they should be unimodular, non-factorizable, and non-semisimple (see [BD21, Subsection 1.1] and [BM02, Section 2]). Quantum groups satisfying all these properties do not seem to lead to interesting invariants of 4-manifolds, but rather to homological refinements of known quantum invariants of their 3-dimensional boundaries [BD22]. On the other hand, if the conjecture is false, every unimodular ribbon Hopf algebra, and more generally every unimodular ribbon category, gives rise to a quantum invariant of 4-dimensional 2-handlebodies up to diffeomorphisms, and may be useful for detecting exotic structures on 4-manifolds.

Apart from 3Alg, there is another interesting quotient of 4Alg, defined in [Bo23] as the symmetric monoidal category freely generated by a BP Hopf algebra with trivial ribbon element (in particular, such a Hopf algebra is cocommutative). Topologically, this quotient describes the category of cobordisms between 2-dimensional CW-complexes up to 2-equivalence, and hence it is designed to study the Andrews–Curtis conjecture. Let us recall that the Andrews–Curtis conjecture states that every balanced[3] presentation of the trivial group can be reduced to the trivial presentation trough balanced presentations (that is, by a sequence of Nielsen transformations on relators and conjugations of relators by generators). This conjecture is open since 1965, and expected to be false. To test potential counterexamples, new cocommutative BP Hopf algebras with symmetric braiding and trivial ribbon element need to be constructed.

The one-to-one correspondence between algebraic and topological structures established in this paper might also be useful for understanding quantum groups or ribbon Hopf algebras, since it provides new graphical methods for establishing identities or constructing central elements. Indeed, every time we happen to know that a complicated tangle can be trivialized, then it follows that the associated morphism in 4Alg is the identity.

1.1. Strategy of the proof of Theorem A

Let us explain the main ideas behind the proof of Theorem A. A Hopf algebra H in a braided monoidal category $\mathscr{C}$ comes equipped with the following structure morphisms:

- ◇ a product $\mu : H \otimes H \to H$ and a unit $\eta : \mathbb{1} \to H$;
- ◇ a coproduct $\Delta : H \to H \otimes H$ and a counit $\varepsilon : H \to \mathbb{1}$;
- ◇ an invertible antipode $S : H \to H$.

These structure morphisms are required to satisfy the standard axioms depicted in Table 2.2.1. A Bobtcheva–Piergallini Hopf algebra (or BP Hopf algebra for short) is a Hopf algebra in $\mathscr{C}$ equipped with the following additional morphisms:

- ◇ an integral form $\lambda : H \to \mathbb{1}$ and an integral element $\Lambda : \mathbb{1} \to H$;
- ◇ an invertible ribbon morphism $\tau : H \to H$;
- ◇ a copairing $w : \mathbb{1} \to H \otimes H$.

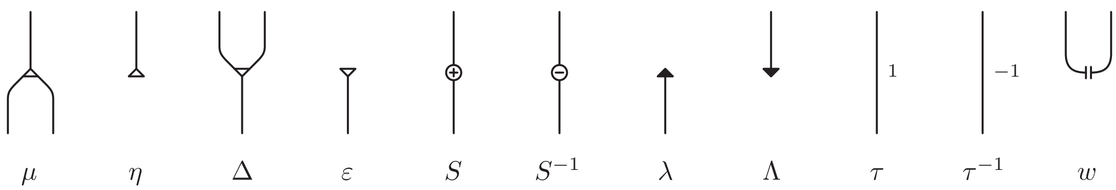

FIGURE 1.1.1

[2]A ribbon category is unimodular if it is finite and if the projective cover of its tensor unit is self-dual.
[3]A presentation of a group is balanced if it has the same number of generators and relators.

These morphisms are required to satisfy a set of axioms, which can be found in Subsection 2.4. To present the generating morphisms and relations between them we will use the graphical notation shown in Figure 1.1.1. We define 4Alg as the PROB freely generated by a BP Hopf algebra.

In order to construct the functor $\Phi : 4\mathrm{Alg} \to 4\mathrm{KT}$, we need to assign Kirby tangles to generating morphisms, and to check all relations. The images of the structure morphisms under Φ are given in Figure 1.1.2 and the relations are checked in Subsection 4.1.

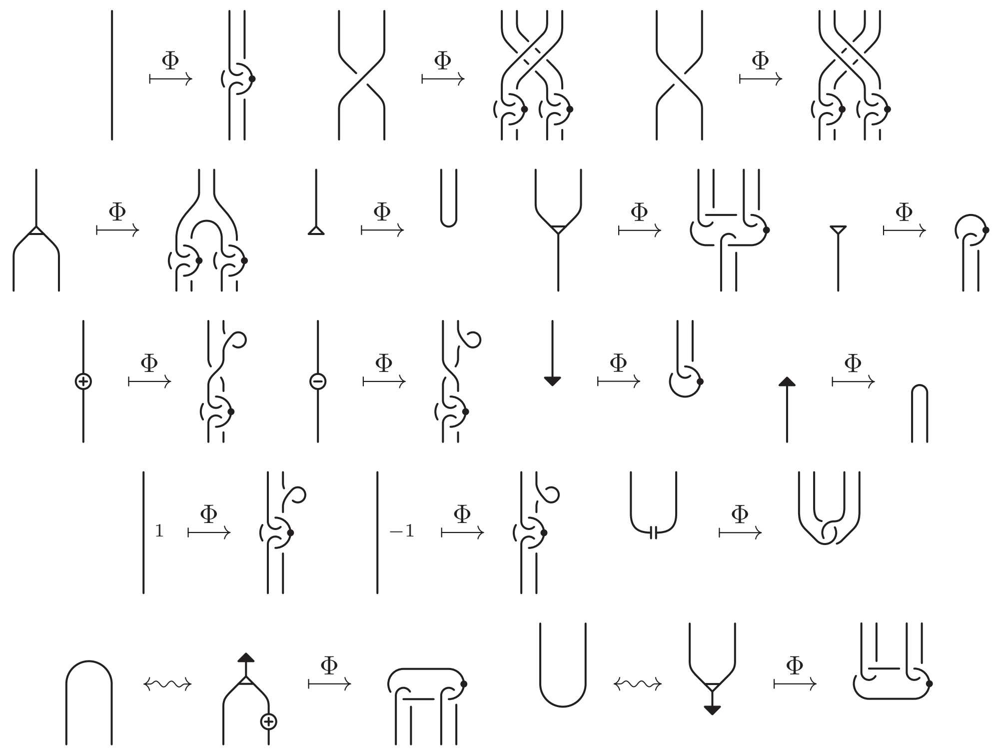

FIGURE 1.1.2. Definition of the functor Φ for the generating morphisms and the evaluation and coevaluation in 4Alg.

Notice that the assignment defined in Figure 1.1.2 replaces each strand representing a copy of the BP Hopf algebra H with two undotted parallel strands representing (a portion of) a 2-handle in 4KT. The claim that the functor Φ is full might then be surprising, since a generic tangle in 4KT does not have this property. However, for any diagram D of a Kirby tangle T, we can choose a so-called *bi-ascending* state for all undotted components. This reduces to the choice of a collection of crossings that need to be reversed in order to trivialize the undotted link representing the 2-handles. Then, we can build a connected sum of each undotted component with its trivialization along chosen bands. The resulting diagram still represents T, and has the property that each undotted component is doubled by a trivial copy which lies below it. An example is given by the first and the last diagrams in Figure 1.1.3, where the doubling is drawn in gray for convenience.

An algebra morphism $\overline{\Phi}(T)$ with the property that $\Phi(\overline{\Phi}(T)) = T$ is constructed as follows. Given a diagram of a Kirby tangle T, we specify a bi-ascending state by marking (with gray disks) those crossings that should be changed in order to trivialize the undotted link. Then, we pick a family of bands α connecting the undotted link to the bottom base of the projection plane, and we call the resulting diagram T_α. Next, we decompose T_α into elementary pieces and assign algebra morphisms to each piece as prescribed in Figures 4.4.4, 4.4.5, and 4.4.6. Finally, we tensor and compose all these morphisms together. This process is illustrated in Figure 1.1.3. Notice that the algebra morphism we assign to a crossing depends on whether this crossing is affected by the trivialization or not. By applying the functor Φ to the resulting algebra morphism $\overline{\Phi}(T)$, we can verify that $\Phi(\overline{\Phi}(T))$ is isotopic to the original tangle T.

The main body of the proof consists in checking that our assignment actually extends to a well-defined functor $\overline{\Phi} : 4\mathrm{KT} \to 4\mathrm{Alg}$ that is inverse to Φ. For this purpose, we need to prove that $\overline{\Phi}(T)$ does not depend on the various choices we made, meaning that it is independent of the bi-ascending state, of the set of bands, and of the diagram we picked.

Moreover, we need to check that our assignment is invariant under isotopies and 2-deformations of T, and that it is compatible with identities, compositions, tensor products, and braidings. The main tool

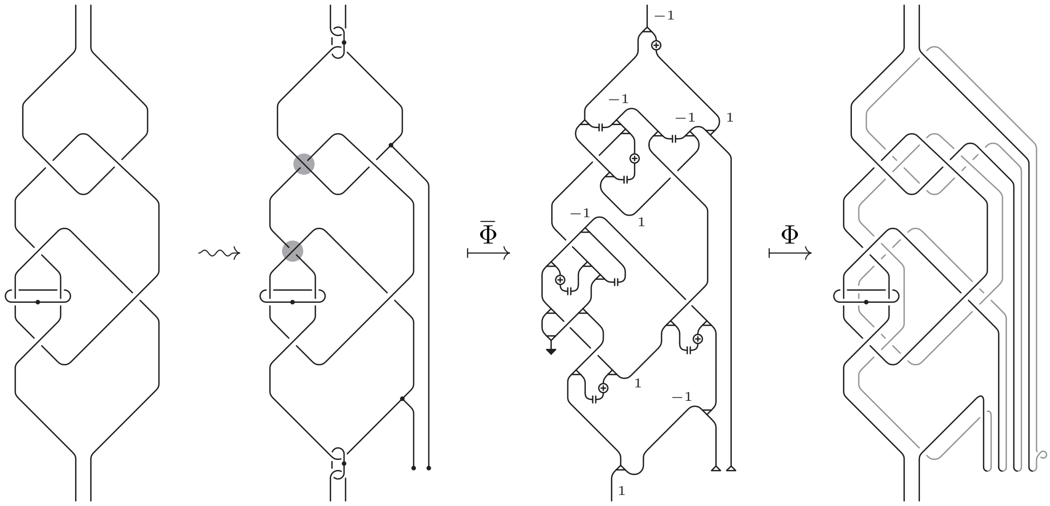

T $\quad T_\alpha$ $\quad \overline{\Phi}(T)$ $\quad \Phi(\overline{\Phi}(T))$

FIGURE 1.1.3. Example of assignment of the algebraic morphism $\overline{\Phi}(T)$ to a Kirby tangle T satisfying $\Phi(\overline{\Phi}(T)) = T$.

in the proof of these properties will be provided by some recursively constructed collection of morphisms $\Theta = \{\Theta_k : H^{\otimes k+1} \to H^{\otimes k}\}_{k\in\mathbb{N}}$ that intertwines all morphisms in a natural subcategory TAlg of 4Alg generated (under tensor products and compositions) by some morphisms in the image of $\overline{\Phi}$ (shown in Figure 4.4.4). More precisely, if $\iota : \mathrm{TAlg} \hookrightarrow 4\mathrm{Alg}$ denotes the inclusion functor, then $\Theta : \iota \otimes H \Rightarrow \iota$ defines a natural transformation, meaning that, for a morphism $F : H^{\otimes s} \to H^{\otimes t}$ in TAlg, we have

$$\Theta_t \circ (F \otimes \mathrm{id}) = F \circ \Theta_s.$$

Geometrically, Θ implements a 1-handle embracing all the strands of $\Phi(\overline{\Phi}(T))$ corresponding to the trivialized copy of T in gray. To check independence of the bi-ascending state, we will also need to implement algebraically a 1-handle embracing the trivialized copy of a single component of T, which will require the construction of a family of labeled versions of Θ.

1.2. Organization

We start our paper with some algebraic background, in Section 2. After recalling the notion of a braided monoidal category, we introduce BP Hopf algebras, and define 4Alg as the braided monoidal category freely generated by a BP Hopf algebra. For each of these algebraic structures we give a diagrammatic presentation of the defining set of axioms. We prove that 4Alg admits the structure of a ribbon category, and that its generating object also admits the structure of a Frobenius algebra.

We introduce the notions of factorizable and anomaly-free BP Hopf algebras, which lead to the definition of the quotient category 3Alg of 4Alg. Then, after recalling the definition of $3\mathrm{Alg}^{\mathrm{H}}$, we construct a functor $\Gamma : 3\mathrm{Alg}^{\mathrm{H}} \to 3\mathrm{Alg}$, and prove that it is an equivalence. Furthermore, we deduce another presentation $3\mathrm{Alg}^{\mathrm{K}}$ of 3Alg, which is obtained from the list of axioms found by Kerler in [Ke01] by adding the braided cocommutativity relation for the adjoint action.

In Section 3, we collect some topological background. First, we recall the definition of the categories 4HB and 3Cob, which are equivalent to the categories of Kirby tangles 4KT and 3KT, respectively. They are naturally related by a functor $\partial_+ : 4\mathrm{HB} \to 3\mathrm{Cob}$ that maps each 4-dimensional 2-handlebody to its front boundary. Finally, we recall (an upside-down version of) Habiro's graphical notation for morphisms in 3Cob as top tangles in handlebodies.

Section 4 is devoted to the proof of Theorem A. After defining the functor $\Phi : 4\mathrm{Alg} \to 4\mathrm{KT}$, we proceed with the construction of its inverse. In order to do this, we start by introducing a certain subcategory TAlg of 4Alg whose image under Φ consist of Kirby tangles whose 2-handles are separated by the projection plane in two levels. We describe generators of TAlg explicitly in terms of decorated crossings, and show that TAlg admits two different ribbon structures. Next, we define two natural transformations Θ and Θ' that will be extensively used in the proof of our main result.

In Subsection 4.3, we introduce bi-ascending states of link diagrams, and we describe a complete set of moves relating any two bi-ascending states of the same link diagram. Subsection 4.4 is devoted to the construction of the inverse functor $\overline{\Phi} : 4\mathrm{KT} \to 4\mathrm{Alg}$. In the following one, we define yet another pair of natural transformations Θ_j^{L} and $\widehat{\Theta}_j^{\mathrm{L}}$ on a labeled version of 4Alg. In the last subsection, we prove independence of $\overline{\Phi}$ on the choice of bands, of the bi-ascending state, and of the representative of T within its 2-equivalence class. Finally, we show that $\overline{\Phi}$ preserves compositions, identities, tensor products, and braidings, and that it is the inverse of Φ.

For convenience of the reader, we collect all relations and their consequences in Appendix A, and we recall (and sometimes establish) their proof in Appendix B.

1.3. Acknowledgments

The authors would like to thank Kazuo Habiro for explaining them how to define integral form and elements in $3\mathrm{Alg}^{\mathrm{H}}$. AB and MDR were supported by the NCCR SwissMAP and Grant 200020_207374 of the Swiss National Science Foundation. IB and RP thank the UZH Institut für Mathematik for its hospitality during the initial conception of this article.

2. Algebraic categories

2.1. Monoidal categories

We list here some basic definitions from the general theory of monoidal categories, which are used repeatedly in the paper. Standard references are provided by [Ma71, EGNO15].

Definition 2.1.1 ([EGNO15, Definitions 2.1.1 & 2.8.1]). A *strict monoidal category* is a category $\mathscr{C}$ equipped with a functor $\otimes : \mathscr{C} \times \mathscr{C} \to \mathscr{C}$, called the *tensor product*, and an object $\mathbb{1} \in \mathscr{C}$, called the *tensor unit*, satisfying:

$$(X \otimes Y) \otimes Z = X \otimes (Y \otimes Z) \text{ for all } X, Y, Z \in \mathscr{C};$$
$$\mathbb{1} \otimes X = X = X \otimes \mathbb{1} \text{ for every } X \in \mathscr{C}.$$

Notice that, thanks to the associativity axiom, bracketing can be ignored in tensor products.

Morphisms in a strict monoidal category $\mathscr{C}$ can be efficiently represented using Penrose graphical notation, which is based on planar graphs and their diagrams. Edges are labeled by objects of $\mathscr{C}$ and are required to be nowhere-horizontal, while vertices are labeled by morphisms of $\mathscr{C}$ and are represented as boxes (called *coupons*) with distinguished opposite bases (an incoming one, on the bottom, and an outgoing one, on the top). Composition of diagrams is given by vertical stacking (and is read from bottom to top), while tensor product is given by horizontal juxtaposition (and is read from left to right).

In the following, all the objects we will consider will be tensor products of a single one, typically denoted by H, and we will adopt the following notations:

$$H^0 = \mathbb{1} \text{ and } H^1 = H;$$
$$H^n = H^{\otimes n} \text{ for every } n \geqslant 2;$$
$$\mathrm{id}_n = \mathrm{id}_{H^n} \text{ for every } n \geqslant 0;$$
$$\mathrm{id} = \mathrm{id}_1.$$

In this setting, up to replacing each edge labeled by H^n with n parallel edges labeled by H, we will always assume that all the edges share the same label H, so we will drop labels for edges altogether. Furthermore, we will usually replace vertices by special symbols encoding their label.

We point out that diagrams are considered up to the equivalence relation induced by planar isotopies (through diagrams with nowhere-horizontal edges). In particular, the planar isotopy depicted in Figure 2.1.1 relates equivalent morphisms.

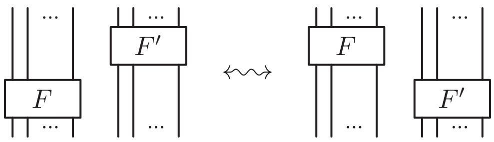

Figure 2.1.1. Example of planar isotopy, with F and F' arbitrary morphisms.

Definition 2.1.2 ([EGNO15, Definitions 8.1.1 & 8.1.2]). A *braided strict monoidal category* is a strict monoidal category $\mathscr{C}$ equipped with a natural isomorphism of components

$$c_{X,Y} : X \otimes Y \to Y \otimes X$$

for all $X, Y \in \mathscr{C}$, called the *braiding*, satisfying:

$$c_{X \otimes Y, Z} = (c_{X,Z} \otimes \mathrm{id}_Y) \circ (\mathrm{id}_X \otimes c_{Y,Z}) \text{ for all } X, Y, Z \in \mathscr{C};$$
$$c_{X, Y \otimes Z} = (\mathrm{id}_Y \otimes c_{X,Z}) \circ (c_{X,Y} \otimes \mathrm{id}_Z) \text{ for all } X, Y, Z \in \mathscr{C}.$$

In Penrose graphical notation, braidings are represented as crossings, and their naturality translates to the invariance of these planar diagrams under the moves shown in Table 2.1.2, where F denotes any morphism, including braidings themselves (these moves correspond to isotopies of embedded versions of these graphs in 3-dimensional space). In the following, since all objects will be tensor powers of a single object $H \in \mathscr{C}$, we will adopt the following short notations:

$$c_{n,m} = c_{H^n, H^m} \text{ for all } n, m \geqslant 0;$$
$$c = c_{1,1}.$$

Strict braided monoidal category axioms

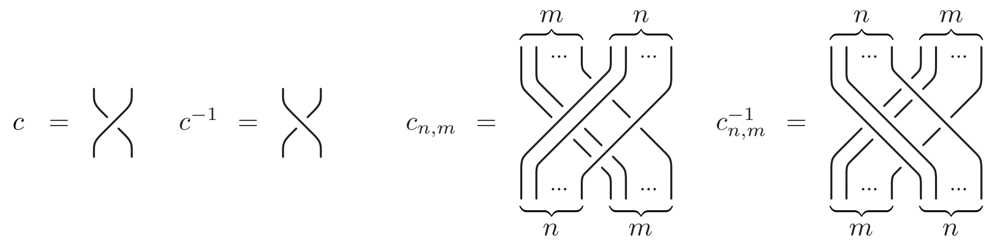

Braiding morphisms and their inverses

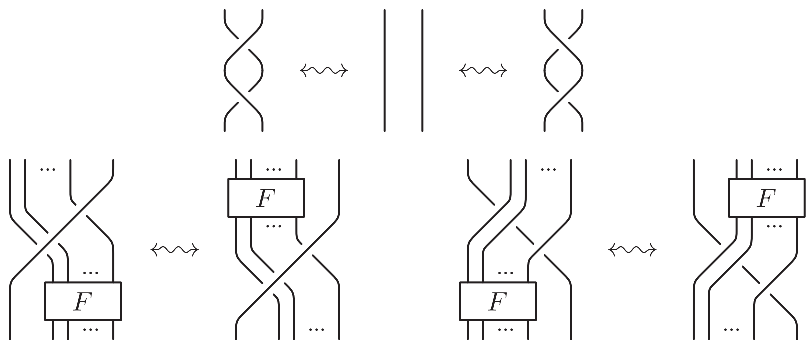

Braiding axioms

TABLE 2.1.2

DEFINITION 2.1.3 ([EGNO15, Definitions 2.10.1, 2.10.2, & 2.10.11]). A strict monoidal category $\mathscr{C}$ is *left rigid* if every $X \in \mathscr{C}$ admits a *left dual* $X^* \in \mathscr{C}$ and two morphisms

$$\overleftarrow{\mathrm{ev}}_X : X^* \otimes X \to \mathbb{1} \quad \text{and} \quad \overleftarrow{\mathrm{coev}}_X : \mathbb{1} \to X \otimes X^*,$$

called the *left evaluation* and *coevaluation*, satisfying

$$(\mathrm{id}_X \otimes \overleftarrow{\mathrm{ev}}_X) \circ (\overleftarrow{\mathrm{coev}}_X \otimes \mathrm{id}_X) = \mathrm{id}_X \quad \text{and} \quad (\overleftarrow{\mathrm{ev}}_X \otimes \mathrm{id}_{X^*}) \circ (\mathrm{id}_{X^*} \otimes \overleftarrow{\mathrm{coev}}_X) = \mathrm{id}_{X^*}.$$

Given any morphism $F \in \mathrm{Hom}_{\mathscr{C}}(X, Y)$, its *left dual* $F^* \in \mathrm{Hom}_{\mathscr{C}}(Y^*, X^*)$ is defined as

$$F^* = (\overleftarrow{\mathrm{ev}}_Y \otimes \mathrm{id}_{X^*}) \circ (\mathrm{id}_{Y^*} \otimes F \otimes \mathrm{id}_{X^*}) \circ (\mathrm{id}_{Y^*} \otimes \overleftarrow{\mathrm{coev}}_X).$$

REMARK 2.1.4. When they exist, left duals are unique up to unique isomorphisms (see [EGNO15, Proposition 2.10.5.]). In particular, if $\mathscr{C}$ is a left rigid strict monoidal category, then for all objects $X, Y \in \mathscr{C}$ we have

$$(X \otimes Y)^* = Y^* \otimes X^*,$$

and for all morphisms $F \in \mathrm{Hom}_{\mathscr{C}}(X, Y)$ and $G \in \mathrm{Hom}_{\mathscr{C}}(Y, Z)$ we have (see [EGNO15, Exercise 2.10.7])

$$(G \circ F)^* = F^* \circ G^*.$$

DEFINITION 2.1.5 ([EGNO15, Definitions 4.7.7 & 4.7.8]). A *pivotal category* is a left rigid strict monoidal category $\mathscr{C}$ equipped with a natural isomorphism of components

$$\psi_X : X \to X^{**}$$

for every $X \in \mathscr{C}$, called the *pivotal structure*, satisfying

$$\psi_{X \otimes Y} = \psi_X \otimes \psi_Y \text{ for all } X, Y \in \mathscr{C}.$$

The existence of a pivotal structure ensures that all duals are two-sided, since it induces morphisms

$$\overrightarrow{\mathrm{ev}}_X : X \otimes X^* \to \mathbb{1} \quad \text{and} \quad \overrightarrow{\mathrm{coev}}_X : \mathbb{1} \to X^* \otimes X,$$

called the *right evaluation* and *coevaluation*, defined as

$$\overrightarrow{\mathrm{ev}}_X = \overleftarrow{\mathrm{ev}}_{X^*} \circ (\psi_X \otimes \mathrm{id}_{X^*}) \quad \text{and} \quad \overrightarrow{\mathrm{coev}}_X = (\mathrm{id}_{X^*} \otimes \psi_X^{-1}) \circ \overleftarrow{\mathrm{coev}}_{X^*},$$

and satisfying

$$(\overrightarrow{\mathrm{ev}}_X \otimes \mathrm{id}_X) \circ (\mathrm{id}_X \otimes \overrightarrow{\mathrm{coev}}_X) = \mathrm{id}_X \quad \text{and} \quad (\mathrm{id}_{X^*} \otimes \overrightarrow{\mathrm{ev}}_X) \circ (\overrightarrow{\mathrm{coev}}_X \otimes \mathrm{id}_{X^*}) = \mathrm{id}_{X^*}.$$

Given any morphism $F \in \mathrm{Hom}_{\mathscr{C}}(X,Y)$, its left dual $F^* \in \mathrm{Hom}_{\mathscr{C}}(Y^*,X^*)$ satisfies

$$F^* = (\mathrm{id}_{X^*} \otimes \overrightarrow{\mathrm{ev}}_Y) \circ (\mathrm{id}_{X^*} \otimes F \otimes \mathrm{id}_{Y^*}) \circ (\overrightarrow{\mathrm{coev}}_X \otimes \mathrm{id}_{Y^*}).$$

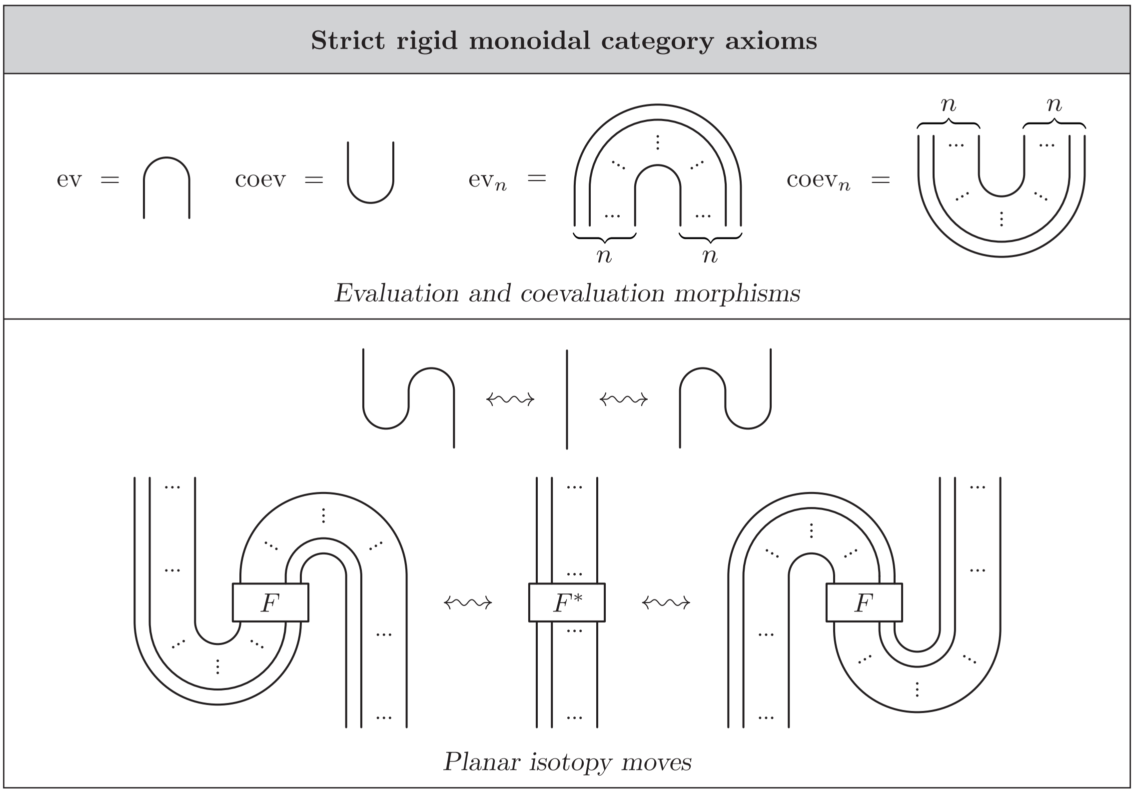

Table 2.1.3

In Penrose graphical notation, duality morphisms (evaluations and coevaluations) can be represented, at the level of diagrams, as maxima and minima (caps and cups), by dropping the requirement on nowhere-horizontal edges. In a pivotal category, their properties translate to the invariance of these diagrams under all planar isotopies, see Table 2.1.3. In general, duals can be encoded by orientations on edges, which allow for the distinction between left and right duality morphisms. However, we will never actually orient edges in what follows. Indeed, in our setting, all edges will be understood as being labeled by a single self-dual object $H \in \mathscr{C}$, whose left and right duality morphisms coincide, and whose pivotal isomorphism is the identity, so no further distinctions will be needed. Therefore, we will adopt the following short notations:

$$\begin{aligned} \mathrm{ev}_n &= \overleftarrow{\mathrm{ev}}_{H^n} = \overrightarrow{\mathrm{ev}}_{H^n} \text{ for every } n \geqslant 0; \\ \mathrm{coev}_n &= \overleftarrow{\mathrm{coev}}_{H^n} = \overrightarrow{\mathrm{coev}}_{H^n} \text{ for every } n \geqslant 0; \\ \mathrm{ev} &= \overleftarrow{\mathrm{ev}}_1 = \overrightarrow{\mathrm{ev}}_1; \\ \mathrm{coev} &= \overleftarrow{\mathrm{coev}}_1 = \overrightarrow{\mathrm{coev}}_1. \end{aligned}$$

If the rigid monidal category is also braided, as a consequence of the planar isotopy moves in Table 2.1.3 and the naturality of the braiding, we can rotate any crossing as shown in Figure 2.1.4.

Figure 2.1.4. Rotating crossing in a strict rigid monidal braided category.

DEFINITION 2.1.6 ([EGNO15, Definition 8.10.1]). A *ribbon category* is a braided pivotal category $\mathscr{C}$ equipped with a natural isomorphism of components

$$\theta_X : X \to X$$

for every $X \in \mathscr{C}$, called the *twist*, satisfying:

$$\theta_{X \otimes Y} = c_{Y,X} \circ c_{X,Y} \circ (\theta_X \otimes \theta_Y) \text{ for all } X, Y \in \mathscr{C};$$
$$(\theta_X)^* = \theta_{X^*} \text{ for every } X \in \mathscr{C}.$$

We will use the notations:

$$\theta_n = \theta_{H^n} \text{ for every } n \geqslant 0;$$
$$\theta = \theta_1.$$

REMARK 2.1.7. According to [EGNO15, Equation (8.35)], in a sufficiently nice braided strict monoidal category, a pivotal structure determines a ribbon structure, and vice versa, by setting

$$\theta_X = \left(\mathrm{id}_X \otimes (\overleftarrow{\mathrm{ev}}_{X^*} \circ c^{-1}_{X^{**},X^*})\right) \circ (\overleftarrow{\mathrm{coev}}_X \otimes \psi_X) \text{ for every } X \in \mathscr{C}.$$

In Penrose graphical notation, twists can be represented by kinks (at least in those ribbon categories where [EGNO15, Equation (8.35)] holds). Then, their properties translate to the invariance of diagrams under all framing-preserving isotopies of embedded versions of the corresponding graphs in 3-dimensional space, see Table 2.1.5. In our setting, where $H \in \mathscr{C}$ is a self-dual object whose pivotal isomorphism is the identity, we have

$$\theta_n = (\mathrm{id}_n \otimes \mathrm{coev}_n) \circ (c_{n,n} \otimes \mathrm{id}_n) \circ (\mathrm{id}_n \otimes \mathrm{ev}_n) \text{ for every } n \geqslant 0.$$

Ribbon structure on a strict rigid braided monoidal category

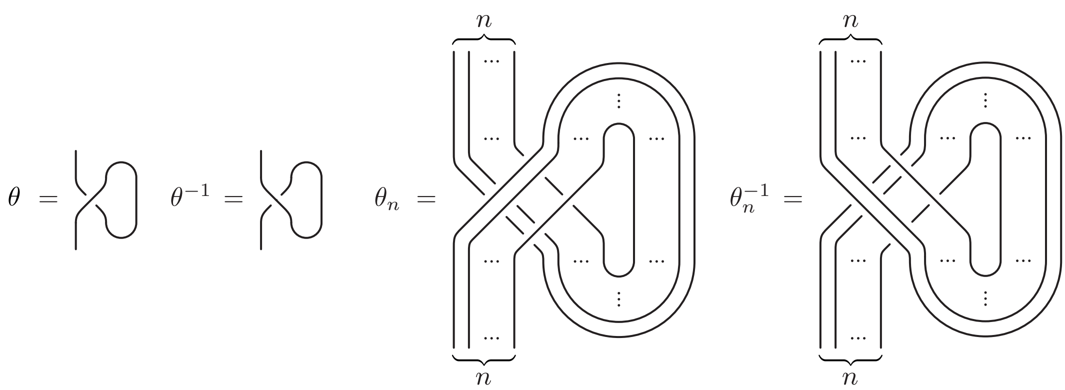

Twist morphisms and their inverses

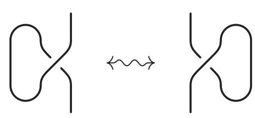

Ribbon axiom

TABLE 2.1.5

2.2. Braided Hopf algebras and the category Alg

Let $\mathscr{C}$ be a braided monoidal category with tensor product $\otimes$, tensor unit $\mathbb{1}$, and braiding c. A *braided Hopf algebra* in $\mathscr{C}$, or simply a *Hopf algebra* in $\mathscr{C}$, is an object $H \in \mathscr{C}$ equipped with the following structure morphisms:

- a *product* $\mu : H \otimes H \to H$ and a *unit* $\eta : \mathbb{1} \to H$;
- a *coproduct* $\Delta : H \to H \otimes H$ and a *counit* $\varepsilon : H \to \mathbb{1}$;
- an *antipode* $S : H \to H$ and its inverse $S^{-1} : H \to H$.

These structure morphisms are subject to the following axioms:

$$\mu \circ (\mu \otimes \mathrm{id}) = \mu \circ (\mathrm{id} \otimes \mu), \tag{a1}$$

$$\mu \circ (\eta \otimes \mathrm{id}) = \mathrm{id} = \mu \circ (\mathrm{id} \otimes \eta), \tag{a2-2$'$}$$

$$(\Delta \otimes \mathrm{id}) \circ \Delta = (\mathrm{id} \otimes \Delta) \circ \Delta, \tag{a3}$$

$$(\varepsilon \otimes \mathrm{id}) \circ \Delta = \mathrm{id} = (\mathrm{id} \otimes \varepsilon) \circ \Delta, \tag{a4-4$'$}$$

$$(\mu \otimes \mu) \circ (\mathrm{id} \otimes c \otimes \mathrm{id}) \circ (\Delta \otimes \Delta) = \Delta \circ \mu, \tag{a5}$$

$$\varepsilon \circ \mu = \varepsilon \otimes \varepsilon, \tag{a6}$$

$$\Delta \circ \eta = \eta \otimes \eta, \tag{a7}$$

$$\varepsilon \circ \eta = \mathrm{id}_{\mathbb{1}}, \tag{a8}$$

$$\mu \circ (S \otimes \mathrm{id}) \circ \Delta = \eta \circ \varepsilon = \mu \circ (\mathrm{id} \otimes S) \circ \Delta, \tag{s1-1$'$}$$

$$S \circ S^{-1} = \mathrm{id} = S^{-1} \circ S. \tag{s2-3}$$

A graphical representation of the generators and the defining axioms of a Hopf algebra can be found in Table 2.2.1, where all edges are assumed to carry the label H (compare with [BP11, Tables 4.7.12 & 4.7.13]). As a well known consequence of these axioms, the antipode satisfies the properties represented in Table 2.2.2. The reader can find the diagrammatic proofs in Appendix B (see also [BP11, Propositions 4.1.4]).

Notice that all these structure morphisms, except for the antipode, feature triangles that point either up or down. This choice is not arbitrary. Indeed, as we will see in Subsection 4.1, triangles pointing up

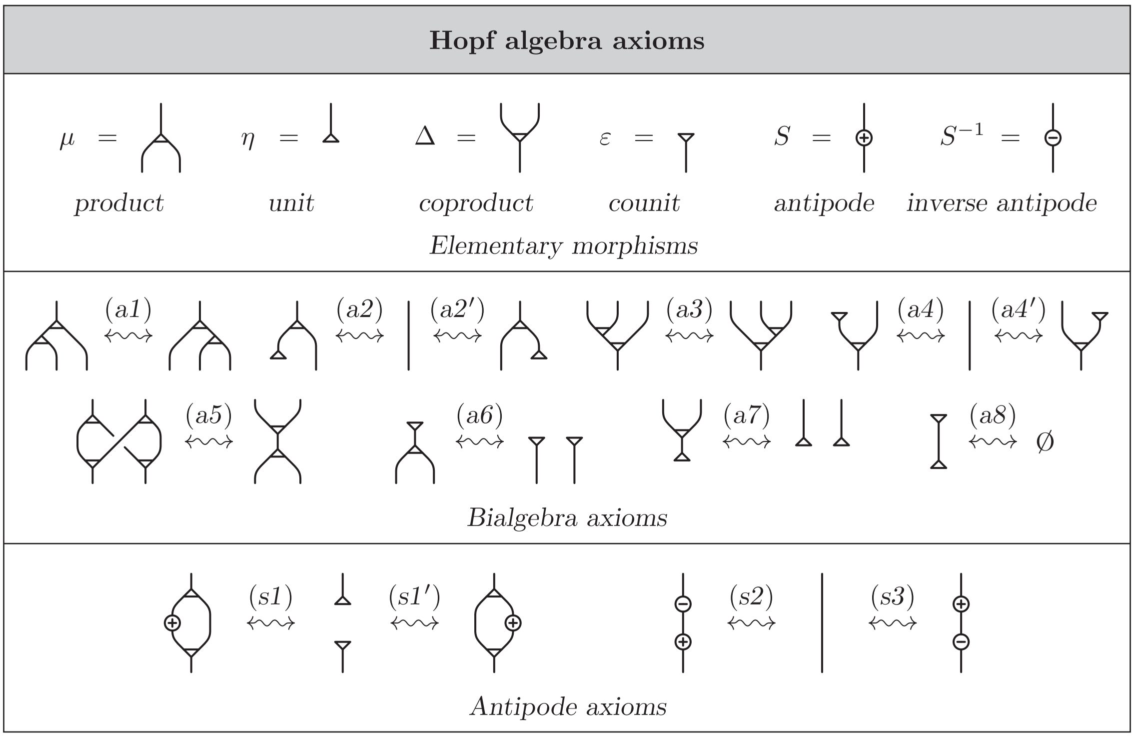

TABLE 2.2.1

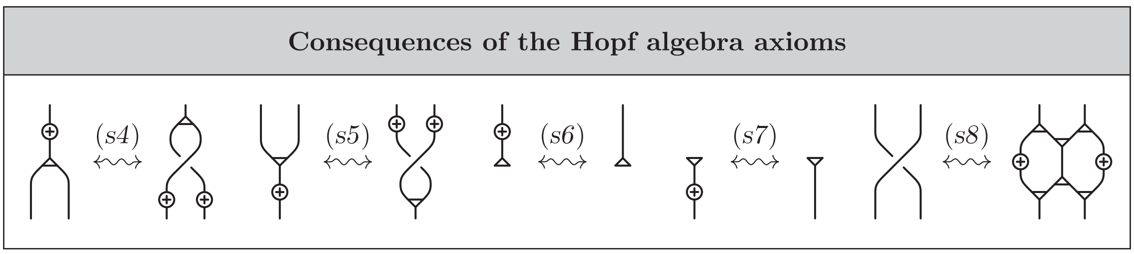

TABLE 2.2.2

correspond to 2-handles, while those pointing down correspond to 1-handles in the category of Kirby tangles 4KT introduced in Subsection 3.3.

DEFINITION 2.2.1. We denote by Alg the strict braided monoidal category freely generated by a Hopf algebra object H. In other words, objects of Alg are tensor powers of H, while morphisms of Alg are compositions of tensor products of identities, braidings, and structure morphisms μ, η, Δ, ε, S, S^{-1}, modulo the defining axioms in Table 2.2.1.

By definition, the category Alg satisfies the following universal property.

UNIVERSAL PROPERTY 2.2.2. *If $\mathscr{C}'$ is a braided monoidal category and $H' \in \mathscr{C}'$ is a Hopf algebra, then there exists a unique braided monoidal functor $\Xi_{H'} : \mathrm{Alg} \to \mathscr{C}'$ sending H to H'.*

PROPOSITION 2.2.3. *There is an involutive anti-monoidal equivalence functor* sym : Alg $\to$ Alg, *called the symmetry functor, that sends H to itself, where anti-monoidal means*

$$\mathrm{sym}(F \otimes F') = \mathrm{sym}(F') \otimes \mathrm{sym}(F)$$

for all morphisms F, F' in Alg.

Proof. The statement follows from the fact that the axioms are invariant under sym. □

2.3. Adjoint action

Let $\mathscr{C}$ be a strict braided monoidal category, let $(H, \mu_H, \eta_H, \Delta_H, \varepsilon_H, S_H)$ be a braided Hopf algebra in $\mathscr{C}$, and let (A, μ_A, η_A) be an algebra in $\mathscr{C}$. We recall that a morphism $\alpha : H \otimes A \to A$ defines a left action of H on A if the following holds:

$$\begin{aligned}
\alpha \circ (\eta_H \otimes \mathrm{id}_A) &= \mathrm{id}_A, \\
\alpha \circ (\mu_H \otimes \mathrm{id}_A) &= \alpha \circ (\mathrm{id}_H \otimes \alpha), \\
\alpha \circ (\mathrm{id}_H \otimes \eta_A) &= \eta_A \circ \varepsilon_H, \\
\alpha \circ (\mathrm{id}_H \otimes \mu_A) &= \mu_A \circ (\alpha \otimes \alpha) \circ (\mathrm{id}_H \otimes c_{H,A} \otimes \mathrm{id}_A) \circ (\Delta_H \otimes \mathrm{id}_{A \otimes A}).
\end{aligned}$$

The first two conditions express the fact that A is a left H-module, while the last two conditions express the fact that the action intertwines the product and the unit of A. The notion of right action is symmetric, and corresponds to a right H-algebra structure on A.

DEFINITION 2.3.1. For every $n \geqslant 0$, the left adjoint action $\mathrm{ad}_n : H \otimes H^n \to H^n$ is inductively defined by the following identities (see Table 2.3.1):

$$\mathrm{ad}_0 = \varepsilon$$

$$\mathrm{ad}_1 = \mathrm{ad} = \mu \circ (\mu \otimes S) \circ (\mathrm{id} \otimes c) \circ (\Delta \otimes \mathrm{id}), \tag{d1}$$

$$\mathrm{ad}_n = (\mathrm{ad} \otimes \mathrm{ad}_{n-1}) \circ (\mathrm{id} \otimes c \otimes \mathrm{id}_{n-1}) \circ (\Delta \otimes \mathrm{id}_n). \tag{d2}$$

We also define the symmetric right adjoint action $\mathrm{ad}'_n : H^n \otimes H \to H^n$ as (see Table 2.3.1):

$$\mathrm{ad}'_n = \mathrm{sym}(\mathrm{ad}_n). \tag{d1'-2'}$$

We denote by $\mathscr{Ad}$ the collection of morphisms $\{\mathrm{ad}_n\}_{n \in \mathbb{N}}$, and similarly by $\mathscr{Ad}'$ the collection $\{\mathrm{ad}'_n\}_{n \in \mathbb{N}}$. The fact that these are indeed left and right actions is a classical result in the theory of Hopf algebras, and the reader can find the proof in Proposition 2.3.2 below. In particular, the adjoint action intertwines the product and the unit.

PROPOSITION 2.3.2. *If H is a Hopf algebra in $\mathscr{C}$, then its structure morphisms satisfy the identities appearing in Table 2.3.1. In particular, for every integer $n \geqslant 0$, the adjoint morphisms ad_n and ad'_n define a left and a right action of H on H^n respectively.*

Proof. Observe that it is enough to prove the statements for ad_n, since the ones for ad'_n follow by applying the functor sym.

Identity (*d3*) is an immediate consequence of relations (*a2*-*2'*), (*a7*), and (*s6*) in Tables 2.2.1 and 2.2.2. In order to show (*d4*), we first prove the special case $n = 1$ in Figure 2.3.2; then the general case follows by the inductive argument shown in Figure 2.3.3. Identity (*d5*) follows from axioms (*a2'*) and (*s1'*) in Table 2.2.1. Identity (*d6*) is proved in Figure 2.3.4, identity (*d7*) is verified in Figure 2.3.5, while

($d8$) can be proved in a similar way, by using ($s1'$) instead of ($s1$). Finally, we derive ($d9$) as described in Figure 2.3.6. ☐

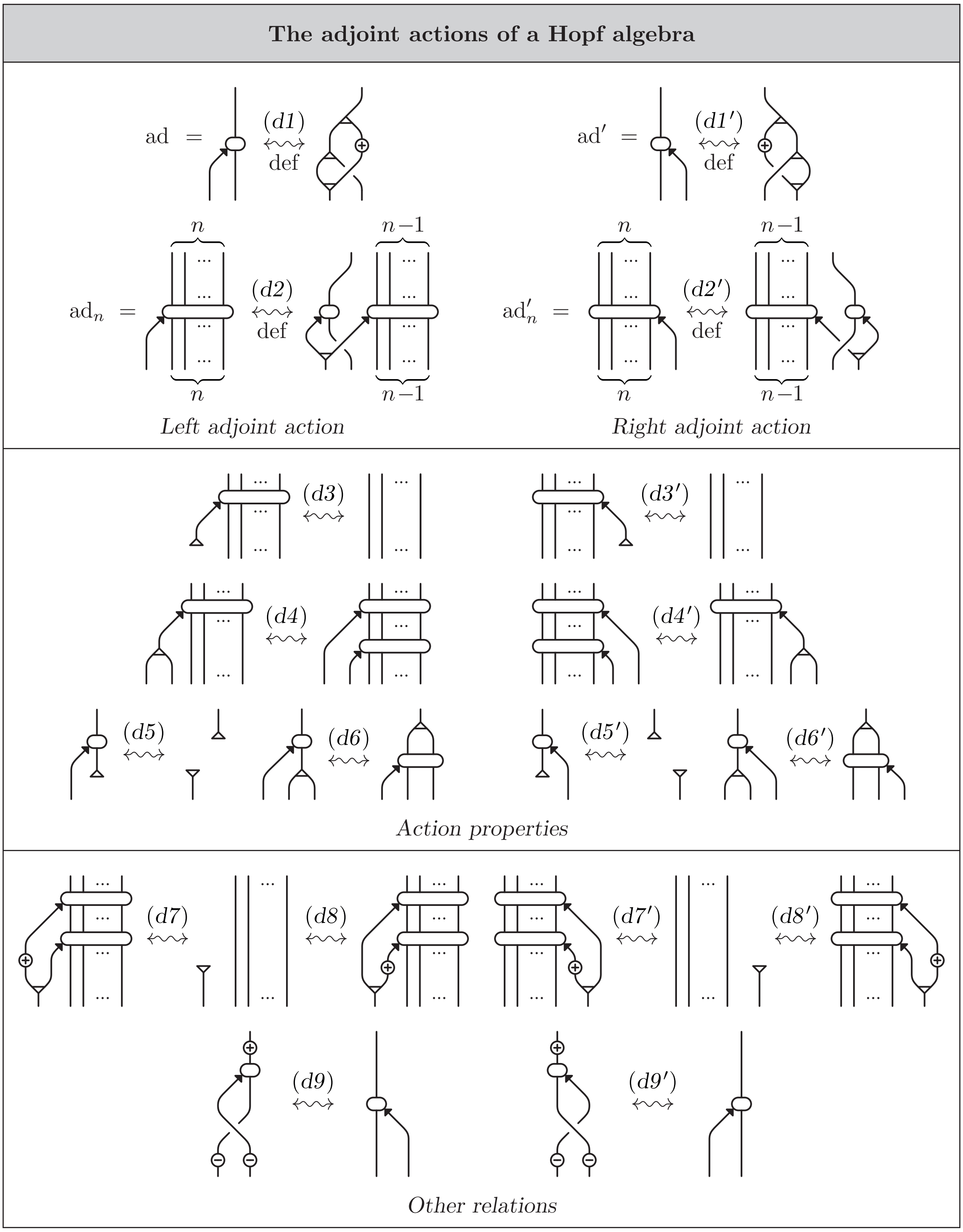

TABLE 2.3.1

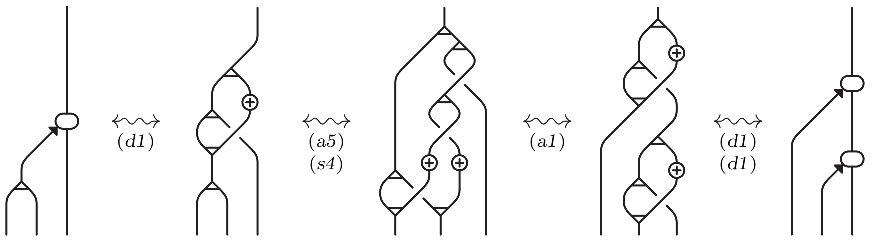

FIGURE 2.3.2. Proof of (d4): case $n = 1$.

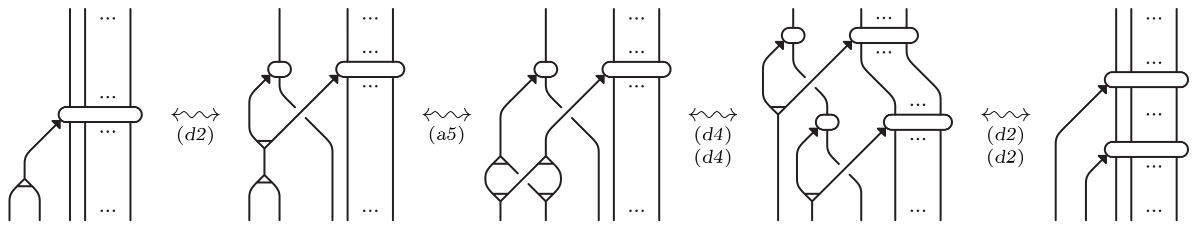

FIGURE 2.3.3. Proof of (d4): inductive step.

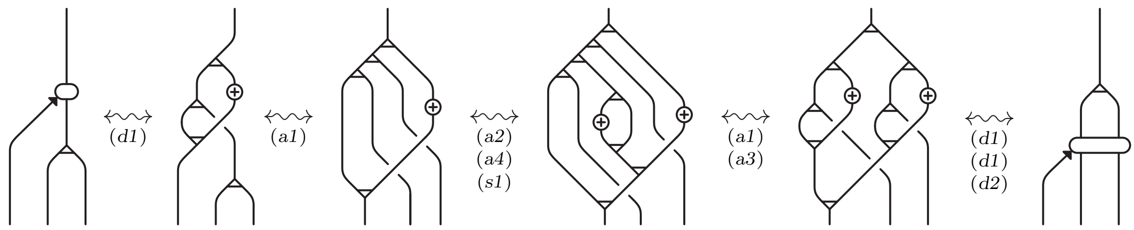

FIGURE 2.3.4. Proof of (d6).

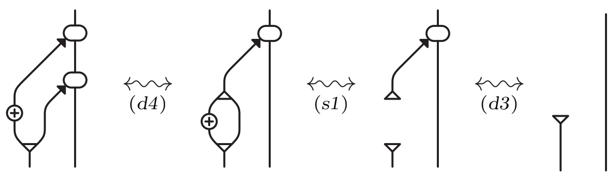

FIGURE 2.3.5. Proof of (d7).

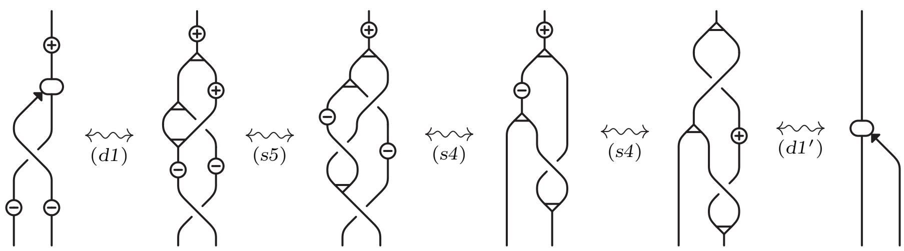

FIGURE 2.3.6. Proof of (d9).

If $\mathscr{C}$ is the category of left modules over a ring R, equipped with its standard symmetric braiding, then the adjoint action is only known to intertwine the coproduct and the antipode when the Hopf algebra is *cocommutative*, that is, when $c \circ \Delta = \Delta$, see [Mo93, Lemma 5.7.2]. The following definition provides a weaker condition on the Hopf algebra that ensures this intertwining property in the case of an arbitrary braided category. This condition was first introduced by Majid under the name *$\mathscr{C}$-cocommutative* action, see [Ma93, Definition 2.3], or *braided cocommutative* action, see [Ma94, Definition 2.9].

DEFINITION 2.3.3. The left adjoint action $\mathrm{ad} : H \otimes H \to H$ of a Hopf algebra H in a braided monoidal category $\mathscr{C}$ is *braided cocommutative* if the following holds:

$$(\mathrm{ad} \otimes \mathrm{id}) \circ (\mathrm{id} \otimes c) \circ (\Delta \otimes \mathrm{id}) = c^{-1} \circ (\mathrm{id} \otimes \mathrm{ad}) \circ (\Delta \otimes \mathrm{id}). \tag{h0}$$

Analogously, the right adjoint action $\mathrm{ad} : H \otimes H \to H$ of a Hopf algebra H in a braided monoidal category $\mathscr{C}$ is *braided cocommutative* if the following holds:

$$(\mathrm{id} \otimes \mathrm{ad}') \circ (c \otimes \mathrm{id}) \circ (\mathrm{id} \otimes \Delta) = c^{-1} \circ (\mathrm{ad}' \otimes \mathrm{id}) \circ (\mathrm{id} \otimes \Delta). \qquad (h0')$$

A graphical representation of the braided cocommutativity axiom for adjoint actions is given in Table 2.3.7. Notice that, when the braiding of $\mathscr{C}$ is symmetric, relations ($h0$) and ($h0'$) are implied by the cocommutativity condition $c \circ \Delta = \Delta$, although they are not equivalent to it.

Braided cocommutative adjoint actions

Braided cocommutativity axiom for left and right adjoint actions

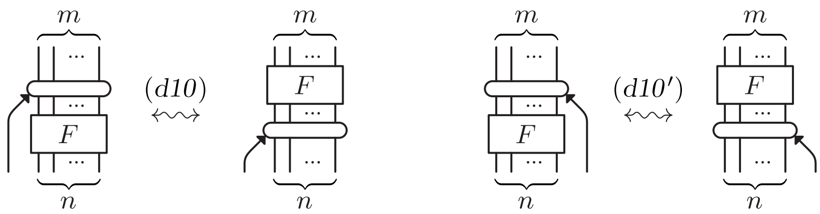

Intertwining properties

Some consequences of the intertwining properties

Table 2.3.7

Lemma 2.3.4. *If* $\mathrm{Alg}^{\mathrm{L}}$ *(respectively* $\mathrm{Alg}^{\mathrm{R}}$*) denotes the strict braided monoidal category freely generated by a Hopf algebra* H *with braided cocomutative left (respectively right) adjoint action, then the latter defines a natural transformation* $\mathscr{A}\!d : H \otimes \mathscr{I}\!d \Rightarrow \mathscr{I}\!d$ *(respectively* $\mathscr{A}\!d' : \mathscr{I}\!d \otimes H \Rightarrow \mathscr{I}\!d$*), where* $\mathscr{I}\!d$ *denotes the identity functor, meaning that, for every morphism* $F : H^n \to H^m$ *in* $\mathrm{Alg}^{\mathrm{L}}$*, we have*

$$\mathrm{ad}_m \circ (\mathrm{id} \otimes F) = F \circ \mathrm{ad}_n, \qquad (d10)$$

and that for every morphism $F : H^n \to H^m$ *in* $\mathrm{Alg}^{\mathrm{R}}$ *we have*

$$\mathrm{ad}'_m \circ (F \otimes \mathrm{id}) = F \circ \mathrm{ad}'_n. \qquad (d10')$$

Moreover, identities (d11-11′) in Table 2.3.7 hold in both $\mathrm{Alg}^{\mathrm{L}}$ *and* $\mathrm{Alg}^{\mathrm{R}}$*.*

Proof. Observe that the category $\mathrm{Alg}^{\mathrm{L}}$ (respectively $\mathrm{Alg}^{\mathrm{R}}$) is the quotient of Alg by the braided cocommutativity axiom ($h0$) (respectively ($h0'$)) and that the functor $\mathrm{sym} : \mathrm{Alg} \to \mathrm{Alg}$ induces an equivalence of categories $\mathrm{sym} : \mathrm{Alg}^{\mathrm{R}} \to \mathrm{Alg}^{\mathrm{L}}$. Therefore, the statements for $\mathrm{Alg}^{\mathrm{R}}$ will follow by applying sym, once the ones for $\mathrm{Alg}^{\mathrm{L}}$ have been proved.

In order to prove ($d10$), it is enough to consider the case when F is a structure morphism of H. For $F = \mu$ and for $F = \eta$ it was already established in Proposition 2.3.2 (see relations ($d5$) and ($d6$)), while for $F = \varepsilon$ the statement follows from ($a6$) in Table 2.2.1. Moreover, since relation ($s8$) in Table 2.2.2 allows us to express c in terms of the rest of the generating morphisms, and since, whenever F is invertible, the identity ($d10$) for F^{-1} is implied by the one for F, we only need to prove ($d10$) for $F = \Delta, S$. This is done in Figures 2.3.8 and 2.3.9.

Now ($d11$) and ($d11'$) follow directly from ($d9$) and ($d9'$), respectively, by intertwining the adjoint action and the antipode. □

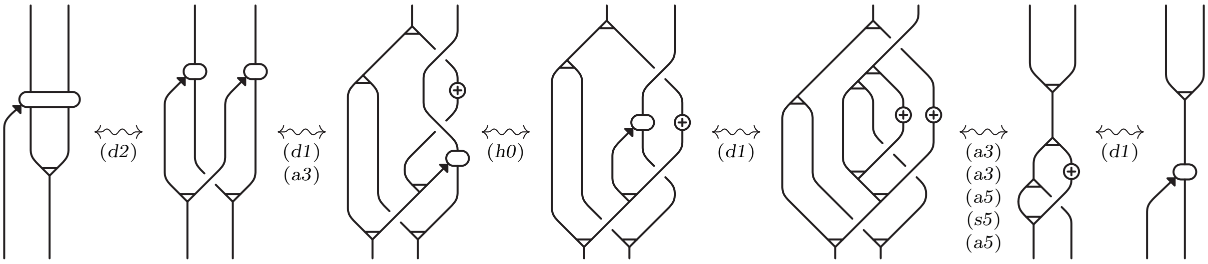

FIGURE 2.3.8. Proof of (*d10*) for $F = \Delta$.

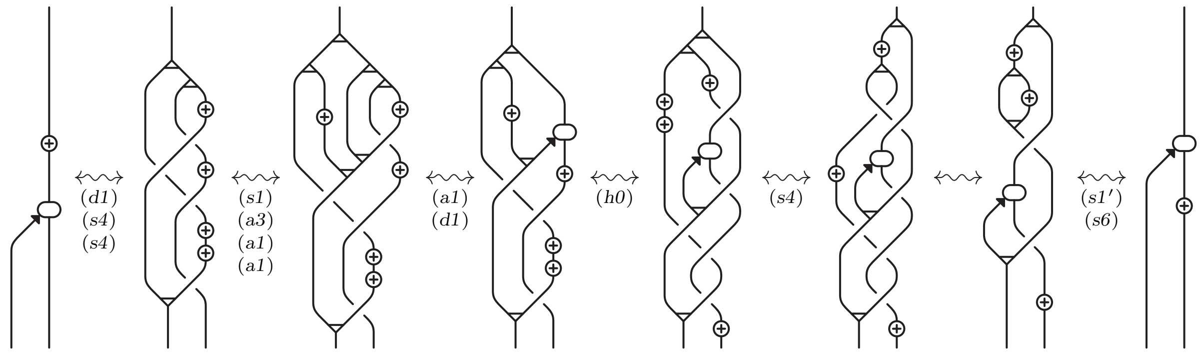

FIGURE 2.3.9. Proof of (*d10*) for $F = S$.

2.4. BP Hopf algebras and the category 4Alg

In this subsection, we recall the definition and the properties of BP Hopf algebras. These algebraic structures were first defined and studied in [BP11] in the general context of *groupoid Hopf algebras*, where all the edges of the diagrams representing the structure morphisms of the algebra are labeled by elements of a groupoid $\mathscr{G}$. The notion of a BP Hopf algebra was introduced in [BD21] and corresponds to the special case of the trivial groupoid $\mathscr{G} = \{1\}$.

DEFINITION 2.4.1. If $\mathscr{C}$ is a braided monoidal category with tensor product $\otimes$, tensor unit $\mathbb{1}$, and braiding c, a *Bobtcheva–Piergallini Hopf algebra*, or *BP Hopf algebra*, is a Hopf algebra H in $\mathscr{C}$ equipped with the following structure morphisms:

- ◇ an *integral form* $\lambda : H \to \mathbb{1}$ and an *integral element* $\Lambda : \mathbb{1} \to H$;
- ◇ a *ribbon morphism* $\tau : H \to H$ and its inverse $\tau^{-1} : H \to H$;
- ◇ a *copairing* $w : \mathbb{1} \to H \otimes H$.

These structure morphisms are subject to the following axioms:

$$(\mathrm{id} \otimes \lambda) \circ \Delta = \eta \circ \lambda, \tag{i1}$$

$$\mu \circ (\Lambda \otimes \mathrm{id}) = \Lambda \circ \varepsilon, \tag{i2}$$

$$\lambda \circ \Lambda = \mathrm{id}_{\mathbb{1}}, \tag{i3}$$

$$S \circ \Lambda = \Lambda, \tag{i4}$$

$$\lambda \circ S = \lambda, \tag{i5}$$

$$S \circ \tau = \tau \circ S, \tag{r3}$$

$$\varepsilon \circ \tau = \varepsilon, \tag{r4}$$

$$\mu \circ (\tau \otimes \mathrm{id}) = \tau \circ \mu, \tag{r5}$$

$$w = (\tau \otimes \tau) \circ \Delta \circ \tau^{-1} \circ \eta \tag{r6}$$

$$(\mathrm{id} \otimes \Delta) \circ w = (\mu \otimes \mathrm{id}_2) \circ (\mathrm{id} \otimes w \otimes \mathrm{id}) \circ w, \tag{r7}$$

$$\Delta \circ \tau^{-1} = (\tau^{-1} \otimes \tau^{-1}) \circ \Omega \circ c^{-1} \circ \Delta, \tag{r8}$$

$$(\mu \otimes \mu) \circ (S \otimes (\Omega \circ c^{-1} \circ \Omega) \otimes S) \circ (\rho_L \otimes \rho_R) = c, \tag{r9}$$

where

$$\Omega = (\mu \otimes \mu) \circ (\mathrm{id} \otimes w \otimes \mathrm{id}) : H \otimes H \to H \otimes H$$

is called the *monodromy*, while the morphisms

$$\rho_L = (\mathrm{id} \otimes \mu) \circ (w \otimes \mathrm{id}) : H \to H \otimes H \quad \text{and} \quad \rho_R = (\mu \otimes \mathrm{id}) \circ (\mathrm{id} \otimes w) : H \to H \otimes H$$

define a left and a right H-comodule structure on H, respectively.

A graphical representation of the additional generators and defining axioms of a BP Hopf algebra can be found in Table 2.4.1, to be added to the list of generators and defining axioms of Hopf algebras given in Table 2.2.1 (compare with [BP11, Tables 4.7.12 & 4.7.13]).

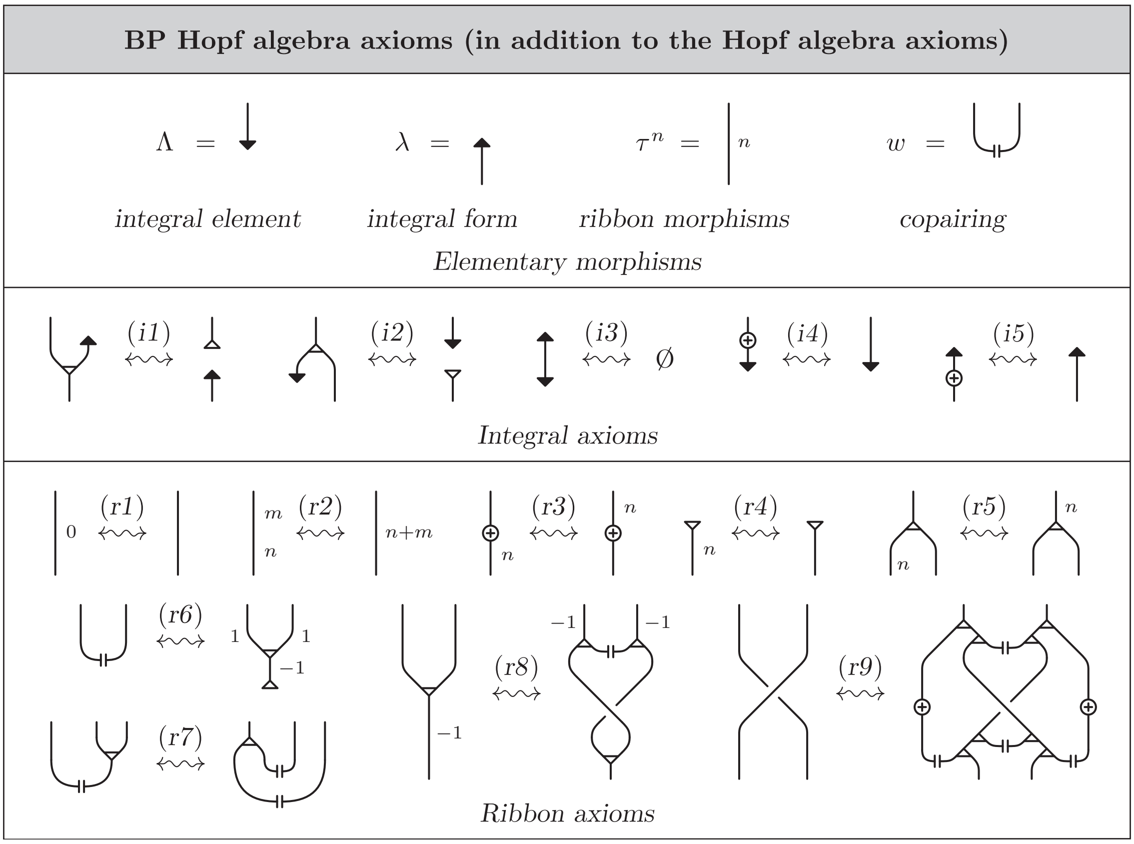

TABLE 2.4.1

DEFINITION 2.4.2. We denote by 4Alg the strict braided monoidal category freely generated by a BP Hopf algebra H. In other words, objects of 4Alg are tensor powers of H, while morphisms of 4Alg are compositions of tensor products of identities, braidings, and structure morphisms μ, η, Δ, ε, S, S^{-1}, λ, Λ, τ, τ^{-1}, w, modulo the defining axioms listed in Definition 2.4.1.

Observe that, since H is a Hopf algebra in 4Alg, then, according to the Universal Property 2.2.2, there exists a unique functor $4\Xi : \mathrm{Alg} \to 4\mathrm{Alg}$ that sends H to itself. Moreover, by definition, we have the following universal property.

UNIVERSAL PROPERTY 2.4.3. *If $\mathscr{C}'$ is a braided monoidal category and $H' \in \mathscr{C}'$ is a BP Hopf algebra, then the braided monoidal functor $\Xi_{H'} : \mathrm{Alg} \to \mathscr{C}'$ given by the universal property of* Alg *factors through* $4\Xi : \mathrm{Alg} \to 4\mathrm{Alg}$.

REMARK 2.4.4. As it is shown in Figure 2.4.2, relation (*r6*) is not an independent axiom, but it is a consequence of (*r8*) and the Hopf algebra axioms. We present it as an axiom, first of all, because it gives an explicit expression for the copairing in terms of the ribbon morphism and the coproduct, and in second place since, as it will be shown in Proposition 2.5.2, in the presence of (*r6*) axiom (*r8*) can be expressed in terms of the adjoint action by its equivalent forms (*d12*) or (*d12′*).

Moreover, the original definition of BP Hopf algebra in [BP11, Table 4.7.13] uses as an axiom relation (*p4*) in Table 2.4.4 in place of (*r6*). As it is shown by Kerler in [Ke01, Lemma 4] (see also Figure B.3.4

in Appendix B), those two relations are equivalent modulo the axioms of braided Hopf algebra and the ribbon axioms (*r1*) to (*r5*) and (*r7*). Therefore Definition 2.4.1 is equivalent to the one in [BP11].

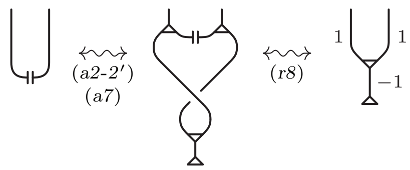

FIGURE 2.4.2. Proof of (*r6*) using the rest of the axioms of a BP Hopf algebra.

The reader can find the diagrammatic proofs of the following propositions in Appendix B (see also [BP11, Propositions 4.1.4, 4.1.5, 4.1.6, 4.1.9, 4.1.10, Lemmas 4.2.5, 4.2.6, Propositions 4.2.7, 4.2.11, 4.2.13] and [Ke01, Lemmas 1 to 8]).

PROPOSITION 2.4.5. *The identities in Table 2.4.3 hold in any braided monoidal category with a Hopf algebra H, an integral form $\lambda : H \to \mathbb{1}$, and an integral element $\Lambda : \mathbb{1} \to H$ satisfying axioms (i1)–(i5) in Table 2.4.1. In particular, they hold in* 4Alg.

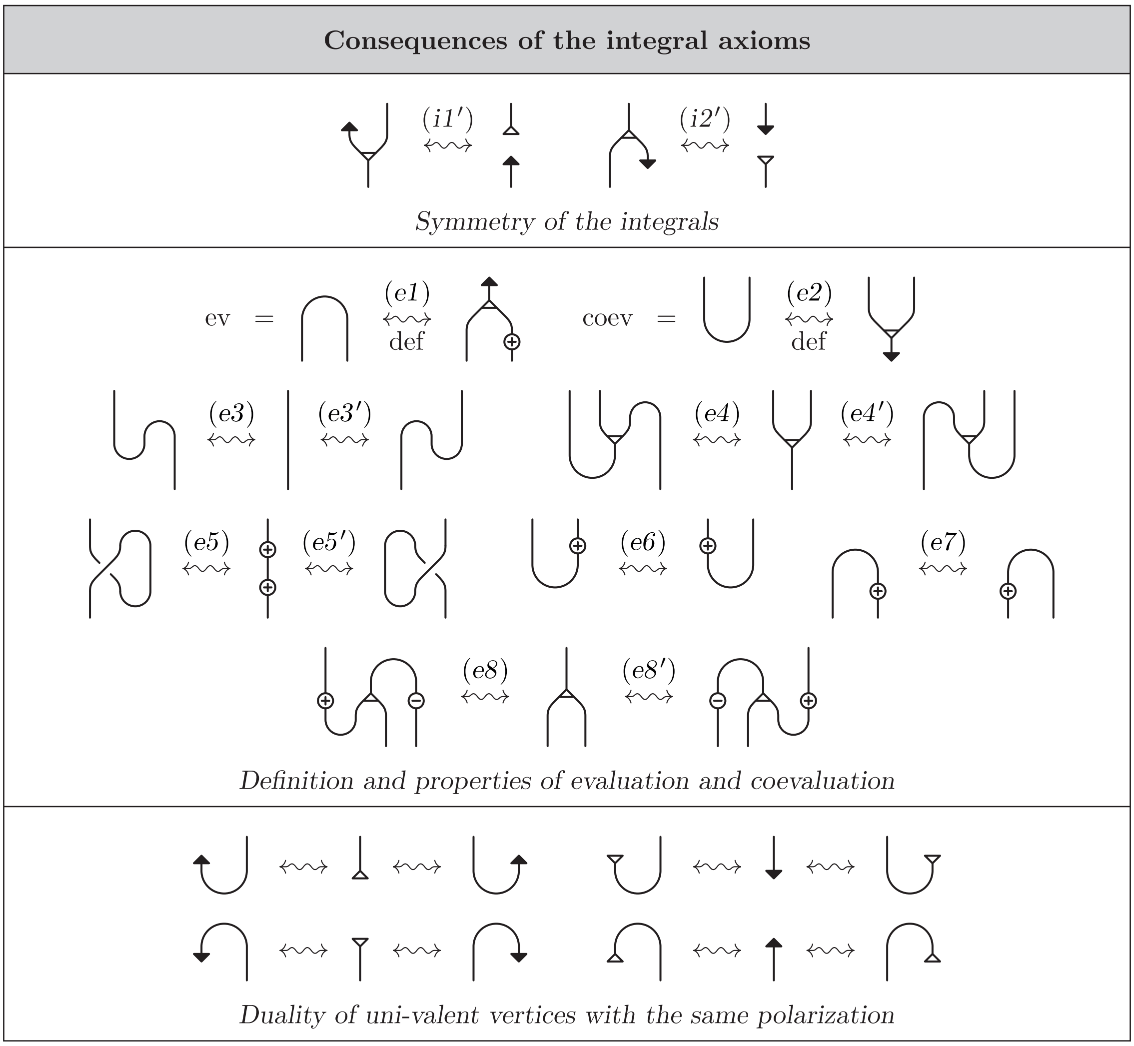

TABLE 2.4.3

Proposition 2.4.6. *The identities in Table 2.4.4 hold in any braided monoidal category with Hopf algebra H and a family of ribbon morphisms $\tau^n : H \to H$ satisfying axioms (r1) to (r7) in Table 2.4.1. In particular, they hold in* 4Alg.

Consequences of the ribbon axioms (r1) to (r7) - Part I

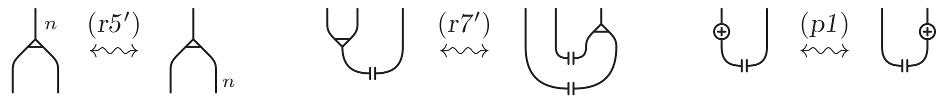

Symmetry of 4Alg *(not using the integrals)*

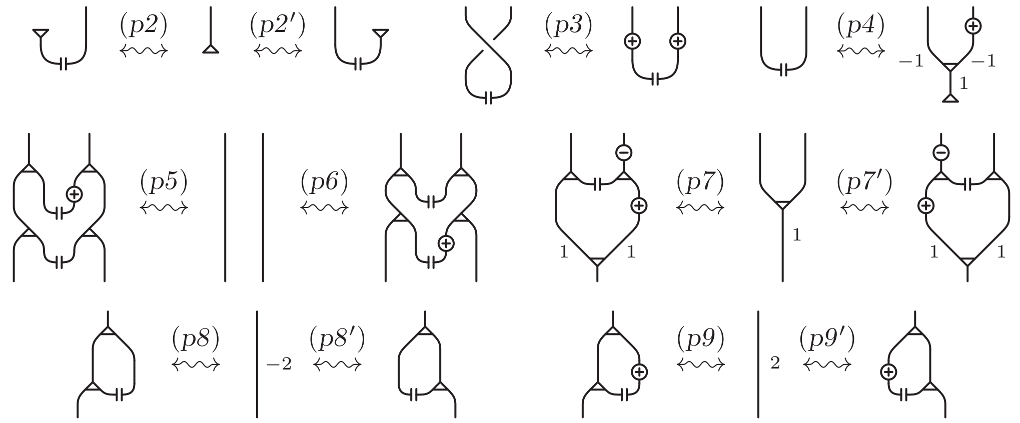

Other consequences not using the integrals

Table 2.4.4

Proposition 2.4.7. *The identities in Table 2.4.5 hold in any braided monoidal category with Hopf algebra H, a family of ribbon morphisms $\tau^n : H \to H$ satisfying axioms (r1) to (r7) in Table 2.4.1, and an integral form $\lambda : H \to \mathbb{1}$ and an integral element $\Lambda : \mathbb{1} \to H$ satisfying axioms (i1) to (i5) in the same table. In particular, the identities in Table 2.4.4 hold in* 4Alg.

Consequences of the ribbon axioms (r1) to (r7) - Part II

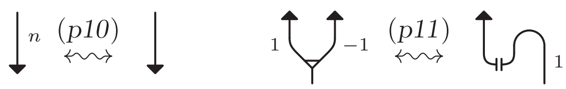

Some consequence regarding the integrals

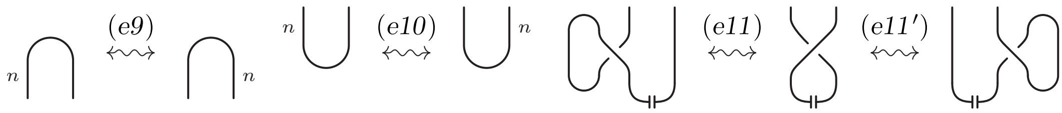

Extended isotopy moves

Table 2.4.5

Proposition 2.4.8. *The identities in Table 2.4.6 are satisfied in* 4Alg. *Moreover, modulo the rest of the defining axioms, relation* (*p12*) *is an equivalent reformulation of axiom* (*r8*), *while relation* (*p13*) *is an equivalent reformulation of axiom* (*r9*).

Consequences of the ribbon axioms (*r8*) and (*r9*)

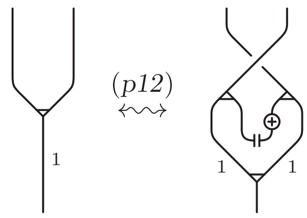

Equivalent form of the axiom (r8)

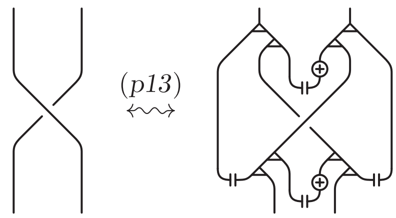

Equivalent form of the axiom (r9)

Inverting the antipode through the copairing

Table 2.4.6

The propositions above have the following implications.

Proposition 2.4.9. 4Alg *is a ribbon category (see Definition 2.1.3), with dual* $(H^n)^* = H^n$ *for every* $n \geqslant 0$, *and with two-sided evaluation* $\mathrm{ev}_{H^n} : H^n \otimes H^n \to \mathbb{1}$ *and coevaluation* $\mathrm{coev}_{H^n} : \mathbb{1} \to H^n \otimes H^n$ *defined inductively by* $\mathrm{ev}_0 = \mathrm{coev}_0 = \mathrm{id}_{\mathbb{1}}$ *and*

$$\mathrm{ev} = \mathrm{ev}_H = \lambda \circ \mu \circ (\mathrm{id} \otimes S), \tag{e1}$$

$$\mathrm{coev} = \mathrm{coev}_H = \Delta \circ \Lambda, \tag{e2}$$

and by

$$\mathrm{ev}_n = \mathrm{ev}_{H^n} = \mathrm{ev} \circ (\mathrm{id} \otimes \mathrm{ev}_{n-1} \otimes \mathrm{id}),$$

$$\mathrm{coev}_n = \mathrm{coev}_{H^n} = (\mathrm{id} \otimes \mathrm{coev}_{n-1} \otimes \mathrm{id}) \circ \mathrm{coev},$$

for every $n > 1$. *The twist* $\theta_{H^n} : H^n \to H^n$ *is defined for every* $n \geqslant 0$ *by*

$$\theta_n = \theta_{H^n} = (\mathrm{ev}_n \otimes \mathrm{id}_n) \circ (\mathrm{id}_n \otimes c_{n,n}) \circ (\mathrm{coev}_n \otimes \mathrm{id}_n).$$

Proof. The statement follows from the definitions of ev and coev, and from identities (*e3*-*3′*) and (*e5*-*5′*) in Table 2.4.3. □

Proposition 2.4.10. *There is an involutive anti-monoidal equivalence functor* sym : 4Alg → 4Alg *that sends every object and every structure morphism to itself. Moreover,* sym *fits into the commutative diagram of functors:*

$$\begin{tikzcd} \mathrm{Alg} \arrow[r, "\mathrm{sym}"] \arrow[d, "4\Xi"'] & \mathrm{Alg} \arrow[d, "4\Xi"] \\ 4\mathrm{Alg} \arrow[r, "\mathrm{sym}"'] & 4\mathrm{Alg} \end{tikzcd}$$

Proof. The statement is a direct consequence of the fact that the symmetric versions (*r5′*) and (*r7′*) of axioms (*r5*) and (*r7*) hold in 4Alg, while all other axioms of 4Alg remain unchanged under sym. □

By a certain abuse of terminology, we will say that two diagrams representing morphisms in 4Alg are *isotopic* if they are related by a sequence of the following moves: braiding axioms in Table 2.1.2, moves (*e3*-*3′*), (*e5*-*5′*), and (*e6*-*7*) in Table 2.4.3, and relations (*e9*) to (*e11*-*11′*) in Table 2.4.5. An example of a non-standard isotopy is presented in Figure 2.4.7. Such generalized isotopy moves will be frequently used in our diagrammatic proofs without explicitly indicating them.

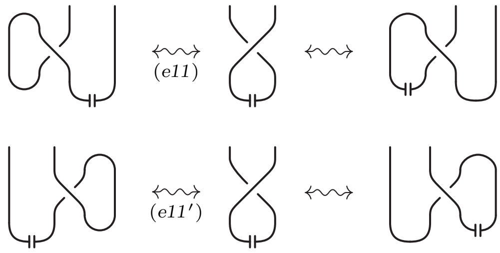

FIGURE 2.4.7. Examples of isotopies.

2.5. Frobenius structure and braided cocommutativity in 4Alg

Let us sidetrack for a moment, and introduce a modified product $\widetilde{\mu}$ which, together with the modified unit $\widetilde{\eta} = \Lambda$, and with the standard coproduct Δ and counit ε, provides every BP Hopf algebra H with a Frobenius algebra structure.

PROPOSITION 2.5.1. *If we set* $\widetilde{\mu} = (\mathrm{id} \otimes \mathrm{ev}) \circ (\Delta \otimes \mathrm{id})$ *and* $\widetilde{\mu}' = (\mathrm{ev} \otimes \mathrm{id}) \circ (\mathrm{id} \otimes \Delta)$, *then the following identities hold in* 4Alg*:*

$$\widetilde{\mu} = \widetilde{\mu}', \tag{q1}$$
$$(\Delta \otimes \mathrm{id}) \circ \mathrm{coev} = (\mathrm{id}_2 \otimes \widetilde{\mu}) \circ \mathrm{coev}_2, \tag{q2}$$
$$(\widetilde{\mu} \otimes \mathrm{id}_2) \circ \mathrm{coev}_2 = (\mathrm{id} \otimes \Delta) \circ \mathrm{coev}, \tag{q2'}$$
$$\mathrm{ev}_2 \circ (\Delta \otimes \mathrm{id}_2) = \mathrm{ev} \circ (\mathrm{id} \otimes \widetilde{\mu}), \tag{q3}$$
$$\mathrm{ev}_2 \circ (\mathrm{id}_2 \otimes \Delta) = \mathrm{ev} \circ (\widetilde{\mu} \otimes \mathrm{id}), \tag{q3'}$$
$$\mu \circ (\mathrm{id} \otimes \widetilde{\mu}) = \widetilde{\mu} \circ (\mu \otimes \mu) \circ (\mathrm{id} \otimes c \otimes \mathrm{id}) \circ (\Delta \otimes \mathrm{id}_2), \tag{q4}$$
$$\mu \circ (\widetilde{\mu} \otimes \mathrm{id}) = \widetilde{\mu} \circ (\mu \otimes \mu) \circ (\mathrm{id} \otimes c \otimes \mathrm{id}) \circ (\mathrm{id}_2 \otimes \Delta). \tag{q4'}$$

The morphism $\widetilde{\mu}$

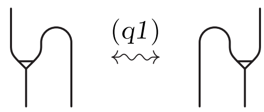

The defining relation for $\widetilde{\mu}$

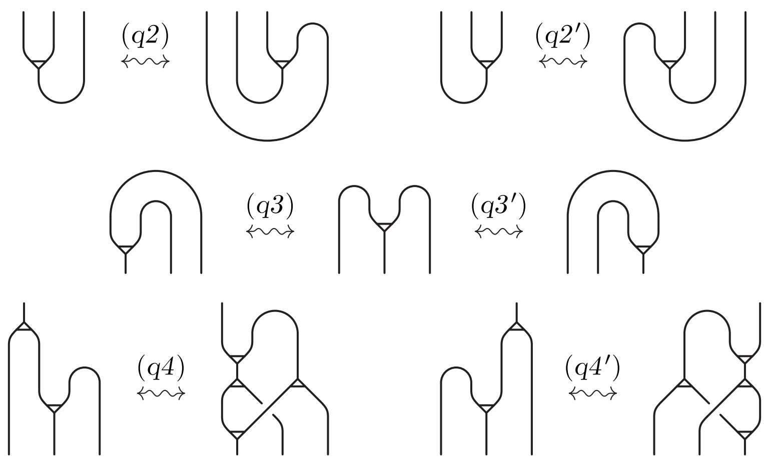

Some properties of $\widetilde{\mu}$

TABLE 2.5.1

A graphical representation of relations (*q1*) to (*q4′*) can be found in Table 2.5.1. Notice that relations (*q2*), (*q2′*), (*q3*), and (*q3′*) imply that $\widetilde{\mu}$ and Δ are dual to each other with respect to the coevaluation. Furthermore, as mentioned above, H admits the structure of a Frobenius algebra in 4Alg, determined by the product $\widetilde{\mu}$, the unit $\widetilde{\eta} = \Lambda$, the coproduct Δ, and the counit ε (see [FS10, Appendix A.2]).

Proof. Relation (*q1*) follows directly from (*e3*) and (*e4′*). Relations (*q2*), (*q3*), and (*q4*) are proved in Figure 2.5.2 (where the reader should ignore for now the dashed boxes and arrows), while relations (*q2′*), (*q3′*), and (*q4′*) follow by applying the symmetry functor. □

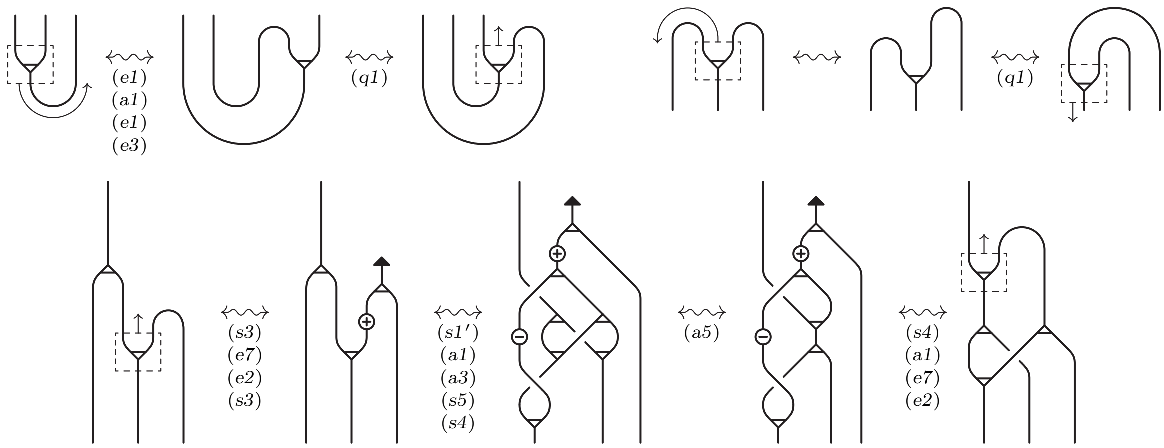

FIGURE 2.5.2. Proof of (*q2*), (*q3*), and (*q4*).

Next, let us establish some properties of the adjoint actions of a BP Hopf algebra. Such properties have already been proved in [BP11, Subsection 4.4], but we present here an alternative argument, based on the fact that the left and right adjoint actions of a BP Hopf algebra are braided cocommutative.

Proposition 2.5.2. *In a BP Hopf algebra, modulo the other axioms,* (*r8*) *and* (*r9*) *admit the equivalent forms presented in Table 2.5.3. Namely,* (*d12-12′*) *are equivalent to* (*r8*)*, while* (*d13-13′*) *and* (*d14-14′*) *are equivalent to* (*r9*)*.*

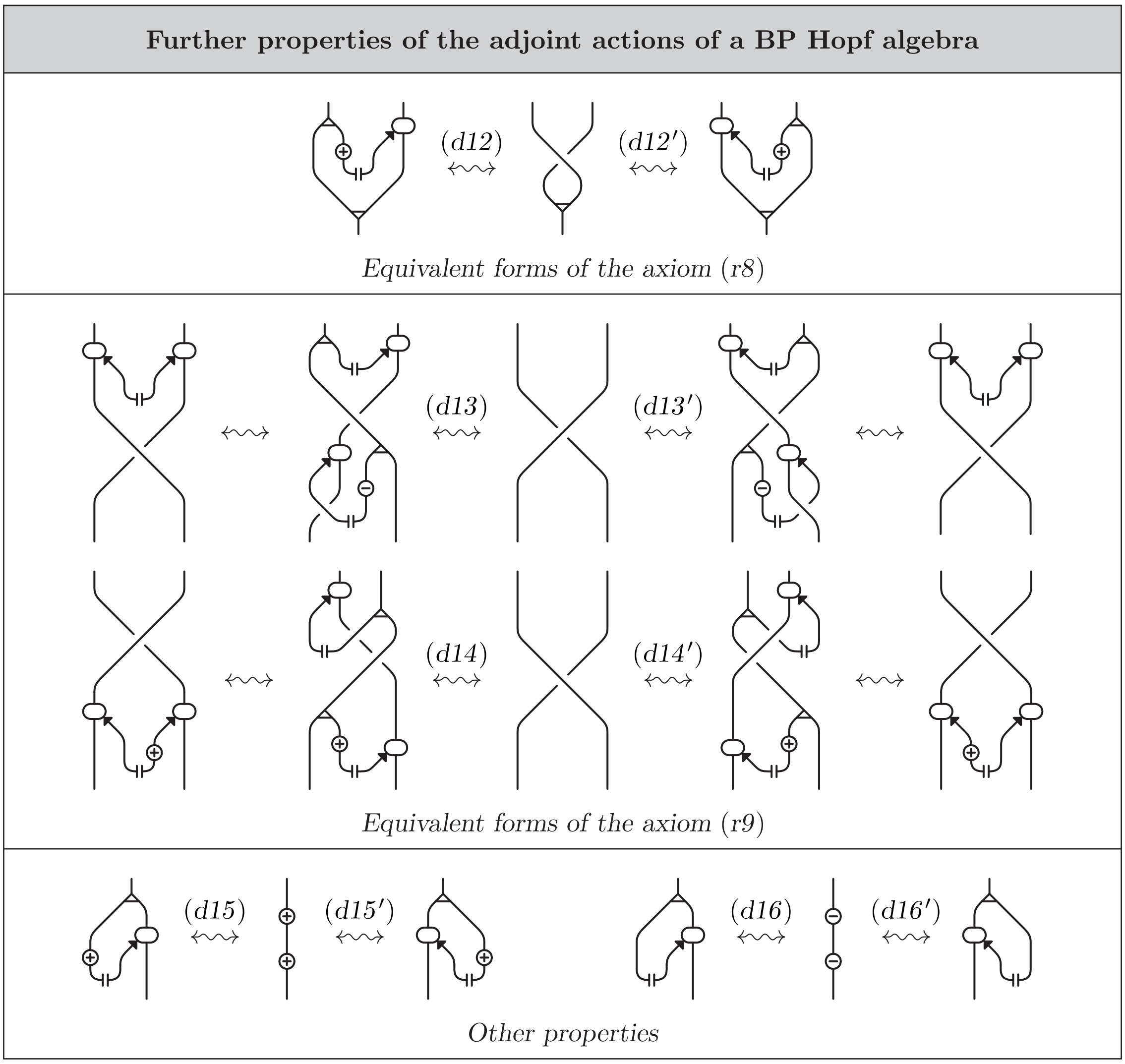

Table 2.5.3

Proof. In Figure 2.5.4 we prove that, modulo the rest of the BP Hopf algebra axioms, excluded (*r9*), axiom (*r8*) implies (*d12*) and the other way around. Therefore, (*d12*) is an equivalent reformulation of (*r8*). Analogously, we show in Figure 2.5.5 that (*r9*) is equivalent to (*d13*) modulo the rest of the BP Hopf algebra axioms, except (*r8*). Then a straightforward application of (*d7-7′*) and (*d8-8′*) shows that the diagrams in (*d14*) represent the inverse morphisms of those represented by the diagrams in (*d13*), which gives the equivalence between (*r8*) and (*d14*). Then the statements for (*d12′*), (*d13′*) and (*d14′*) are obtained by applying the functor sym. □

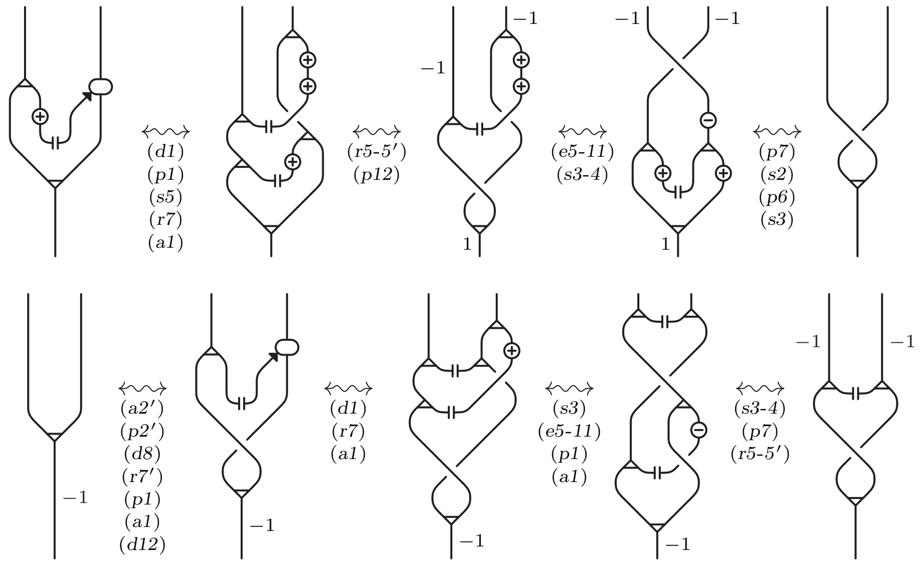

FIGURE 2.5.4. Equivalence between (*r8*) and (*d12*).

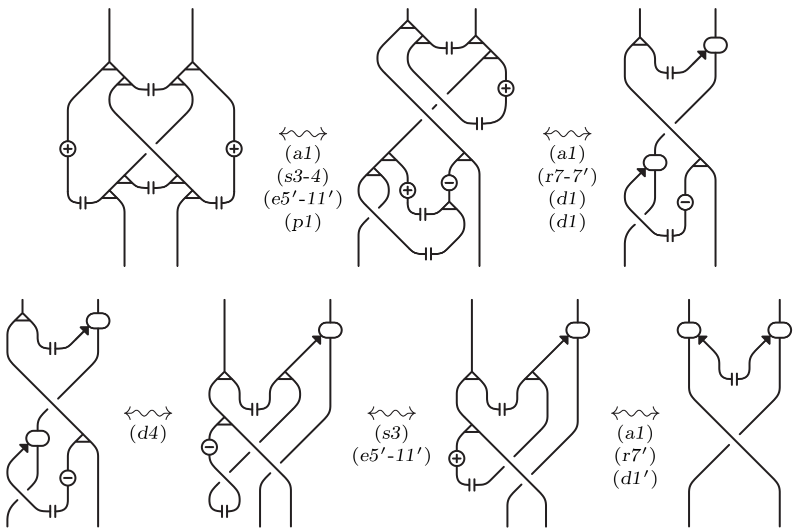

FIGURE 2.5.5. Equivalence between (*r9*) and (*d13*).

PROPOSITION 2.5.3. *The left and right adjoint actions of a BP Hopf algebra satisfy the braided cocommutativity axiom (h0-0′), which implies the intertwining properties (d10-10′) and relations (d11-11′) in Table 2.3.7. In particular, left and right adjoint actions intertwine all morphisms in* 4Alg*. Moreover, they satisfy relations (d15-15′) and (d16-16′) in Table 2.5.3.*

Proof. Concerning the left adjoint action, relation (*h0*) is proven in Figure 2.5.6. Then, Lemma 2.3.4 implies that (*d10*) holds for the product, the coproduct, the unit, the counit, the antipode and its inverse, and also that (*d11-11′*) are satisfied. We have to show that (*d10*) holds for the integrals, for the ribbon morphism, and for the copairing. For the integral element it follows from (*i2*), (*i2′*) and (*s7*), while for the integral form it is shown in Figure 2.5.7. For the ribbon morphism it follows from (*r5*), and (*p4*) implies that it holds for the copairing as well. Then, by applying the functor sym, we get the analogous properties for the right adjoint action. Finally, the proofs of (*d15*) and (*d16*) are shown in Figure 2.5.8, while (*d15′*) and (*d16′*) are obtained by applying sym once again. □

REMARK 2.5.4. Notice that the proofs of (*d15*) and (*d16*) presented above only use identities (*d10*), (*d12*), the Hopf algebra axioms, and their consequences for the adjoint action presented in Table 2.3.1. This fact is going to be important later, when we will prove that 3Alg is equivalent to the category $3\mathrm{Alg}^{\mathrm{H}}$ introduced in Subsection 2.6.

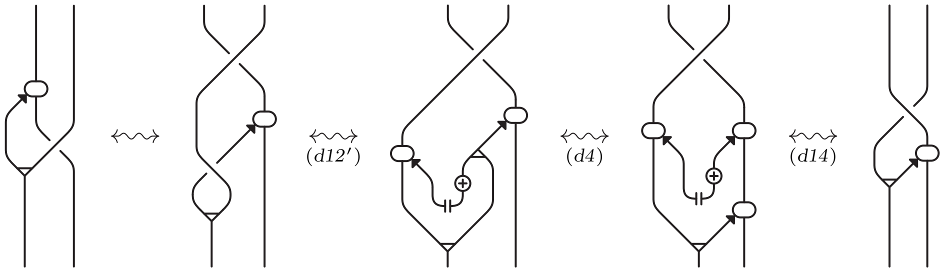

FIGURE 2.5.6. Proof of (*h0*).

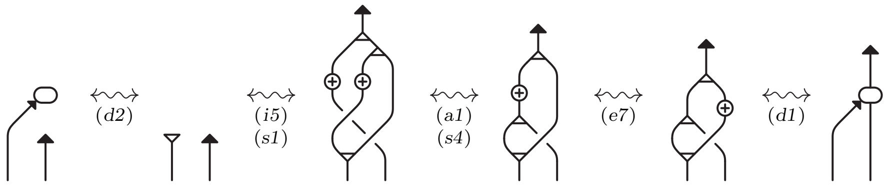

FIGURE 2.5.7. Proof of (*d10*) for $F = \lambda$.

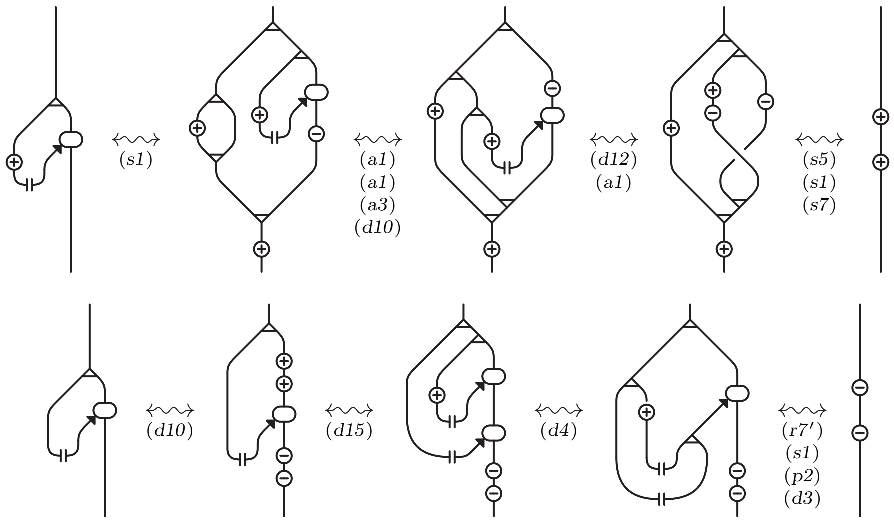

FIGURE 2.5.8. Proof of (*d15*) and (*d16*).

2.6. Factorizable BP Hopf algebras and the categories 3Alg and 3Alg$^{\mathbf{H}}$

In this subsection, we will introduce an important non-degeneracy condition for BP Hopf algebras, called *factorizability*. We will prove that factorizable anomaly-free BP Hopf algebras[4] are equivalent to *Habiro Hopf algebras*, a notion due to Habiro that was first defined in [As11].

DEFINITION 2.6.1. A BP Hopf algebra H in $\mathscr{C}$ is *factorizable* if it satisfies

$$(\lambda \otimes \mathrm{id}) \circ w = \Lambda, \tag{f}$$

and it is *anomaly-free* if it satisfies

$$\lambda \circ \tau \circ \eta = \mathrm{id}_{\mathbb{1}}. \tag{n}$$

The axioms of anomaly-free factorizable BP Hopf algebras are presented in Table 2.6.1. These axioms imply the relations in Table 2.6.2, as it is shown in Section B.4 of Appendix B (see also [BP11, Propositions 5.4.2 & 5.4.3]). In particular, axiom (f) implies the existence of a Hopf pairing $\overline{w} : H \otimes H \to \mathbb{1}$ which, together with the copairing w, satisfies the zigzag identities (*f2-2′*) in Table 2.6.2. Therefore, both $\overline{w}$ and w are non-degenerate. By analogy with the standard theory of ribbon Hopf algebras, we use the term factorizability to denote this property.

[4]Factorizable anomaly-free BP Hopf algebras were introduced [BP11] under the name *boundary ribbon Hopf algebras*.

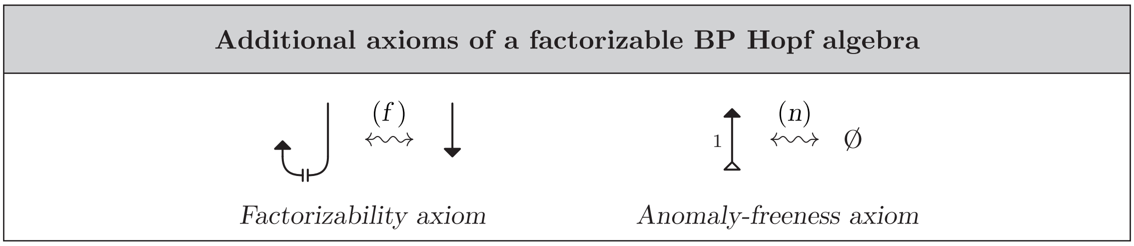

Table 2.6.1

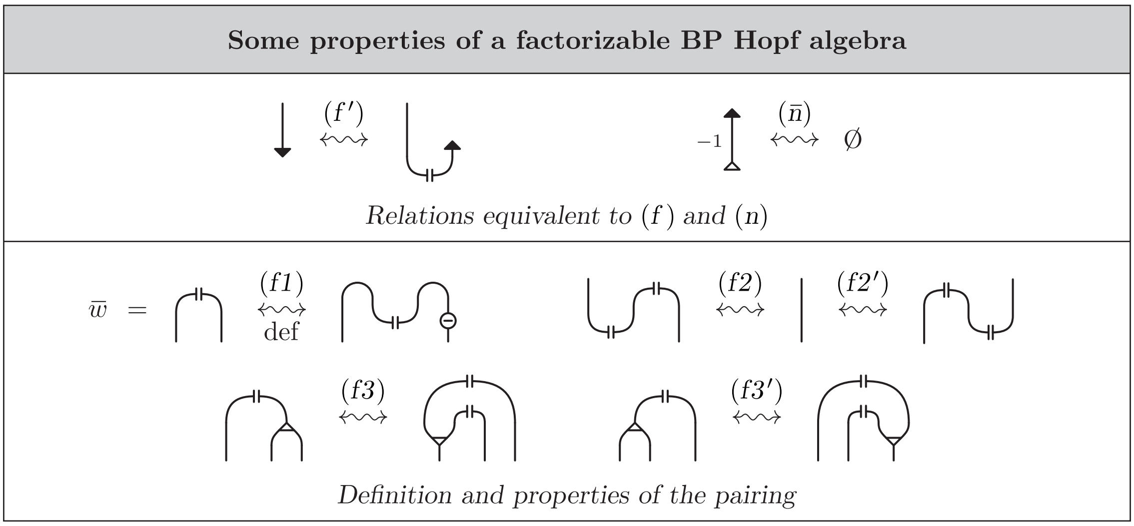

Table 2.6.2

Definition 2.6.2. We denote by 3Alg the strict braided monoidal category freely generated by an anomaly-free factorizable BP Hopf algebra H. In other words, 3Alg is the quotient of 4Alg by relations (f) and (n).

Definition 2.6.3. Let $\mathscr{C}$ be a braided monoidal category with tensor product $\otimes$, tensor unit $\mathbb{1}$, and braiding c. A *Habiro Hopf algebra* is a Hopf algebra H in $\mathscr{C}$ with braided cocommutative left adjoint action, equipped with the following structure morphisms:

- a *copairing* $w : \mathbb{1} \to H \otimes H$ and a pairing $\overline{w} : H \otimes H \to \mathbb{1}$;
- a *ribbon element* $v_+ : \mathbb{1} \to H$ and its multiplicative inverse $v_- : \mathbb{1} \to H$.

These structure morphisms are subject to the following axioms:

$$\mu \circ (v_+ \otimes \mathrm{id}) = \mu \circ (\mathrm{id} \otimes v_+), \tag{h1}$$
$$\mu \circ (v_+ \otimes v_-) = \eta, \tag{h2}$$
$$\varepsilon \circ v_+ = \mathrm{id}_{\mathbb{1}}, \tag{h3}$$
$$S \circ v_+ = v_+, \tag{h4}$$
$$w = (\mu \otimes \mu) \circ (v_- \otimes \mathrm{id}_2 \otimes v_-) \circ \Delta \circ v_+, \tag{h5}$$
$$(\mathrm{id} \otimes \Delta) \circ w = (\mu \otimes \mathrm{id}_2) \circ (\mathrm{id} \otimes w \otimes \mathrm{id}) \circ w, \tag{h6}$$
$$(\mathrm{id} \otimes \overline{w}) \circ (w \otimes \mathrm{id}) = \mathrm{id} = (\overline{w} \otimes \mathrm{id}) \circ (\mathrm{id} \otimes w), \tag{h7-7′}$$
$$\overline{w} \circ (\mu \otimes v_+) \circ (v_+ \otimes v_+) = \mathrm{id}_{\mathbb{1}}, \tag{h8}$$
$$S^2 = (\mathrm{id} \otimes \overline{w}) \circ (c \otimes \mathrm{id}) \circ (\mathrm{id} \otimes w). \tag{h9}$$

We denote by $3\mathrm{Alg}^{\mathrm{H}}$ the strict braided monoidal category freely generated by a Habiro Hopf algebra H.

A diagrammatic representation of the generators and the axioms of a Habiro Hopf algebra can be found in Table 2.6.3. Notice that the notation adopted for all structure morphisms, with the exception of the ribbon elements, is the same as the one used for the analogous structure morphisms of BP Hopf algebras in Tables 2.4.1 and 2.6.1. This should not cause any confusion since, as we will see below, the functor from $3\mathrm{Alg}^{\mathrm{H}}$ to 3Alg matches the corresponding structure morphisms.

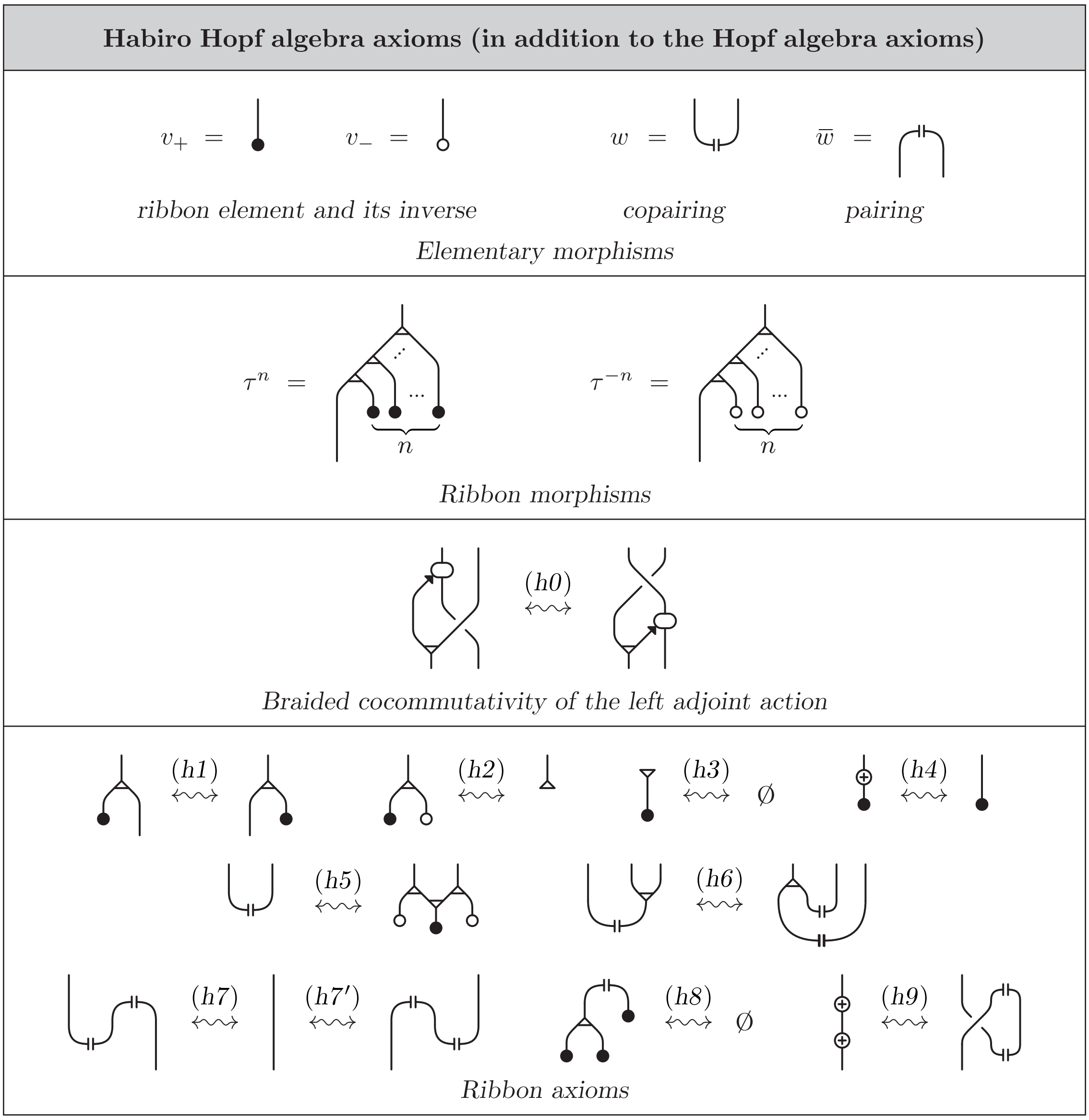

TABLE 2.6.3

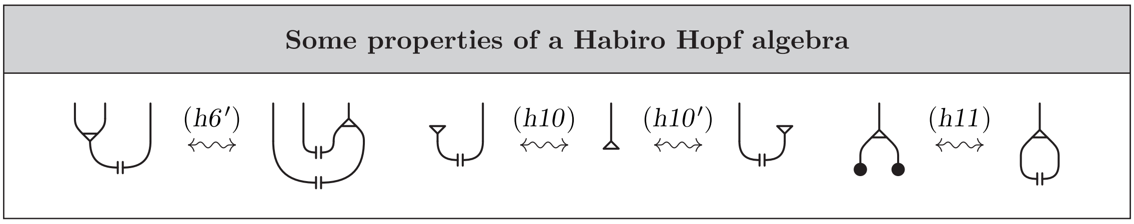

TABLE 2.6.4

LEMMA 2.6.4. *The ribbon morphisms of* $3\mathrm{Alg}^{\mathrm{H}}$*, defined in Table 2.6.3, satisfy the ribbon axioms* (*r1*) *to* (*r5*) *of a BP Hopf algebra in Table 2.4.1. Moreover, the relations in Table 2.4.4 are satisfied in* $3\mathrm{Alg}^{\mathrm{H}}$.

Proof. The fact that the ribbon morphism of $3\mathrm{Alg}^{\mathrm{H}}$ satisfy axioms (*r1*) to (*r5*) in Table 2.4.1 is a straightforward consequence of axioms (*h1*) to (*h4*) and the associativity of the product. Moreover, axiom (*h5*) and (*h6*) are equal correspondingly to (*r6*) and (*r7*). Therefore, relations (*r1*) to (*r7*) are satisfied in $3\mathrm{Alg}^{\mathrm{H}}$. According to Proposition 2.4.5, this implies that the relations in Table 2.4.4 hold in $3\mathrm{Alg}^{\mathrm{H}}$. □

Remark 2.6.5. The set of axioms of a Habiro Hopf algebra, as originally presented in [As11], contains also the relations in Table 2.6.4. Proposition 2.6.4 implies that those relations are actually consequences of the axioms in Table 2.6.3. Indeed, (*h6′*) is equal to (*r7′*), (*h10-10′*) are equal to (*p2-2′*) while (*h11*) is obtained by composing (*p8*) with the unit morphism.

Proposition 2.6.6. *There exists a braided monoidal functor* $\Gamma : 3\mathrm{Alg}^{\mathrm{H}} \to 3\mathrm{Alg}$ *which preserves the Hopf algebra structure morphisms, sends the pairing and the copairing in* $3\mathrm{Alg}^{\mathrm{H}}$ *to the corresponding ones in* $3\mathrm{Alg}$ *(see Table 2.6.1) and sends the ribbon elements to the morphisms represented in Figure 2.6.5, meaning*

$$\Gamma(v_+) = \tau^{-1} \circ \eta \quad \text{and} \quad \Gamma(v_-) = \tau \circ \eta.$$

Figure 2.6.5. Images under $\Gamma : 3\mathrm{Alg}^{\mathrm{H}} \to 3\mathrm{Alg}$ of the ribbon element and its inverse.

Proof. Since $3\mathrm{Alg}$ and $3\mathrm{Alg}^{\mathrm{H}}$ are both braided Hopf algebras with braided cocommutative left actions (see Proposition 2.5.2), it is enough to show that the defining ribbon axioms of $3\mathrm{Alg}^{\mathrm{H}}$ in Table 2.6.3 are satisfied in $3\mathrm{Alg}$, once each elementary morphism has been replaced by its image under Γ. All of them, with the exception of (*h8*) and (*h9*), coincide or follow directly from axioms or properties of $3\mathrm{Alg}$ in Tables 2.4.1, 2.4.4 and 2.6.1. The proofs of (*h8*) and (*h9*) are presented in Figures 2.6.6 and 2.6.7. □

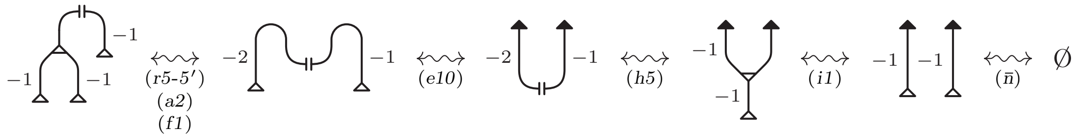

Figure 2.6.6. Proof of (*h8*).

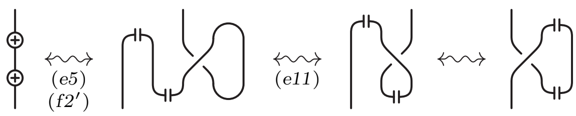

Figure 2.6.7. Proof of (*h9*).

In order to prove that Γ is an equivalence of categories, we need some preliminary results.

Lemma 2.6.7. *Identities* (*d10*) *and* (*d11-11′*) *in Table 2.3.7 hold in* $3\mathrm{Alg}^{\mathrm{H}}$. *In particular, the left adjoint action intertwines all morphisms in* $3\mathrm{Alg}^{\mathrm{H}}$.

Proof. Since the left adjoint action in $3\mathrm{Alg}^{\mathrm{H}}$ is braided cocommutative, Lemma 2.3.4 implies that (*d10*) for $F = c, \mu, \eta, \Delta, \varepsilon, S$ and (*d11-11′*) hold in $3\mathrm{Alg}^{\mathrm{H}}$. On the other hand, (*d10*) for $v_\pm$ follows directly from axioms (*h1*), (*h2*) and (*a3*). Moreover axiom (*h5*) implies that (*d10*) for $F = w$ follows from (*d10*) for $v_\pm$, Δ, and μ. Finally, as it is shown in Figure 2.6.8, (*d10*) for $F = \overline{w}$ follows from (*d10*) for w and axioms (*h7-7′*). □

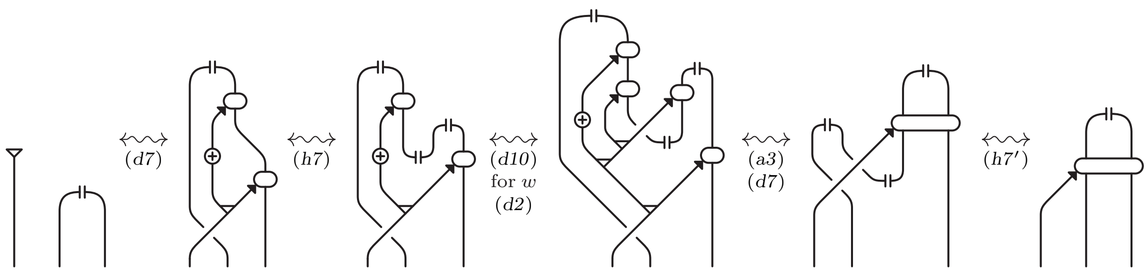

Figure 2.6.8. Proof of (*d10*) for $\overline{w}$.

LEMMA 2.6.8. *Identities (d12), (d13), (d15) and (d16) in Table 2.5.3 are satisfied in* $3\mathrm{Alg}^{\mathrm{H}}$.

Proof. The proofs of (*d12*) and (*d13*) are presented in Figures 2.6.9 and 2.6.10, while (*d15*) and (*d16*) follow from (*d10*) and (*d12*) as it is shown in Figure 2.5.8 (see Remark 2.5.4). □

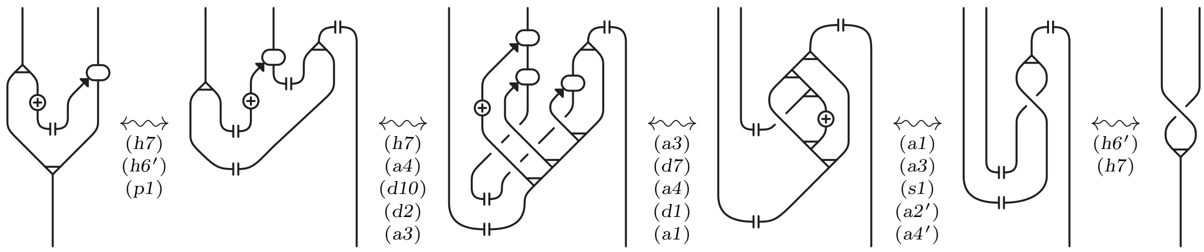

FIGURE 2.6.9. Proof of (*d12*) in $3\mathrm{Alg}^{\mathrm{H}}$.

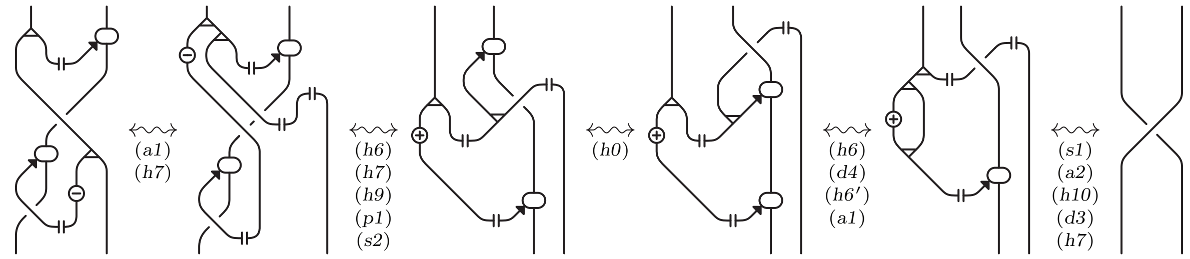

FIGURE 2.6.10. Proof of (*d13*) in $3\mathrm{Alg}^{\mathrm{H}}$.

Recall that 4Alg, and hence 3Alg, are ribbon categories whose evaluation and coevaluation are constructed using the integral form and element. Our next goal will be to show that $3\mathrm{Alg}^{\mathrm{H}}$ admits another ribbon structure, with evaluation and coevaluation given by the Hopf pairing and copairing. We will use the notation $H^\vee$ for the dual of H with respect to the Hopf pairing.

PROPOSITION 2.6.9. $3\mathrm{Alg}^{\mathrm{H}}$ *is a ribbon category (see Definition 2.1.3), with dual* $(H^n)^\vee = H^n$ *for every* $n \geqslant 0$*, and with two-sided evaluation* $\overline{w}_{H^n} : H^n \otimes H^n \to \mathbb{1}$ *and coevaluation* $w_{H^n} : \mathbb{1} \to H^n \otimes H^n$ *inductively defined by* $\overline{w}_0 = \overline{w}_{\mathbb{1}} = w_0 = w_{\mathbb{1}} = \mathrm{id}_{\mathbb{1}}$,

$$\overline{w}_1 = \overline{w}_H = \overline{w},$$
$$w_1 = w_H = w,$$

and by

$$\overline{w}_n = \overline{w}_{H^n} = \overline{w} \circ (\mathrm{id} \otimes \overline{w}_{n-1} \otimes \mathrm{id}),$$
$$w_n = w_{H^n} = (\mathrm{id} \otimes w_{n-1} \otimes \mathrm{id}) \circ w,$$

for every $n > 1$*. The twist* $\vartheta_{H^n} : H^n \to H^n$ *is defined for every* $n \geqslant 0$ *by*

$$\vartheta_n = \vartheta_{H^n} = (\overline{w}_n \otimes \mathrm{id}_n) \circ (\mathrm{id}_n \otimes c_{n,n}) \circ (w_n \otimes \mathrm{id}_n).$$

Moreover, in $3\mathrm{Alg}^{\mathrm{H}}$ *we have*

$$\mu^\vee = \Delta, \quad \eta^\vee = \varepsilon, \quad S^\vee = S, \quad w^\vee = \overline{w}.$$

Proof. The statement concerning the ribbon structure follows from relations (*h7-7′*) and (*h9*) in Table 2.6.3, together with the fact that $S^\vee = S$. Indeed, $S^\vee = (\mathrm{id} \otimes \overline{w}) \circ (\mathrm{id} \otimes S \otimes \mathrm{id}) \circ (w \otimes \mathrm{id})$ is equal to S due to (*p1*) in Table 2.4.4 and (*h7*). The identities concerning the rest of the dual morphisms follow directly from relations (*h6-6′*) and (*h7-7′*) in Table 2.6.3 and (*h10-10′*) in Table 2.6.4. □

Proposition 2.6.9 implies that, if a morphism F is a composition of tensor products of structure morphisms, other than the ribbon elements, then the diagram representing $F^\vee$ is obtained from the diagram representing F by rotating it of an angle π. Moreover, by dualizing each side of a given relation between morphisms of $3\mathrm{Alg}^{\mathrm{H}}$, we obtain another relation between the corresponding dual morphisms, to which we will refer as the *dual* relation, or property. For example, the dual of relation (*p1*) states that $\overline{w} \circ (S \otimes \mathrm{id}) = \overline{w} \circ (\mathrm{id} \otimes S)$, and we will refer to it as ($p1^\vee$).

The following result is due to Habiro.

PROPOSITION 2.6.10 (Habiro). *In* $3\mathrm{Alg}^{\mathrm{H}}$, *the morphisms* $\lambda = \overline{w} \circ (\mu \otimes \mathrm{id}) \circ (\mathrm{id} \otimes v_+ \otimes v_+)$ *and* $\Lambda = \lambda^\vee$ *are S-invariant integral form and integral element satisfying relations* (*i1*) *to* (*i5*) *in Table* 2.4.1.

Integrals for a Habiro Hopf algebra

TABLE 2.6.11

Proof. Observe that axioms (*h1*) and (*h4*) and relations (*s4*) and ($p1^\vee$) imply that the integral form is S-invariant, meaning that $\lambda \circ S = \lambda$. Therefore, if we show that λ is a right integral form, meaning that it satisfies relations (*i1*) and (*i5*), then, by considering the dual relation, we would get that $\Lambda = \lambda^\vee$ is an S-invariant integral element.

The proof that λ is a right integral form is shown in Figures 2.6.12 and 2.6.13. Finally, the relation $\lambda \circ \Lambda = \mathrm{id}_{\mathbb{1}}$ is proved in Figure 2.6.14. ☐

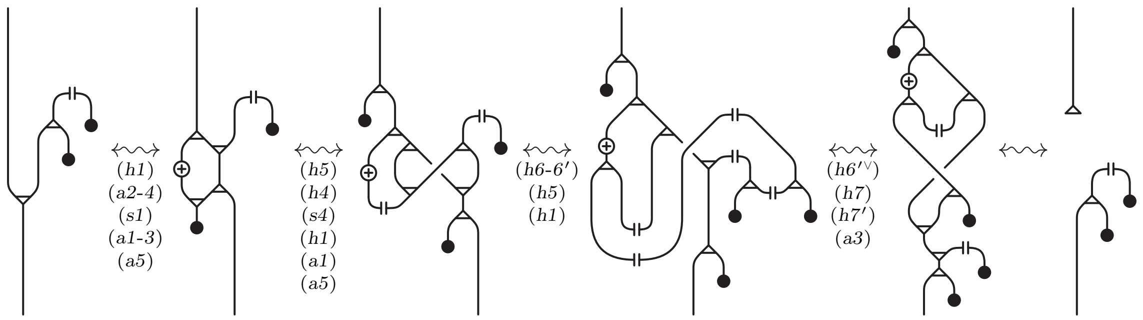

FIGURE 2.6.12. Proof of (*i1*) in $3\mathrm{Alg}^{\mathrm{H}}$ (see Figure 2.6.13 for the last step).

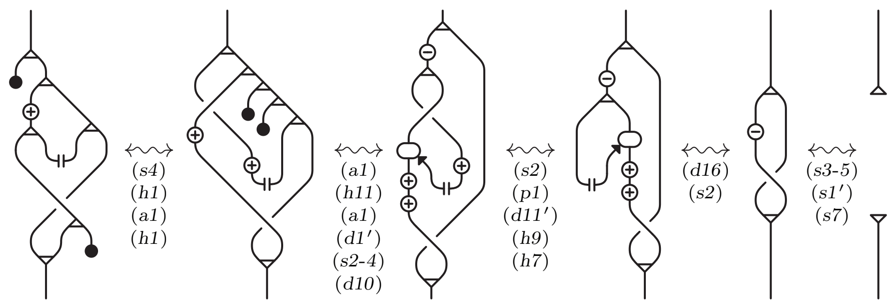

FIGURE 2.6.13. Last step in the proof of (*i1*) in $3\mathrm{Alg}^{\mathrm{H}}$.

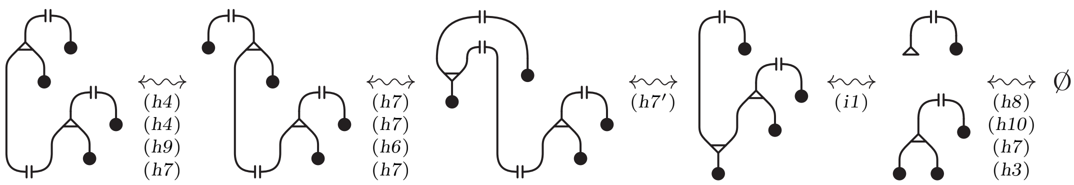

FIGURE 2.6.14. Proof of (*i3*) in $3\mathrm{Alg}^{\mathrm{H}}$, that is, $\lambda \circ \Lambda = \mathrm{id}_{\mathbb{1}}$.

Theorem 2.6.11. *The braided monoidal functor* $\Gamma : 3\mathrm{Alg}^{\mathrm{H}} \to 3\mathrm{Alg}$ *is an equivalence of categories.*

Proof. We recall that, modulo the other axioms of 4Alg, (*r8*) and (*r9*) are equivalent to (*d12*) and (*d13*) in Table 2.5.3, respectively. Therefore, the quotient 3Alg is equivalent to the category freely generated by the elementary morphisms and relations presented in Tables 2.2.1, 2.4.1 and 2.6.1, where axioms (*r8*) and (*r9*) have been replaced by (*d12*) and (*d13*) in Table 2.5.3.

We define now a braided monoidal functor $\bar{\Gamma} : 3\mathrm{Alg} \to 3\mathrm{Alg}^{\mathrm{H}}$ by sending all elementary morphisms of 3Alg to the corresponding morphisms of $3\mathrm{Alg}^{\mathrm{H}}$. In order to see that the functor is well defined we have to check that all axioms of 3Alg are satisfied in its image. For the integral axioms and for relations (*d12*) and (*d13*) this follows correspondingly from Proposition 2.6.10 and from Lemma 2.6.8. The ribbon axioms (*r1*) to (*r7*) are equivalent to (*h1*) to (*h6*), while axiom (*n*) in Table 2.6.1 follows from (*h2*), (*h3*) and (*h10*). Now it is left to observe that $\bar{\Gamma} \circ \Gamma = \mathrm{id}_{3\mathrm{Alg}^{\mathrm{H}}}$ and $\Gamma \circ \bar{\Gamma} = \mathrm{id}_{3\mathrm{Alg}}$. □

Let us finish this subsection by introducing yet another equivalent presentation of 3Alg. More precisely, we will show that, by adding the braided cocommutativity relation for the adjoint action to Kerler's original list of axioms, we obtain a category that is equivalent to 3Alg.

Definition 2.6.12. Let $\mathscr{C}$ be a braided monoidal category with tensor product $\otimes$, tensor unit $\mathbb{1}$, and braiding c. A *Kerler Hopf algebra* is a Hopf algebra H in $\mathscr{C}$ with braided cocommutative left adjoint action, equipped with the following structure morphisms:

- ⋄ an *integral form* $\lambda : H \to \mathbb{1}$ and an *integral element* $\Lambda : \mathbb{1} \to H$;
- ⋄ a *copairing* $w : \mathbb{1} \to H \otimes H$;
- ⋄ a *ribbon element* $v_+ : \mathbb{1} \to H$ and its multiplicative inverse $v_- : \mathbb{1} \to H$.

These structure morphisms are subject to the following axioms:

$$(\mathrm{id} \otimes \lambda) \circ \Delta = \eta \circ \lambda, \tag{$i1$}$$
$$\mu \circ (\Lambda \otimes \mathrm{id}) = \Lambda \circ \varepsilon, \tag{$i2$}$$
$$\lambda \circ \Lambda = \mathrm{id}_{\mathbb{1}}, \tag{$i3$}$$
$$S \circ \Lambda = \Lambda, \tag{$i4$}$$
$$\lambda \circ S = \lambda, \tag{$i5$}$$
$$\mu \circ (v_+ \otimes \mathrm{id}) = \mu \circ (\mathrm{id} \otimes v_+), \tag{$h1$}$$
$$\mu \circ (v_+ \otimes v_-) = \eta, \tag{$h2$}$$
$$\varepsilon \circ v_+ = \mathrm{id}_{\mathbb{1}}, \tag{$h3$}$$
$$S \circ v_+ = v_+, \tag{$h4$}$$
$$w = (\mu \otimes \mu) \circ (v_- \otimes \mathrm{id}_2 \otimes v_-) \circ \Delta \circ v_+, \tag{$h5$}$$
$$(\mathrm{id} \otimes \Delta) \circ w = (\mu \otimes \mathrm{id}_2) \circ (\mathrm{id} \otimes w \otimes \mathrm{id}) \circ w, \tag{$h6$}$$
$$(\lambda \otimes \mathrm{id}) \circ w = \Lambda, \tag{f}$$
$$\lambda \circ v_+ = \mathrm{id}_{\mathbb{1}}. \tag{n}$$

We denote by $3\mathrm{Alg}^{\mathrm{K}}$ the strict braided monoidal category freely generated by a Kerler Hopf algebra H.

A diagrammatic representation of the generators and the axioms of a Kerler Hopf algebra are presented in Table 2.6.15.

Corollary 2.6.13. *There exists a braided monoidal equivalence between the categories* $3\mathrm{Alg}^{\mathrm{K}}$ *and* $3\mathrm{Alg}^{\mathrm{H}}$ *that preserves the corresponding Hopf algebra structures.*

Proof. By definition, the Hopf algebra in $3\mathrm{Alg}^{\mathrm{K}}$ has S-invariant integral form and element. Moreover, the copairing and the ribbon morphisms defined in Table 2.6.15 satisfy axioms (*r1*)–(*r7*) in Table 2.4.1. This implies that sym induces a well defined equivalence functor from $3\mathrm{Alg}^{\mathrm{K}}$ to itself, and that, according to Propositions 2.4.5, 2.4.6, and 2.4.7, the properties in Tables 2.4.3, 2.4.4, and 2.4.5 hold in $3\mathrm{Alg}^{\mathrm{K}}$. In particular, we can define evaluation and coevaluation morphisms by relations (*e1*-*2*) in Table 2.4.3 and a pairing by the expansion (*f1*) in Table 2.6.2. Moreover, we can see that relations (*h7*-*7′*), (*h8*) and (*h9*) in Table 2.6.3 and ($\bar{n}$) in Table 2.6.2 hold in $3\mathrm{Alg}^{\mathrm{K}}$ as well. Indeed, the proofs of (*h7*), (*h8*), (*h9*), and ($\bar{n}$), which are presented in Figures B.4.1, 2.6.6, 2.6.7, and B.4.2, respectively, use only axioms and

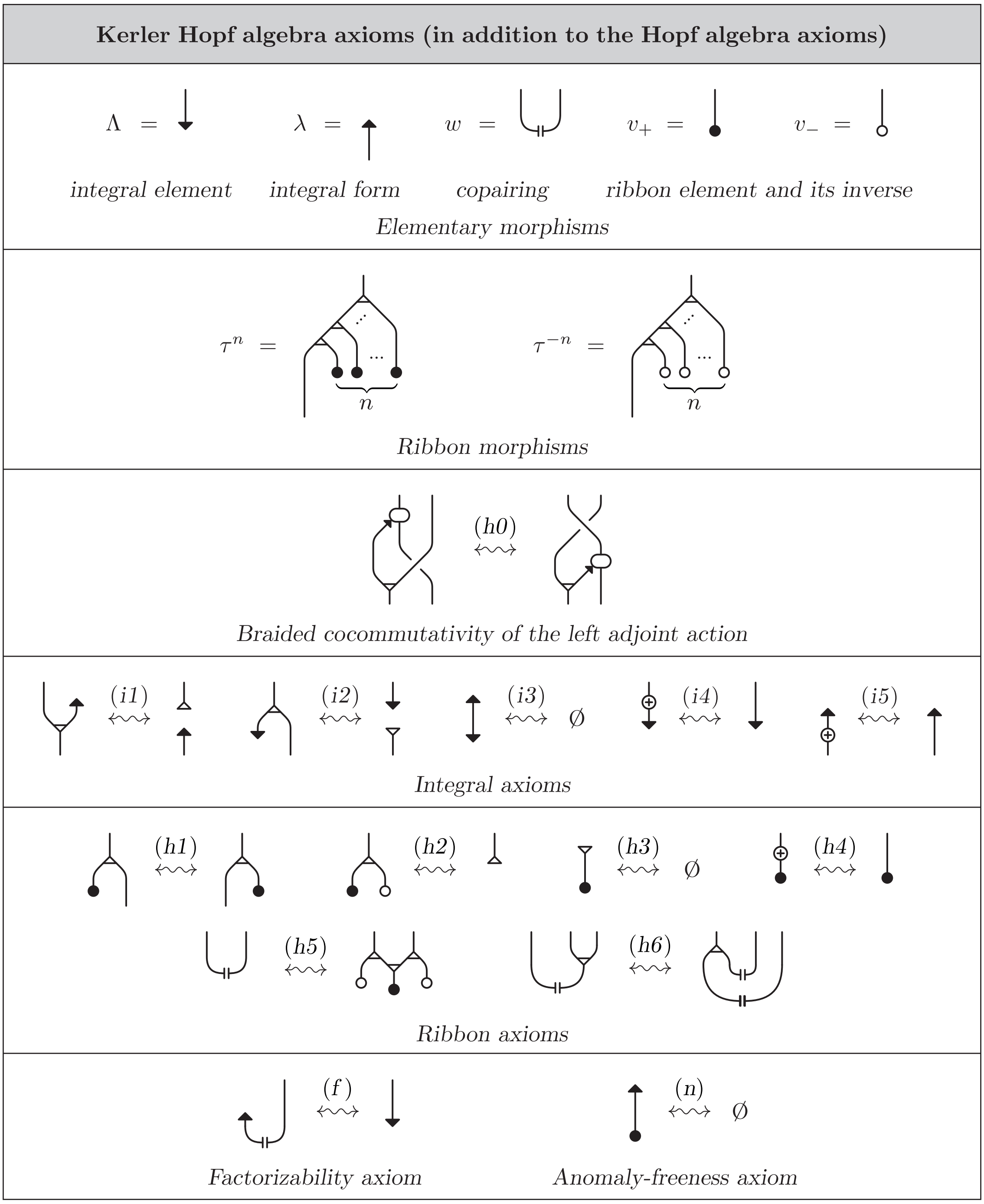

TABLE 2.6.15

relations which are satisfied in $3\mathrm{Alg}^{\mathrm{K}}$, while $(h7')$ follows by symmetry. Therefore, there exists a well-defined braided monoidal functor from $3\mathrm{Alg}^{\mathrm{H}}$ to $3\mathrm{Alg}^{\mathrm{K}}$ sending the elementary morphisms of $3\mathrm{Alg}^{\mathrm{H}}$ to the corresponding morphisms of $3\mathrm{Alg}^{\mathrm{K}}$.

The inverse functor from $3\mathrm{Alg}^{\mathrm{K}}$ to $3\mathrm{Alg}^{\mathrm{H}}$ is defined by sending the integral form and element in $3\mathrm{Alg}^{\mathrm{K}}$ to the ones shown in Table 2.6.11 in $3\mathrm{Alg}^{\mathrm{H}}$. Then the only non trivial relations to be checked are the integral relations, which are satisfied by Proposition 2.6.10. □

Notice that, in his original definition [Ke01], Kerler used the non-degeneracy of the copairing instead of the integral axioms, but he also showed that these axioms are interchangeable.

3. Topological categories

3.1. The category KT of Kirby tangles

Our main object of interest will be the category of oriented 4-dimensional relative 2-handlebodies (see Subsection 3.2) modulo 2-equivalence, which is an equivalence relation generated by slides and cancellations of 1-handles and 2-handles. Following [Ki89, GS99, BP11], morphisms in this category will be described in terms of a particular class of tangles, called admissible Kirby tangles (compare with Definition 3.3.3 below), considered up to 2-deformations, which implement the above handle moves. In this section, we will discuss the general notion of Kirby tangle, which will be further restricted in Subsection 3.3 to the notion of admissible Kirby tangle, in order to represent 4-dimensional 2-handlebodies.

We start by fixing the following notation. For any integer $k \geqslant 0$, we set

$$E_k := \{e_{k,1}, e_{k,2}, \ldots, e_{k,k}\} \subset [0,1]^2,$$

with the k points $e_{k,i}$ uniformly distributed along $]0,1[\times \{1/2\}$. In particular, $E_0 = \varnothing$.

Definition 3.1.1. Given two integers $k, \ell \geqslant 0$ such that $k+\ell$ is even, a *Kirby tangle* from E_k to E_ℓ consists of the following data:

(a) a collection of $m \geqslant 0$ dotted unknots $U_1, U_2, \ldots, U_m$, together with disjoint flat spanning disks $D_1, D_2, \ldots, D_m$ embedded into $]0,1[^3$;

(b) an undotted tangle properly and smoothly embedded into $[0,1]^3$, which is transversal to the spanning disks, and which consists of a link $L = L_1 \cup L_2 \cup \cdots \cup L_n$ formed by $n \geqslant 0$ closed components, and of $(k+\ell)/2$ arcs whose endpoints belong to $(E_k \times \{0\}) \cup (E_\ell \times \{1\})$, all endowed with the blackboard framing with respect to the projection $[0,1]^3 \to [0,1]^2$ that forgets the second coordinate.

Definition 3.1.2. Two Kirby tangles are said to be 2-*equivalent* if they are related by a finite sequence of the following operations, called 2-*deformations*:

(a) performing an ambient isotopy of the tangle in $[0,1]^3$ that fixes the boundary and preserves the intersections between the disks spanned by the dotted unknots and the undotted components;

(b) pushing an arc of any undotted (possibly open) component C through the disk D spanned by any dotted unknot U in such a way that two opposite transversal intersection points between C and D appear/disappear;

(c) adding/deleting a dotted unknot U and an undotted closed component C such that the disk D spanned by U is pierced only once by C and by no other undotted component;

(d) sliding any (possibly open) undotted component C over any different closed one C', that is, replacing C by a (blackboard parallel) band connected sum of itself with a parallel copy of C'.

Next, 2-equivalence classes of Kirby tangles can be organized as the morphisms of a strict monoidal category, as specified by the following definition.

Definition 3.1.3. We denote by KT the strict monoidal category whose objects are the sets E_k for $k \geqslant 0$, and whose morphisms from E_k to E_ℓ are 2-equivalence classes of Kirby tangles from E_k to E_ℓ.

The composition $T' \circ T$ of two morphisms $T : E_k \to E_\ell$ and $T' : E_{k'} \to E_{\ell'}$ with $\ell = k'$ is given by vertical juxtaposition, with T' on top of T, and by rescaling the third coordinate of a factor $1/2$.

The tensor product, denoted $\sqcup$, is given by horizontal juxtaposition, followed by a suitable reparameterization of the first coordinate, in such a way that

$$E_k \sqcup E_{k'} = E_{k+k'}$$

on the level of objects. For the tensor product of two morphisms $T : E_k \to E_\ell$ and $T' : E_{k'} \to E_{\ell'}$, the reparameterization of the first coordinate depends on the third one, in order to simultaneously realize the above equality at both the source and the target level, and to get in this way a Kirby tangle from $E_{k+k'}$ to $E_{\ell+\ell'}$ representing $T \sqcup T'$.

For each $k \geqslant 0$, the identity id_{E_k} is represented by the product $E_k \times [0,1]$, interpreted as a Kirby tangle consisting of k undotted arcs. In particular, the empty Kirby tangle represents $\mathrm{id}_{\mathbb{1}}$, since $\mathbb{1} = E_0 = \varnothing$.

Kirby tangles live in $]0,1[^2 \times [0,1]$ and will be always represented through their planar diagrams by the projection to the square $]0,1[\times [0,1]$ that forgets the second coordinate, in such a way that the factor $]0,1[^2$ projects to $]0,1[$. As usual, we require that the restriction of the projection to the tangle, including both dotted and undotted components, is regular, and that it is injective except for a finite number of transversal double points, which give rise to crossings. We will use the same letter to denote both a Kirby tangle and its plane projection.

In the following, we will need to consider particular planar diagrams of Kirby tangles whose projection satisfies an extra regularity property, as specified by the next definition.

Definition 3.1.4. Given a Kirby tangle T as in Definition 3.1.1, we say a planar diagram of T is *strictly regular* if the disks $D_1, \dots, D_m$ spanned by the dotted unknots project bijectively onto disjoint planar disks, and if the projection of the undotted tangle intersects each of such disks as presented on the top right figure in Table 3.1.1.

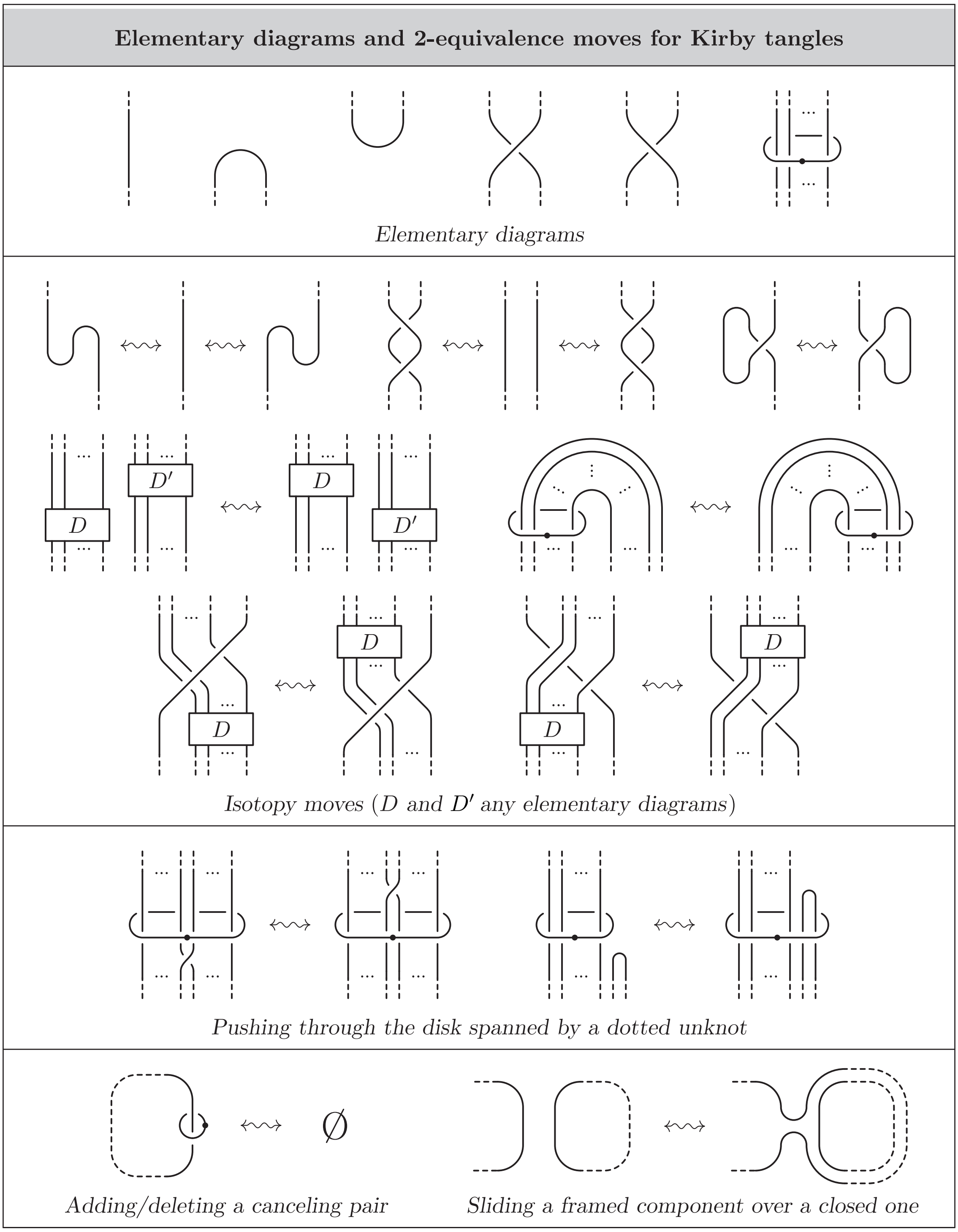

Table 3.1.1

All the planar diagrams we have drawn until now are strictly regular, but using strictly regular diagrams to represent admissible Kirby tangles sometimes makes pictures quite heavy. In the following, when this will not cause confusion, we will often draw planar diagrams that are not strictly regular. However, we will always keep the condition that the disks $D_1, \dots, D_m$ project bijectively onto disjoint planar disks.

The next proposition provides a presentation of the monoidal category KT in terms of the generators and relations represented in Table 3.1.1. Here, the isotopy moves correspond to those ambient isotopies of Kirby tangles in $[0,1]^3$ that preserve the intersections between the undotted components and the disks spanned by the dotted unknots in the standard form shown as the rightmost elementary diagram, while the pushing-through moves are needed to relax this last condition. On the other hand, the diagram operations on the bottom correspond to operations (c) and (d) in Definition 3.1.2.

Proposition 3.1.5. *Up to ambient isotopy in* $[0,1]^3$*, any Kirby tangle* $T \in \mathrm{KT}$ *can be expressed as a composition of tensor products of the elementary diagrams in Table 3.1.1 that yields a strictly regular planar diagram of* T*. Moreover, any two strictly regular planar diagrams expressed in this way represent* 2*-equivalent Kirby tangles if and only if, up to planar isotopy preserving the expression as composition of tensor products, they are related by a finite sequence of the isotopy moves and the diagram operations in the same Table 3.1.1.*

Proof. The first part of the statement concerning generators immediately follows from a standard transversality argument. On the other hand, all the moves and operations in Table 3.1.1 clearly represent 2-deformations of Kirby tangles, so we only need to prove that they are sufficient to realize any 2-equivalence. Since operations (c) and (d) in Definition 3.1.2 correspond to the last two moves in Table 3.1.1, we are left to prove that the remaining moves in that table can generate any isotopy of Kirby tangles.

Modulo the pushing-through moves in Table 3.1.1, we can assume that, during the isotopy, the disks spanned by the dotted unknots are rigidly moved in space, and that the intersections between the disks spanned by the dotted unknots and the undotted components are preserved, as in point (a) of Definition 3.1.2. Actually, this would require also the move where a cup is pushed through the disk spanned by a dotted unknot from above, but up to the isotopy moves this is equivalent to the second pushing-through move in Table 3.1.1, where a cap is pushed through that disk from below.

Furthermore, modulo the isotopy move where a dotted component passes from one side of a multiple cap to the other, we can also assume that, at the end of the isotopy, each disk spanned by a dotted unknot is sent into its image in such a way that the orientation induced by the plane projection of the diagram is preserved.

These assumptions allow us to consider the last elementary diagram in Table 3.1.1 as a coupon with the same number of incoming and outgoing edges, and hence to apply [Tu94, Chapter I, Lemma 3.4]. Then, it is enough to observe that the relations in that lemma can be generated by the moves in Table 3.1.1. ☐

We conclude this subsection with a simple proposition, which reduces the slide operation in Table 3.1.1 to a special case. This will be useful to prove our main theorem.

Proposition 3.1.6. *In a Kirby tangle, any slide of a (possibly open) undotted component over a closed one can be realized, up to isotopy and addition/deletion of canceling pairs, by a sequence of slides over undotted components that form at most one self-crossing, and hence are unknots with framing* 0 *or* ± 1.

Proof. Consider a slide over a closed undotted component C, and proceed by induction on the number $c \geqslant 0$ of self-crossings of C. If $c \leqslant 1$, there is nothing to prove. So assume $c > 1$, and look at any self-crossing of C. Here, we modify the diagram as indicated in Figure 3.1.2. The original diagram on the left-hand side can be obtained from the one on the right-hand side by sliding C', first over C'' and then over C''', and by deleting in sequence two canceling $1/2$-pairs. Since both C'' and C''' have less than c self-crossings, we can realize the slides over them by using the inductive hypothesis. To complete the

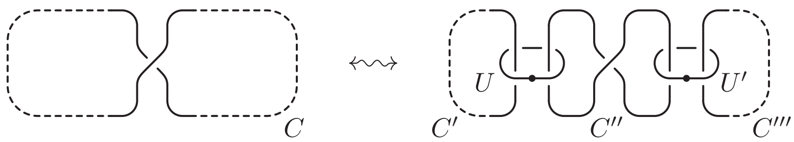

Figure 3.1.2. Proof of Proposition 3.1.6.

proof, it is enough to observe that, up to the modification in the figure, a slide over C is the same as a sequence of slides over C', C'', and C''', and hence we can use the inductive hypothesis once again, since also C' has less than c self-crossing. $\square$

3.2. 4-dimensional relative 2-handlebodies

We review now the notion of an oriented 4-dimensional relative 2-handlebody built over a connected 3-manifold with (possibly empty) boundary. For the basic definitions about handle decompositions we refer to [GS99], while a detailed discussion of the specific topic mentioned above can be found in [BP11, Subsections 2.1 & 2.2], where the notion is actually considered in the more general context of multiple 0-handles.

Definition 3.2.1. Given a compact connected oriented 3-manifold M with (possibly empty) boundary, an oriented 4-dimensional *relative 2-handlebody* built on M is an oriented smooth 4-manifold with a given handle decomposition

$$W = W_0 \cup_{i=1}^m H_i^1 \cup_{j=1}^n H_j^2,$$

where $W_0 = M \times [0,1] \subset W$ is a smooth collar of $M \times \{0\}$ with product orientation, $W_1 = W_0 \cup_{i=1}^m H_i^1 \subset W$ is a smooth submanifold obtained by attaching the 1-handles $H_i^1 = B^1 \times B^3$ to the interior of the *front boundary* $\partial_+ W_0 = M \times \{1\}$, and finally $W = W_1 \cup_{j=1}^n H_j^2$ is obtained by attaching the 2-handles $H_j^2 = B^2 \times B^2$ to the interior of the *front boundary* $\partial_+ W_1 = \partial W_1 \smallsetminus \partial\big(M \times [0,1[\big)$.

By identifying M with $M \times \{0\} \subset W$, we think of it as a smooth submanifold of ∂W, and we call the family of handles forming W starting from $M \times [0,1]$ a *relative 2-handlebody decomposition* of the pair (W, M).

We remark that this definition reduces to the standard one when M is a closed 3-manifold (compare with [GS99, Definition 4.2.1]). In particular, for $M \cong S^3$, we can fill $S^3 \cong S^3 \times \{0\}$ with B^4 and get in this way the notion of an (absolute) connected oriented 4-dimensional 2-handlebody, by thinking of B^4 as the starting 0-handle.

For a handlebody decomposition of (W, M) as above, the connectedness of M and the orientability of W imply that there is a unique way to attach the 1-handles, up to ambient isotopy of their attaching balls in $\partial_+ W_0$, which does not change the diffeomophism type of the pair (W, M). On the other hand, the 2-handles can be specified by a framed link in $\partial_+ W_1$, whose jth component uniquely determines up to isotopy an embedding $S^1 \times B^2 \to \partial_+ W_1$ giving the attaching map of a single 2-handle H_j^2, once it is identified with $B^2 \times B^2$. In this case too, an ambient isotopy in $\partial_+ W_1$ of the framed link representing the 2-handles does not affect the diffeomorphism type of (W, M).

Definition 3.2.2. Two oriented 4-dimensional relative 2-handlebodies W and W' built on the same compact connected oriented 3-manifold M are said to be *2-equivalent* if the relative 2-handlebody decompositions of (W, M) and (W', M) are related by a *2-deformation*, meaning a finite sequence of the following operations:
(a) isotoping the attaching maps of the handles;
(b) adding/deleting a canceling pair consisting of a 1-handle and a 2-handle;
(c) sliding a 2-handle over another one.

It is worth noticing that also the operation of sliding a 1-handle over another one is admitted, as it can be obtained from (b) and (c), see for instance [BP11, Figure 2.2.11].

We already observed that the operations of type (a) preserve the diffeomorphism type of the handlebody, and it is easy to see that the same holds for the those of type (b) and (c). Hence, if two oriented 4-dimensional relative 2-handlebodies are 2-equivalent, then they are diffeomorphic.

Viceversa, whether diffeomorphic oriented 4-dimensional relative 2-handlebodies are always 2-equivalent is an open question, which is expected to have negative answer (see [Ki89, Section I.6] and [GS99, Section 5.1]). A list of 4-dimensional 2-handlebodies which are diffeomorphic but conjecturally not 2-equivalent can be found in [Go91].

On the other hand, it is known that homeomophic oriented 4-dimensional relative 2-handlebodies are not necessarily diffeomorphic. See [Ak16, Section 9.1] for examples of such exotic handlebodies.

In the following, we will focus on the special case when $M = M_{s,t} \cong M_s \natural M_t$ is the boundary connected sum of two (absolute) connected oriented 3-dimensional 1-handlebodies

$$M_s \cong H^0 \cup_{i=1}^s H_i^1 \quad \text{and} \quad M_t \cong H^0 \cup_{i=1}^t H_i^1,$$

with $s, t \geqslant 0$. We assume that M_s and M_t are canonically realized inside $\mathbb{R}^3$, by identifying H^0 with $[0,1]^3$ and attaching each 1-handle H^1_i to $]0,1[^2 \times \{1\}$. So, we can set

$$M_{s,t} = (M_s \times \{0\}) \cup ([0,1]^2 \times \{0\} \times [0,1]) \cup (M_t \times \{1\}) \subset \mathbb{R}^4,$$

as depicted on the left-hand side of Figure 3.2.1. Then, we consider a canonical identification

$$M_{s,t} \times [0,1] \cong (M_s \times [0,0.1]) \cup ([0,1]^3 \times [0.1,0.9]) \cup (M_t \times [0.9,1]) \subset \mathbb{R}^4$$

such that $M_{s,t}$ corresponds to $M_{s,t} \times \{0\}$ (see the right-hand side of Figure 3.2.1). Notice that, since $M_{s,t}$ is a subset of $\mathbb{R}^4$, the cylinder $M_{s,t} \times [0,1]$ is defined as a subset of $\mathbb{R}^5$. Under the canonical identification represented on the right-hand side of Figure 3.2.1, the last coordinate of $M_{s,t} \times [0,1]$ can no longer be interpreted as the height in the picture, but rather as a parametrization of the thickness of the cylinder. In particular, $M_{s,t} \times \{0\}$ corresponds to the union of top, back, and bottom face, while $M_{s,t} \times \{1\}$ corresponds to the intersection between the front face and the strip $\mathbb{R}^3 \times [0.1, 0.9]$.

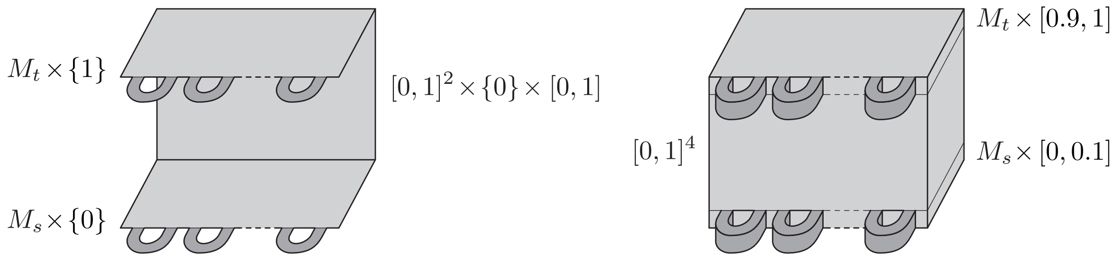

FIGURE 3.2.1. Canonical realization of $M_{s,t}$ and $M_{s,t} \times [0,1]$ in $\mathbb{R}^4$.

We observe that $M_{s,t} \times [0,1]$ consists of $[0,1]^4$ with $s+t$ 4-dimensional 1-handles attached to it, s on the bottom part of the front face $[0,1]^2 \times \{1\} \times [0,1]$ and t on the top part of the same front face (see Figure 3.2.1).

Any 4-dimensional 2-handlebody $W = W_0 \cup_{i=1}^m H^1_i \cup_{j=1}^n H^2_j$ has a Kirby tangle representation, obtained in the following way. Assuming that both of the attaching balls of a 1-handle H^1_i are contained in a local chart $A_i \cong \mathbb{R}^3$ of $\partial_+ W_0$, we can think of H^1_i as the result of removing from W_0 a complementary 2-handle living inside a collar of A_i in W_0, whose attaching map into A_i is determined by a trivially framed unknot $U_i \subset A_i$. A dotted unframed version of the unknot U_i, together with a spanning disk $D_i \subset A_i$ of it, is usually taken to represent H^1_i in the so called dot notation.

Once the dot notation is used for all the 1-handles, with the disks D_i taken to be pairwise disjoint, also the framed link determining the 2-handles can be completely drawn in $\partial_+ W_0$, instead of $\partial_+ W_1$, with each transversal intersection between a framed component and a disk D_i corresponding to a passage of that component through the 1-handle H^1_i. In this way, all the picture is contained in ∂W_0, and isotoping it in ∂W_0 corresponds to isotoping the attaching maps of the handles as said above.

Then, by using the dot notation for such 1-handles, the handlebody structure of any oriented 4-dimensional relative 2-handlebody W built on $M_{s,t}$ can be described by drawing the attaching data of the handles directly on the front face of $[0,1]^4$. In particular, this makes the notion of natural framing (represented by an integer) well-defined.

At this point, by adopting the dot notation also for the 1-handles of W, and by projecting to $[0,1]^2$, we get a Kirby tangle representation of W as in Figure 3.2.2.

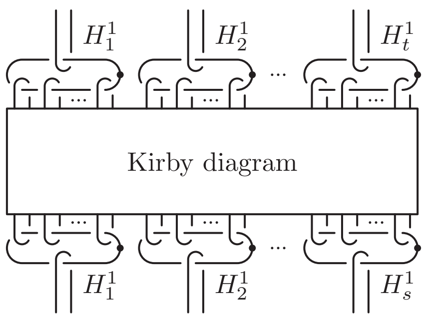

FIGURE 3.2.2. The Kirby tangle of a relative handlebody built on $M_{s,t}$.

Here, each of the open undotted components appearing at the top and bottom stands for "half of a 2-handle" connecting a 1-handle of $M_{s,t} \times [0,1]$, denoted by a dotted unknot as if it were a 1-handle of W, to the corresponding 1-handle of $M_{s,t}$. Moreover, we can assume all the undotted components, including the open ones, are endowed with the blackboard framing, since any framing can be reduced to the blackboard one by adding some positive or negative kinks.

We observe that, in such a Kirby tangle, an operation of type (b) in Definition 3.2.2 can be realized by adding/deleting the dotted and undotted components corresponding to the 1-handle and 2-handle in question, respectively (as in Definition 3.1.2 (c)). On the other hand, an operation of type (c) in the Definition 3.2.2 can be realized by replacing the undotted component representing the 2-handle to be slided by its band connected sum with a parallel copy of the undotted component representing the 2-handle over which the slide is performed (as in Definition 3.1.2 (d)).

3.3. The categories 4HB and 4KT

We start by observing that 2-equivalence classes of oriented 4-dimensional relative 2-handlebodies built over the 3-manifolds $M_{s,t}$ with $s,t \geqslant 0$ form a strict monoidal category 4HB and then we describe the diagrammatic counterpart of such category, namely the monoidal category 4KT, whose morphisms are 2-equivalence classes of admissible Kirby tangles.

Definition 3.3.1. We denote by 4HB the strict monoidal category whose objects are connected oriented 3-dimensional 1-handlebodies M_s for $s \geqslant 0$, and whose morphisms from M_s to M_t are 2-equivalence classes of oriented 4-dimensional relative 2-handlebodies built on $M_{s,t}$ of the form described in Subsection 3.2.

The composition of two morphisms $W = (W, M_{s,t})$ and $W' = (W', M_{s',t'})$ in 4HB with $t = s'$ is obtained by a taking their vertical juxtaposition, with W' on top of W, by gluing the two morphisms (identifying canonically the target of the first with the source of the second), and then by rescaling by a factor $1/2$, that is,

$$W' \circ W \cong (W \cup_{M_t \times \{1\} = M_{s'} \times \{0\}} W', M_{s,t'}),$$

with $M_{s,t'}$ canonically contained in $M_{s,t} \cup_{M_t \times \{1\} = M_{s'} \times \{0\}} M_{s',t'}$, and with handlebody decomposition consisting of all the handles of W and W' plus the 1-handles deriving from the thickening of $M_t = M_{s'}$.

The tensor product, denoted by $\natural$, is given by horizontal juxtaposition, from left to right. For two objects M_s and $M_{s'}$ it corresponds to the boundary connected sum $M_s \natural M_{s'}$, which is canonically identified with $M_{s+s'}$, while for two morphisms $W = (W, M_{s,t})$ and $W' = (W', M_{s',t'})$ it corresponds to the boundary connected sum of pairs, that is,

$$W \natural W' \cong (W \natural W', M_{s,t} \natural M_{s',t'} \cong M_{s+s',t+t'}),$$

with $M_{s+s',t+t'}$ canonically identified to $M_{s,t} \natural M_{s',t'}$, and handlebody decomposition consisting of all the handles of W and W'.

For each $s \geqslant 0$, the identity id_{M_s} is represented by the product $M_s \times [0,1]$ with the natural handlebody decomposition. In particular, $\mathrm{id}_{\mathbb{1}} = M_0 \times [0,1]$, since $\mathbb{1} = M_0$.

Remark 3.3.2. The category 4HB is the skeleton of a category whose objects are arbitrary connected oriented 3-dimensional 1-handlebodies. It is convenient however to restrict our attention to the standard models for objects we are considering here, as this allows us to define a braided monoidal structure on 4HB.

Now, we define admissible Kirby tangles, which are Kirby tangles that actually represent relative 2-handlebodies built on $M_{s,t}$ for $s,t \geqslant 0$, like the one in Figure 3.2.2.

Definition 3.3.3. A Kirby tangle from E_k to E_ℓ as in Definition 3.1.1 is said to be *admissible* if the following properties hold:

(a) both k and ℓ are even, say $k = 2s$ and $\ell = 2t$;
(b) the open components of the undotted tangle consist of s arcs $A_{1,0}, A_{2,0}, \dots, A_{s,0}$ such that the endpoints of $A_{i,0}$ are $(e_{2s,2i-1}, 0)$ and $(e_{2s,2i}, 0)$ in $E_{2s} \times \{0\}$ for each $i = 1, 2, \dots, s$, and t arcs $A_{1,1}, A_{2,1}, \dots, A_{t,1}$ such that the endpoints of $A_{j,1}$ are $(e_{2t,2j-1}, 1)$ and $(e_{2t,2j}, 1)$ in $E_{2t} \times \{1\}$ for each $j = 1, 2, \dots, t$.

In particular, in an admissible Kirby tangle, no undotted arc connects a point at level 0 to one at level 1 (compare with [MP92, KL01]). Two admissible Kirby tangles are 2-equivalent if they are 2-equivalent as Kirby tangles.

PROPOSITION 3.3.4. *2-equivalence classes of admissible Kirby tangles form a category* 4KT *whose objects are the sets* E_{2s} *with* $s \geqslant 0$*, and whose morphisms from* E_{2s} *to* E_{2t} *are 2-equivalence classes of admissible Kirby tangles. The composition in* 4KT *is induced by the one in* KT *(see Definition 3.1.3), while the identity morphism* id_s *of* E_{2s} *is defined inductively as follows:* id_0 *is the empty diagram,* id_1 *is the first diagram in Figure 3.3.1, and* $\mathrm{id}_s = \mathrm{id}_1 \sqcup \mathrm{id}_{s-1}$ *for any* $s > 1$.

4KT *has a braided (strict) monoidal structure whose tensor product is induced by the one of* KT *(see Definition 3.1.3), ans whose tensor unit is* $\mathbb{1} = E_0$*; the braiding isomorphisms* $c_{1,1} = c : E_4 \to E_4$ *and* $c_{1,1}^{-1} = c^{-1} : E_4 \to E_4$ *are presented in Figure 3.3.1, while* $c_{s,s'} : E_{2(s+s')} \to E_{2(s+s')}$ *for* $s + s' > 2$ *are obtained inductively using the relations in Definition 2.1.2 (see Table 2.1.2).*

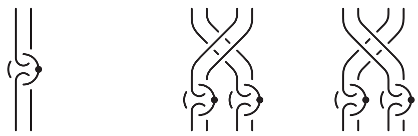

id_1 c c^{-1}

FIGURE 3.3.1. Identity and braiding morphisms in 4KT.

Proof. We only need to show that id_s are indeed identity morphisms. In other words, for any admissible Kirby tangle T from E_{2s} to E_{2t}, both $T \circ \mathrm{id}_s$ and $\mathrm{id}_t \circ T$ are 2-equivalent to T. To see this, it is enough to observe that in $T \circ \mathrm{id}_s$ the upper undotted components of id_s get closed and we can slide the lower open components over the closed ones and then cancel them with the dotted components; a symmetric argument works for the top part of $\mathrm{id}_t \circ T$. □

REMARK 3.3.5. We observe that Kirby tangles which describe oriented 4-dimensional relative 2-handlebodies, as depicted in Figure 3.2.2, are always admissible, and vice-versa, up to 2-equivalence, every admissible Kirby tangle can be arranged in that form, by composing it on the top and on the bottom with identity morphisms.

REMARK 3.3.6. Since 2-equivalence preserves admissibility, morphisms from E_{2s} to E_{2t} in 4KT form a subset of the morphisms with the same source and target in KT. Therefore, we have a set-theoretic inclusion of 4KT in KT at both the levels of objects and morphisms, and this inclusion respects compositions and products. However, the identity of E_{2s} in KT is not represented by an admissible Kirby tangle for $s > 0$, and hence it is not a morphism of 4KT, so 4KT is not a subcategory of KT.

Finally, the following proposition is an immediate consequence of the definitions, and in particular of the fact that 2-equivalence of 4-dimensional relative 2-handlebodies corresponds to 2-equivalence of admissible Kirby tangles.

PROPOSITION 3.3.7 ([BP11, Proposition 2.3.1]). *The map sending any morphism of* 4KT *given by the 2-equivalence class of a Kirby tangle* T *to the morphism of* 4HB *given by the 2-equivalence class of the* 4*-dimensional relative* 2*-handlebody represented by* T *defines an equivalence of strict monoidal categories* $4\mathrm{KT} \cong 4\mathrm{HB}$.

3.4. 3-dimensional relative cobordisms

For any $s \geqslant 0$, let F_s denote the connected oriented surface of genus s with connected non-empty boundary, canonically realized in $\mathbb{R}^3$ as the *front boundary* $\partial_+ M_s$ of the 3-dimensional handlebody $M_s \subset \mathbb{R}^3$ considered in Subsection 3.2, given by

$$\partial_+ M_s = \partial M_s \smallsetminus \partial\big([0,1]^2 \times [0,1[\big).$$

We remark that $\partial F_s = (\partial[0,1]^2) \times \{1\} \cong S^1$ does not depend on s, hence it is the same for every $s \geqslant 0$. Then, for any $s, t \geqslant 0$, we can consider the connected closed surface of genus $s + t$ given by

$$F_{s,t} = \partial M_{s,t} = (F_s \times \{0\}) \cup ((\partial[0,1]^2) \times \sqsubset) \cup (F_t \times \{1\}) \subset \mathbb{R}^4,$$

oriented according to the identifications $F_t \times \{1\} \cong F_t$ and $-F_s \times \{0\} \cong -F_s$, where

$$\sqsubset = (\partial[0,1]^2) \smallsetminus \,]0,1[\times \{1\} = ([0,1] \times \{0\}) \cup (\{0\} \times [0,1]) \cup ([0,1] \times \{1\})$$

is a piece-wise linear arc embedded into $\mathbb{R}^2$ (notice that $(\partial[0,1]^2) \times \sqsubset$ is represented as a pair of horseshoe-shaped arcs yielding the side boundary of $M_{s,t}$ in left-hand part of Figure 3.2.1).

By an oriented 3-dimensional relative cobordism, we mean an oriented cobordism between the compact connected oriented surfaces F_s and F_t which is relative to the common boundary $\partial F_s = \partial F_t$ in the sense of the following definition.

DEFINITION 3.4.1. An oriented 3-dimensional *relative cobordism* from F_s to F_t, with $s, t \geqslant 0$, is a compact connected oriented 3-manifold M whose boundary coincides with $F_{s,t}$, that is, $\partial M = F_{s,t}$.

Two relative cobordisms M and M' from F_s to F_t are said to be *equivalent* if there exists a homeomorphism $h : M \to M'$ that coincides with the identity on the common boundary $\partial M = \partial M' = F_{s,t}$.

According to this definition, if W is an oriented relative 4-dimensional handlebody built on $M_{s,t}$, then its *front boundary*

$$\partial_+ W = \partial W \smallsetminus \partial\big(M_{s,t} \times [0,1[\big)$$

is a relative cobordism from F_s to F_t, since $\partial(\partial_+ W) = F_{s,t} \times \{1\}$ can be canonically identified with $F_{s,t}$.

In particular, the front boundary

$$\partial_+(M_{s,t} \times [0,1]) = M_{s,t} \times \{1\}$$

of the trivial handlebody $M_{s,t} \times [0,1]$ (with no handles) is a relative cobordism from F_s to F_t that can be canonically identified with $M_{s,t}$. See the left-hand part of Figure 3.4.1 for an "ironed-out" picture of $\partial_+(M_{s,t} \times [0,1])$, to be compared with the "horseshoe" version of $M_{s,t}$ represented in the left-hand part of Figure 3.2.1. This can be considered as a basic relative cobordism from which any other relative cobordism between F_s and F_t can be obtained by surgery. Since attaching handles to a 4-dimensional relative handlebody induces surgery on its front boundary, this is a immediate consequence of the following extension of the Lickorish-Rokhlin-Wallace's theorem about the surgery presentation of closed 3-manifolds (see [KL01]).

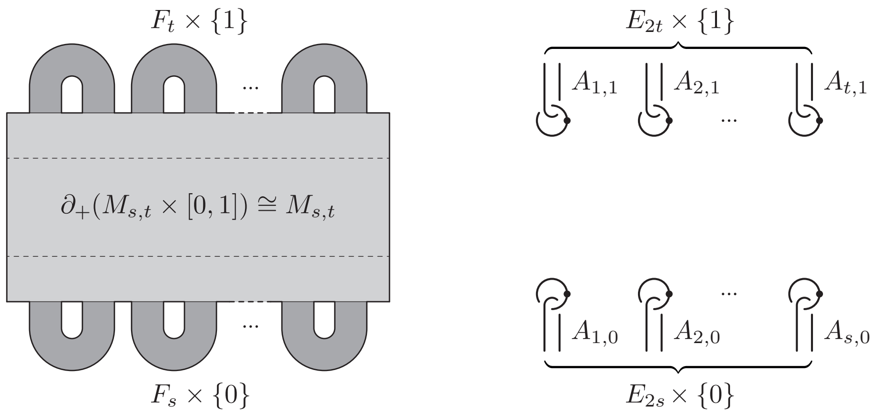

FIGURE 3.4.1. The relative cobordism $\partial_+(M_{s,t} \times [0,1])$ and the corresponding Kirby tangle.

PROPOSITION 3.4.2. *Any 3-dimensional relative cobordism M from F_s to F_t is homeomorphic to the front boundary $\partial_+ W$ of a 4-dimensional relative 2-handlebody W built over $M_{s,t}$, hence, up to homeomorphism, it can be obtained by surgery on $M_{s,t}$. Moreover, W can be assumed to have only 2-handles, so only 2-surgery is needed to realize M starting from $M_{s,t}$.*

Similarly, Kirby calculus relating surgery presentations of homeomorphic closed 3-manifolds can be extended to 3-dimensional relative cobordisms, as stated by the following proposition (see [KL01]).

PROPOSITION 3.4.3. *Two oriented 4-dimensional relative 2-handlebodies W and W' have equivalent front boundaries $\partial_+ W$ and $\partial_+ W'$ (as relative cobordisms) if and only if they are related by a finite sequence of the operations* (a), (b), *and* (c) *in Definition 3.2.2, and of the following further two operations:*
(d) *replacing a 1-handle by a trivially attached 2-handle and vice-versa (handle trading);*
(e) *adding/deleting a 2-handle attached along a separate unknot with framing ± 1 (blow-up/down).*
Moreover, operations (a)–(d) *suffice to relate W and W' if these have equivalent front boundaries and the same signature $\sigma(W) = \sigma(W')$, since operation* (e) *is the unique one that changes the signature of the handlebody by ± 1.*

In light of the above proposition, operation (d) allows us to replace all the 1-handles in any Kirby tangle presentation of a 4-dimensional relative 2-handlebodies W while preserving both the front boundary

∂W up to homeomorphism and the signature $\sigma(W)$. In this way, any surgery presentation of a 3-dimensional relative cobordism can be changed into one consisting of 2-surgeries only, simply by erasing all the dots from the corresponding Kirby tangle.

We observe that, according to Proposition 3.4.2, any "consistent" family of 3-dimensional relative cobordisms from F_s to F_t for all $s, t \geqslant 0$ could be chosen, instead of $M_{s,t}$, as the base for the surgery presentation of any such cobordism. For example, this is the case for the relative cobordisms $T_{s,t}$ schematically depicted in Figure 3.4.2, which are obtained by attaching s c1-handles to the bottom face of $[0,1]^3$, and removing open tubular neighborhoods of t arcs whose endpoints lie on the top face. Here, the bottom part of the boundary is canonically identified with F_s, while the blackboard framing of the tangle is used to determine an identification of the top part of the boundary with F_t.

This alternative choice leads to the top-tangle surgery presentation of 3-dimensional relative cobordisms considered in [BD21]. This is an upside-down version of Habiro's bottom-tangles in handlebodies (see [Ha05, As11]), to which surgery is applied. The reason for the vertical inversion is that we read cobordisms from bottom to top, like in [BP11, BD21], while in [Ha05, As11] they are read from top to bottom.

For the reader convenience, in Figure 3.4.3, we show the top-tangle presentation of the structure morphisms of 3Alg. Here, the thick blackboard framed arcs stand for removed open tubular neighborhoods, as in Figure 3.4.2, while the thin blackboard framed closed curves stand for 2-surgery. They are obtained by performing 2-surgery on the top-tangle in Figure 3.4.2, followed by suitable slidings and cancellations. Observe that most of the cobordisms in the figure can be realized without any 2-surgery, which means that they embed directly into $\mathbb{R}^3$.

3.5. The quotient categories 3Cob and 3KT

We will show that equivalence classes of oriented 3-dimensional relative cobordisms form a monoidal category 3Cob, which admits a quotient front boundary functor $\partial_+ : 4\mathrm{HB} \to 3\mathrm{Cob}$. This will give rise to a corresponding quotient functor $\partial_+ : 4\mathrm{KT} \to 3\mathrm{KT}$, once 3Cob is shown to be equivalent to the category 3KT of admissible Kirby tangles up to a suitable front boundary equivalence.

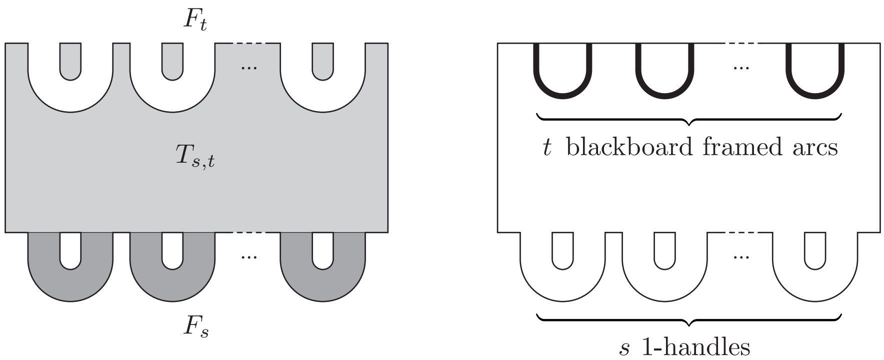

FIGURE 3.4.2. The relative cobordism $T_{s,t}$ and its top-tangle diagram.

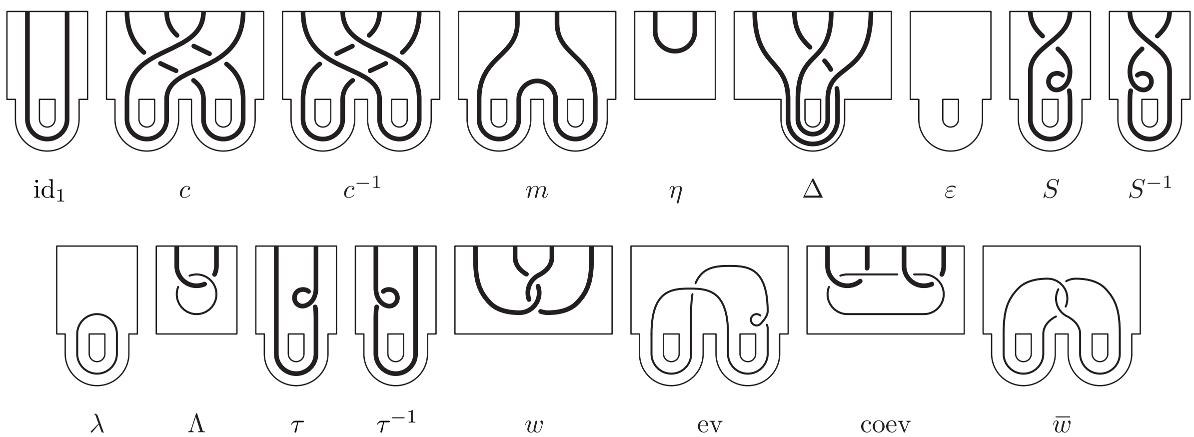

FIGURE 3.4.3. Top-tangle diagrams corresponding to the Kirby diagrams in Figure 3.3.1.

Definition 3.5.1. We denote by 3Cob the strict monoidal category whose objects are connected oriented surfaces (with boundary) F_s for $s \geqslant 0$, and whose morphisms from F_s to F_t are equivalence classes of 3-dimensional relative cobordisms from F_s to F_t, as defined in Subsection 3.4.

The composition of two morphisms M from F_s to F_t and M' from $F_{s'}$ to $F_{t'}$ with $t = s'$ is given by vertical juxtaposition, with M' on top of M, and by rescaling by a factor $1/2$, which corresponds to gluing the two morphisms by canonically identifying the target of the first with the source of the second, that is,

$$M' \circ M \cong M \cup_{F_t \times \{1\} = F_{s'} \times \{0\}} M',$$

with $\partial(M' \circ M) \cong F_{s,t'}$ canonically contained in $F_{s,t} \cup_{F_t \times \{1\} = F_{s'} \times \{0\}} F_{s',t'}$.

The tensor product, denoted by $\natural$, is given by horizontal juxtaposition, from left to right, and it corresponds to the boundary connected sum for both the objects and the morphisms, with canonical identifications $F_s \natural F_{s'} \cong F_{s+s'}$ for the product of objects, and $\mathrm{Bd}(M \natural M') = \mathrm{Bd}\, M \# \mathrm{Bd}\, M' = F_{s,t} \# F_{s',t'} \cong F_{s+s',t+t'}$ for the product $M \natural M'$ of morphisms M from F_s to F_t and M' from $F_{s'}$ to $F_{t'}$.

For each $s \geqslant 0$, the identity id_{F_s} is represented by the product cobordism $F_s \times [0,1]$. In particular, $\mathrm{id}_{\mathbb{1}} = F_0 \times [0,1]$, since $\mathbb{1} = F_0$.

Remark 3.5.2. The category 3Cob can be understood as the skeleton of a category whose objects are arbitrary connected oriented surface with connected non-empty boundary. Once again, it is convenient to work with the standard models for objects we are considering here, as this allows us to define a braided monoidal structure on 3Cob.

In light Definitions 3.3.1 and 3.5.1, the front boundary operator ∂_+ introduced in Subsection 3.4 induces a monoidal functor from 4HB to 3Cob. In fact, we have the following proposition.

Proposition 3.5.3. *There is a quotient monoidal functor* $\partial : 4\mathrm{HB} \to 3\mathrm{Cob}$ *such that* $\partial M_s = F_s$ *for all* $s \geqslant 0$*, which sends any morphism of* 4HB *given by the 2-equivalence class of the relative* 2*-handlebody* W *to the morphism of* 3Cob *given by the equivalence class of its front boundary* $\partial_+ W$.

Proof. The claim that ∂_+ is well-defined as a monoidal functor immediately follows from the definition of the front boundary of a 4-dimensional relative 2-handlebody, the "if" part of Proposition 3.4.3, and the fact that vertical and horizontal juxtaposition of 4-dimensional relative 2-handlebodies restrict to analogous operations on their front boundaries. Notice that, for all $W = (W, M_{s,t})$ and $W' = (W', M_{s',t'})$ with $t = s'$, the front boundary $\partial_+(W' \circ W)$ and the composition $\partial_+(W') \circ \partial_+(W)$ differ only by a canonical collar of the middle surface $F_t = F_{s'}$, and so they are equivalent. On the other hand, the functor ∂_+ is trivially surjective on objects, while Proposition 3.4.2 implies its surjectivity on morphisms. □

Now, based on the front boundary equivalence moves shown Table 3.5.1, which provide a Kirby tangle interpretation of operations (d) and (e) in Proposition 3.4.3, we can define the category 3KT, which is the diagrammatic counterpart of 3Cob.

Front boundary equivalence moves for Kirby tangles	
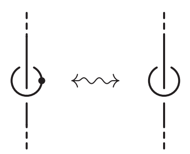	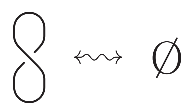
1/2-handle trading	*Positive blow down/up*

Table 3.5.1

Definition 3.5.4. Two admissible Kirby tangles are said to be *front boundary equivalent* if they are related by a finite sequence of the moves and the operations in Tables 3.1.1 and 3.5.1.

Actually, the relations in Table 3.5.1 imply any 1/2-handle trading and negative blow-up/down, as specified by the next proposition (compare with [Ki89] and [GS99]).

Proposition 3.5.5 ([BP11, Lemma 5.2.1]). *Modulo* 1/2*-handle cancellation and* 2*-handle sliding, any* 1/2*-handle trading can be reduced to one presented on the left-hand side of Table 3.5.1. Moreover,* *modulo 2-handle sliding and 1/2-handle trading, positive and negative blow-up/down are inverse to one another.*

Definition 3.5.6. We denote by 3KT the quotient category of 4KT with respect to the front boundary equivalence relations presented in Table 3.5.1. Then 3KT inherits the structure of a braided (strict) monoidal category making the quotient functor $\partial : 4\mathrm{KT} \to 3\mathrm{KT}$ into a braided monoidal functor.

As an immediate consequence of the above definitions and of Proposition 3.5.5, we have the following proposition.

Proposition 3.5.7 ([BP11, Proposition 5.2.2]). *The maps sending any morphism of* 3KT *given by the front boundary equivalence class of a Kirby tangle T to the morphism of* 3Cob *given by the equivalence class of the relative cobordism represented by T defines an equivalence of braided monoidal categories* $3\mathrm{KT} \cong 3\mathrm{Cob}$. *Furthermore, the following diagram commutes:*

$$\begin{tikzcd} 4\mathrm{KT} \arrow[r, "\partial_+"] \arrow[d, "\cong"'] & 3\mathrm{KT} \arrow[d, "\cong"] \\ 4\mathrm{HB} \arrow[r, "\partial_+"'] & 3\mathrm{Cob} \end{tikzcd}$$

4. Algebraic presentation of 4HB and 3Cob

This section is devoted to the proof of Theorem A, which provides an algebraic presentation of 4HB $\cong$ 4KT. We start by recalling the definition of the functor $\Phi : 4\mathrm{Alg} \to 4\mathrm{KT}$. Its inverse $\overline{\Phi} : 4\mathrm{KT} \to 4\mathrm{Alg}$ is constructed in Subsection 4.4, and its independence of many auxiliary choices is shown in subsequent subsections. A crucial role in the proof is played by a subcategory TAlg and its labeled version MAlg as well as a natural transformation Θ (Subsection 4.2) and its labeled version Θ^{L}_j (Subsection 4.5). The proof of Theorem A is given in Subsection 4.7.

4.1. The functor $\Phi : 4\mathrm{Alg} \to 4\mathrm{KT}$

It was first shown in [CY94] that the category 3Cob of 3-dimensional cobordisms contains a braided Hopf algebra, the punctured torus. It was later shown in [Ke01] that this braided Hopf algebra, together with a ribbon element and an integral, generates 3Cob, or equivalently the category 3KT of admissible framed tangles (see also [Ha05] for a similar statement concerning the category of bottom tangles in handlebodies). We recall here a generalization of these results established in [BP11], where it is proved that the solid torus in 4HB satisfies axioms (*r8*) and (*r9*), and is thus a BP Hopf algebra.

Theorem 4.1.1 ([BP11, Theorem 4.3.1]). *There exists a braided monoidal functor $\Phi : 4\mathrm{Alg} \to 4\mathrm{KT}$ that sends H to E_2 (see Proposition 3.3.4) and each structure morphism of H to the corresponding Kirby tangle represented in Figure 4.1.1.*

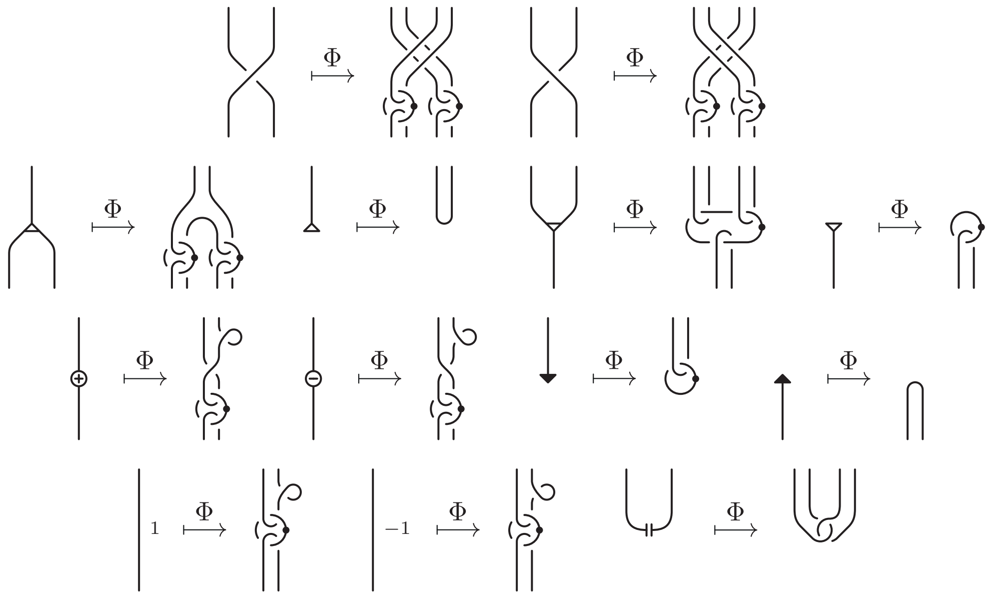

Figure 4.1.1. The functor $\Phi : 4\mathrm{Alg} \to 4\mathrm{KT}$.

Notice that the image of the copairing w is the rotation along a horizontal axis in $\mathbb{R}^3$ of the bottom tangle defining Lyubashenko's pairing in [Ly94].

For completeness, we present the proof.

Proof of Theorem 4.1.1. We have to check that the images under Φ of the structure morphisms of H satisfy the axioms of a BP Hopf algebra.

This is easy to check for most of the Hopf algebra axioms and for the integral axioms in Tables 2.4.1 and 2.4.3. In particular, the proof reduces to an isotopy for the braid axioms, and to the removal of canceling 1/2-pairs for axioms (*a4-4′*), (*a6*), (*a8*), (*i3*), and (*i4*), while a few handle slides are also required for axioms (*a1*), (*a2-2′*), (*a3*), (*a7*), (*s2-3*), (*i1*), (*i2*), and (*i5*).

Axiom (*a5*) and the first part of axiom (*s1-1′*) are proved in Figures 4.1.2 and 4.1.3 respectively. The second part of axiom (*s1-1′*) is analogous to the first.

Compatibility with axioms (*r3*)–(*r5*) can be easily established, once again, by the removal of canceling 1/2-handle pairs after suitable handle slides. The rest of the ribbon axioms are dealt with in Figures 4.1.4, 4.1.5, 4.1.6, and 4.1.7. Here, in the rightmost diagrams of the last two figures, some removal of canceling 1/2-handle pairs has been performed. □

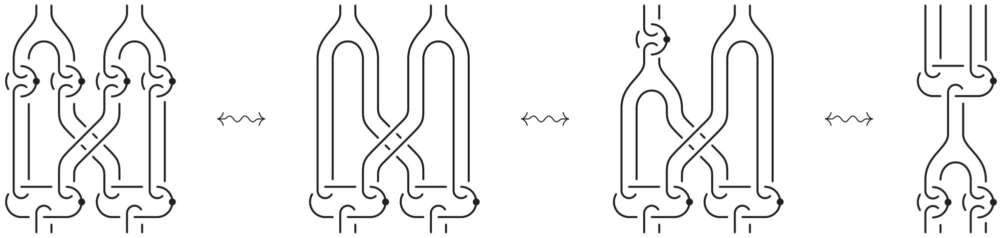

FIGURE 4.1.2. The definition of Φ is compatible with axiom (*a5*).

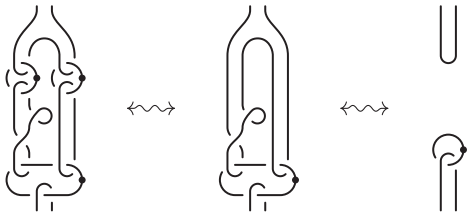

FIGURE 4.1.3. The definition of Φ is compatible with axiom (*s1-1'*).

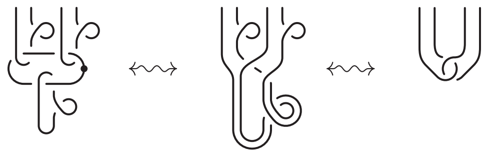

FIGURE 4.1.4. The definition of Φ is compatible with axiom (*r6*).

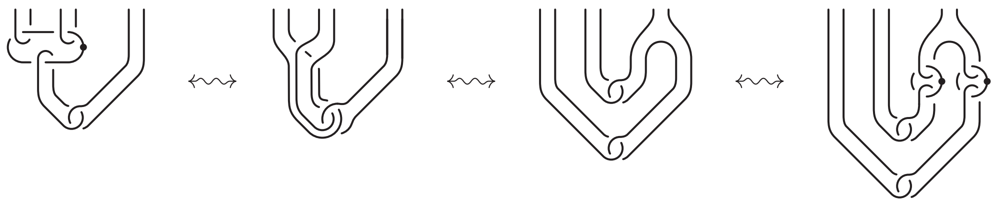

FIGURE 4.1.5. The definition of Φ is compatible with axiom (*r7*).

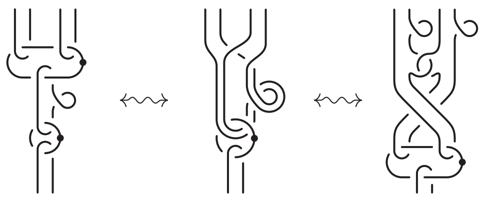

FIGURE 4.1.6. The definition of Φ is compatible with axiom (*r8*).

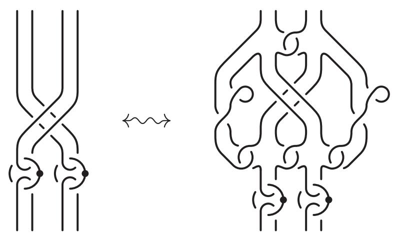

FIGURE 4.1.7. The definition of Φ is compatible with axiom (*r9*).

We observe that the images under Φ of the evaluation, the coevaluation, and the adjoint action are equivalent, in 4KT, to the tangles represented in Figure 4.1.8. The proof is straightforward and left to the reader.

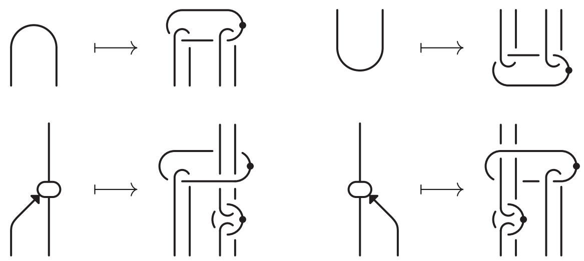

FIGURE 4.1.8. Images under Φ of ev, coev, ad, and ad$'$.

4.2. The subcategory TAlg of 4Alg

In this subsection, we define a monoidal subcategory TAlg of 4Alg whose morphisms are sent by Φ to a family of special two-level Kirby tangles. TAlg will play an essential role in the definition of the inverse functor $\overline{\Phi}$ of Φ in Subsection 4.4, where the image of any Kirby tangle in 4KT under $\overline{\Phi}$ will be defined as some sort of closure of morphisms in TAlg. We will show below that TAlg has some interesting algebraic properties. In particular, it admits two ribbon structures. Moreover, there exist two families of morphisms in 4Alg that intertwine all morphisms in TAlg, and whose images under Φ are given by 1-handles which embrace the upper/lower level of the tangle.

We start by introducing in Table 4.2.1 a compact notation for certain decorations (featuring copairings) of the braiding morphisms $c^{\pm 1}$ of 4Alg. A decoration of a crossing is a wavy line attached to the two edges which form the crossing, and it is entirely contained in one of the four regions that make up

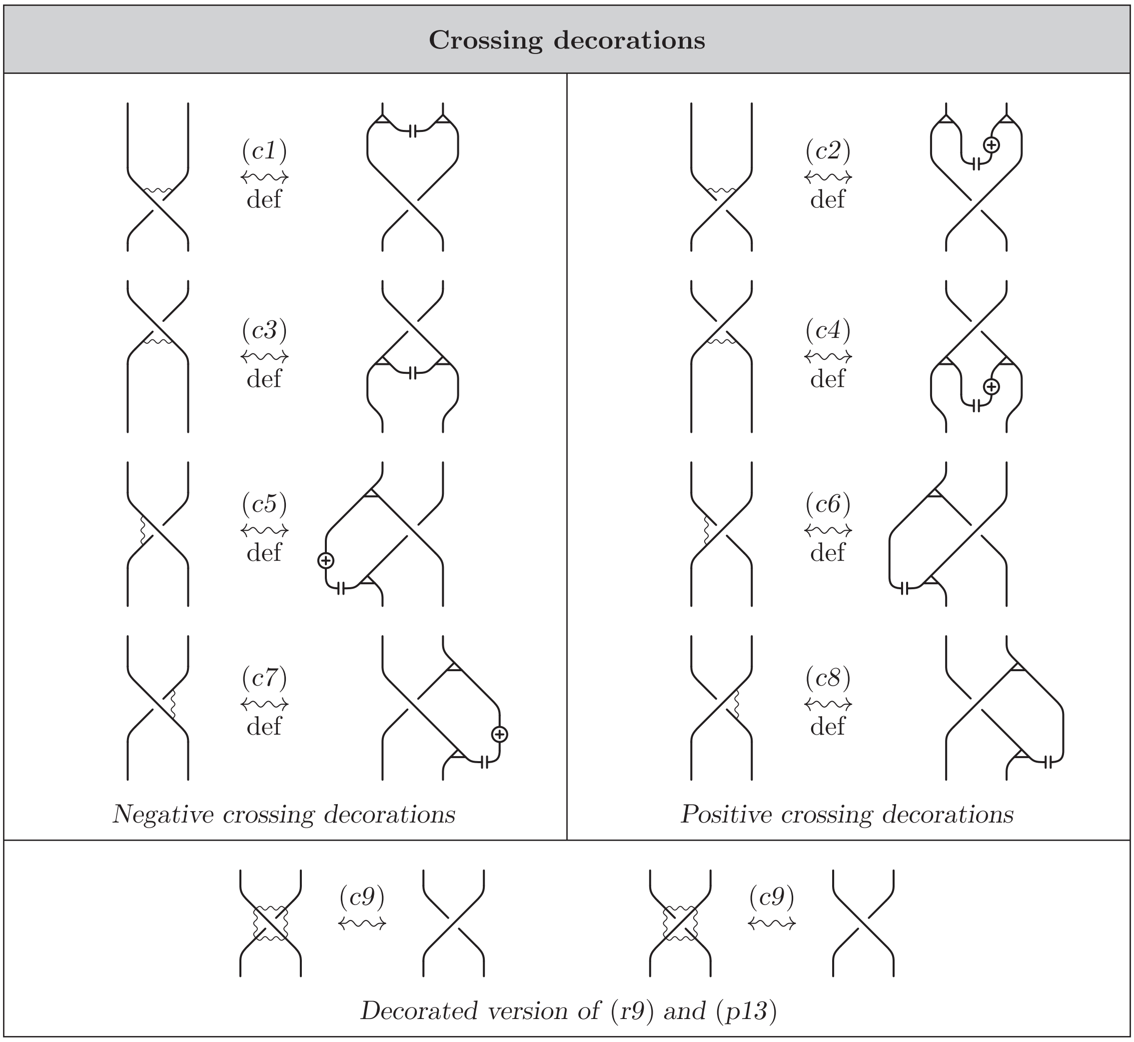

TABLE 4.2.1

the complement of the crossing inside a circular neighborhood in the projection plane. In particular, we have four possible decorations for both positive and negative crossings, and the relations (*c1*)–(*c8*) in Table 4.2.1 define these decorations as morphisms in 4Alg.

Observe that a decoration, which is a wavy line attached to arbitrary edges, doesn't have a meaning on its own; it acquires one only in a neighborhood of a crossing, and it has to appear in one of the forms shown in Table 4.2.1. In particular, to a crossing we can attach at most four decorations. To understand the meaning of decorations, we observe that the image of c (respectively of c^{-1}) under Φ consists of four positive (respectively negative) crossings between two double strands (see Figure 4.1.1), and adding a decoration corresponds to inverting one of these four crossings (see Figure 4.1.7). Notice that inverting all four of them transforms $\Phi(c)$ into $\Phi(c^{-1})$, or the other way round. The algebraic versions of these moves are the relations shown in the bottom section of Table 4.2.1, which are the representation of axiom (*r9*) in Table 2.4.1 and relation (*p13*) in Table 2.4.6 in terms of decorated crossings. Moreover, these two relations can be generalized as stated in the following proposition.

Proposition 4.2.1. *Any decorated crossing is equivalent to the opposite crossing with complementary decorations. We will denote by (c9) this general class of relations.*

Proof. The statement follows from axiom (*r9*) in Table 2.4.1 and relation (*p13*) in Table 2.4.6, by applying relations (*p5*-*6*) in Table 2.4.4. □

We will focus now on studying the properties of the decorated crossings X, $\widehat{X}$, Y, and $\widehat{Y}$ defined in the top two lines of Figure 4.2.2, which will play an important role in the definition of $\overline{\Phi}$ in the next subsection.

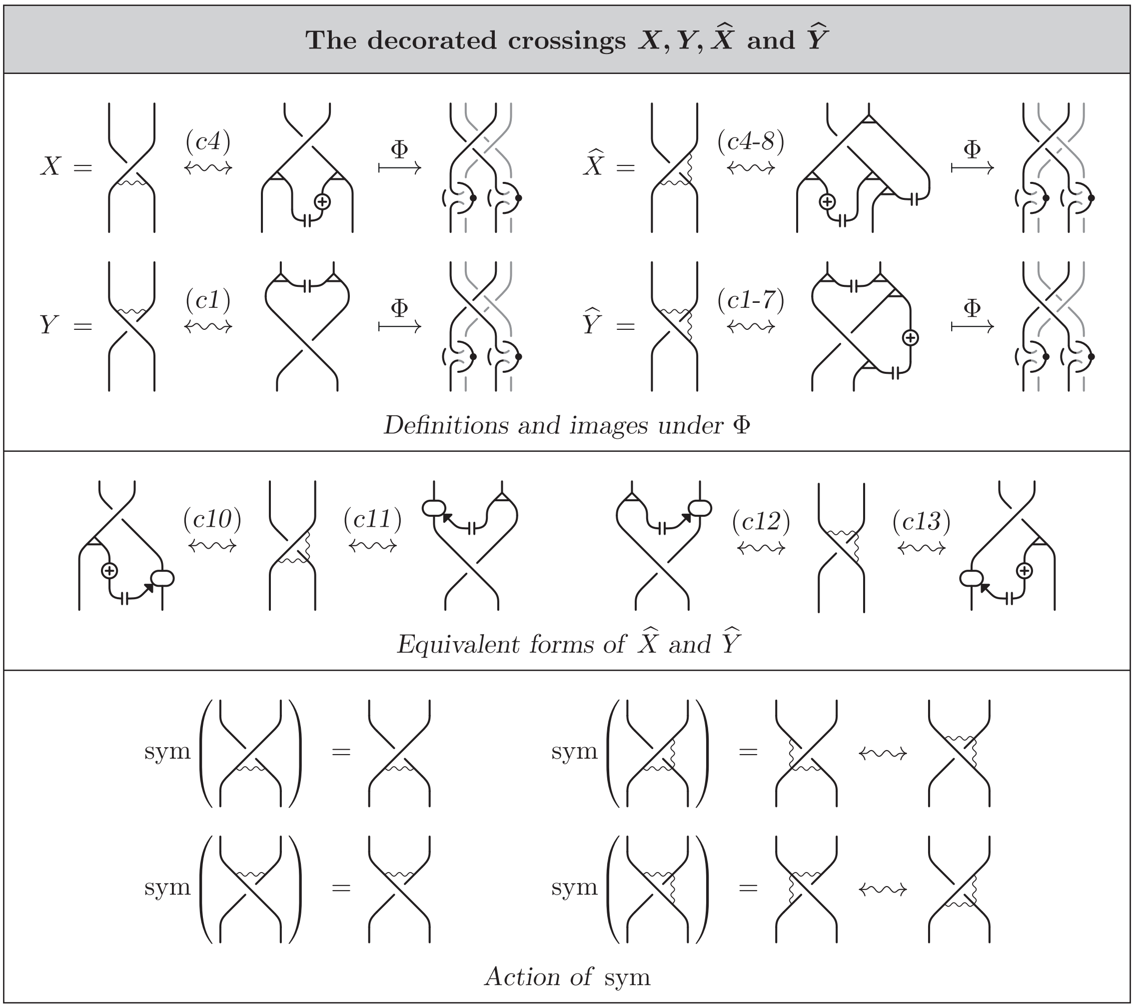

Table 4.2.2

LEMMA 4.2.2. *$\widehat{X}$ and $\widehat{Y}$ can be presented in the equivalent forms represented in Table 4.2.2. Moreover, we have the following identities (see Tables 4.2.2 and 4.2.10):*

$$\mathrm{sym}(X) = X, \quad \mathrm{sym}(Y) = Y,$$
$$\mathrm{sym}(\widehat{X}) = \widehat{Y}, \quad \mathrm{sym}(\widehat{Y}) = \widehat{X},$$
$$Y = X^{-1}, \tag{c14-15}$$
$$\widehat{Y} = \widehat{X}^{-1}, \tag{c20-21}$$

Proof. The identities (*c14-15*) and (*c20-21*) follow from the properties of the copairing, the adjoint action, and the antipode, as indicated in Figure 4.2.3, while (*c10-11*), (*c12-13*) and the identities involving the symmetry functor are proved in Figure 4.2.4. □

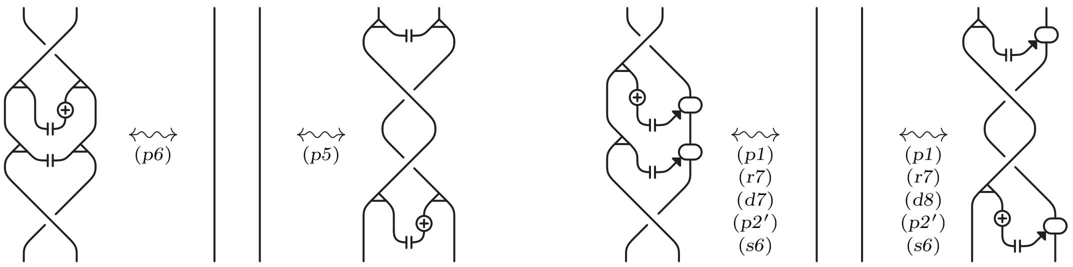

FIGURE 4.2.3. Proof of (*c14-15*) and (*c20-21*).

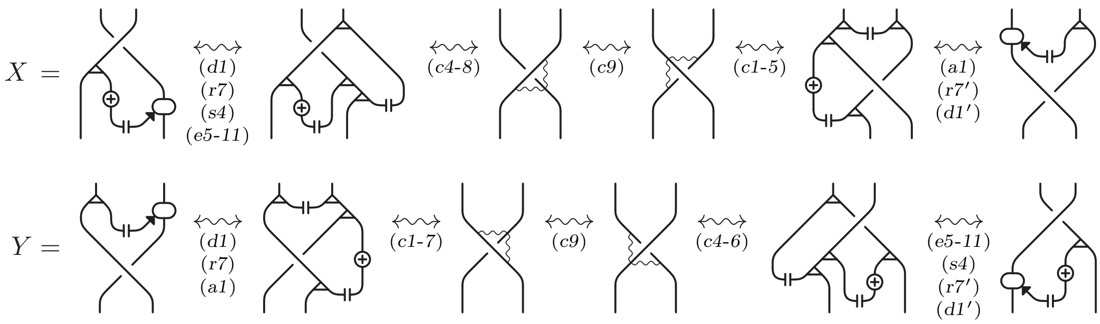

FIGURE 4.2.4. Equivalent forms of $\widehat{X}$ and $\widehat{Y}$.

REMARK 4.2.3. The images of X, $\widehat{X}$, Y, and $\widehat{Y}$ under Φ are represented in Figure 4.2.2. Notice that such images satisfy the following properties.

(a) The intersection of the projection plane with the Kirby tangle coincides with some of the disks spanned by the 1-handles, and the intersections with such disks divide the tangle of undotted components, and in particular each open component, into two parts: one which stays above and one which stays below the projection plane, represented respectively in black and gray.

(b) In the projection plane, the lower arc of each undotted component projects onto the right of the upper one.

Notice that the images under Φ of Δ, ε, Λ, τ, ev, coev (see Figures 4.1.1 and 4.1.8), and therefore any composition of these morphisms as well, satisfy properties (a) and (b) as well.

We will now define two families of morphisms Θ_k and Θ'_k, with $k \geqslant 0$, designed to provide an algebraic analogue of a dotted component that embraces either the lower (gray) or the upper (black) strands of a two-level tangle.

DEFINITION 4.2.4. For every $k \geqslant 0$, the morphism $\Theta_k : H^k \otimes H \to H^k$ in 4Alg is recursively defined by the following identities (compare with Figure 4.2.5):

$$\Theta_0 = \varepsilon, \quad \Theta_1 = \mu,$$
$$\Theta_k = (\Theta_1 \otimes \Theta_{k-1}) \circ (\mathrm{id} \otimes c_{k-1,1} \circ \mathrm{id}) \circ (\mathrm{id}_{k-1} \otimes \Delta).$$

Define also $\Theta'_k = \mathrm{sym}(\Theta_k) : H \otimes H^k \to H^k$ to be the symmetric morphism (see Proposition 2.4.10).

We denote by Θ the collection of morphisms $\{\Theta_k\}_{k\in\mathbb{N}}$, and similarly by Θ' the collection $\{\Theta'_k\}_{k\in\mathbb{N}}$.

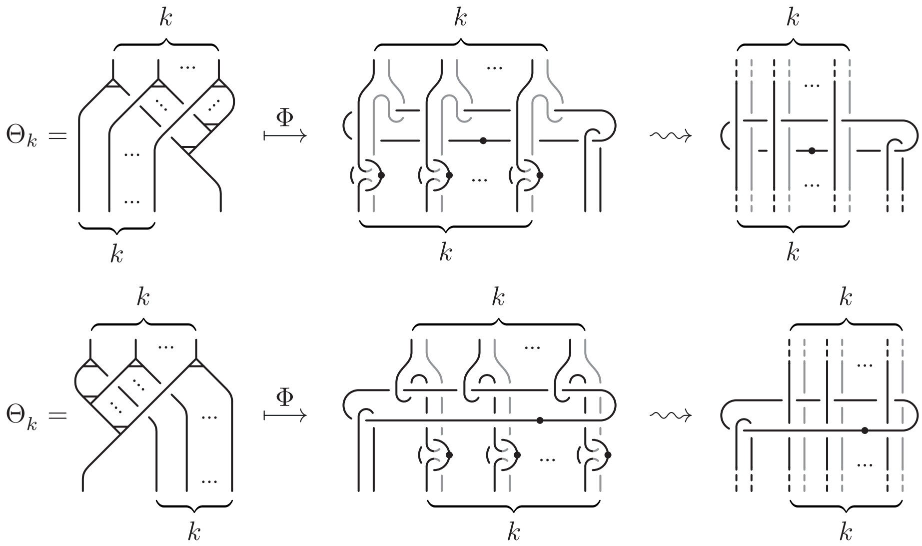

FIGURE 4.2.5. The morphisms Θ_k and Θ'_k and their images under Φ, $k \geqslant 0$.

For every $k \geqslant 0$, we also introduce the morphisms[5]

$$U'_k = \Theta_k \circ (\mathrm{id}_k \otimes \Lambda) \text{ and } U_k = \Theta'_k \circ (\Lambda \otimes \mathrm{id}_k),$$

see Figure 4.2.6. Notice that their images under Φ satisfy Properties (a) and (b) in Remark 4.2.3 as well. This motivates the definition of the category TAlg below.

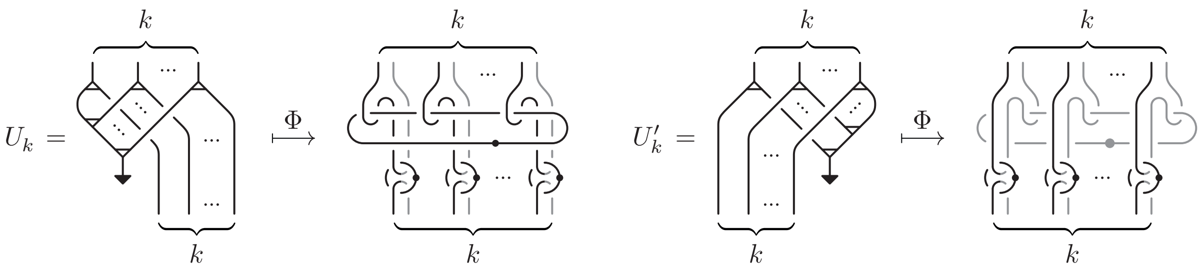

FIGURE 4.2.6. The morphisms U_k and U'_k and their images under Φ.

DEFINITION 4.2.5. We denote by TAlg the strict monoidal subcategory of 4Alg generated by the morphisms Δ, ε, Λ, ev, τ, X, $\widehat{X}$, Y, $\widehat{Y}$, U_k, and U'_k defined in Tables 2.2.1, 2.4.1, and 4.2.2, and Figure 4.2.6.

Notice that coev and $\widetilde{\mu}$ belong to TAlg, since they are compositions of morphisms in TAlg, while the product μ, the unit η, the antipode S, and the copairing w are not in TAlg.

As an immediate consequence of Lemma 4.2.2 and Definition 4.2.5, we have the following corollary.

COROLLARY 4.2.6. *The subcategory* TAlg *of* 4Alg *is invariant under the action of the symmetry functor* sym : 4Alg → 4Alg *defined in Proposition 2.4.10.*

[5] Θ' and U' are just auxiliary morphisms which will be used to simplify some proofs, while Θ and U will play an essential role in the following. This is why we swap the prime in the notation.

Lemma 4.2.7. *If* $\iota : \mathrm{TAlg} \hookrightarrow 4\mathrm{Alg}$ *denotes the inclusion functor, then* $\Theta : \iota \otimes H \Rightarrow \iota$ *and* $\Theta' : H \otimes \iota \Rightarrow \iota$ *define natural transformations, meaning that, for every morphism* $F : H^s \to H^t$ *in* TAlg, *we have (see Figure 4.2.7)*

$$\Theta_t \circ (F \otimes \mathrm{id}) = F \circ \Theta_s, \tag{t1}$$

$$\Theta'_t \circ (\mathrm{id} \otimes F) = F \circ \Theta'_s. \tag{t1'}$$

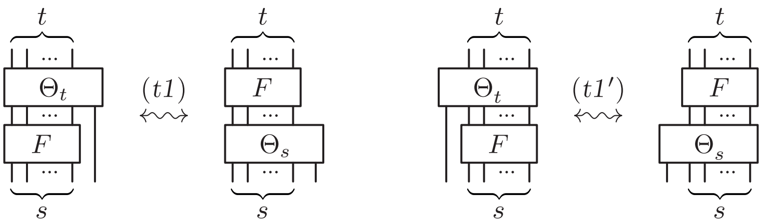

Figure 4.2.7. Naturality of Θ and Θ'.

Proof. According to Corollary 4.2.6, the statement for Θ' can be derived from the one for Θ by applying the functor sym. For what concerns Θ, the coassociativity relation (*a3*) implies that, if the statement is true for two morphisms, then it is true for their product as well. Therefore, it is enough to show that (*t1*) holds whenever F is one of the generating morphisms of TAlg. For $F = \Delta, \varepsilon, \Lambda, \tau$, the statement follows directly from (*a5*), (*a6*), (*i2′*), and (*r5*), while for $F = \mathrm{ev}, U_k, U'_k$ it is shown in Figure 4.2.8. Then, in the first two lines of Figure 4.2.9, we prove (*t1*) for $F = X$, which in turn implies (*t1*) for $F = Y$, since, thanks to Lemma 4.2.2, $Y = X^{-1}$. Finally, in the last line of Figure 4.2.9, by using (*t1*) for Y, we prove the statement for $F = \widehat{X}$, which implies (*t1*) for $F = \widehat{Y} = \widehat{X}^{-1}$. □

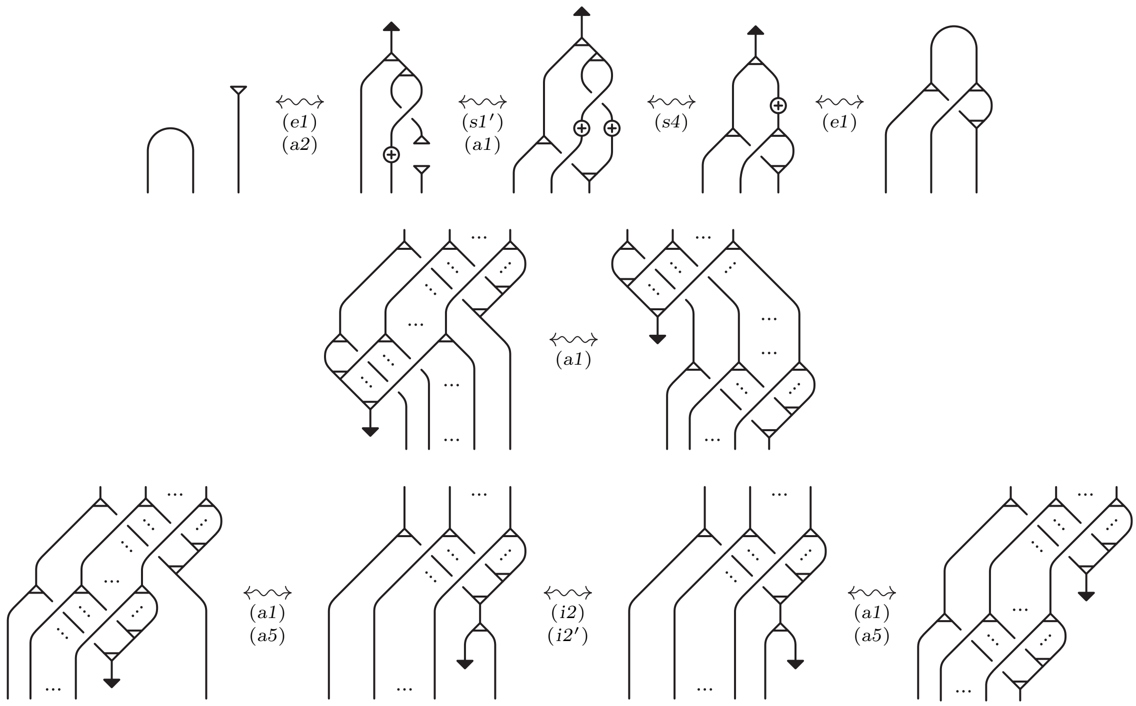

Figure 4.2.8. Proof of relation (*t1*) for $F = \mathrm{ev}, U_k, U'_k$.

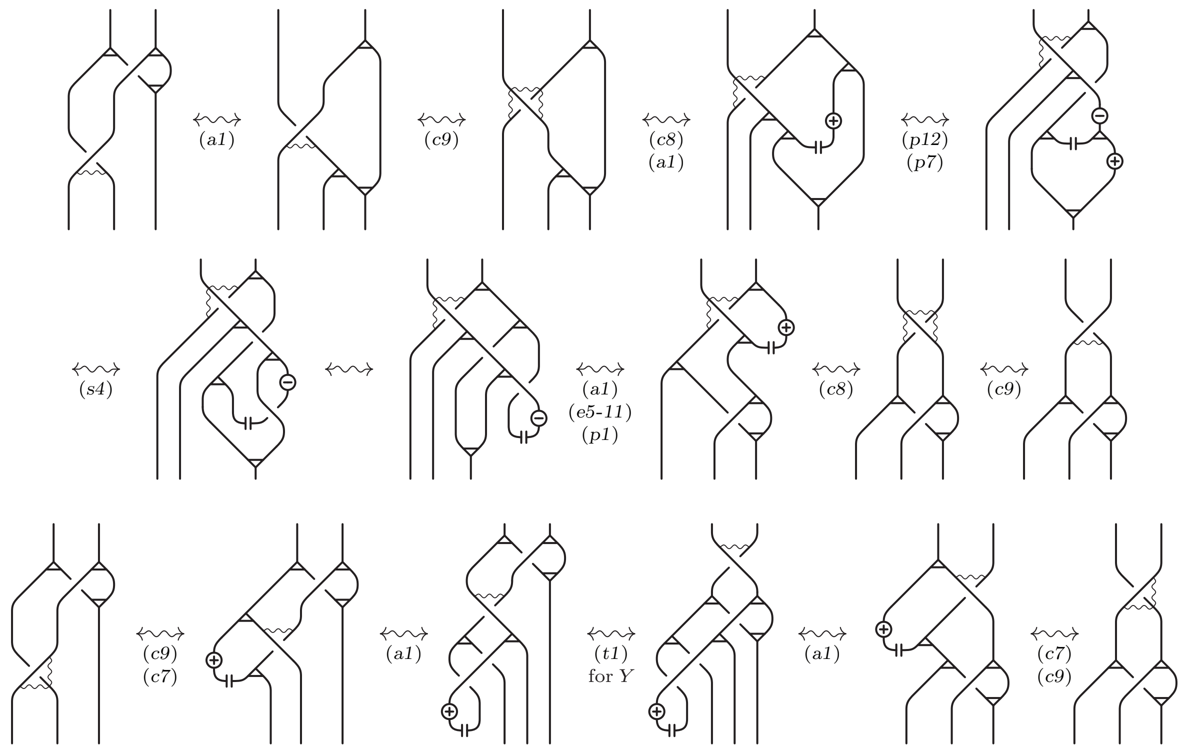

FIGURE 4.2.9. Proof of relation (*t1*) for $F = X, \widehat{X}$.

THEOREM 4.2.8. *The relations in Tables 4.2.10 and 4.2.11 are satisfied in* TAlg*. In particular,* TAlg *admits two distinct ribbon structures, in which braiding morphisms (and their inverses) are given by* $X, X^{-1} = Y : H \otimes H \to H \otimes H$ *and by* $\widehat{X}, \widehat{X}^{-1} = \widehat{Y} : H \otimes H \to H \otimes H$*, respectively.*

Braided ribbon structures on TAlg

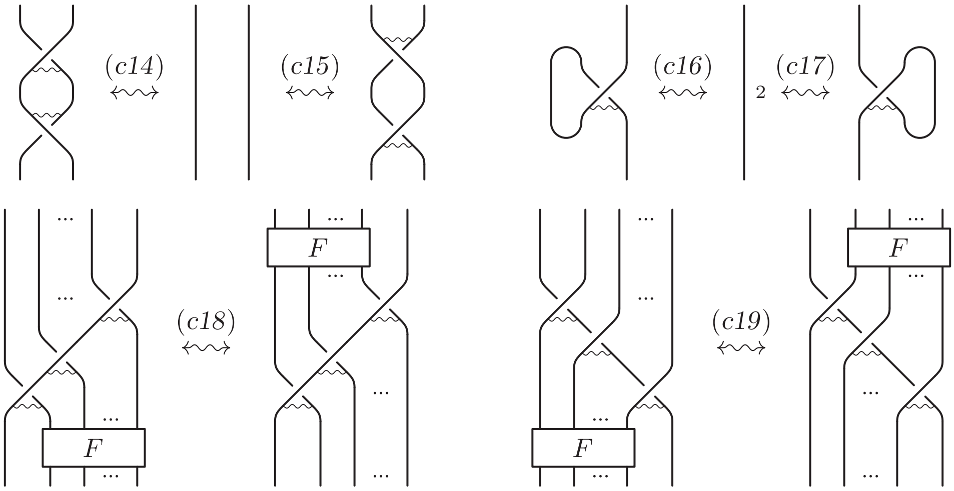

The braided ribbon structure induced by X and Y (F any morphism in TAlg*)*

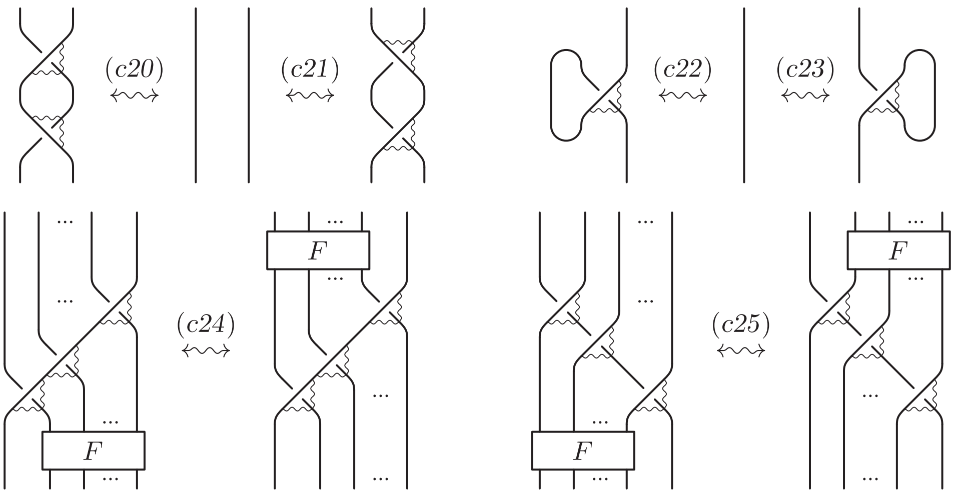

The braided ribbon structure induced by $\widehat{X}$ and $\widehat{Y}$ (F any morphism in TAlg*)*

TABLE 4.2.10

Properties of the morphisms U_k in TAlg

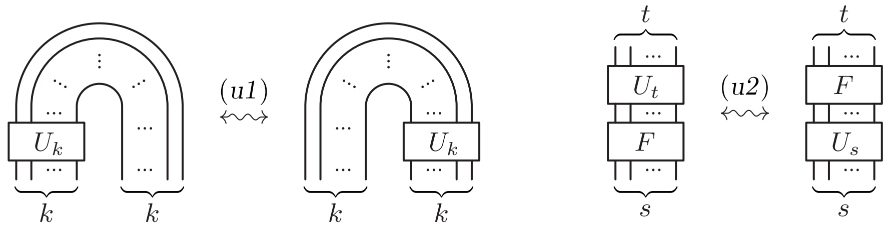

(F *any morphism in* TAlg)

TABLE 4.2.11

Proof. The evaluation and coevaluation morphisms of TAlg are induced by the ones of 4Alg. Relations (*c14*-*15*) and (*c20*-*21*) have been proved in Lemma 4.2.2. Relations (*c16*), (*c22*), and (*c23*) are proved (in this order) in Figure 4.2.12, while (*c17*) follows by symmetry from (*c16*). Relation (*c24*) follows from (*d10*) and Figure 4.2.13, while relations (*c18*) and (*c25*) follow from (*t1′*) and from Figure 4.2.14. Then, (*c19*) follows by symmetry from (*c18*). Relation (*u1*) is proved in Figure 4.2.15, while (*u2*) is a direct consequence of (*t1′*). □

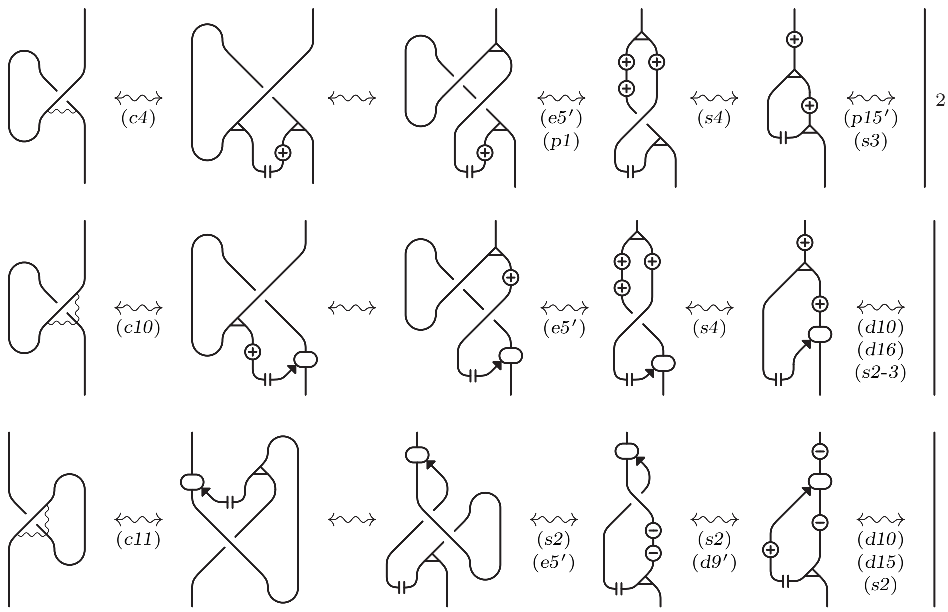

FIGURE 4.2.12. Proof of relations (*c16*), (*c22*), and (*c23*).

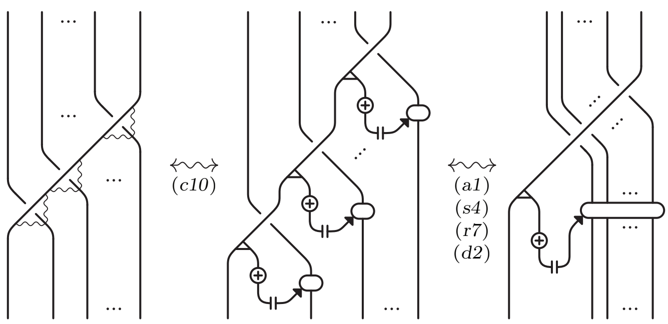

FIGURE 4.2.13. Proof of relation (*c24*).

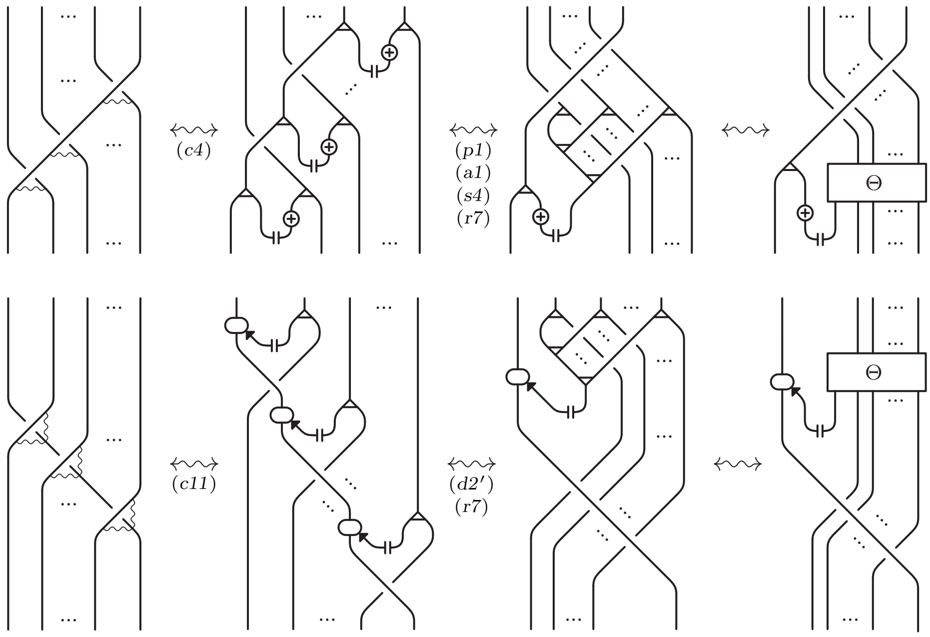

FIGURE 4.2.14. Proof of relations (*c18*) and (*c25*).

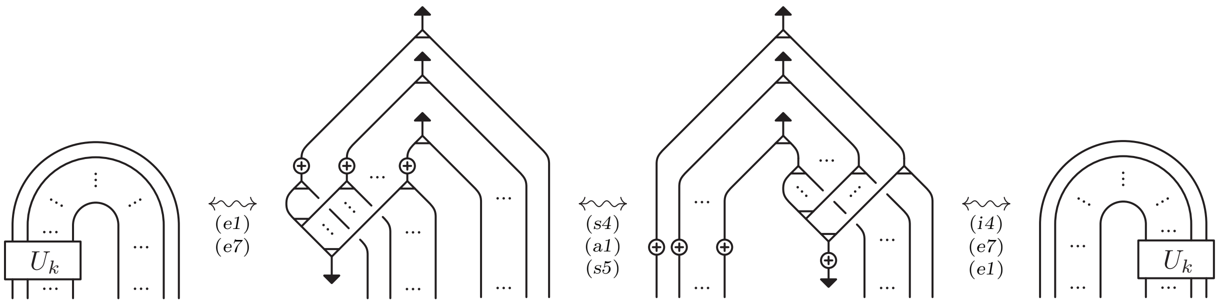

FIGURE 4.2.15. Proof of relation (*u1*).

4.3. Bi-ascending states of link diagrams

In [BP11], a key ingredient for inverting Φ was the notion of vertically trivial state of a link diagram. In the present more algebraic context, based on the presentation of the category 4KT provided by Proposition 3.3.4, it seems convenient to replace that notion with the completely diagrammatic notion of bi-ascending state.

As usual, we represent a link $L \subset \mathbb{R}^3 \subset \mathbb{R}^3 \cup \{\infty\} \cong \mathbb{S}^3$ by a planar *diagram* $D \subset \mathbb{R}^2$ consisting of the orthogonal projection of the link onto $\mathbb{R}^2$, which can be assumed to be self-transversal after a suitable horizontal (that is, height-preserving) isotopy, together with a *crossing state* for each double point, encoding which arc passes over the other. Such a diagram D uniquely determines the link L up to vertical isotopy. On the other hand, link isotopy can be represented in terms of diagrams by crossing-preserving isotopy in $\mathbb{R}^2$ and Reidemeister moves.

It is well-known that any link diagram D can be transformed into the diagram D' of a trivial link by a suitable sequence of crossing changes, that is, by inverting the state of some of its crossings. We say that D' is a *trivial state* of D.

The simplest trivial states of a link diagram D, are given by so-called ascending states (see [Li97]). Bi-ascending states of D form a larger family of trivial states of D satisfying the following crucial property (which does not hold for ascending states): any two bi-ascending states of the same knot diagram can be related by a finite sequence of bi-ascending states, each obtained from the previous by inverting a single crossing (see Proposition 4.3.2 below). Before defining the notion of bi-ascending diagram, we need to introduce some terminology.

Given a diagram D of a link $L = L_1 \cup \dots \cup L_n \subset \mathbb{R}^3$, where each $L_i \subset L$ is a component of L, we write $D = D_1 \cup \dots \cup D_n \subset \mathbb{R}^2$, with each $D_i \subset D$ being the subdiagram of D corresponding to L_i, and we refer to each $D_i \subset D$ as a *component* of D. Similarly, by an *arc* $A \subset D$ we mean any part of

D corresponding to the projection to an arc in L (not only the arcs ending at two consecutive undercrossings, as usual). Moreover, we say that A is an *ascending* arc with respect to a given orientation if, at each of its self-crossings, the subarc that comes first passes under the other one.

DEFINITION 4.3.1. A link diagram D is said to be *bi-ascending* if it is possible to number its components $D_1, \ldots, D_n$ and to choose on each D_i an orientation and two distinct points p_i and q_i away from the crossings of D in such a way that, if we denote by $A_i^\pm$ the two oriented arcs from p_i to q_i in D_i (with the sign $+$ for the arc whose orientation coincides with the chosen one for D_i), the following properties hold:

(a) D_i crosses always over D_j, for every $1 \leqslant i < j \leqslant n$;
(b) A_i^+ crosses always over A_i^-, for every $1 \leqslant i \leqslant n$;
(c) $A_i^\pm$ are both ascending arcs, for every $1 \leqslant i \leqslant n$.

We note that the crossings of a bi-ascending diagram D, as specified in the definition, are compatible with a height function which vertically separates the components, and whose restriction to each component D_i has a single local minimum at p_i and a single local maximum at q_i. Therefore, any bi-ascending diagram represents a trivial link. In particular, bi-ascending diagrams whose arcs A_i^- form no crossing coincide with ascending ones.

In the following, we simply refer to a bi-ascending trivial state of a link diagram D as a *bi-ascending state* of D. Given a link diagram D, for any choice of the numbering and orientations of its components D_i and of different non-crossing points p_i and q_i along each D_i, there is a unique bi-ascending state D' of D which satisfies the properties in the above definition, taking into account the canonical correspondence between the components D_i of D and the components D_i' of D'. On the other hand, different choices can lead to the same bi-ascending state.

The next proposition is an analog of [BP11, Proposition 1.1.3] for bi-ascending states of a diagram.

PROPOSITION 4.3.2. *Any two bi-ascending states D' and D'' of a link diagram D are related by a finite sequence $D^{(0)}, D^{(1)}, \ldots, D^{(k)}$ of bi-ascending states of D such that $D^{(0)} = D'$, $D^{(k)} = D''$ and, for every $1 \leqslant i \leqslant k$, the state $D^{(i)}$ is obtained from $D^{(i-1)}$ either by changing all the crossings between two vertically adjacent components, or by changing a single self-crossing of one component. Moreover, in the second case, the singular diagram between $D^{(i-1)}$ and $D^{(i)}$ (whose changing crossing has been replaced by a singular point) is a bi-ascending diagram of a trivial singular link. Namely, its components are vertically separated, meaning that they satisfy the property* (a) *of Definition 4.3.1, and are all bi-ascending diagrams of unknots but one, which is the 1-point union of two vertically separated bi-ascending diagrams of unknots.*

Proof. Changing all the crossings between two vertically adjacent components in a bi-ascending state of D has the effect of transposing those components. Then, by iterating this kind of operation, we can permute components as we want. Therefore, we are left to address the case when D is a knot diagram.

Let $D' \subset \mathbb{R}^2$ be a bi-ascending state of a knot diagram D. Then, the crossings of D' are uniquely determined by the choice of an orientation on D and two distinct non-crossing points p and q splitting D into two ascending arcs $A^\pm$ from p to q such that A^+ is positively oriented and crosses always over A^-.

Let us fix for the moment the orientation, and see what happens to the induced bi-ascending state D' when we move one of the points p and q along D while keeping it distinct from the other. The crossings of D' do not change until the moving point passes through a crossing of D, in which case we have one of the four situations depicted in Figure 4.3.1, depending on which is the moving point (p on the left-hand side of the figure, q on the right-hand side) and what is the relative position of the other point along the diagram. As a simple inspection shows, in the two top cases only the crossing which is passed through by the moving point changes in D'', while no crossing change occurs in the two bottom cases.

This way, we can relate any two bi-ascending states of D determined by the same orientation and by different choices of the points p and q. In particular, we can relate any bi-ascending state to an ascending one.

Concerning the orientation of D, it is enough to observe that its inversion does not affect the induced state D' when this is an ascending state. In fact, in this case the interchange of the two arcs A^+ and A^- is irrelevant, since there is no crossing between them, and hence property (b) in Definition 4.3.1 is vacuous.

For the second part of the statement, let D' be a bi-ascending state of D, and suppose that we pass from D' to a bi-ascending state D'' of D that differs from D' by a single self-crossing change of a single component. We can focus on the changing component and forget the others, that is, we can assume that

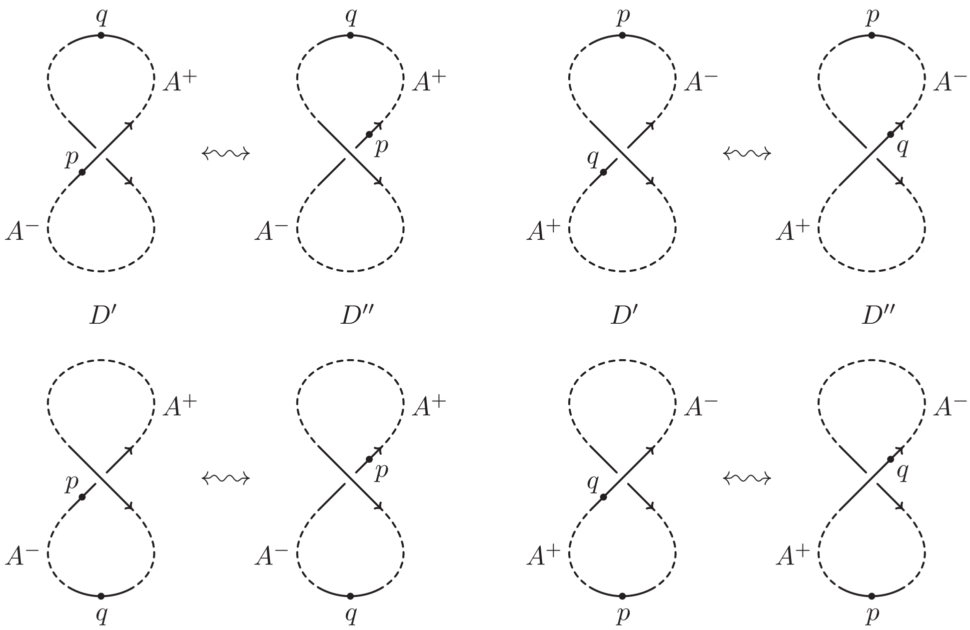

FIGURE 4.3.1. Letting p or q pass through a single crossing of D.

D is a knot diagram. Moreover, according to Definition 4.3.2 and to the proof of the first part of the statement above, we can also assume that D' and D'' are bi-ascending states of D determined by the same orientation and by different choices for the points p and q, and that they are related as in the top line of Figure 4.3.1.

In both cases, once the changing crossing is replaced by a singular point s, the resulting loops are easily seen to be bi-ascending, with one always crossing over the other. Namely, if the moving point is p, then the upper loop is bi-ascending and determined by s and q with the inherited orientation, while the lower one is ascending and starting from s with the opposite orientation. On the other hand, if the moving point is q, then the upper loop is ascending and starting from s with the inherited orientation, while the lower one is bi-ascending and determined by p and s with the opposite orientation. □

4.4. Definition of the inverse functor $\overline{\Phi} : \mathbf{4KT} \to \mathbf{4Alg}$

Given a Kirby tangle $T : E_{2s} \to E_{2t}$ in 4KT, we will now explain how to construct a morphism $\overline{\Phi}(T) : H^s \to H^t$ in 4Alg whose image $\Phi(\overline{\Phi}(T))$ under the functor Φ is the 2-equivalence class of T. The construction depends on some choices, but in the next subsections we will show that different choices lead to equivalent morphisms in 4Alg, so that $\overline{\Phi}(T)$ depends only on the Kirby tangle T up to 2-deformations. Moreover, the assignment respects compositions and identities, therefore it defines a functor $\overline{\Phi} : 4\mathrm{KT} \to 4\mathrm{Alg}$.

We represent T by a strictly regular planar diagram, which is a composition of tensor products of elementary diagrams in Table 3.1.1, and, up to composing it on the top and on the bottom with identity morphisms, we will assume that T is of the form represented in the leftmost diagram of Figure 4.4.1 (see

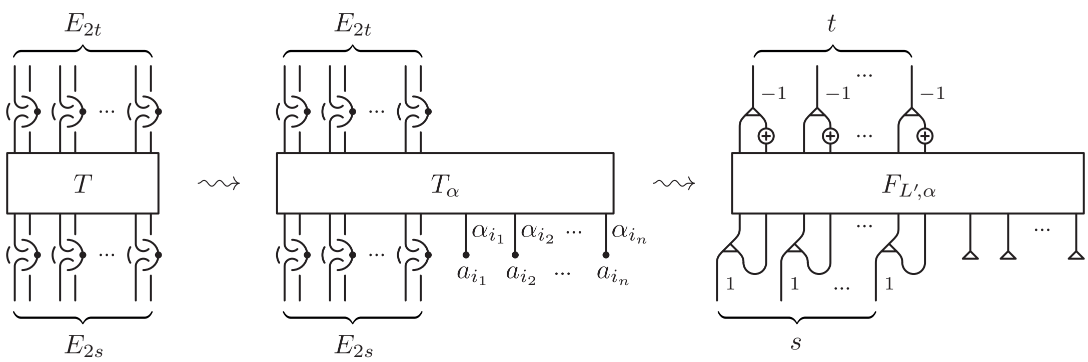

FIGURE 4.4.1. Outline of the construction of $\overline{\Phi}(T)$.

Proposition 3.1.5 and Remark 3.3.5). Let $B_1, \ldots, B_m \subset \,]0,1[^2$ be the planar projections of the disjoint disks spanned by the dotted unknots $U_1, \ldots, U_m$ of T, and let L be the strictly regular planar subdiagram which represents the blackboard framed link formed by the closed undotted components of T. Then, the construction of the morphism $\overline{\Phi}(T)$ is achieved by the following steps, illustrated in Figure 1.1.3):

(1) Choose a numbering $L = L_1 \cup \cdots \cup L_n$ of the components of L and, on each component L_i, choose both an orientation and a pair of points p_i and q_i inducing a bi-ascending state $L' = L'_1 \cup \cdots \cup L'_n$ of L. In particular, we require that L'_i crosses always over L'_j for any $i < j$, and that the positively oriented ascending arc determined by p_i and q_i crosses over the negatively oriented one (see Definition 4.3.1). Mark with small gray disks $C_1, \ldots, C_\ell$ the crossings of L that have to be inverted in order to get L' (see Figure 4.4.2).

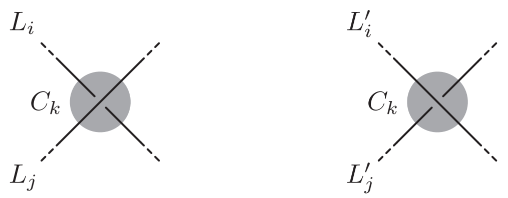

FIGURE 4.4.2. The disk C_k and the diagrams D and D' at a changing crossing, $i \leqslant j$.

(2) Fix n points $a_1, a_2, \ldots, a_n \in [0,1] \times \{0.1\} \subset [0,1]^2$ on the bottom right of the projection plane (their numbering is not required to respect the natural order of the segment $[0,1] \times \{0.1\}$), and choose n embedded arcs $\alpha_i : [0,1] \to [0,1]^2$ such that $\alpha_i(0) = a_i$ and $\alpha_i(1) = b_i \in L_i$. Each α_i is required to form regular crossings both with L and among themselves, with crossing states that can be arbitrarily chosen (see the middle diagram in Figure 4.4.1). Assume also that each α_i avoids the crossings of L, the points p_i and q_i, the disks $B_1, \ldots, B_m$, and local maxima and minima of L in the plane diagram. Since L'_i is a bi-ascending state of L_i, the points p_i, q_i, and b_i divide L_i in three arcs $L_i = L_i^1 \cup L_i^2 \cup L_i^3$, numbered in such a way that either $b_i = L_i^1 \cap L_i^2$ or $b_i = L_i^2 \cap L_i^3$ and that, if we denote by $(L_i^j)'$ the corresponding arcs of L', then $(L_i^j)'$ crosses always over $(L_i^k)'$ if $j < k$ (see Figure 4.4.3, where the arrows indicate the preferred orientation of the bi-ascending state of L_i). For every $1 \leqslant i \leqslant n$, set $L_{i,\alpha} = L_i \cup \alpha_i$ and $L'_{i,\alpha} = L'_i \cup \alpha_i$. Furthermore, set $\alpha = \{\alpha_i\}_{i=1}^n$, $L_\alpha = L_{1,\alpha} \cup \cdots \cup L_{n,\alpha}$, and $L'_\alpha = L'_{1,\alpha} \cup \cdots \cup L'_{n,\alpha}$. Then, for every $1 \leqslant i \leqslant n$, mark with small gray disks as above the crossings formed by the arc α_i and by L in which one of the following things happen:

(a) α_i crosses either under $L_{j,\alpha}$ for $i < j$ or over $L_{j,\alpha}$ for $i > j$;
(b) α_i crosses either under $L_i^2 \cup L_i^3$ or over L_i^1 with $b_i = L_i^1 \cap L_i^2$;
(c) α_i crosses either under L_i^3 or over $L_i^1 \cup L_i^2$ with $b_i = L_i^2 \cap L_i^3$.

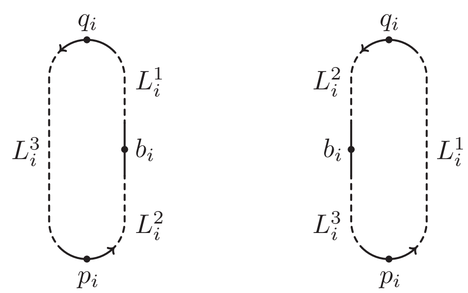

FIGURE 4.4.3. Possible subdivisions of $L_i = L_i^1 \cup L_i^2 \cup L_i^3$.

(3) Replace each elementary diagram of L_α as indicated by the arrows on the left-hand side of Figures 4.4.4 and 4.4.5, where $f_i = 1 - \mathrm{wr}(L'_i)$ with $\mathrm{wr}(L'_i)$ denoting the algebraic sum of the signs of all crossings in L'_i. In particular, the replacement for a crossing depends on whether it is marked as a changing crossing or not, the image being X or Y in the case of a unmarked crossing, and $\widehat{X}$ or $\widehat{Y}$ otherwise. Replace also the dotted components of T and the identity morphisms lying outside of the T_α-labeled box as prescribed by the arrows on the left-hand side of Figure 4.4.6. Then $\overline{\Phi}(T) = \overline{\Phi}_{L',\alpha}(T)$ is defined as (see the right-hand side of Figure 4.4.1)

$$\overline{\Phi}(T) = \overline{\Phi}_{L',\alpha}(T) = \overline{W}^{\otimes t} \circ F_{L',\alpha} \circ \left(W^{\otimes s} \otimes \eta^{\otimes n}\right),$$

where $\overline{W} = \mu \circ (\tau^{-1} \otimes S)$, where $W = (\mu \otimes \tau) \circ (\mathrm{id} \otimes \mathrm{coev})$ (see Figure 4.4.6), and where the morphism $F_{L',\alpha}$ belongs to the subcategory TAlg of 4Alg.

The notation $\overline{\Phi}_{L',\alpha}(T)$ highlights the choice of the bi-ascending state L' and of the arcs α_i for $1 \leqslant i \leqslant n$, as required by the construction. In Subsection 4.6 (see Propositions 4.6.2, 4.6.3, 4.6.6, and 4.6.7) we will show that the 2-equivalence class of $\overline{\Phi}_{L',\alpha}(T)$ is independent of such choices, and that it only depends on the 2-equivalence class of T. This will justify the notation $\overline{\Phi}(T)$.

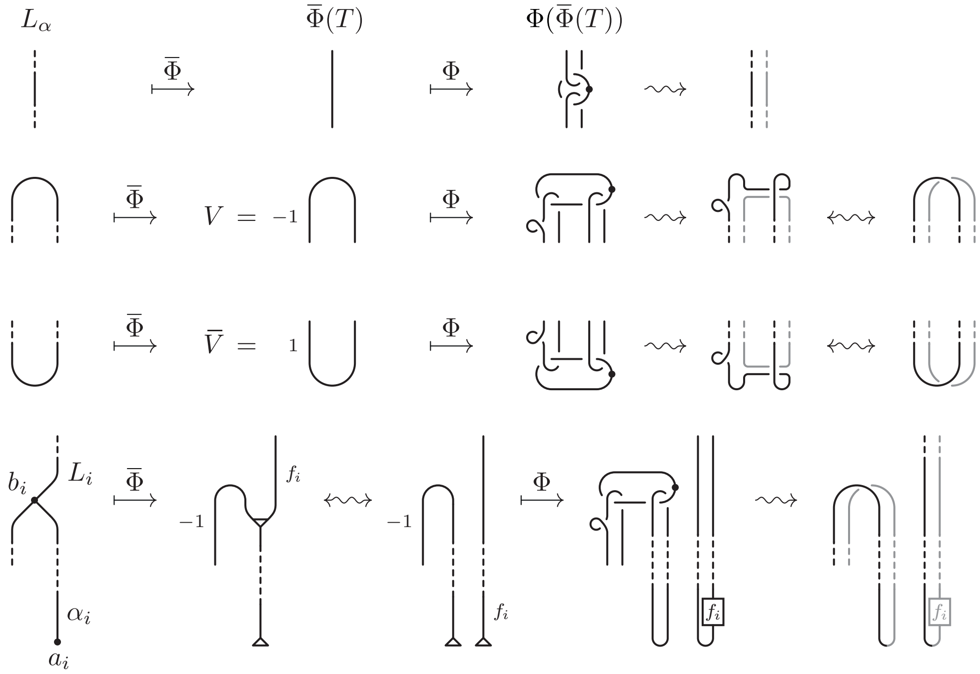

FIGURE 4.4.4. Definition of $\overline{\Phi}(T)$ and its image under Φ – Part 1.

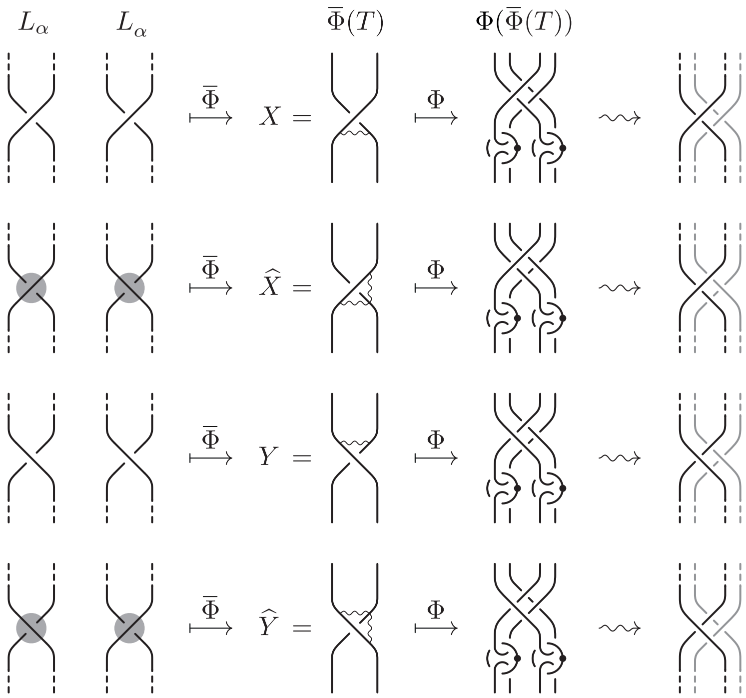

FIGURE 4.4.5. Definition of $\overline{\Phi}(T)$ and its image under Φ – Part 2.

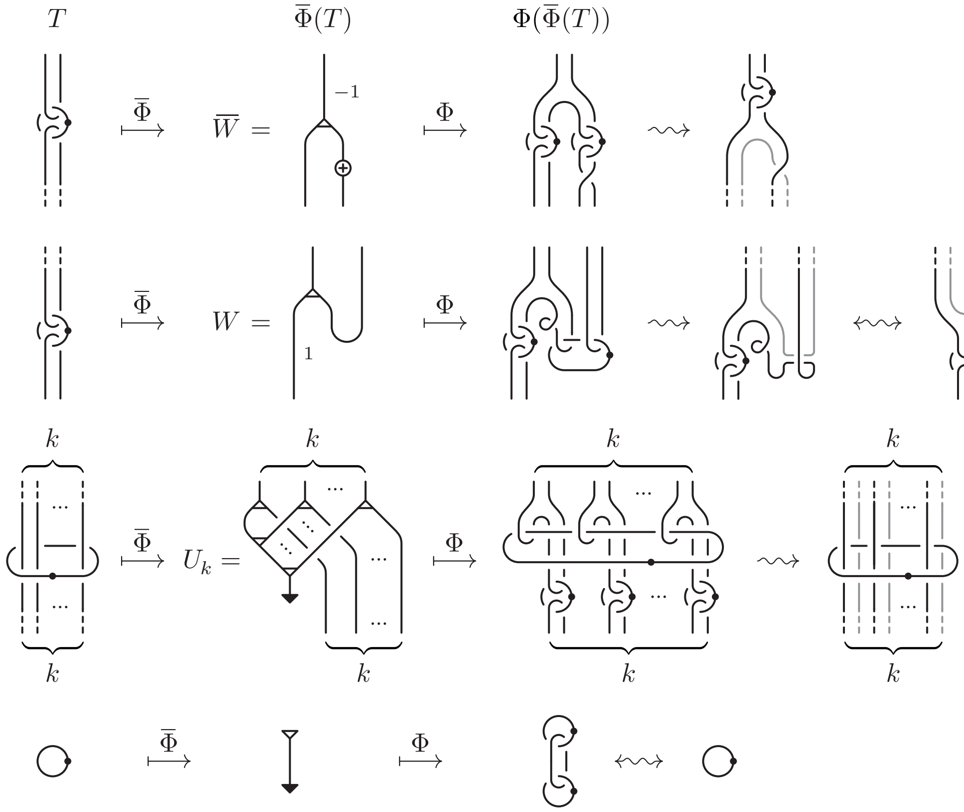

FIGURE 4.4.6. Definition of $\overline{\Phi}(T)$ and its image under Φ – Part 3 ($k \geqslant 1$).

Later, in Proposition 4.6.2, we will show that the conditions imposed in Step (2) on the arcs α_i for $1 \leqslant i \leqslant n$ can be weakened to exclude (b) and (c). Nevertheless, considering for now only arcs α_i that satisfy those two conditions as well makes it much easier to see that $\overline{\Phi}$ is the inverse of Φ in the next proposition.

PROPOSITION 4.4.1. *$\Phi(\overline{\Phi}(T)) = T$ for every Kirby tangle T in* 4KT.

Proof. Before applying the functor Φ, we modify $\overline{\Phi}(T)$ by sliding the coproduct Δ that appears in the image of the attaching point of each α_i (see the last line in Figure 4.4.4) along $\overline{\Phi}(\alpha_i)$ until it reaches the unit at its end. Then, we apply (*a7*) in Table 2.2.1 to split $\overline{\Phi}(\alpha_i)$ into two parallel arcs (see the first two steps in Figure 4.4.7). We recall that sliding along coev and ev morphisms transforms Δ in $\widetilde{\mu}$ and vice-versa (see (*q2*) and (*q3*) in Table 2.5.1 and the first two lines of Figure 2.5.2), while sliding Δ through U_k and through the decorated crossings uses (*u2*), (*c18*), (*c19*), (*c24*), and (*c25*) in Table 4.2.10. We observe that, in this last case, the crossing splits into two crossings of the same type. Therefore, the resulting morphism $F_{L',\beta}$ still lies in the subcategory TAlg of 4Alg.

Since Φ is a monoidal functor, the morphism $\Phi(\overline{\Phi}(T))$ is given by the corresponding composition of tensor products of the diagrams represented on the right-hand side of Figures 4.4.4, 4.4.5, and 4.4.6, where the rightmost diagrams are obtained from the previous ones by 2-handle slides and 1/2-handle cancellations.

Comparing T and $\Phi(\overline{\Phi}(T))$, we observe the following.

- Each component L_i has been isotoped by pulling a small arc in a neighborhood of b_i all the way down to the bottom-right part of the diagram through a narrow blackboard-parallel band β_i obtained by doubling α_i. Denote by $L_\beta = L_{\beta,1} \cup \cdots \cup L_{\beta,n}$ the resulting link diagram. Observe that, in Step (2) above, the signed crossings between α_i and L_α have been chosen in such a way that, by inverting both them and the signed crossings identified in Step (1), we obtain a bi-ascending state $L'_\beta = L'_{\beta,1} \cup \cdots \cup L'_{\beta,n}$ of L_β with respect to the same choice of numbering, orientations, and points p_i and q_i.
- The link L_β, represented in black in the rightmost diagrams in Figures 4.4.4, 4.4.5, and 4.4.6, has been "doubled" by a copy of the trivial link, represented by the bi-ascending diagram L'_β in gray, which lies below the original Kirby tangle T.

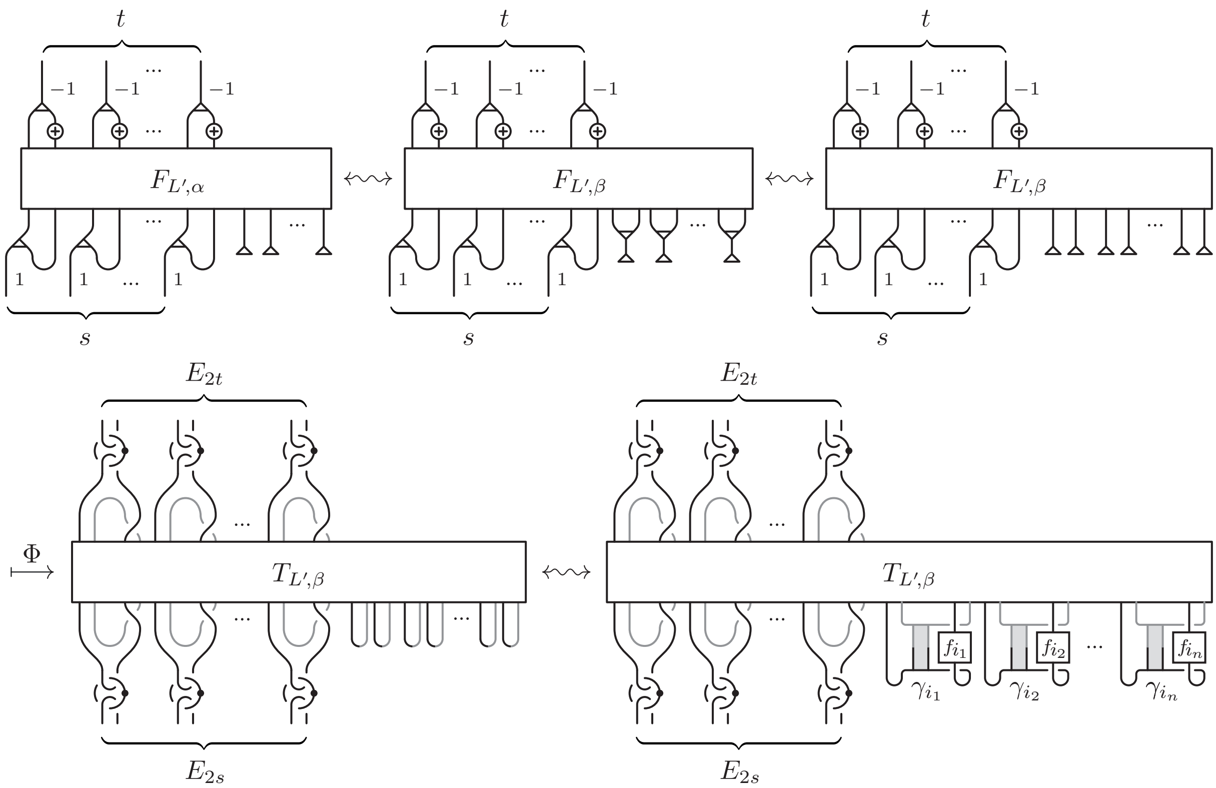

FIGURE 4.4.7. $\Phi \circ \overline{\Phi}(T)$.

- ⋄ Each component $L'_{\beta,i}$ is connected to the corresponding component $L_{\beta,i}$ by a band γ_i, shown in gray in the bottom-right part of Figure 4.4.7, that merge the ends of the two copies of β_i in $L_{\beta,i}$ and $L'_{\beta,i}$.

A three-dimensional view of $\Phi(\overline{\Phi}(T))$ in the spacial case when the points a_i are ordered from left to right is presented in Figure 4.4.8. Therefore, the Kirby tangle $\Phi(\overline{\Phi}(T))$ can be isotoped to the original one T by first contracting all the unknots of $L'_{\beta,i}$, and then retracting the corresponding bands β_i one by one. □

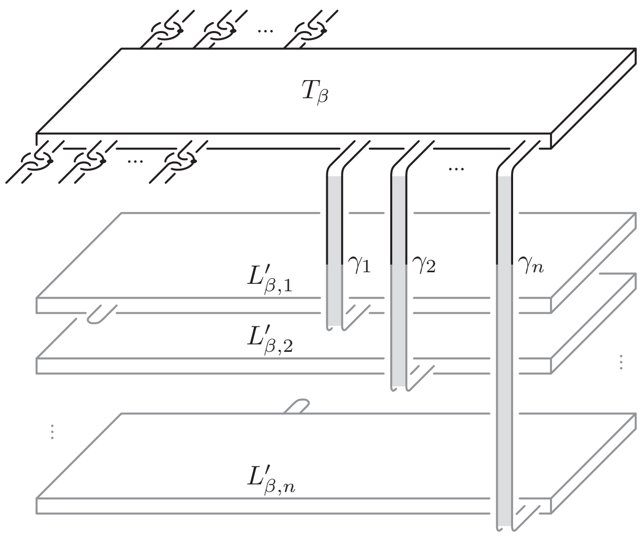

FIGURE 4.4.8. Three-dimensional view of $\Phi(\overline{\Phi}(T))$ in the spacial case when the points a_i are ordered from left to right. Notice that, for levels from 1 to n, there is either a single cap on the top (like for level n in this example), or a single cup on the bottom (like for level 1 in this example), or nothing at all (like for level 2 in this example), depending on whether the corresponding undotted component of the original tangle T, before composing with identities, was either open on the top, or open on the bottom, or closed, respectively.

4.5. The category MAlg

As we have seen in the previous subsection, $\overline{\Phi}(T)$ encodes algebraically a multiple-level Kirby tangle, and in order to prove that $\overline{\Phi}$ is a well-defined functor, we need to develop suitable algebraic tools that allow us to work with such structures. The main idea is to consider a category MAlg that is similar to TAlg, but whose objects and morphisms carry labels. In other words, objects are tensor products $H_{\underline{i}} = H_{i_1} \otimes H_{i_2} \otimes \ldots \otimes H_{i_k}$ with $i_\ell \geqslant 0$ for $0 \leqslant \ell \leqslant k$, while morphisms are labeled versions of the corresponding morphisms of 4Alg. The images of the morphisms of MAlg under Φ satisfy the same conditions (a) and (b) in Remark 4.2.3 as morphisms of TAlg, but, in addition, the lower (grey) arc of each undotted component of label i stays above the lower (grey) arc of each undotted component of label $j > i$; in other words, labels denote the "depth" of those arcs in the corresponding Kirby tangle.

Here is the formal definition.

Definition 4.5.1. We denote by $\mathrm{MAlg}^{\mathrm{F}}$ the strict monoidal category freely generated by objects H_i for $i \geqslant 0$ and by morphisms

$$\begin{gathered}
\mathrm{ev}_i : H_i \otimes H_i \to \mathbb{1} \text{ for } i \geqslant 1, \\
\Delta_i : \mathbb{1} \to H_i \otimes H_i \text{ for } i \geqslant 1, \\
\varepsilon_i : H_i \to \mathbb{1} \text{ for } i \geqslant 1, \\
\Lambda_i : \mathbb{1} \to H_i \text{ for } i \geqslant 1, \\
\tau_i : H_i \to H_i \text{ for } i \geqslant 1, \\
X_{i,j}, \widehat{Y}_{i,j} : H_i \otimes H_j \to H_j \otimes H_i \text{ for } 1 \leqslant i \leqslant j, \\
\widehat{X}_{i,j}, Y_{i,j} : H_i \otimes H_j \to H_j \otimes H_i \text{ for } i \geqslant j \geqslant 1, \\
W_i : H_0 \to H_i \otimes H_i \text{ for } i \geqslant 1, \\
\overline{W}_i : H_i \otimes H_i \to H_0 \text{ for } i \geqslant 1, \\
U_{\underline{i}} = U_{i_1,\ldots,i_k} : H_{i_1} \otimes \ldots \otimes H_{i_k} \to H_{i_1} \otimes \ldots \otimes H_{i_k} \text{ for } k \geqslant 1 \text{ and } i_1, \ldots, i_k \geqslant 1
\end{gathered}$$

Let $\mathscr{F} : \mathrm{MAlg}^{\mathrm{F}} \to 4\mathrm{Alg}$ denote the natural forgetful functor that discards labels; in particular, $\mathscr{F}(H_i) = H$ for every $i \geqslant 0$, $\mathscr{F}(U_{i_1,\ldots,i_k}) = U_k$, and each of the remaining generating morphisms is sent by $\mathscr{F}$ to the morphism of 4Alg carrying the same name without indices. Then, we denote by MAlg the quotient category $\mathrm{MAlg}^{\mathrm{F}} / \ker \mathscr{F}$.

The diagrammatic notation for the morphisms in the image of $\mathscr{F}$ is introduced in Figure 4.5.1. In particular, we represent $\mathscr{F}(F_{\underline{i},\underline{j}})$ by a box that contains in its lower (respectively upper) part the labels of the string in the source (respectively target) of $F_{\underline{i},\underline{j}}$.

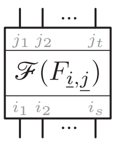

Figure 4.5.1. Diagrammatic notation for $\mathscr{F}(F_{\underline{i},\underline{j}})$, where $\underline{i} = (i_1, \ldots, i_s)$ and $\underline{j} = (j_1, \ldots, j_t)$.

We will now define a family of natural transformations Θ^{L}_k for $k \geqslant 1$ designed to provide the algebraic analogue of a dotted component that embraces the kth level, while passing below the ith level, for $0 \leqslant i \leqslant k-1$, and above the jth level, for $j \geqslant k+1$.

Definition 4.5.2. For all $k \geqslant 1$ and $\underline{i} = (i_1, i_2, \ldots, i_\ell)$, with $\ell \geqslant 0$ and $i_h \geqslant 0$ for every $1 \leqslant h \leqslant \ell$, the morphisms $\gamma_{\underline{i},k} : H^\ell \otimes H \to H \otimes H^\ell$ and $\Theta^{\mathrm{L}}_{\underline{i},k} : H^\ell \otimes H \to H^\ell$ of 4Alg are recursively defined by the following identities:

$$\begin{gathered}
\gamma_{\varnothing,k} = \mathrm{id}, \quad \Theta^{\mathrm{L}}_{\varnothing,k} = \varepsilon, \\
\gamma_{(i),k} = \begin{cases} c & \text{if } i \leqslant k, \\ \widehat{X} & \text{if } i > k, \end{cases} \quad \Theta^{\mathrm{L}}_{(i),k} = \begin{cases} \mu & \text{if } i = k, \\ \mathrm{id} \otimes \varepsilon & \text{if } i \neq k, \end{cases} \\
\gamma_{\underline{i},k} = (\gamma_{(i_1),k} \otimes \mathrm{id}_{\ell-1}) \circ (\mathrm{id} \otimes \gamma_{(i_2,\ldots,i_\ell),k}), \\
\Theta^{\mathrm{L}}_{\underline{i},k} = (\Theta^{\mathrm{L}}_{(i_1),k} \otimes \Theta^{\mathrm{L}}_{(i_2,\ldots,i_\ell),k}) \circ (\mathrm{id} \otimes \gamma_{(i_2,\ldots,i_\ell),k} \otimes \mathrm{id}) \circ (\mathrm{id}_\ell \otimes \Delta).
\end{gathered}$$

We denote by Θ^{L}_k the collection of morphisms $\{\Theta^{\mathrm{L}}_{\underline{i},k} \mid \underline{i} \in \mathbb{N}^\ell, \ell \in \mathbb{N}\}$.

Proposition 4.5.3. *If* $\mathscr{F} : \mathrm{MAlg} \to 4\mathrm{Alg}$ *denotes the forgetful functor that discards labels, then* $\Theta^{\mathrm{L}}_k : \mathscr{F} \otimes H \Rightarrow \mathscr{F}$ *defines a natural transformation, meaning that, for every morphism* $F_{\underline{i},\underline{j}} : H_{\underline{i}} \to H_{\underline{j}}$ *in* MAlg*, we have (see Figure 4.5.2):*

$$\Theta^{\mathrm{L}}_{\underline{j},k} \circ (\mathscr{F}(F_{\underline{i},\underline{j}}) \otimes \mathrm{id}) = \mathscr{F}(F_{\underline{i},\underline{j}}) \circ \Theta^{\mathrm{L}}_{\underline{i},k}. \qquad (t2)$$

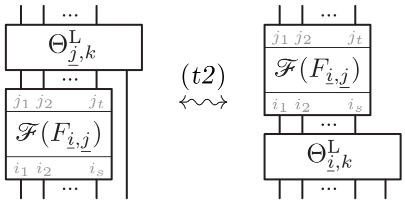

Figure 4.5.2. Naturality of Θ^{L}_k.

Before proceeding to the proof of Proposition 4.5.3, in Figure 4.5.3 we present a specific example of the natural transformation $\Theta^{\mathrm{L}}_{\underline{i},k} : \mathscr{F}(H_{\underline{i}}) \otimes H \to \mathscr{F}(H_{\underline{i}})$ and its image under the functor Φ. Notice that, since Θ^{L}_k is a natural transformation between functors with source MAlg and target 4Alg, it is a collection of morphisms in the target category (which are unlabeled), one for every object in the source category (which are labeled). In other words, $\Theta^{\mathrm{L}}_{\underline{i},k}$ does not really carry labels, but its definition depends on the labeled object $H_{\underline{i}}$. Therefore, the labels attached to the morphisms represented in Figure 4.5.3 and below indicate that these morphisms are in the image of $\mathscr{F}$, but keeping track of labels in pictures will allow us to understand which form of Θ^{L}_k we need to use.

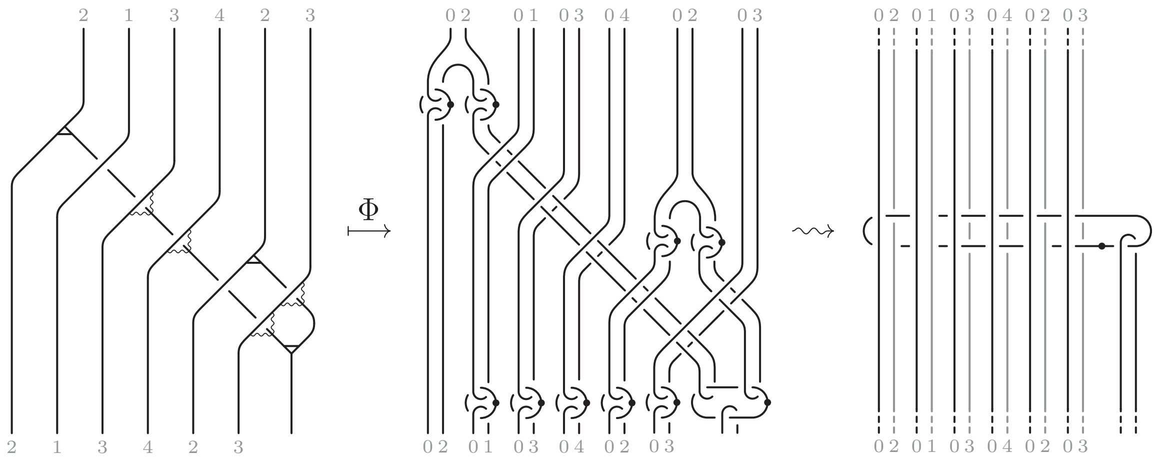

Figure 4.5.3. The morphism $\Theta^{\mathrm{L}}_{\underline{i},k} : \mathscr{F}(H_{\underline{i}}) \otimes H \to \mathscr{F}(H_{\underline{i}})$ for $\underline{i} = (2,1,3,4,2,3)$ and $k = 2$, and its image under the functor $\Phi : 4\mathrm{Alg} \to 4\mathrm{KT}$.

Lemma 4.5.4. *If* $\underline{i} = (i_1, \ldots, i_h, i_{h+1}, \ldots, i_\ell)$ *with* $\ell \geqslant 1$ *and* $1 \leqslant h < \ell$*, then*

$$\Theta^{\mathrm{L}}_{\underline{i},k} = (\Theta^{\mathrm{L}}_{(i_1,\ldots,i_h),k} \otimes \Theta^{\mathrm{L}}_{(i_{h+1},\ldots,i_\ell),k}) \circ (\mathrm{id}_h \otimes \gamma_{(i_{h+1},\ldots,i_\ell),k} \otimes \mathrm{id}) \circ (\mathrm{id}_\ell \otimes \Delta).$$

Proof. For $h = 1$ and for any $\ell \geqslant 1$, the statement is true by definition of $\Theta^{\mathrm{L}}_{\underline{i},k}$. Then the claim follows by induction on h. The proof of the inductive step is presented in Figure 4.5.4, where the first step follows from the definition of $\Theta^{\mathrm{L}}_{\underline{i},k}$, while the second step follows from the inductive hypothesis and the decomposition of $\gamma_{(i_2,\ldots,i_\ell),k}$ as $(\gamma_{(i_2,\ldots,i_h),k} \otimes \mathrm{id}_{\ell-h}) \circ (\mathrm{id}_{h-1} \otimes \gamma_{(i_{h+1},\ldots,i_\ell),k})$. Then, for the third step, we apply the coassociativity axiom (*a3*) to collect together the rightmost strands in the sources of the two copies of $\gamma_{(i_{h+1},\ldots,i_\ell),k}$, and use (*c18-24*) to push the resulting Δ past them. Finally, we apply once more the defining relation of $\Theta^{\mathrm{L}}_{(i_1,\ldots,i_h),k}$. $\square$

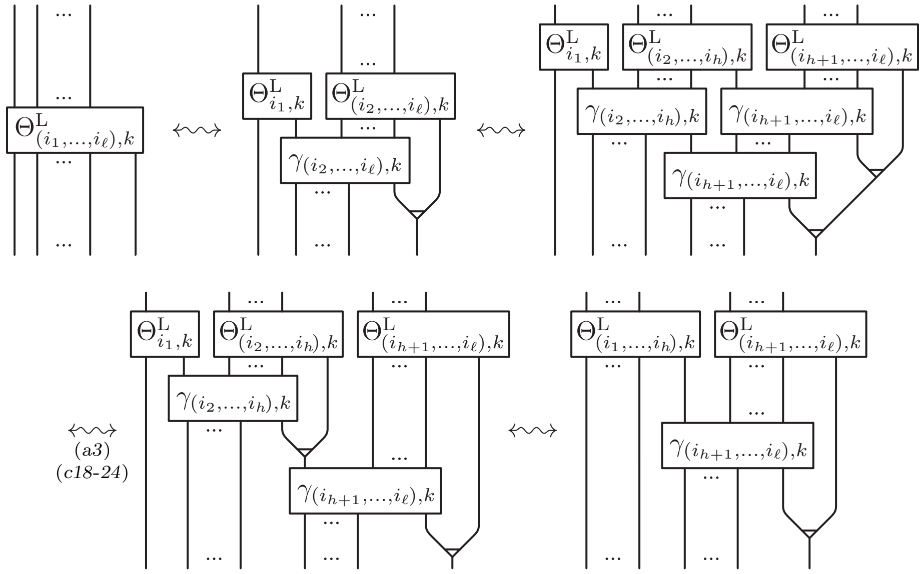

FIGURE 4.5.4. Proof of the inductive step of Lemma 4.5.4.

Proof of Proposition 4.5.3. We will first prove the statement in the case where $F_{\underline{i},\underline{j}}$ is a generating morphism of MAlg. We observe that ($t2$) holds trivially if none of the edges of $F_{\underline{i},\underline{j}}$ is labeled by k, while it follows from ($t1$) in Proposition 4.2.7 if all incoming and outgoing edges of $F_{\underline{i},\underline{j}}$ are labeled by k, since in this case both $\Theta^{\mathrm{L}}_{\underline{i},k}$ and $\Theta^{\mathrm{L}}_{\underline{j},k}$ coincide with Θ_k. Moreover, the proof for $\overline{W}_i$ is identical to the proof of ($t1$) for V in Figure 4.2.9, while ($t2$) for W_i follows directly by applying the bialgebra axiom ($a5$) and the property of the integral element ($i2'$). On the other hand, when $F_{\underline{i},\underline{i}} = U_{\underline{i}}$, then ($t2$) follows directly from the associativity axiom ($a1$).

In order to complete the proof of ($t2$) for the generating morphisms of MAlg, it remains to consider the case where $F_{\underline{i},\underline{j}}$ is a decorated crossing, meaning one of the morphisms $X_{i,j}, Y_{i,j}, \widehat{X}_{i,j}, \widehat{Y}_{i,j}$, with exactly one of the indices i or j equal to k. Since, according to Lemma 4.2.2, we have $Y_{i,j} = X^{-1}_{j,i}$ and $\widehat{Y}_{i,j} = \widehat{X}^{-1}_{j,i}$, it is enough to prove the statement for $X_{i,k}$ and $\widehat{X}_{k,i}$ if $i < k$, and for $\widehat{X}_{i,k}$ and $X_{k,i}$ if $i > k$. This is done in Figure 4.5.5.

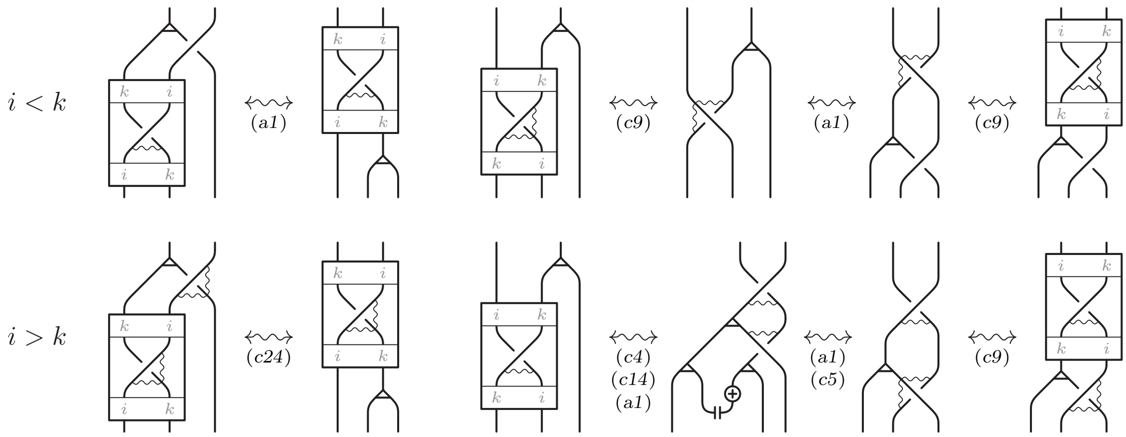

FIGURE 4.5.5. Naturality of Θ^{L}_k with respect to decorated crossings with mixed labels.

Now, by Lemma 4.5.4, the claim will follow for every morphism $F_{\underline{i},\underline{j}} : H_{\underline{i}} \to H_{\underline{j}}$ in MAlg if we can show that

$$\gamma_{\underline{j},k} \circ (\mathscr{F}(F_{\underline{i},\underline{j}}) \otimes \mathrm{id}) = (\mathrm{id} \otimes \mathscr{F}(F_{\underline{i},\underline{j}})) \circ \gamma_{\underline{i},k}. \tag{g1}$$

every time $F_{\underline{i},\underline{j}}$ is a generating morphism of MAlg. Observe that, if no label of $F_{\underline{i},\underline{j}}$ is strictly greater than k, then ($g1$) follows from the naturality of the braiding. On the other hand, if all of its labels are strictly greater than k, then it follows from ($c24$-25).

Therefore, we are left to prove (*g1*) for morphisms $F_{\underline{i},\underline{j}}$ in which some of the labels are strictly greater than k, and some are not. In this case, $F_{\underline{i},\underline{j}}$ is either a decorated crossing, or W_i or $\overline{W}_i$ for $i > k$. For what concerns decorated crossings, we observe that, thanks to Lemma 4.2.2 once again, it is enough to prove (*g1*) for $X_{i,j}$ and $\widehat{X}_{j,i}$ with $i \leqslant k < j$. This is done in Figure 4.5.6. The proofs for $\overline{W}_i$ and W_i with $i > k$ is shown in Figure 4.5.7. □

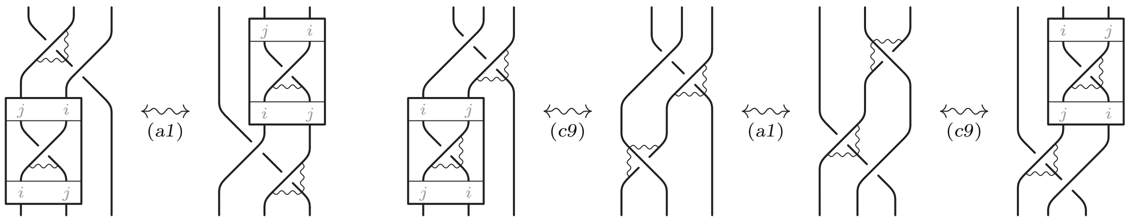

FIGURE 4.5.6. Naturality of $\gamma_{\underline{i},k}$ with respect to decorated crossings with $i \leqslant k < j$.

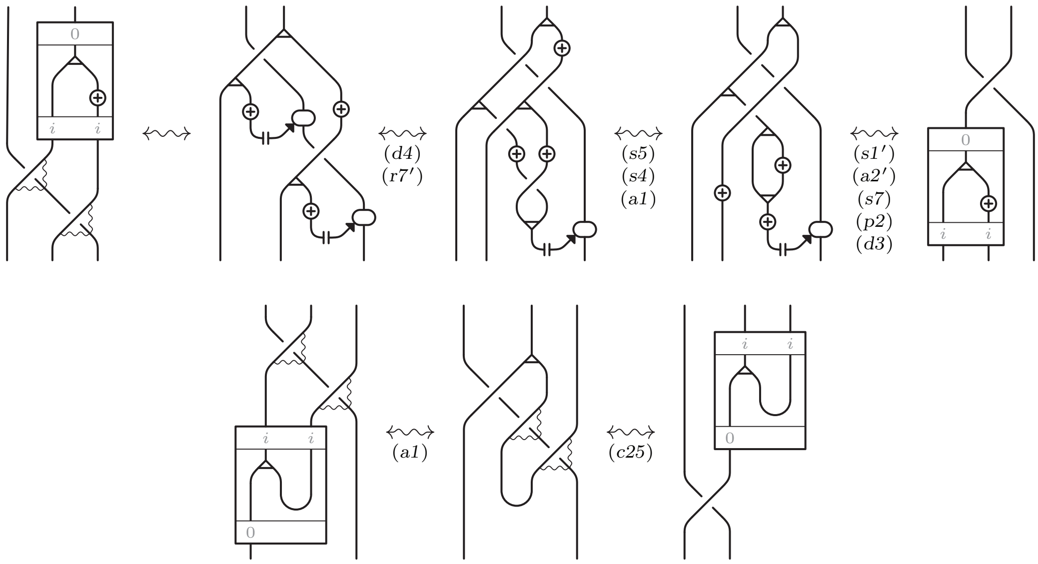

FIGURE 4.5.7. Naturality of $\gamma_{\underline{i},k}$ with respect to the morphisms $\mathscr{F}(\overline{W}_i)$ and $\mathscr{F}(W_i)$ with $i > k$.

Finally, we will define a family of natural transformations $\widehat{\Theta}^{\mathrm{L}}_k$ for $k \geqslant 0$ designed to provide the algebraic analogue of a dotted component that embraces the kth level, while passing below the $i$the level, for $1 \leqslant i \leqslant k-1$, and above the jth level, for $k+1 \leqslant j \leqslant n$, composed with a positive double braiding between the strands of the kth and $(k+1)$st level (see Figure 4.5.8).

DEFINITION 4.5.5. For all $k \geqslant 1$ and $\underline{i} = (i_1, i_2, \ldots, i_\ell)$, with $\ell \geqslant 0$ and $i_h \geqslant 0$ for every $1 \leqslant h \leqslant \ell$, the morphisms $\widehat{\gamma}_{\underline{i},k} : H^\ell \otimes H \to H \otimes H^\ell$ and $\widehat{\Theta}^{\mathrm{L}}_{\underline{i},k} : H^\ell \otimes H \to H^\ell$ in 4Alg are recursively defined by the following identities:

$$\widehat{\gamma}_{\varnothing,k} = \mathrm{id}, \quad \widehat{\Theta}^{\mathrm{L}}_{\varnothing,k} = \varepsilon,$$

$$\widehat{\gamma}_{(i),k} = \begin{cases} c & \text{if } i \leqslant k, \\ X & \text{if } i = k+1, \\ \widehat{X} & \text{if } i > k+1, \end{cases} \quad \widehat{\Theta}^{\mathrm{L}}_{(i),k} = \begin{cases} \mu & \text{if } i = k, \\ \mathrm{id} \otimes \varepsilon & \text{if } i \neq k, \end{cases}$$

$$\widehat{\gamma}_{\underline{i},k} = (\widehat{\gamma}_{(i_1),k} \otimes \mathrm{id}_{\ell-1}) \circ (\mathrm{id} \otimes \widehat{\gamma}_{(i_2,\ldots,i_\ell),k}),$$

$$\widehat{\Theta}^{\mathrm{L}}_{\underline{i},k} = (\widehat{\Theta}^{\mathrm{L}}_{(i_1),k} \otimes \widehat{\Theta}^{\mathrm{L}}_{(i_2,\ldots,i_\ell),k}) \circ (\mathrm{id} \otimes \widehat{\gamma}_{(i_2,\ldots,i_\ell),k} \otimes \mathrm{id}) \circ (\mathrm{id}_\ell \otimes \Delta).$$

We denote by $\widehat{\Theta}^{\mathrm{L}}_k$ the collection of morphisms $\{\widehat{\Theta}^{\mathrm{L}}_{\underline{i},k} \mid \underline{i} \in \mathbb{N}^\ell, \ell \in \mathbb{N}\}$.

A specific example of the natural transformation $\widehat{\Theta}^{\mathrm{L}}_{\underline{i},k}$ can be found in Figure 4.5.8. Observe that the only difference between $\Theta^{\mathrm{L}}_{\underline{i},k}$ and $\widehat{\Theta}^{\mathrm{L}}_{\underline{i},k}$ is in the crossing with the $(k+1)$-labeled strand.

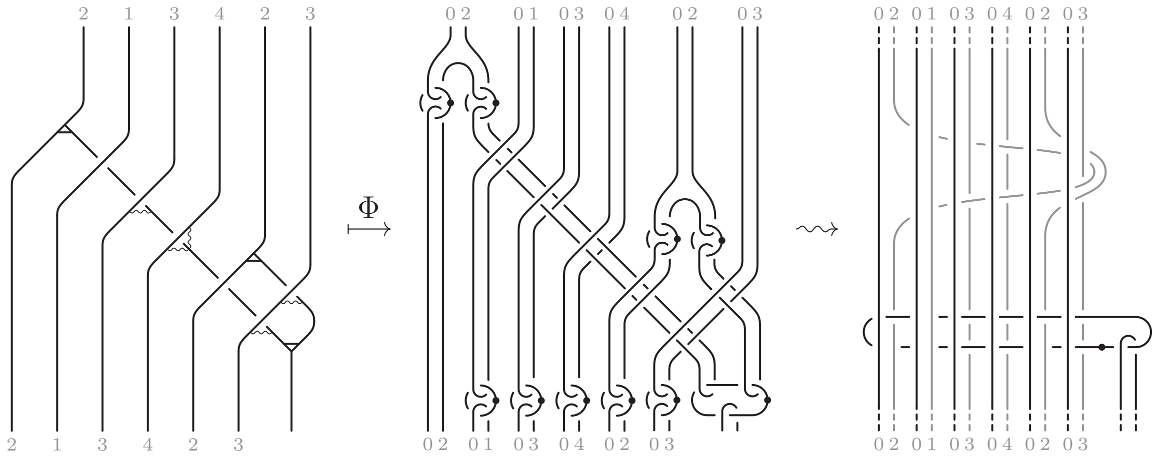

FIGURE 4.5.8. The morphism $\widehat{\Theta}^{\mathrm{L}}_{\underline{i},k} : \mathscr{F}(H_{\underline{i}}) \otimes H \to \widehat{\mathscr{F}}_k(H_{\underline{i}})$ for $\underline{i} = (2,1,3,4,2,3)$ and $k = 2$.

LEMMA 4.5.6. *If $\underline{i} = (i_1, \dots i_h, i_{h+1}, i_\ell)$ with $\ell \geqslant 1$ and $1 \leqslant h < \ell$, then*

$$\widehat{\Theta}^{\mathrm{L}}_{\underline{i},k} = (\widehat{\Theta}^{\mathrm{L}}_{(i_1,\dots i_h),k} \otimes \widehat{\Theta}^{\mathrm{L}}_{(i_{h+1},\dots,i_\ell),k}) \circ (\mathrm{id}_h \otimes \widehat{\gamma}_{(i_{h+1},\dots,i_\ell),k} \otimes \mathrm{id}) \circ (\mathrm{id}_\ell \otimes \Delta).$$

Proof. The proof proceeds by induction on h, and it is completely analogous to the proof of Lemma 4.5.4 (see Figure 4.5.4). □

PROPOSITION 4.5.7. *For every $k \geqslant 1$, there exists a unique functor $\widehat{\mathscr{F}}_k : \mathrm{MAlg} \to 4\mathrm{Alg}$ that first exchanges the object H_k with H_{k+1} and the morphisms $X_{k,k+1}, \widehat{Y}_{k,k+1} : H_k \otimes H_{k+1} \to H_{k+1} \otimes H_k$ with $\widehat{X}_{k+1,k}, Y_{k+1,k} : H_{k+1} \otimes H_k \to H_k \otimes H_{k+1}$, respectively, and then discards labels. Furthermore, $\widehat{\Theta}^{\mathrm{L}}_k : \mathscr{F} \otimes H \Rightarrow \widehat{\mathscr{F}}_k$ defines a natural transformation, meaning that, for every morphism $F_{\underline{i},\underline{j}} : H_{\underline{i}} \to H_{\underline{j}}$ in MAlg, we have (see Figure 4.5.9)*

$$\widehat{\Theta}^{\mathrm{L}}_{\underline{j},k} \circ (\mathscr{F}(F_{\underline{i},\underline{j}}) \otimes \mathrm{id}) = \widehat{\mathscr{F}}_k(F_{\underline{i},\underline{j}}) \circ \widehat{\Theta}^{\mathrm{L}}_{\underline{i},k}. \tag{t3}$$

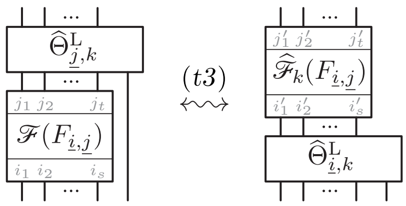

FIGURE 4.5.9. Naturality of $\widehat{\Theta}^{\mathrm{L}}_k$ (the sequences $\underline{i}'$ and $\underline{j}'$ are obtained from $\underline{i}$ and $\underline{j}$, respectively, by exchanging k and $k+1$ at any of their occurrences).

Proof. We start by proving that (t3) holds for any morphism $F_{\underline{i},\underline{j}}$ in MAlg. Lemma 4.5.6 implies that it is enough to show that (t3) and

$$\widehat{\gamma}_{\underline{j},k} \circ (\mathscr{F}(F_{\underline{i},\underline{j}}) \otimes \mathrm{id}) = (\mathrm{id} \otimes \mathscr{F}(F_{\underline{i},\underline{j}})) \circ \widehat{\gamma}_{\underline{i},k} \tag{g2}$$

hold every time $F_{\underline{i},\underline{j}}$ is a generating morphism of MAlg.

For what concerns (t3), we observe that, if all labels of $F_{\underline{i},\underline{j}}$ are different from $k+1$, then (t3) reduces to (t2), while if all labels are different from k, then it becomes trivial by applying (c18) to the counit ε. Therefore, it is enough to show that (t3) holds whenever $F_{\underline{i},\underline{j}}$ is a generating morphism with mixed labels featuring at least one label equal to $k+1$ and another equal to k. In other words, it is enough to consider $F_{\underline{i},\underline{j}} = U_{\underline{i}}, X_{k,k+1}, \widehat{X}_{k+1,k}, Y_{k+1,k}, \widehat{Y}_{k,k+1}$. The statement for $U_{\underline{i}}$ follows directly from the associativity axiom (a1). For what concerns decorated crossings, since $Y_{i,j} = X_{j,i}^{-1}$ and $\widehat{Y}_{i,j} = \widehat{X}_{j,i}^{-1}$ (see Lemma 4.2.2), it is enough to prove (t3) for $X_{k,k+1}$ and $\widehat{X}_{k+1,k}$. This is done in Figure 4.5.10.

For what concerns (g2), if all labels of $F_{\underline{i},\underline{j}}$ are different from $k+1$, then (g2) reduces to (g1), while if all labels are equal to $k+1$, then it follows from (c19). Therefore, it is enough to show that (g2) holds whenever $F_{\underline{i},\underline{j}}$ is a generating morphism of MAlg with mixed labels featuring at least one label equal to

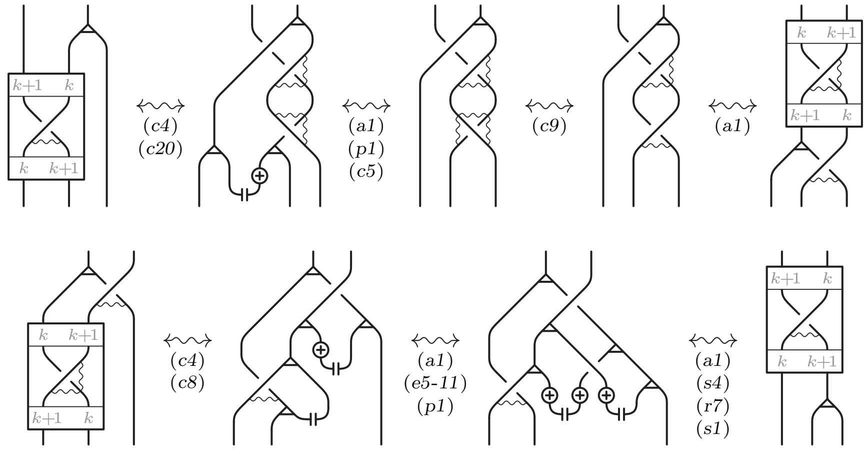

FIGURE 4.5.10. Naturality of $\widehat{\Theta}^{\mathrm{L}}_k$ with respect to decorated crossings with mixed labels.

$k+1$. In other words, it is enough to consider $F_{\underline{i},\underline{j}} = U_{\underline{i}}, \overline{W}_{k+1}, \overline{W}_{k+1}$, or a decorated crossing. Once again, the statement for $U_{\underline{i}}$ follows directly from the associativity axiom ($a1$), while the proofs of ($g2$) for $\overline{W}_{k+1}$ and W_{k+1} are analogous to the ones shown in Figure 4.5.7, where in the first line the adjoint action has to be replaced by the product, and in the second line $\widehat{X}$ has to be replaced by X. For what concerns decorated crossings, we observe that, thanks to relations ($c14$) and ($c20$), it is enough to prove ($g2$) for $X_{i,k+1}$ and $\widehat{X}_{k+1,i}$ with $i \leqslant k$ and for $\widehat{X}_{i,k+1}$ and $X_{k+1,i}$ with $i > k+1$. This is done in Figures 4.5.11 and 4.5.12, respectively.

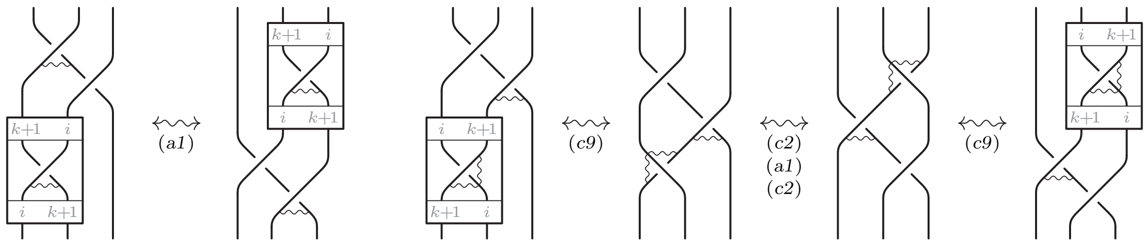

FIGURE 4.5.11. Naturality of $\widehat{\gamma}_k$ with respect to decorated crossings with mixed labels, $i \leqslant k$.

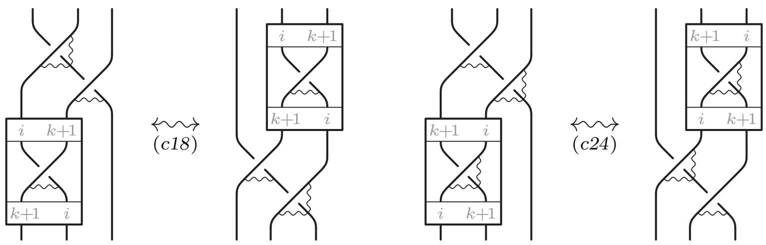

FIGURE 4.5.12. Naturality of $\widehat{\gamma}_k$ with respect to decorated crossings with mixed labels, $i > k+1$.

We will show now that ($t3$) implies that $\widehat{\mathscr{F}}_k : \mathrm{MAlg} \to 4\mathrm{Alg}$ is a functor. In order to see this, consider, for all $\ell \geqslant 0$, $k \geqslant 1$, and $\underline{i} = (i_1, i_2, \ldots, i_\ell)$ with $i_h \geqslant 0$ for all $1 \leqslant h \leqslant \ell$, the morphisms $\Omega_{\underline{i},k}, \Omega^{-1}_{\underline{i},k} : H^\ell \to H^\ell$ in 4Alg defined as

$$\Omega_{\underline{i},k} = \widehat{\Theta}^{\mathrm{L}}_{\underline{i},k} \circ (\mathrm{id}_\ell \otimes \eta),$$
$$\Omega^{-1}_{\underline{i},k} = \breve{\Theta}^{\mathrm{L}}_{\underline{i},k} \circ (\mathrm{id}_\ell \otimes \eta),$$

where $\breve{\Theta}^{\mathrm{L}}_{\underline{i},k}$ is defined recursively, for $\ell \geqslant 0$, as follows:

$$\breve{\Theta}^{\mathrm{L}}_{\varnothing,k} = \varepsilon, \quad \breve{\Theta}^{\mathrm{L}}_{i,k} = \begin{cases} \mu \circ (\mathrm{id} \otimes S) & \text{if } i = k, \\ \mathrm{id} \otimes \varepsilon & \text{if } i \neq k, \end{cases}$$
$$\breve{\Theta}^{\mathrm{L}}_{\underline{i},k} = (\breve{\Theta}^{\mathrm{L}}_{i_1,k} \otimes \mathrm{id}_{\ell-1}) \circ (\mathrm{id} \otimes \widehat{\gamma}_{(i_2,\ldots,i_\ell),k}) \circ (\mathrm{id} \otimes \breve{\Theta}^{\mathrm{L}}_{(i_2,\ldots,i_\ell),k} \otimes \mathrm{id}) \circ (\mathrm{id}_\ell \otimes \Delta).$$

By induction on $\ell \geqslant 0$, we can see that $\Omega^{-1}_{\underline{i},k}$ is the inverse of $\Omega_{\underline{i},k}$. Indeed, for $\ell = 1$, the statement follows by definition. Then, the inductive step is proved in Figures 4.5.13–4.5.16. In particular, in Figures 4.5.13 and 4.5.14, it is shown that, up to the inductive hypotheses, the identities $\Omega^{-1}_{\underline{i},k} \circ \Omega_{\underline{i},k} = \mathrm{id}_\ell$ and $\Omega_{\underline{i},k} \circ \Omega^{-1}_{\underline{i},k} = \mathrm{id}_\ell$ reduce to

$$(\breve{\Theta}^{\mathrm{L}}_{i_1,k} \otimes \mathrm{id}_{\ell-1}) \circ (\mathrm{id} \otimes \widehat{\gamma}_{(i_2,\ldots,i_\ell),k}) \circ (\mathrm{id}_\ell \otimes \eta) \circ (\widehat{\Theta}^{\mathrm{L}}_{i_1,k} \otimes \mathrm{id}_{\ell-1}) \circ (\mathrm{id} \otimes \widehat{\gamma}_{(i_2,\ldots,i_\ell),k}) \circ (\mathrm{id}_\ell \otimes \eta) = \mathrm{id}_\ell, \quad (g3)$$

$$(\widehat{\Theta}^{\mathrm{L}}_{i_1,k} \otimes \mathrm{id}_{\ell-1}) \circ (\mathrm{id} \otimes \widehat{\gamma}_{(i_2,\ldots,i_\ell),k}) \circ (\mathrm{id}_\ell \otimes \eta) \circ (\breve{\Theta}^{\mathrm{L}}_{i_1,k} \otimes \mathrm{id}_{\ell-1}) \circ (\mathrm{id} \otimes \widehat{\gamma}_{(i_2,\ldots,i_\ell),k}) \circ (\mathrm{id}_\ell \otimes \eta) = \mathrm{id}_\ell, \quad (g4)$$

respectively. Equations (g3) and (g4) are proved in Figures 4.5.15 and 4.5.16. Now, (t3) implies that, for every morphism $F_{\underline{i},\underline{j}} : H_{\underline{i}} \to H_{\underline{j}}$ in MAlg, we have $\Omega_{\underline{j},k} \circ \mathscr{F}(F_{\underline{i},\underline{j}}) = \widehat{\mathscr{F}}_k(F_{\underline{i},\underline{j}}) \circ \Omega_{\underline{i},k}$, and therefore

$$\widehat{\mathscr{F}}_k(F_{\underline{i},\underline{j}}) = \Omega_{\underline{j},k} \circ \mathscr{F}(F_{\underline{i},\underline{j}}) \circ \Omega^{-1}_{\underline{i},k}.$$

Since $\mathscr{F}$ is a functor, the last identity implies the functoriality of $\widehat{\mathscr{F}}_k$, while $\Omega_{\underline{j},k}$ defines a natural equivalence between them. □

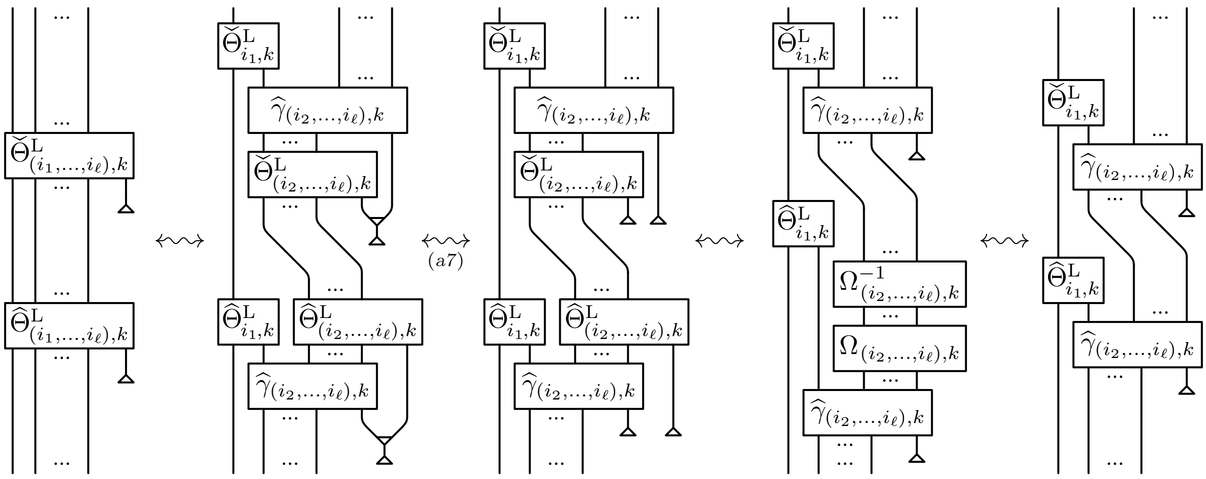

FIGURE 4.5.13. Invertibility of $\Omega_{\underline{i},k}$ – Part 1, reducing $\Omega^{-1}_{\underline{i},k} \circ \Omega_{\underline{i},k} = \mathrm{id}_\ell$ to (g3).

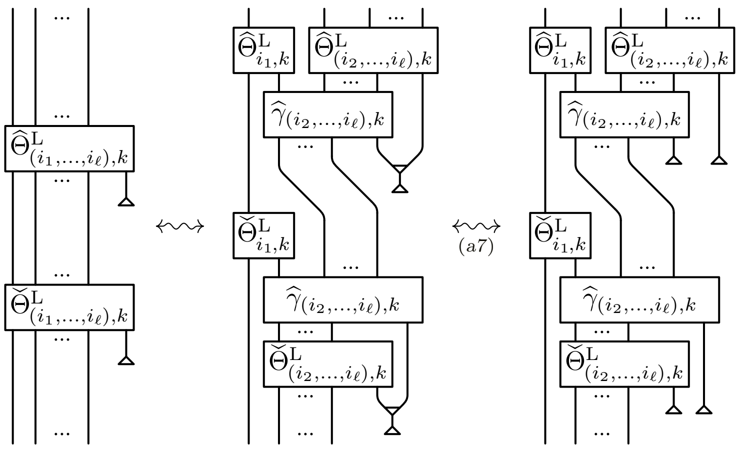

FIGURE 4.5.14. Invertibility of $\Omega_{\underline{i},k}$ – Part 1, reducing $\Omega_{\underline{i},k} \circ \Omega^{-1}_{\underline{i},k} = \mathrm{id}_\ell$ to (g4).

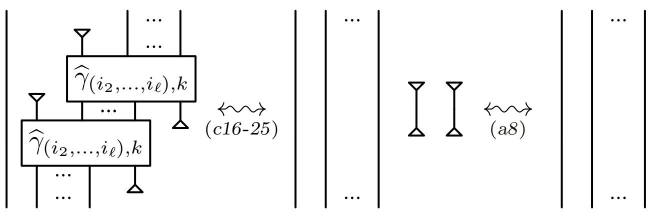

FIGURE 4.5.15. Invertibility of $\Omega_{\underline{i},k}$ – Part 2, establishing (g3) and (g4) when $i_1 \neq k$.

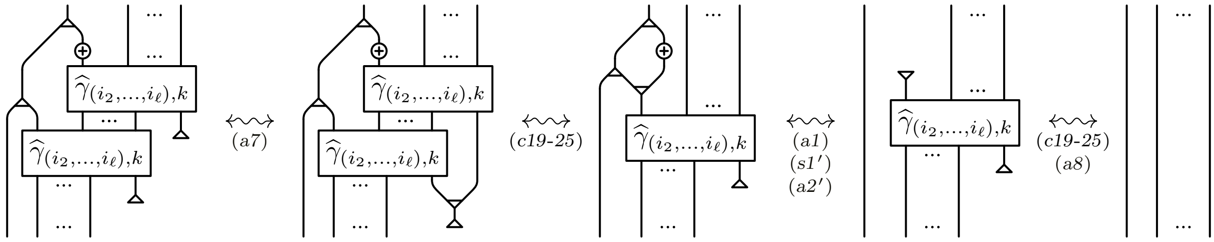

FIGURE 4.5.16. Invertibility of $\Omega_{\underline{i},k}$ – Part 2, establishing (g3) when $i_1 = k$ (establishing (g4) requires using (s1) instead of (s1′)).

4.6. Invariance of $\overline{\Phi}(T)$

Let $T : E_{2s} \to E_{2t}$ be a tangle in 4KT presented by a strictly regular planar diagram of the form represented in the leftmost part of Figure 4.4.1, and let L be the subdiagram which represents the blackboard framed link formed by the closed undotted components of T.

The construction of the morphism $\overline{\Phi}(T) = \overline{\Phi}_{L',\alpha}(T)$ in 4Alg presented in Subsection 4.4 required the following choices:

(1) a numbering of the components L_i of $L = L_1 \cup \cdots \cup L_n$, an orientation of each component L_i, and two points p_i and q_i in L_i, all inducing a bi-ascending state $L' = L'_1 \cup \cdots \cup L'_n$ of L, as in Step (1) in Subsection 4.4;

(2) n embedded arcs $\alpha_i : [0,1] \to [0,1]^2$ such that $\alpha_i(0) = a_i$, $\alpha_i(1) = b_i \in L_i$ satisfying the conditions listed in Step (2) in Subsection 4.4.

We are going to prove now that $\overline{\Phi}(T)$ is independent of such choices, and that it is invariant under 2-deformations of T. We will use the notations introduced in Subsection 4.4. In particular, $L_{i,\alpha} = L_i \cup \alpha_i$ and $L'_{i,\alpha} = L'_i \cup \alpha_i$ for every $1 \leqslant i \leqslant n$, with $L_\alpha = L_{1,\alpha} \cup \cdots \cup L_{n,\alpha}$ and $L'_\alpha = L'_{1,\alpha} \cup \cdots \cup L'_{n,\alpha}$.

PROPOSITION 4.6.1. *There exists a morphism $G_{L',\alpha} : H_0^{\otimes s} \otimes H_{(i_1,i_2,\dots,i_n)} \to H_0^{\otimes t}$ in* MAlg, *with $\{i_1, i_2, \dots, i_n\} = \{1, 2, \dots, n\}$, such that*

$$\overline{\Phi}_{L',\alpha}(T) = \mathscr{F}(G_{L',\alpha}) \circ (\mathrm{id}_s \otimes \eta^{\otimes n}),$$

where $\mathscr{F} : \mathrm{MAlg} \to \mathrm{4Alg}$ is the forgetful functor which discards labels.

Proof. Recall that, by definition (see the right-hand side of Figure 4.4.1),

$$\overline{\Phi}_{L',\alpha}(T) = \overline{W}^{\otimes t} \circ F_{L',\alpha} \circ \big(W^{\otimes s} \otimes \mathrm{id}_n\big) \circ (\mathrm{id}_s \otimes \eta^{\otimes n}),$$

where the morphism $\overline{W}^{\otimes t} \circ F_{L',\alpha} \circ (W^{\otimes s} \otimes \mathrm{id}_n)$ is assembled using the images of the elementary tangles making up T, as presented in the second column of Figures 4.4.4, 4.4.5, and 4.4.6, with the exception of the unit morphisms that are images of the ends a_i for $1 \leqslant i \leqslant n$.

Then, we only need to show that there exists a morphism $G_{L',\alpha} : H_0^{\otimes s} \otimes H_{(i_1,i_2,\dots,i_n)} \to H_0^{\otimes t}$ in MAlg such that $\mathscr{F}(G_{L',\alpha}) = \overline{W}^{\otimes t} \circ F_{L',\alpha} \circ (W^{\otimes s} \otimes \mathrm{id}_{H^n})$. We can obtain $G_{L',\alpha}$ simply by attaching labels to the morphisms appearing in the decomposition of $\overline{W}^{\otimes t} \circ F_{L',\alpha} \circ (W^{\otimes s} \otimes \mathrm{id}_n)$, making sure that the assignment is compatible with the definition of the category MAlg, see Definition 4.5.1. This is done in Figure 4.6.1, where we label by 0 the source of W and the target of $\overline{W}$, and where we label the remaining morphisms according to the numbering of the components of L_α. Observe that, since the number attached to a component of the link corresponds to its depth in the bi-ascending state L' of L, the decorated crossings which appear are exactly the ones in the definition of the category MAlg, see Definition 4.5.1. Hence, $G_{L',\alpha}$ is a morphism in MAlg, as required. □

PROPOSITION 4.6.2. *For a fixed choice of the bi-ascending state L', and hence of the numbering of the components of L, the morphism $\overline{\Phi}_{L',\alpha}(T)$ of* 4Alg *does not depend on the choice of the family α of embedded arcs $\alpha_i : [0,1] \to [0,1]^2$ for $1 \leqslant i \leqslant n$. Moreover, every arc α_i can be chosen to intersect the component L_i to which it is attached in an arbitrary way, provided it still crosses below $L_{j,\alpha}$ for $j < i$ and above $L_{j,\alpha}$ for $j > i$. In other words, the conditions on α_i in Step* (2) *of Subsection 4.4 can be weakened to exclude* (b) *and* (c).

Proof. In order to see that $\overline{\Phi}_{L',\alpha}(T)$ is independent of the choice of the family of arcs α, we have to show that $\overline{\Phi}_{L',\alpha}(T) = \overline{\Phi}_{L',\widehat{\alpha}}(T)$ for any other family of arcs $\widehat{\alpha}$ satisfying the same conditions required in Step (2), except for (b) and (c). We can do that by assuming the additional hypothesis that α intersects

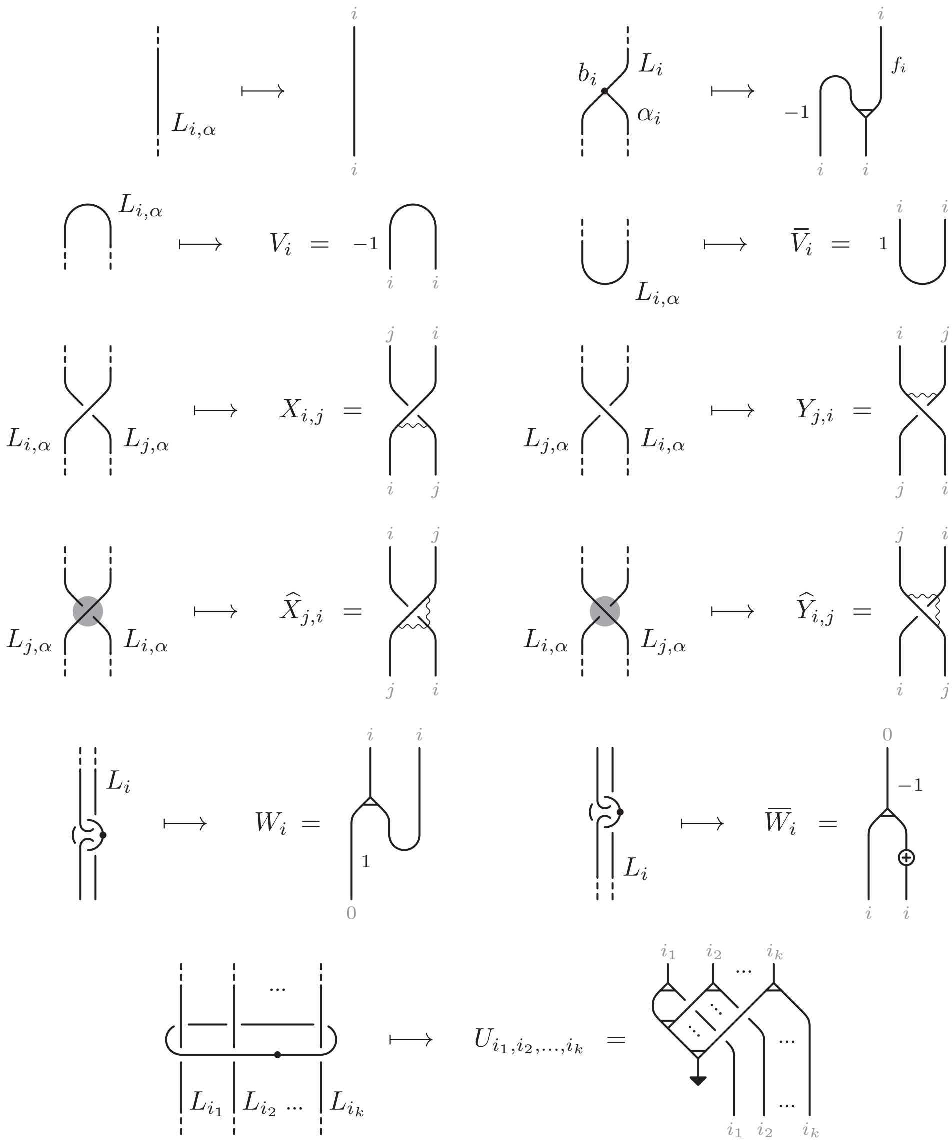

FIGURE 4.6.1. Construction of the morphism $G_{L',\alpha} : H_0^{\otimes s} \otimes H_{(1,2,\ldots,n)} \to H_0^{\otimes t}$ in MAlg, with $1 \leqslant i \leqslant j \leqslant n$.

$\widehat{\alpha}$ regularly and, in particular, that $\widehat{\alpha}_i(1) = \widehat{b}_i \neq b_i = \alpha_i(1)$ for every $1 \leqslant i \leqslant n$. In fact, if this were not the case, we could always consider a third family $\widehat{\widehat{\alpha}}$ of arcs satisfying such additional hypothesis with respect to both α and $\widehat{\alpha}$, and then show that $\overline{\Phi}_{L',\alpha}(T) = \overline{\Phi}_{L',\widehat{\widehat{\alpha}}}(T) = \overline{\Phi}_{L',\widehat{\alpha}}(T)$.

Therefore, we can proceed to replace the arcs of α with those of $\widehat{\alpha}$ one at a time. In other words, it is enough to show that $\overline{\Phi}_{L',\alpha}(T) = \overline{\Phi}_{L',\widehat{\alpha}}(T)$ whenever $\overline{\Phi}_{L',\widehat{\alpha}}(T)$ is the morphism obtained by replacing the arc α_k with an arc $\widehat{\alpha}_k : [0,1] \to [0,1]^2$ that satisfies the conditions in Step (2) of Subsection 4.4 except for (b) and (c), and by keeping every other arc α_i with $i \neq k$ fixed.

The main idea behind the proof is the following. We consider the graph diagram $T_{\alpha,\widehat{\alpha}_k} = T_\alpha \cup \widehat{\alpha}_k = T \cup_{j=1}^n \alpha_j \cup \widehat{\alpha}_k$ in which both arcs α_k and $\widehat{\alpha}_k$ are simultaneously attached to L_k, and we choose the crossing state for the crossings between α_k and $\widehat{\alpha}_k$ in an arbitrary way. We can assume for instance that $\widehat{\alpha}_k$ crosses always over α_k, and we do not mark these crossings. Under the conditions listed above, $T_{\alpha,\widehat{\alpha}_k}$ has only regular intersections, and we can associate to it a morphism in 4Alg following the same rules used in the definition of $\overline{\Phi}$. Then, we will show (see equations (*v1*) and (*v2*) below) that if, in this last morphism, the unit η in the image of $\widehat{a}_k$ (respectively a_k) is replaced by the integral element Λ, then the resulting morphism is equivalent to $\overline{\Phi}_{L',\alpha}(T)$ (respectively $\overline{\Phi}_{L',\widehat{\alpha}}(T)$). Finally, we will show that the two morphisms that are obtained by exchanging η and Λ, which are associated to a_k and $\widehat{a}_k$, are 2-equivalent in 4Alg (see equation (*v3*) below). This last step will require the use of the natural transformation Θ_k^{L}, which means that we will interpret the essential part of the above morphisms as the image under the forgetful functor of a labeled morphism in TAlg. Here are the details.

By Proposition 4.6.1, there exist morphisms

$$G_{L',\alpha} : H_0^{\otimes s} \otimes H_{(i_1,\dots,i_{\ell-1},i_\ell=k,i_{\ell+1},\dots,i_n)} \to H_0^{\otimes t}$$

and

$$G_{L',\widehat{\alpha}} : H_0^{\otimes s} \otimes H_{(i_1,\dots,i_{\ell-1},i_{\ell+1},\dots,i_h,k,i_{h+1},\dots,i_n)} \to H_0^{\otimes t}$$

in MAlg such that

$$\overline{\Phi}_{L',\alpha}(T) = \mathscr{F}(G_{L',\alpha}) \circ (\mathrm{id}_s \otimes \eta^{\otimes n}) \text{ and } \overline{\Phi}_{L',\widehat{\alpha}}(T) = \mathscr{F}(G_{L',\widehat{\alpha}}) \circ (\mathrm{id}_s \otimes \eta^{\otimes n}).$$

Then $\overline{\Phi}_{L',\alpha}(T) = \overline{\Phi}_{L',\widehat{\alpha}}(T)$ will follow if we can find a third morphism

$$G_{L',\alpha,\widehat{\alpha}_k} : H_0^{\otimes s} \otimes H_{(i_1,\dots,i_{\ell-1},k,i_{\ell+1},\dots,i_h,k,i_{h+1},\dots,i_n)} \to H_0^{\otimes t}$$

in MAlg such that

$$\mathscr{F}(G_{L',\alpha}) = \mathscr{F}(G_{L',\alpha,\widehat{\alpha}_k}) \circ (\mathrm{id}_{s+h} \otimes \Lambda \otimes \mathrm{id}_{n-h-1}), \tag{v1}$$

$$\mathscr{F}(G_{L',\widehat{\alpha}}) = \mathscr{F}(G_{L',\alpha,\widehat{\alpha}_k}) \circ (\mathrm{id}_{s+\ell-1} \otimes \Lambda \otimes \mathrm{id}_{n-\ell}), \tag{v2}$$

$$\begin{aligned}\mathscr{F}(G_{L',\alpha,\widehat{\alpha}_k}) &\circ (\mathrm{id}_{s+\ell-1} \otimes \Lambda \otimes \mathrm{id}_{h-\ell} \otimes \eta \otimes \mathrm{id}_{n-h-1}) \\ &= \mathscr{F}(G_{L',\alpha,\widehat{\alpha}_k}) \circ (\mathrm{id}_{s+\ell-1} \otimes \eta \otimes \mathrm{id}_{h-\ell} \otimes \Lambda \otimes \mathrm{id}_{n-h-1}).\end{aligned} \tag{v3}$$

In order to construct $G_{L',\alpha,\widehat{\alpha}_k}$, consider the graph diagram $T_{\alpha,\widehat{\alpha}_k}$. The morphism $G_{L',\alpha,\widehat{\alpha}_k}$ is obtained by associating to the elementary morphisms making up $T_{\alpha,\widehat{\alpha}_k}$ the morphisms of MAlg listed in Figures 4.6.1 and 4.6.2-(a). Notice that the edges in the image of $\widehat{b}_k$ shown in Figure 4.6.2-(a) are not weighted by the ribbon morphism, as opposed to the ones corresponding to b_k. The global form of the morphism $\mathscr{F}(G_{L',\alpha,\widehat{\alpha}_k})$ is represented in Figure 4.6.2-(b).

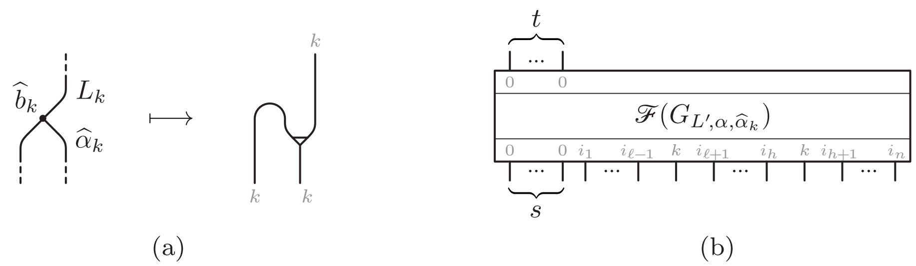

FIGURE 4.6.2. Image of b'_k in MAlg and global form of $\mathscr{F}(G_{L',\alpha,\widehat{\alpha}_k})$.

Consider now the morphism $\mathscr{F}(G_{L',\alpha,\widehat{\alpha}_k}) \circ (\mathrm{id}_{s+h} \otimes \Lambda \otimes \mathrm{id}_{n-h-1})$ of 4Alg obtained by composing the image of $\widehat{\alpha}_k$ with the integral element Λ (see the second diagram in Figure 4.6.3). Since Λ belongs to TAlg, and since the image of $\widehat{\alpha}_k$ is made up entirely of decorated crossings of type X, $\widehat{X}$, Y, and $\widehat{Y}$, which also belong to TAlg, and of ev and coev morphisms, we can apply relations (*c18*), (*c19*), (*c24*), and (*c25*) in Table 4.2.10 and the duality between ε and Λ in Table 2.4.3 to pull up Λ towards the image of $\widehat{b}_k$, thus obtaining $\mathscr{F}(G_{L',\alpha})$ (see the last two steps in Figure 4.6.3). This proves (*v1*), and the proof of (*v2*) is completely analogous.

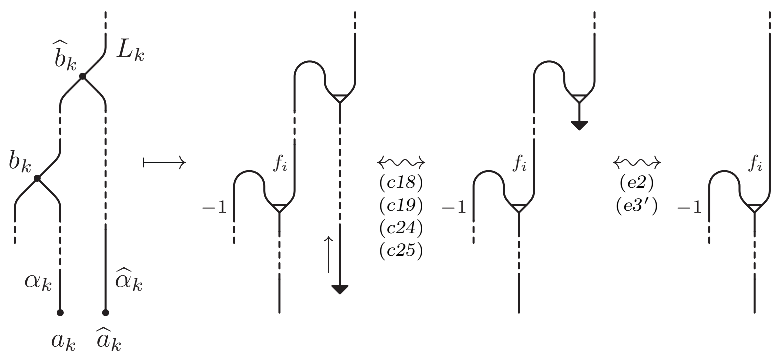

FIGURE 4.6.3. Independence of the choice of α_k: proof of (*v1*).

The proof of ($v3$) is shown in Figure 4.6.4. Here, in the second diagram, $\gamma^{-1}_{(i_{h+1},\dots,i_n),k}$ is the inverse of the morphism $\gamma_{(i_{h+1},\dots,i_n),k} : H^{n-h} \otimes H \to H \otimes H^{n-h}$ (see Definition 4.5.2), and can be represented as a composition of tensor products of identities, inverse braidings c^{-1}, and decorated crossings of type $\widehat{Y}$. To implement this first step, we are using the fact that the counit ε belongs to TAlg, and can thus be pulled up to the top-right using the naturality of the braided structures of 4Alg and TAlg. Then, the top part of the second diagram can be interpreted as $\mathrm{id}_t \otimes \varepsilon = \Theta^{\mathrm{L}}_{(0,\dots,0),k}$, which allows us to use, in the second step, the naturality property ($t2$) of Θ^{L}_k to intertwine it with $\mathscr{F}(G_{L',\alpha,\widehat{\alpha}_k})$. $\square$

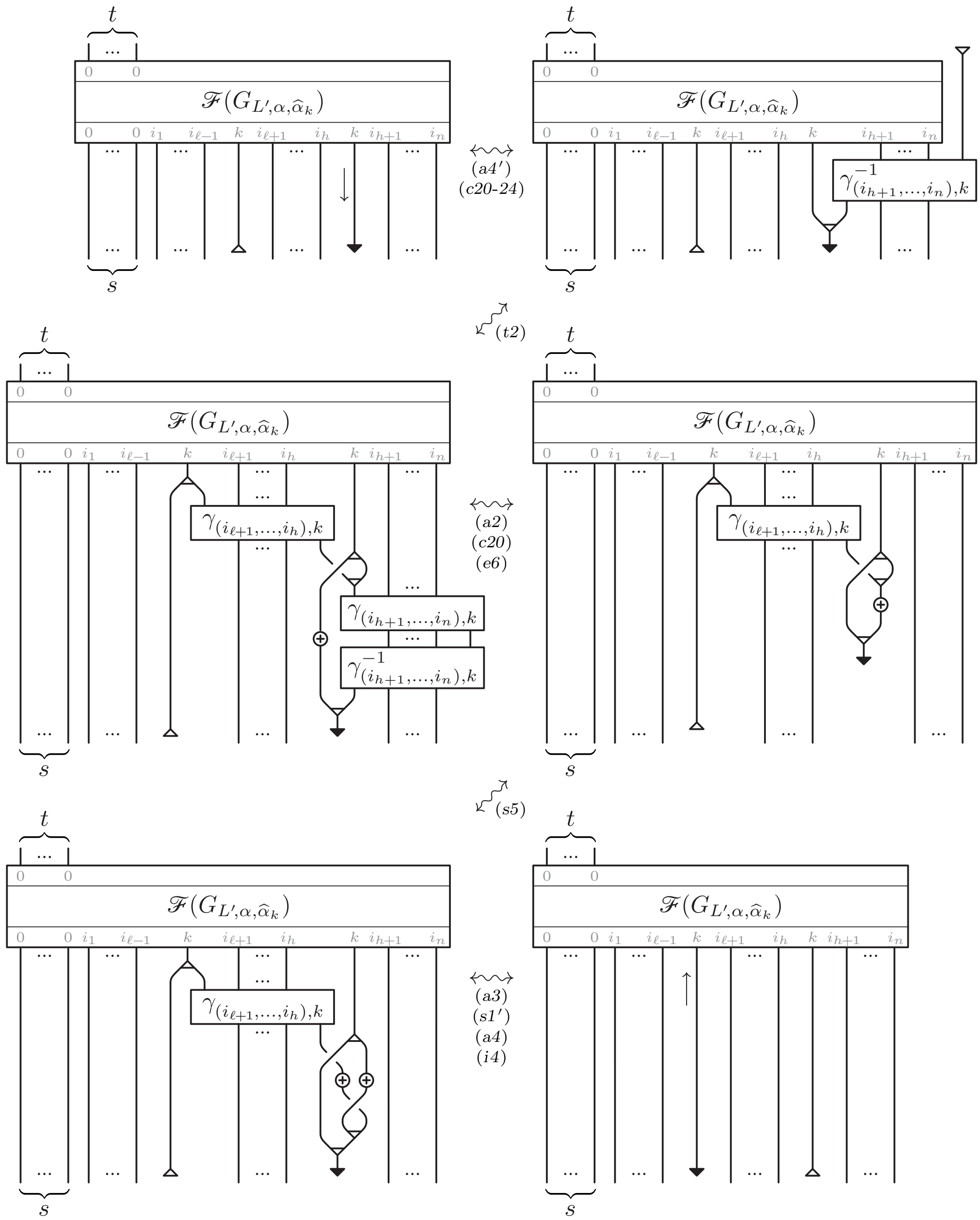

FIGURE 4.6.4. Independence of the choice of α_k: proof of ($v3$).

Since $\overline{\Phi}_{L',\alpha}(T)$ is independent of the choice of the arcs α_i for all $1 \leqslant i \leqslant n$, from now we will denote this morphism simply as $\overline{\Phi}_{L'}(T)$.

PROPOSITION 4.6.3. *The morphism $\overline{\Phi}_{L'}(T)$ does not depend on the numbering of the components of L, that is, on the vertical order of the components of the bi-ascending state L'.*

Proof. In order to show that $\overline{\Phi}_{L'}(T)$ is independent of the numbering of the components of L, it is enough to show that $\overline{\Phi}_{L'}(T) = \overline{\Phi}_{L''}(T)$ when L'' is obtained from L' by exchanging the order of two consecutive components L_k and L_{k+1}, for some $1 \leqslant k \leqslant n-1$. This implies that L'' is obtained from L' by setting $L''_{k+1} = L'_k$, $L''_k = L'_{k+1}$, and by inverting all crossings between these two components, while $L''_i = L'_i$ for every $i \neq k, k+1$. Then, according to Proposition 4.6.1 and to the definition of the functor $\widehat{\mathscr{F}}_k$ in Proposition 4.5.7, $\overline{\Phi}_{L'}(T) = \mathscr{F}(G_{L',\alpha}) \circ (\mathrm{id}_s \otimes \eta^{\otimes n})$, while $\overline{\Phi}_{L''}(T) = \widehat{\mathscr{F}}_k(G_{L',\alpha}) \circ (\mathrm{id}_s \otimes \eta^{\otimes n})$. Hence, the statement will follow if we show that

$$\mathscr{F}(G_{L'}) \circ (\mathrm{id}_s \otimes \eta^{\otimes n}) = \widehat{\mathscr{F}}_k(G_{L'}) \circ (\mathrm{id}_s \otimes \eta^{\otimes n}).$$

This is done in Figure 4.6.5, where we have assumed that the endpoints $a_1, a_2, \ldots, a_n$ of $\alpha_1, \alpha_2, \ldots, \alpha_n$ have been positioned in the lower right corner of the diagram in increasing order from the left to the right, as it is allowed by Proposition 4.6.2. In the first step in Figure 4.6.5, we insert $\varepsilon \circ \eta$ between the kth and the $(k+1)$st strand, and pull the counit ε through the $n-k$ vertical strands to its right using the naturality of the two braided structures of TAlg. Since $\mathrm{id}_t \otimes \varepsilon = \widehat{\Theta}^{\mathrm{L}}_{(0,\ldots,0),k}$, in the second step we use the naturality property (*t3*) of $\widehat{\Theta}^{\mathrm{L}}_k$ (see Proposition 4.5.7) to intertwine it with $\mathscr{F}(G_{L',\alpha})$, thus obtaining $\widehat{\mathscr{F}}_k(G_{L',\alpha})$. □

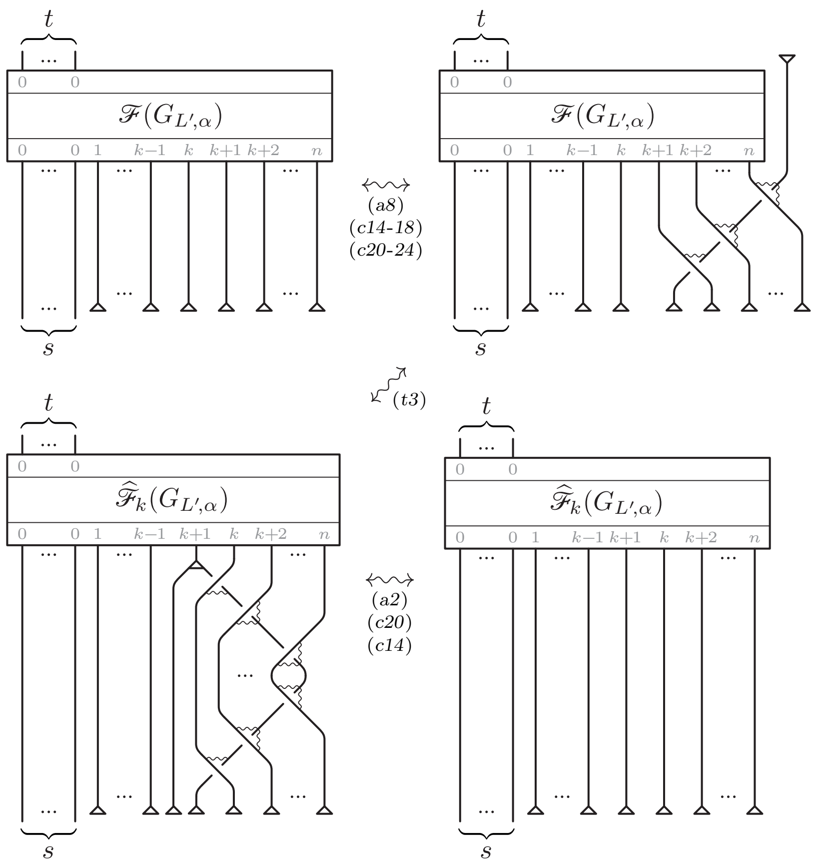

FIGURE 4.6.5. Proof of the independence of the choice of numbering of the components of L.

In order to prove that $\overline{\Phi}_{L'}(T)$ is independent of the choice of the bi-ascending state of the single components of L', we need the following lemma.

LEMMA 4.6.4. *Let $T = T_2 \circ T_1$ be a tangle of the form represented on the left-hand side of Figure 4.6.6, where two adjacent strands belonging to the same component L_n of the undotted link $L = L_1 \cup \cdots \cup L_n$ of T are joined by a flat band δ. Assume that surgering L_n along δ yields two different components $\widehat{L}_n$ and $\widehat{L}_{n+1}$ of the undotted link $\widehat{L} = L_1 \cup \cdots \cup L_{n-1} \cup \widehat{L}_n \cup \widehat{L}_{n+1}$ of a new tangle $\widehat{T}$, where an extra dotted component is added to encircle δ, as shown on the right-hand side of Figure 4.6.6. Assume also that $L' = L'_1 \cup \cdots \cup L'_n$ and $\widehat{L}' = L'_1 \cup \cdots \cup L'_{n-1} \cup \widehat{L}'_n \cup \widehat{L}'_{n+1}$ are bi-ascending states of L and $\widehat{L}$, respectively, whose components are vertically ordered according to the numbering, and such that surgering L'_n along*

δ gives the two components $\widehat{L}'_n$ and $\widehat{L}'_{n+1}$. In other words, L' and $\widehat{L}'$ are obtained by inverting the same crossings in L and $\widehat{L}$, respectively. Then $\overline{\Phi}_{L'}(T) = \overline{\Phi}_{\widehat{L}'}(\widehat{T})$.

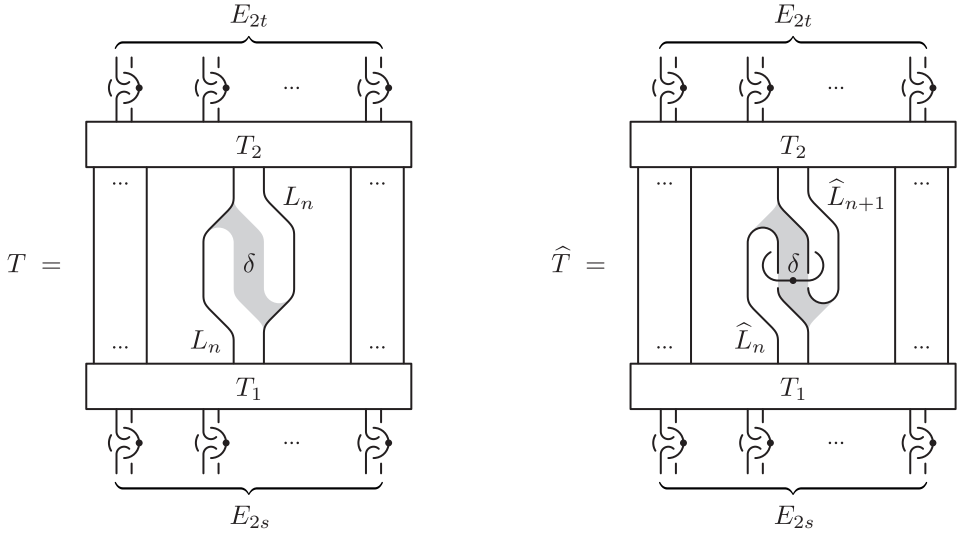

FIGURE 4.6.6. Cutting the component L_n.

Proof. Choose a set of arcs $\alpha_1, \dots, \alpha_{n+1}$ for $\widehat{L}$ that is consistent with the requirements in Step (2) of Subsection 4.4 except for (b) and (c), as allowed by Proposition 4.6.2). This yields the graph diagrams T_α and $\widehat{T}_\alpha$ shown in Figure 4.6.7. Here, α_n and α_{n+1} are two parallel arcs which cross over the vertical strands belonging to $\widehat{L}_{n+1}$ and under all the others. In particular, they form the same sequence of crossing states along the pair of gray boxes.

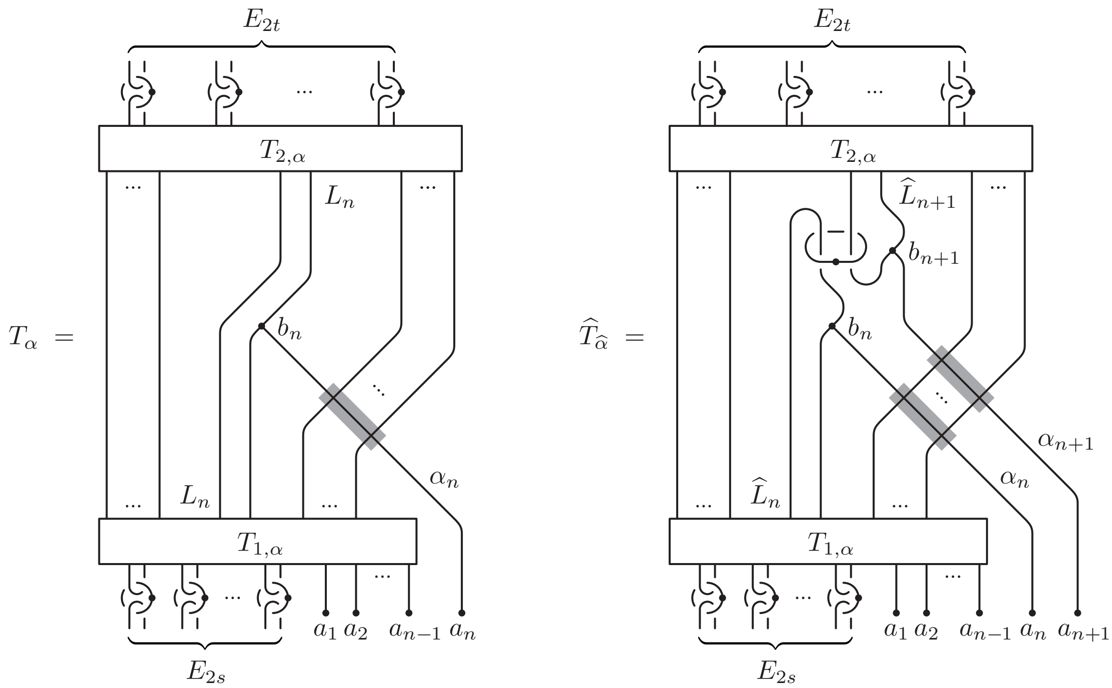

FIGURE 4.6.7. Choice of the arcs α_n and α_{n+1} in the proof of Lemma 4.6.4: α_n and α_{n+1} cross over the vertical strings which belong to $\widehat{L}_{n+1}$ and under all the others.

Now, the equality $\overline{\Phi}_{\widehat{L}'}(\widehat{T}) = \overline{\Phi}_{L'}(T)$ is proved in Figure 4.6.8, where in the last step we have used that $\widehat{f}_n + \widehat{f}_{n+1} = 2 - \mathrm{wr}(\widehat{L}_n) - \mathrm{wr}(\widehat{L}_{n+1}) = 2 - \mathrm{wr}(L_n) = 1 + f_n$. $\square$

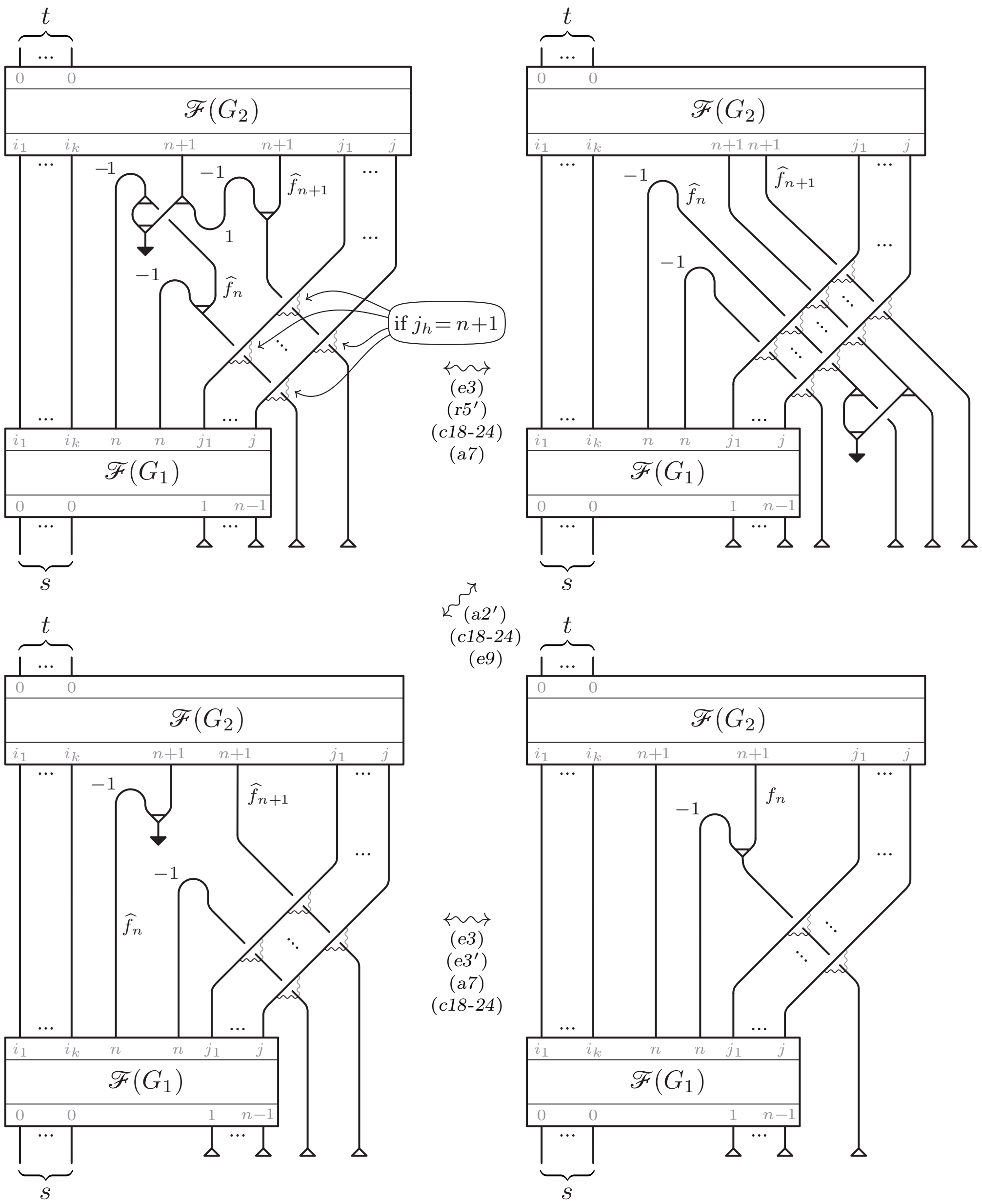

FIGURE 4.6.8. Proof of Lemma 4.6.4.

REMARK 4.6.5. We observe that replacing $T = T_2 \circ T_1$ by $\widehat{T}$, as described in Lemma 4.6.4, is a 2-deformation. Indeed, one can go back by sliding $\widehat{L}_n$ over $\widehat{L}_{n+1}$, and then by canceling the extra 1-handle with $\widehat{L}_{n+1}$.

PROPOSITION 4.6.6. *The morphism $\overline{\Phi}_{L'}(T)$ does not depend on the choice of the bi-ascending state of the single components of L'.*

Proof. Using Proposition 4.6.3, we can assume that the component whose bi-ascending state we want to change is the last one, L_n. According to Proposition 4.3.2, it is enough to prove that $\overline{\Phi}_{L'}(T) = \overline{\Phi}_{L''}(T)$ whenever the bi-ascending state L'' is obtained from L' by a single crossing change in L'_n.

Notice that $\overline{\Phi}_{L'}(T)$ is invariant under the planar isotopy moves in Figure 2.1.4, which rotate crossings. Indeed, by definition, the images under $\overline{\Phi}$ of all crossings of T_α are in the subcategory TAlg which, according to Theorem 4.2.8, is a rigid monoidal category whose rigid structure is iduced by the morphisms ev and coev. Therefore, we can assume that the changing crossing is oriented in one of the two ways shown in the top line in Figure 4.6.9.

In both cases, we cut the component L_n by performing a surgery on it, as described in Lemma 4.6.4 and in Figure 4.6.6, along a band δ which is located immediately above the changing crossing, as shown

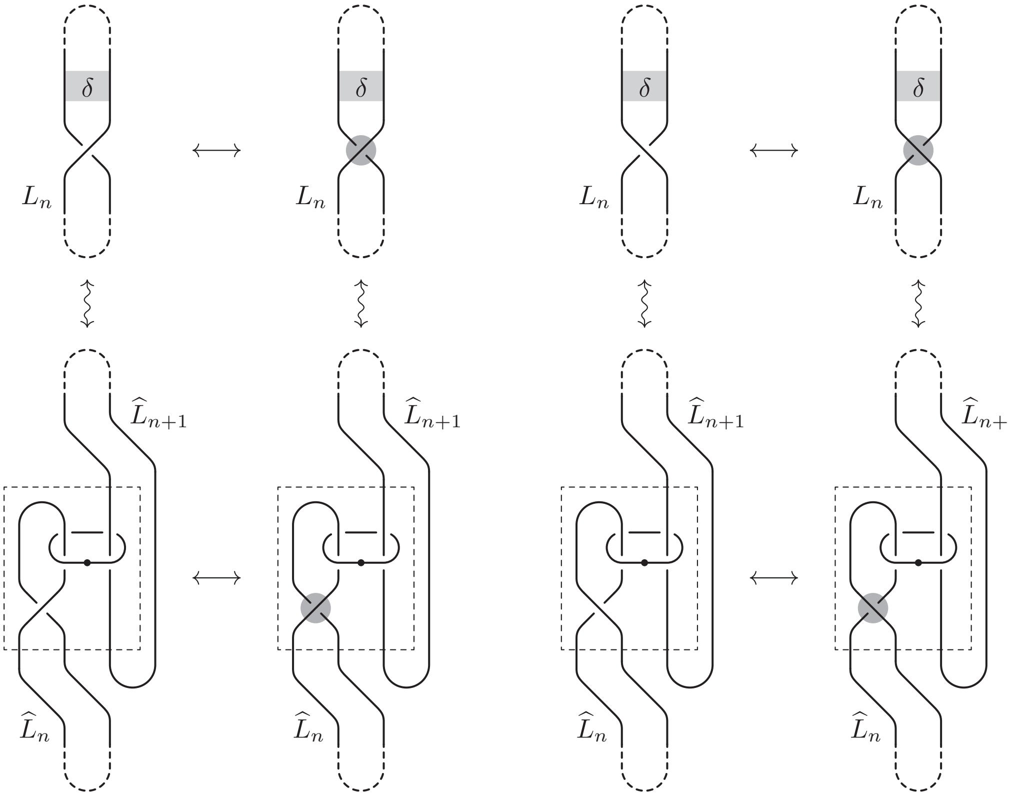

FIGURE 4.6.9. Orienting the changing crossing and cutting the component L_n.

in Figure 4.6.9. We obtain this way the two new components $\widehat{L}_n$ and $\widehat{L}_{n+1}$. According to the second part of Proposition 4.3.2, we can assume that $\widehat{L}_n$ and $\widehat{L}_{n+1}$ are vertically separated unknots. Actually, Proposition 4.3.2 tells us that this is true for the two component obtained by cutting L_n at the changing crossing, but since there is no other crossing inside the dashed boxes in Figure 4.6.9, we are free to vertically isotope $\widehat{L}_n$ and $\widehat{L}_{n+1}$ inside those boxes in such a way that the same holds for them.

Then, L' and $\widehat{L}'$ satisfy the hypotheses of Lemma 4.6.4, and hence we have $\overline{\Phi}_{L'}(T) = \overline{\Phi}_{\widehat{L}'}(\widehat{T})$ and $\overline{\Phi}_{L''}(T) = \overline{\Phi}_{\widehat{L}''}(\widehat{T})$. So, we are left to prove that $\overline{\Phi}_{\widehat{L}'}(\widehat{T}) = \overline{\Phi}_{\widehat{L}''}(\widehat{T})$. This is done in Figure 4.6.10, where

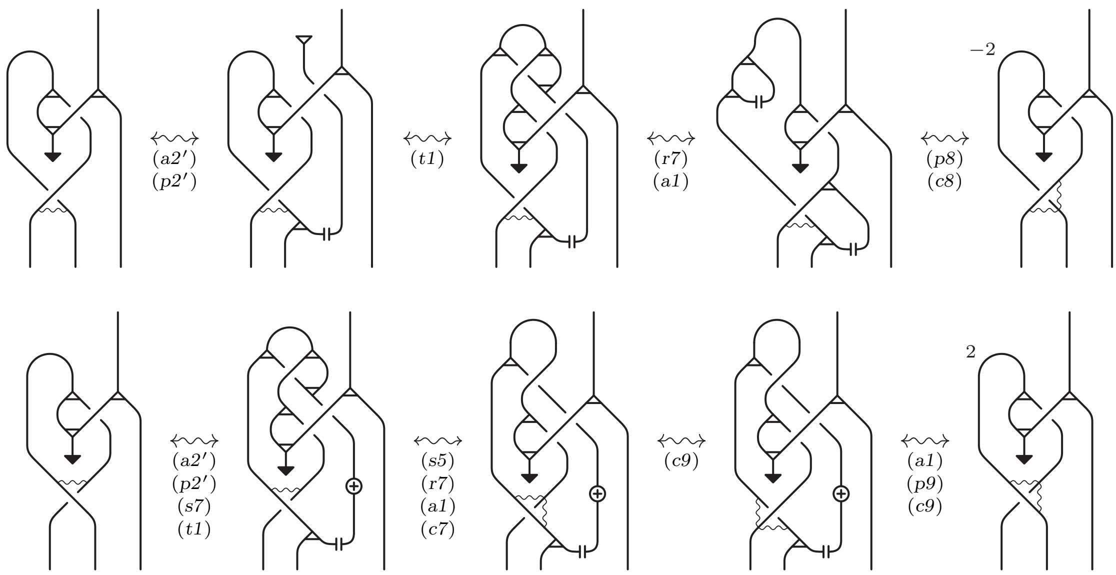

FIGURE 4.6.10. Proof of the invariance of $\overline{\Phi}$ under change of crossing.

only the parts of the images corresponding to the parts of the diagrams inside the dashed rectangles in Figure 4.6.9 are compared, since the rest is fixed. □

It is left to show that $\overline{\Phi}$ is invariant under the 2-equivalence moves in Table 3.1.1.

PROPOSITION 4.6.7. *The morphism $\overline{\Phi}(T)$ depends only on the 2-equivalence class of T in 4KT.*

Proof. In order to see that $\overline{\Phi}(T)$ is invariant under the isotopy moves presented in Table 3.1.1, we observe that, using Propositions 4.6.3 and 4.6.6, the bi-ascending state L' can be chosen so that the image under $\overline{\Phi}$ of the isotopy move we are interested in reduces to one of the identities in Tables 4.2.10 and 4.2.11. On the other hand, the invariance under the pushing-through move in Table 3.1.1 reduces to (*t1′*) in Figure 4.2.7.

The proof of the invariance under 1/2-handle cancellation of an undotted component L_i with a dotted meridian is illustrated in Figure 4.6.11. We start by using the integral axiom (*i2*) to express multiplication by Λ as the composition $\Lambda \circ \varepsilon$. Then, since ε and Λ belong to the subcategory TAlg, and since they are dual to each other with respect to ev and coev, we use moves (*c18*), (*c19*), (*c24*), (*c25*), and (*u2*) in Table 4.2.10 to slide them along the image of the undotted component L_i until it is transformed in the composition $\varepsilon \circ \eta$, which is removed through relation (*a8*).

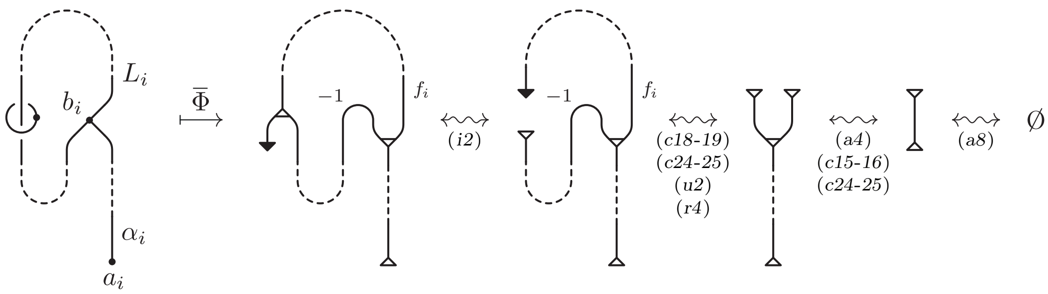

FIGURE 4.6.11. Invariance of $\overline{\Phi}(T)$ under 1/2-handle cancellation.

It remains to prove that $\overline{\Phi}(T)$ is invariant under 2-handle slide of a component L_j over another component L_i, that is, under the replacement of L_j by the band connected sum of L_j and a parallel copy $L_i^{\|}$ of L_i. Since we have already proved the invariance of $\overline{\Phi}(T)$ under isotopy and 1/2-handle cancellations, we can assume, thanks to Proposition 3.1.6, that L_i has at most one self-crossing, and that the components L_i and L_j and the sliding band β have one of the forms outlined on the left-hand sides of Figures 4.6.12, 4.6.14, and 4.6.16 below. In these pictures, using the independence of $\overline{\Phi}(T)$ of the choice of the bi-ascending state, we have assumed that, in the first two cases, it is $L_j = L_2$ that slides over $L_i = L_1$, while, in the third case, it is $L_j = L_1$ that slides over $L_i = L_2$. We are also assuming that the visible part of the diagram has been pulled down outside the box T_α (see Figure 4.4.1), except for the dashed lines which interact with the rest of the diagram inside T_α. In particular, the dashed part of L_i cannot form self-crossings, but it can cross the dashed part of L_j, which can also form self-crossings.

We consider the three cases separately, starting from the one where L_i has no self-crossings. In this case, Figure 4.6.12 shows the two tangles before and after the slide, together with suitable choices for arcs $\alpha_i = \alpha_1$ and $\alpha_j = \alpha_2$ and for the data determining bi-ascending (actually ascending) states of $L_i = L_1$ and $L_j = L_2$.

Then, the images in 4Alg of the two tangles under $\overline{\Phi}$, constructed according to those choices, are shown to be the same in Figure 4.6.13. Here, we first apply (*a7*) to split the image of α_2 into two units, and then attach together the left one to the image of $L_{\alpha,1}$, thus obtaining the morphism $\widetilde{\mu}$ highlighted inside the dashed box in the second diagram of the figure. Then, we use the properties of $\widetilde{\mu}$ in Table 2.5.1, as well as (*c18*), (*c19*), (*c24*), (*c25*), and (*u2*) in Tables 4.2.10 and 4.2.11, to slide $\widetilde{\mu}$ all around the dashed arc, creating this way a parallel copy of the arc. Observe that, according to Proposition 2.5.1, when the product $\widetilde{\mu}$ passes through ev, it turns into the coproduct Δ, and when Δ passes through coev, it turns back into $\widetilde{\mu}$. This means that, in the process of sliding, the morphism $\widetilde{\mu}$ always moves upwards, while the morphism Δ always moves downwards. In particular, when we arrive to left end of the dashed arc, we get the Δ highlighted inside the dashed box in the third diagram of the figure. Moreover, when $\widetilde{\mu}$ or Δ slide through a crossing, two crossings of the same type are created, while when they slide through a morphism U_k, they turn it into U_{k+1}. Therefore, we have indeed doubled the dashed arc.

Now, we pass to the second case, when L_i forms a positive self-crossing. The two tangles before and after the slide, together with suitable choices for the bi-ascending states and the arcs α, are given by the

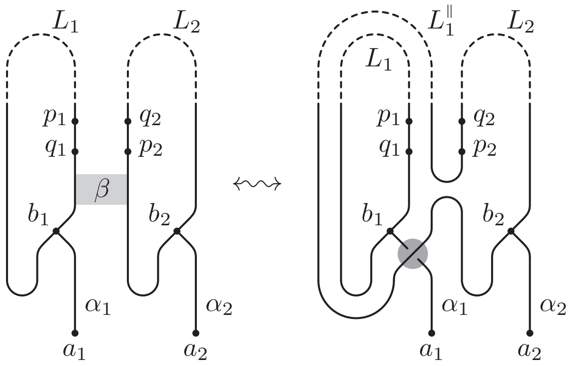

FIGURE 4.6.12. Sliding L_2 over L_1, for L_1 with no self-crossings.

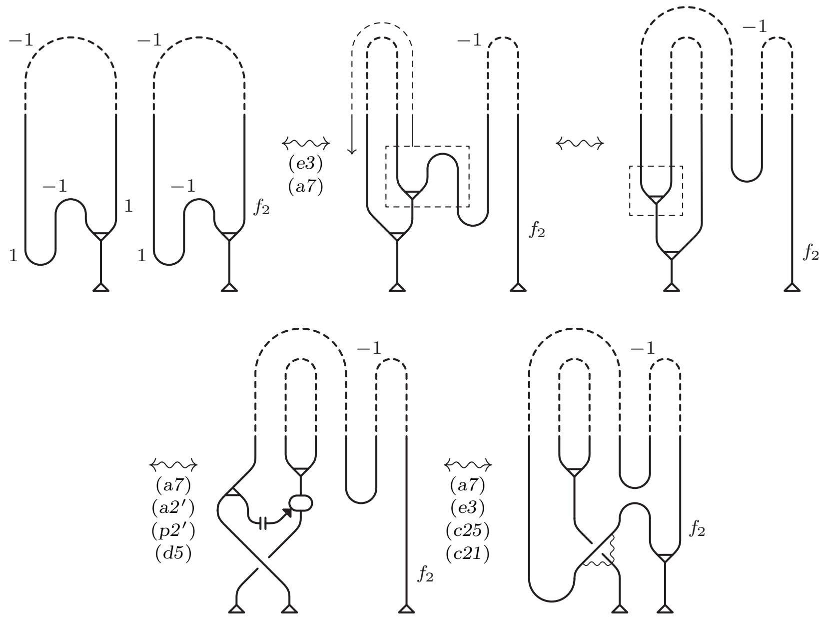

FIGURE 4.6.13. Proof of the invariance of $\overline{\Phi}(T)$ under the slide of L_2 over L_1, for L_1 with no self-crossings.

first two diagrams in Figure 4.6.14, while the third is an equivalent form of the second, up to isotopy. The proof that the images of the first and third diagrams under $\overline{\Phi}$ are the same in 4Alg is presented in Figure 4.6.15, where the first diagram has been obtained by applying relation (*c22*) to replace the decorated kink in the image of $L_i = L_1$ by the identity morphism, then observing that the total ribbon weight of the image of L_1 is $f_1 - 1 = 1 - \mathrm{wr}(L_1') - 1 = 1$, and finally repeating the first step in Figure 4.6.13.

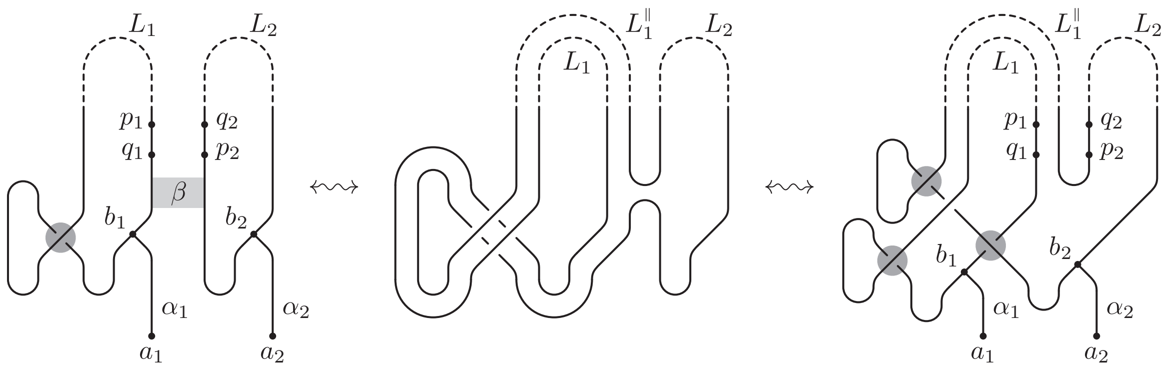

FIGURE 4.6.14. Sliding L_2 over L_1, for L_1 with one positive self-crossing.

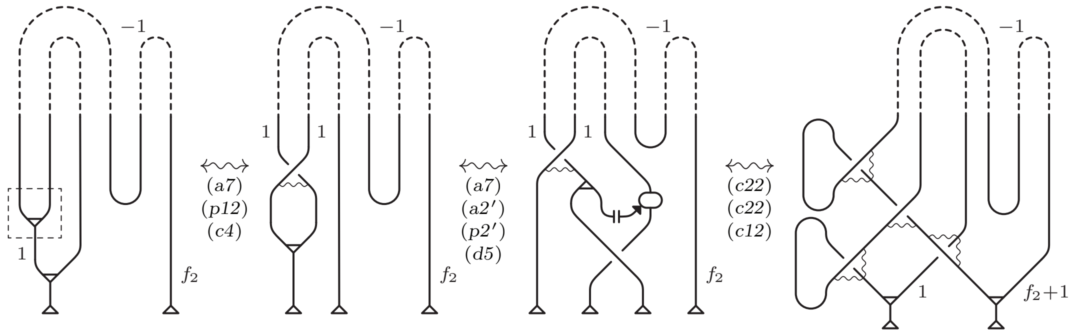

FIGURE 4.6.15. Proof of the invariance of $\overline{\Phi}(T)$ under the slide of L_2 over L_1, for L_1 with one positive self-crossing.

In the third case, we slide $L_j = L_1$ over $L_i = L_2$, and assume that L_2 forms a single negative self-crossing. The result of the slide is presented in Figure 4.6.16, where the third diagram is again an equivalent form of the second, up to isotopy.

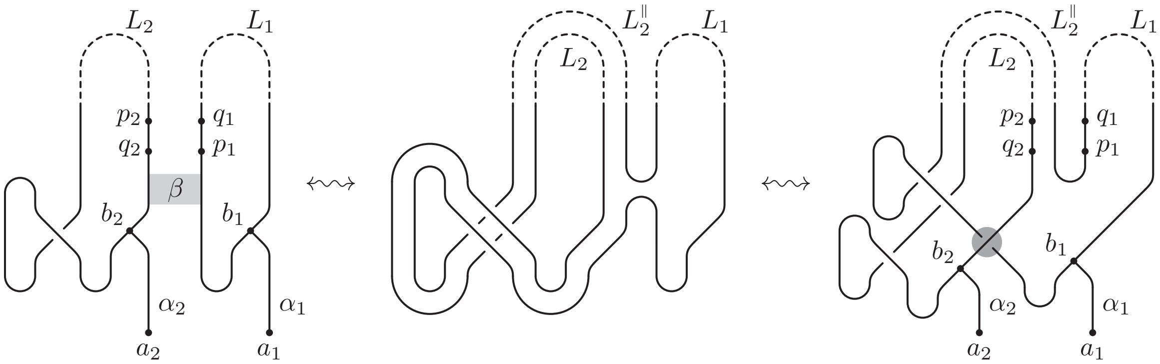

FIGURE 4.6.16. Sliding L_1 over L_2, for L_2 with one negative self-crossing.

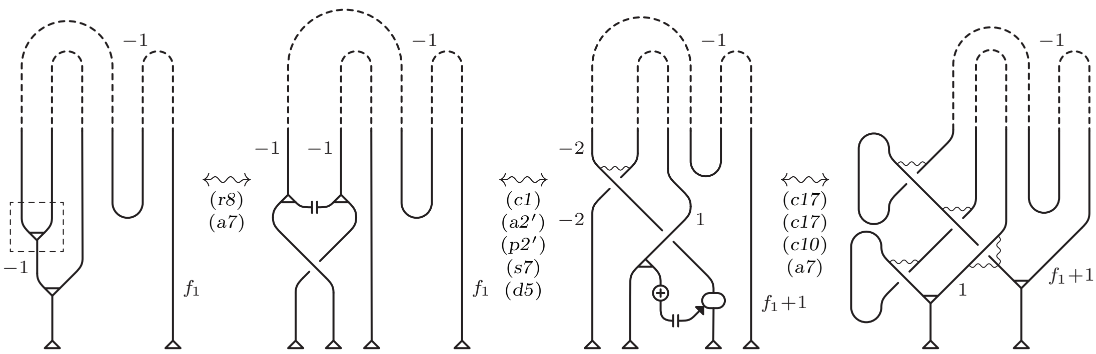

FIGURE 4.6.17. Proof of the invariance of $\overline{\Phi}(T)$ under the slide of L_2 over L_1, for L_1 with one negative self-crossing.

In Figure 4.6.17, we prove that the images of the first and third diagrams under $\overline{\Phi}$ are the same in 4Alg. Notice that, in this case, as a consequence of relations (*c16-17*), the decorated kink in the image of L_2 is equal to τ^{-2}, and hence the total ribbon weight of the component is $f_2-1-2 = 1-\mathrm{wr}(L_2')-3 = -1$. Then, the first diagram in Figure 4.6.17 has been obtained by repeating the first step in Figure 4.6.13. □

4.7. Proof of Theorem A

In this subsection, we prove one of the main results of this paper, which can be rephrased as follows.

THEOREM 4.7.1. *The map* $T \to \overline{\Phi}(T)$ *extends to a braided monoidal functor* $\overline{\Phi} : 4\mathrm{KT} \to 4\mathrm{Alg}$ *such that* $\overline{\Phi} \circ \Phi = \mathrm{id}_{4\mathrm{Alg}}$ *and* $\Phi \circ \overline{\Phi} = \mathrm{id}_{4\mathrm{KT}}$. *In particular,* $\overline{\Phi}$ *and* Φ *are equivalences of braided monoidal categories.*

Proof. Since we have already proved in Proposition 4.6.7 that $\overline{\Phi}(T)$ depends only on the 2-equivalence class of the Kirby tangle T, in order to show that $\overline{\Phi}$: 4KT $\to$ 4Alg is a well-defined monoidal functor, we only need to prove that it preserves identities, compositions, and tensor producta. The proof that it preserves identities is shown in Figure 4.7.1.

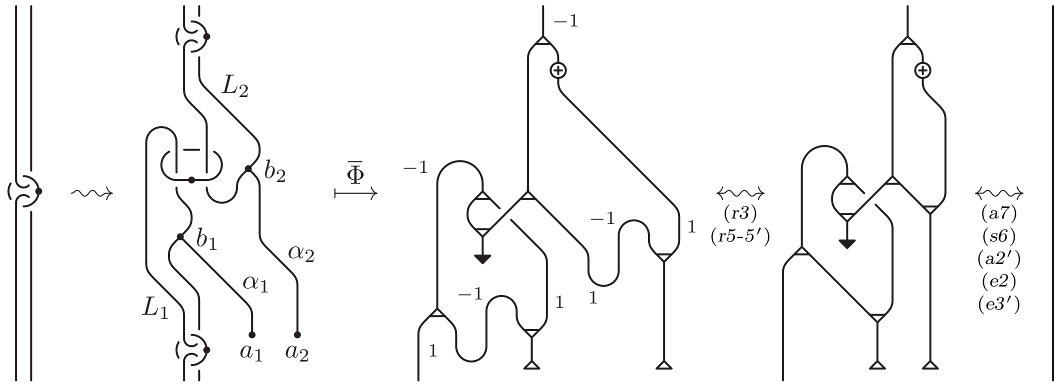

FIGURE 4.7.1. Proof that $\overline{\Phi}$ preserves identities.

Let now $T_1 : E_{2s} \to E_{2t}$ and $T_2 : E_{2t} \to E_{2r}$ be Kirby tangles with n and m undotted components, respectively. Then, the link L of undotted components of their composition $T_2 \circ T_1$ will have exactly $n + m - t$ components. In order to show that $\overline{\Phi}(T_2 \circ T_1) = \overline{\Phi}(T_2) \circ \overline{\Phi}(T_1)$, we make the special choice of bi-ascending state and arcs for $T_2 \circ T_1$ shown in Figure 4.7.2, where the undotted components of $L = L_1 \cup L_2 \cup \cdots \cup L_{n+m-t}$ are numbered in such way that:

- ◇ $L_1, L_2, \ldots, L_{n-t}$ are the components of T_1 that are not attached to its target;
- ◇ $L_{n-t+1}, L_{n-t+2}, \ldots, L_n$ are the components obtained from the gluing of the open components of T_1 to the ones of T_2 along E_{2t}, numbered following the order of the intervals in E_{2t};
- ◇ $L_{n+1}, L_2, \ldots, L_{n+m-t}$ are the components of T_2 that are not attached to its source.

Then, the choice of the arcs α_{n-t+i} for $i = 1, \ldots, t$ is presented in Figure 4.7.2. Notice that each α_{n-t+i} forms only positive crossings with the components L_{n-t+j} for $j = i + 1, \ldots, t$.

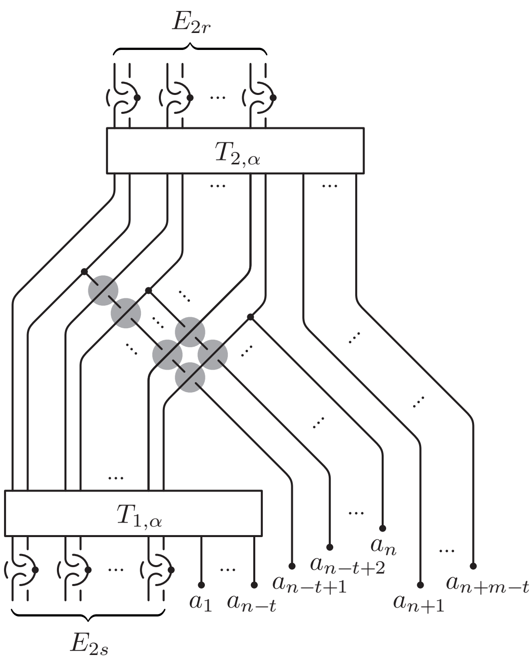

FIGURE 4.7.2. Special choice of arcs for $T_2 \circ T_1$.

Then, $\overline{\Phi}(T_2 \circ T_1)$ is presented in Figure 4.7.3. In order to see that it is equivalent to $\overline{\Phi}(T_2) \circ \overline{\Phi}(T_1)$, we first retract the images of the arcs α_{n-t+i} for $i = 1, \ldots, t$ by passing the identity morphisms through the

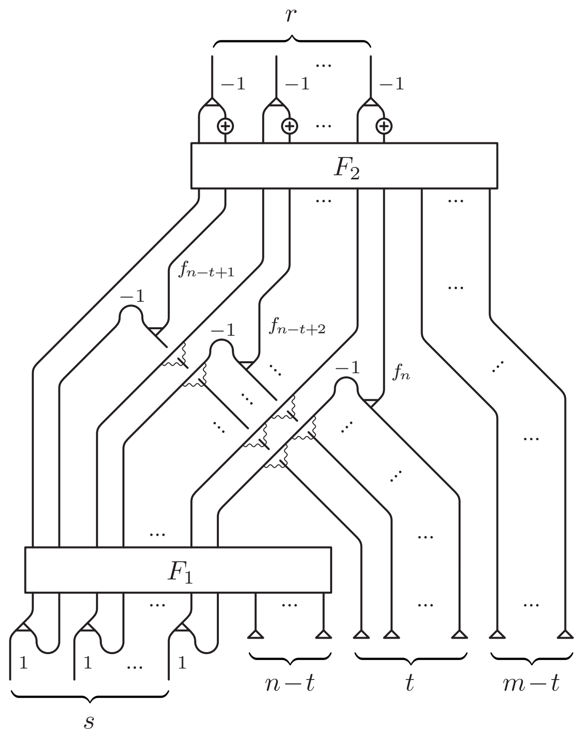

FIGURE 4.7.3. $\overline{\Phi}(T_2 \circ T_1)$.

the adjoint morphisms in the decorated crossings of type $\widehat{X}$, as shown in Figure 4.7.4. Then, we double the image of each arc through the move shown in Figure 4.7.5, and separate its weight as

$$f_{n-t+i} - 1 = -\mathrm{wr}(L'_{n-t+i}) = -(1 - f_{1,n-t+i}) - (1 - f_{2,i}) = f_{1,n-t+i} + f_{2,i} - 2,$$

where $(1 - f_{1,n-t+i})$ is equal to the writhe of the bi-ascending state of the $(n-t+i)$th component of T_1, and $(1 - f_{2,i})$ is equal to the writhe of the bi-ascending state of the ith component of T_2 (the numbering and the biascending states of the undotted components of T_1 and T_2 are induced by the ones of $T_2 \circ T_1$). Finally, by the inverse of the move presented in Figure 4.7.4, we pull down all identity morphisms back to the bottom-right corner of the diagram, thus creating new decorated crossings of type $\widehat{X}$. The resulting diagram is exactly $\overline{\Phi}(T_2) \circ \overline{\Phi}(T_1)$.

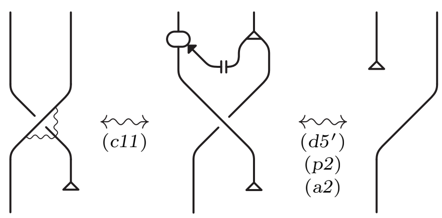

FIGURE 4.7.4. Retracting the images of the arcs $\alpha_{n-t+1}, \dots, \alpha_n$ in $T_2 \circ T_1$.

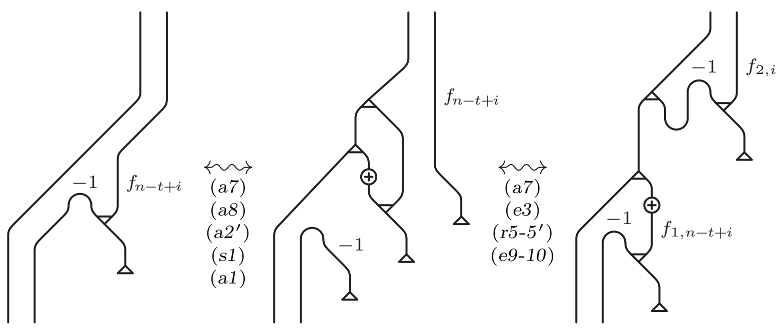

FIGURE 4.7.5. Doubling the retracted images of the arcs $\alpha_{n-t+1}, \dots, \alpha_n$.

In order to prove the monoidality of the functor $\overline{\Phi}$, let $T_1 : E_{2s_1} \to E_{2t_1}$ and $T_2 : E_{2s_2} \to E_{2t_2}$ be morphisms in 4KT. Consider $T_1 \sqcup T_2$, and order its undotted components by letting the ones of T_1 precede the ones of T_2; moreover, choose the arcs α_i by pulling the ones of T_1 across the s_2 vertical strands connected to the source of T_2, forming positive crossings with them. Then, the images under $\overline{\Phi}$ of such crossings are decorated crossings of type $\widehat{X}$, and we can transform $\overline{\Phi}(T_1 \sqcup T_2)$ into $\overline{\Phi}(T_1) \otimes \overline{\Phi}(T_2)$ by retracting the units at the end of the images of the arcs α_i of T_1 through the decorated crossings, by the move presented in Figure 4.7.4.

Finally, we recall that $\Phi \circ \overline{\Phi} = \mathrm{id}_{4\mathrm{KT}}$ has been proved in Proposition 4.4.1, so it remains to prove that $\overline{\Phi} \circ \Phi = \mathrm{id}_{4\mathrm{Alg}}$. In order to see this, it is enough to show that $\overline{\Phi}(\Phi(F)) = F$ when F is a generating morphism of 4Alg. The proofs for all elementary morphisms, with the exception of S^{-1} and τ^{-1}, are presented (up to compositions with identity morphisms) in Figures 4.7.6–4.7.13. We observe that, in the second-to-last move of Figure 4.7.8 and in the last move of Figure 4.7.10, we have expressed the decorated crossings of type $\widehat{X}$ and $\widehat{Y}$ in terms of the adjoint morphism, and we have intertwined the adjoint and the identity morphisms as we did in Figure 4.7.4. Now, the statements for S^{-1} and τ^{-1} follow from the ones for S and τ, while the ones for c and w follow from relation (*s8*), axiom (*r6*), and the fact that $\overline{\Phi}$ preserves compositions. □

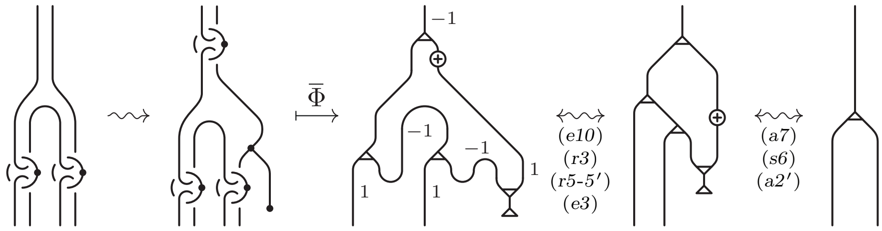

FIGURE 4.7.6. $\overline{\Phi}(\Phi(\mu)) = \mu$.

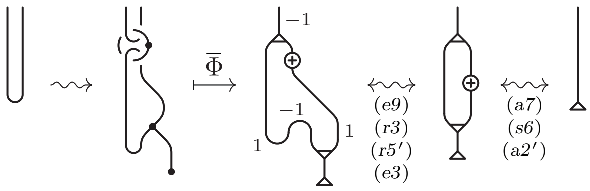

FIGURE 4.7.7. $\overline{\Phi}(\Phi(\eta)) = \eta$.

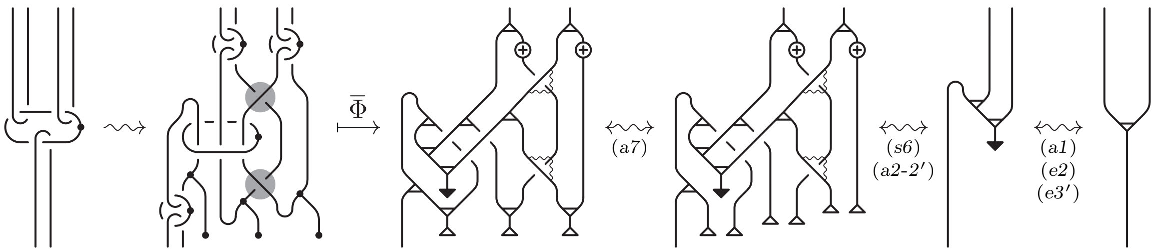

FIGURE 4.7.8. $\overline{\Phi}(\Phi(\Delta)) = \Delta$.

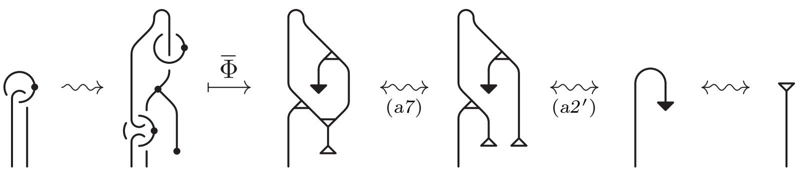

FIGURE 4.7.9. $\overline{\Phi}(\Phi(\varepsilon)) = \varepsilon$.

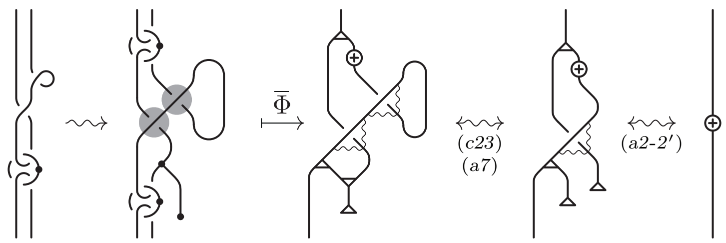

Figure 4.7.10. $\overline{\Phi}(\Phi(S)) = S$.

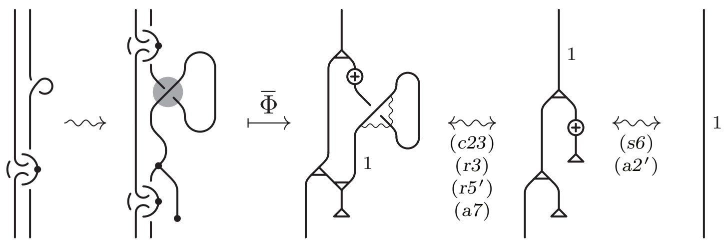

Figure 4.7.11. $\overline{\Phi}(\Phi(\tau)) = \tau$.

Figure 4.7.12. $\overline{\Phi}(\Phi(\lambda)) = \lambda$.

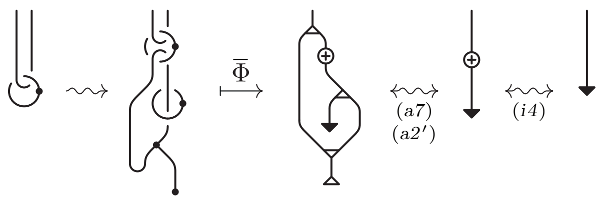

Figure 4.7.13. $\overline{\Phi}(\Phi(\Lambda)) = \Lambda$.

Appendix A. Tables.

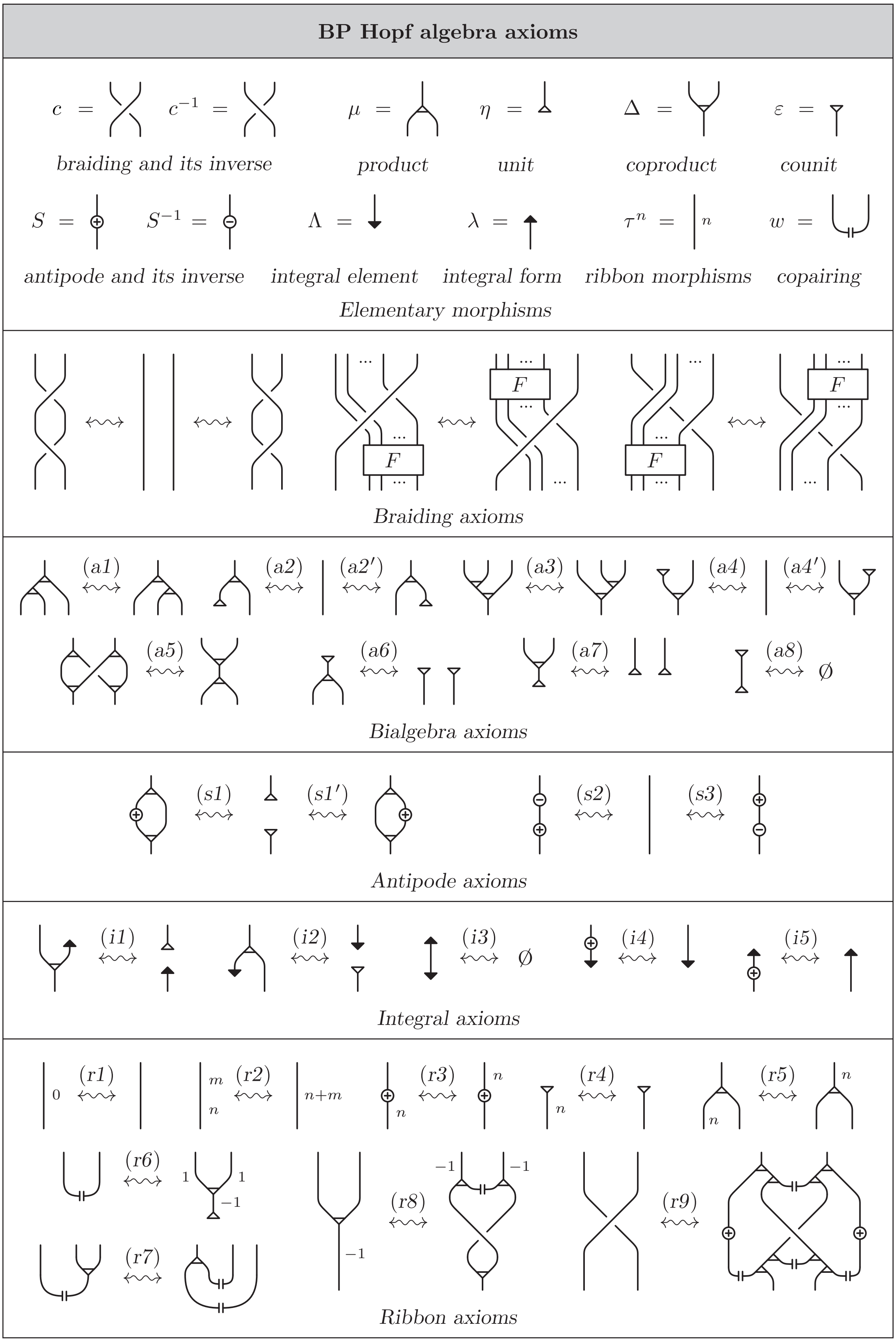

TABLE A.1. (Compare with Tables 2.1.2, 2.2.1, and 2.4.1)

Consequences of the Hopf algebra axioms

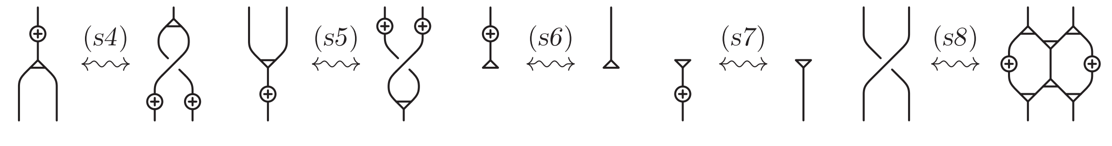

TABLE A.2. (Compare with Table 2.2.2)

The adjoint actions of a Hopf algebra

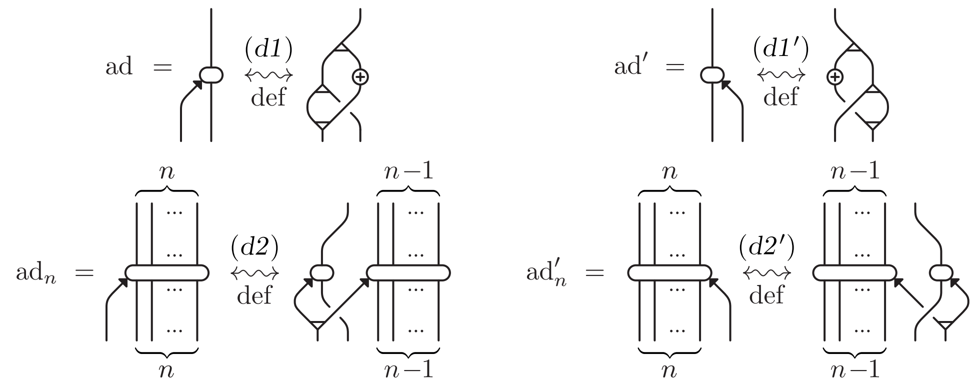

Left adjoint action *Right adjoint action*

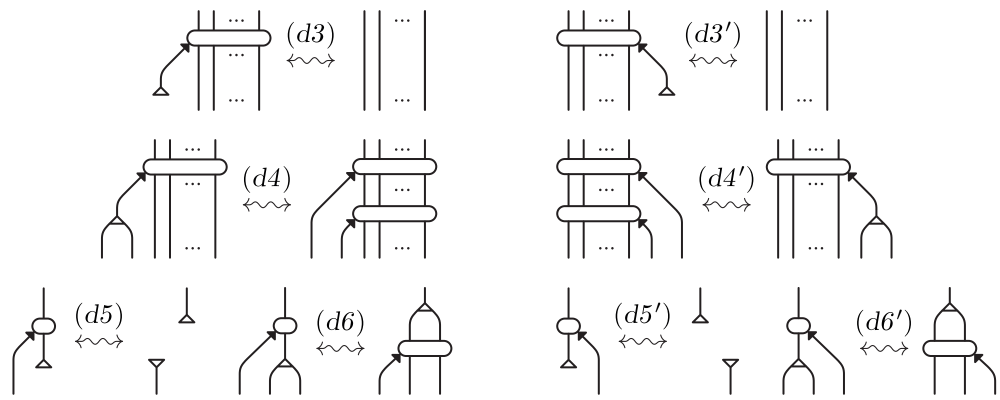

Action properties

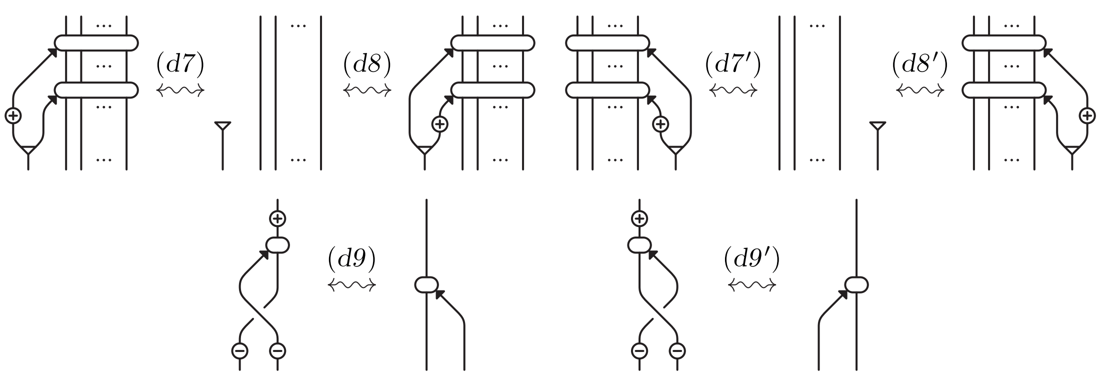

Other relations

TABLE A.3. (Compare with Table 2.3.1)

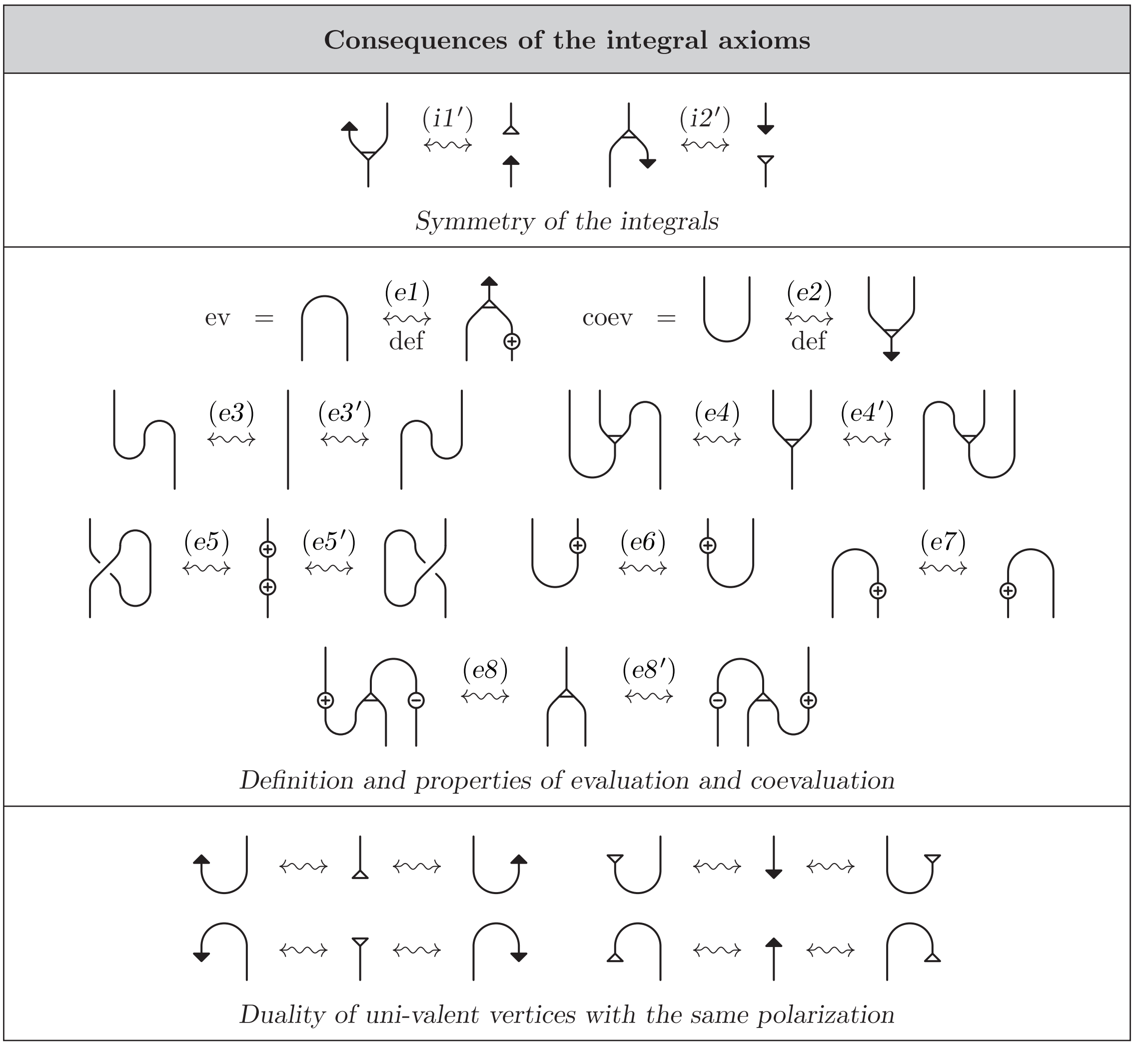

Table A.4. (Compare with Table 2.4.3)

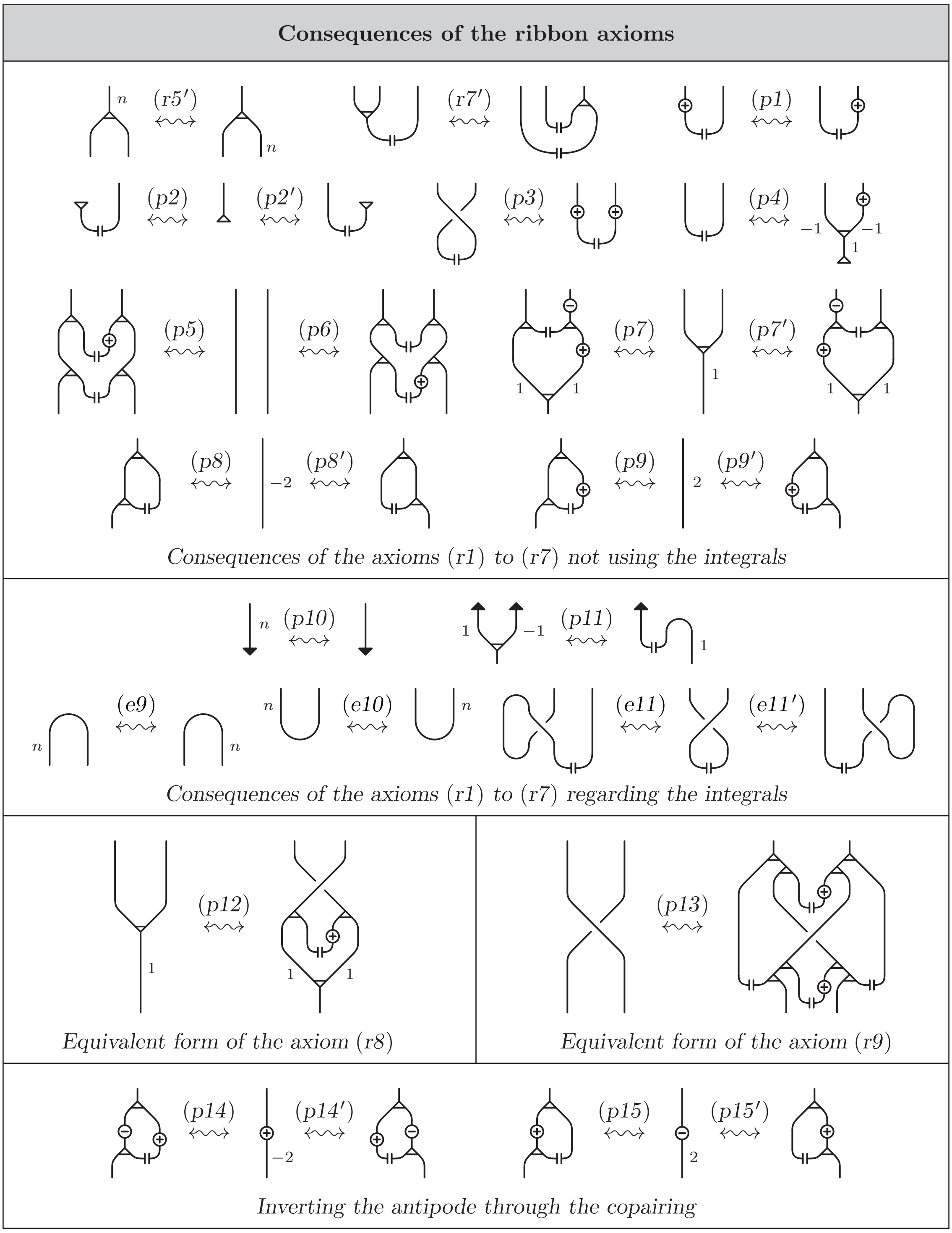

TABLE A.5. (Compare with Tables 2.4.4, 2.4.5, and 2.4.6)

Further properties of the adjoint actions of a BP Hopf algebra

Braided cocommutativity axiom for left and right adjoint actions

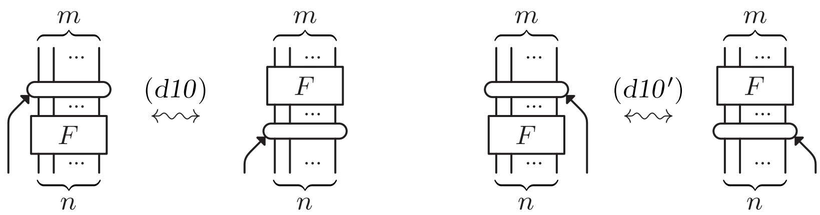

Intertwining properties

Some consequences of the intertwining properties

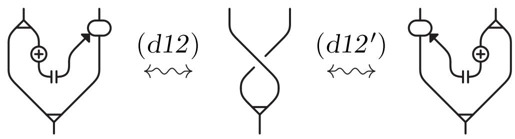

Equivalent forms of the axiom (r8)

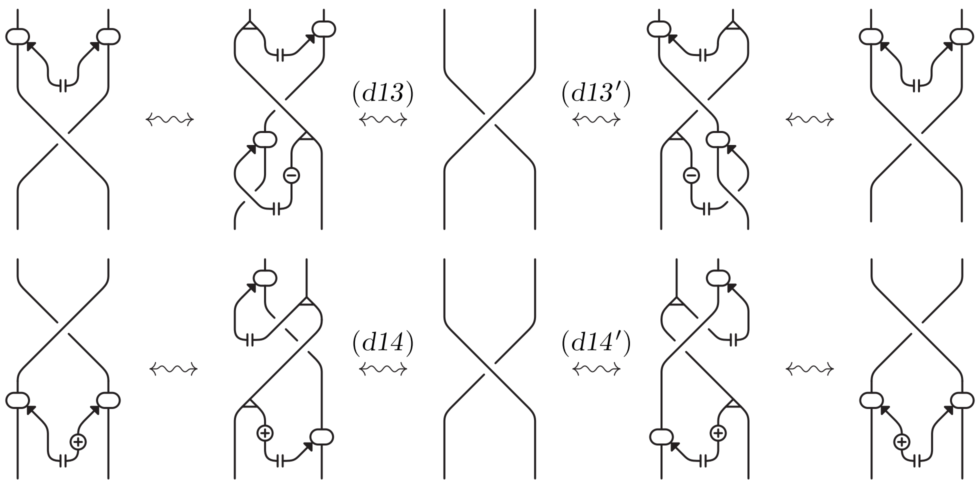

Equivalent forms of the axiom (r9)

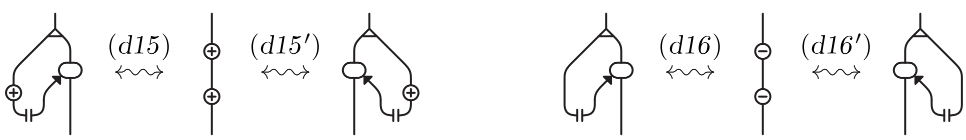

Other properties

Table A.6. (Compare with Tables 2.3.7 and 2.5.3)

Additional axioms and properties of a factorizable BP Hopf algebra

Factorizability axiom *Anomaly-freeness axiom*

Relations equivalent to (*f*) *and* (*n*)

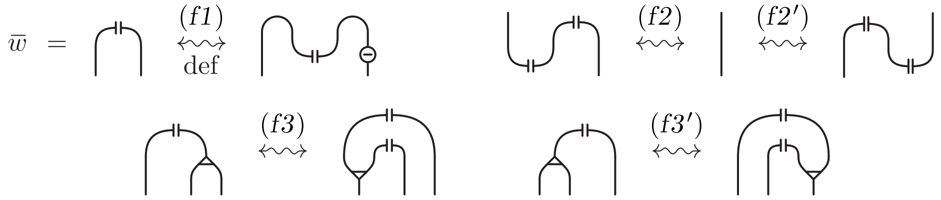

Definition and properties of the pairing

TABLE A.7. (Compare with Table 2.6.1)

Appendix B. Proofs.

In this appendix, we give the proofs of the properties of a BP Hopf algebra presented in Tables A.2, A.4, A.5, and A.7. Some of them, like the ones concerning the antipode in Table A.2 and the symmetry of the integrals in Table A.4, are well-known, and can be found in any basic textbook on Hopf algebras. Also, the rest of the properties have already appeared in the literature. For example, the non-degeneracy of ev and coev (relations (*e8*-*8'*)) were proven by Kerler in [Ke01, Lemma 7]. He also showed[6] in [Ke01, Lemmas 3 & 4] that relation (*p4*) is equivalent to the ribbon axiom (*r6*) modulo the Hopf algebra axioms together with the ribbon axioms (*r1*)–(*r5*), and that those ribbon axioms imply (*p1*) and (*r7'*). The diagrammatic proofs of all relations, with the exception of (*s8*) and (*p3*), appear in [BP11, Propositions/Lemmas 4.1.4, 4.1.5, 4.1.6, 4.1.9, 4.1.10, 4.2.5, 4.2.6, 4.2.7, 4.2.11, and 4.2.13] in the more general context of a groupoid Hopf algebra. The reason why we present the proofs here is, on the one hand, for the sake of completeness, and, on the other hand, because the equivalence results in Subsection 2.6 require the precise knowledge of which properties of the algebra follow from which set of axioms.

B.1. Consequences of the braided Hopf algebra axioms in Table A.2

Properties (*s5*), (*s7*), and (*s8*) are proved in Figures B.1.1, B.1.2, and B.1.3. Then, (*s4*) and (*s6*) are obtained by a dual argument (rotating the diagrams in Figures B.1.1 and B.1.2 upside down).

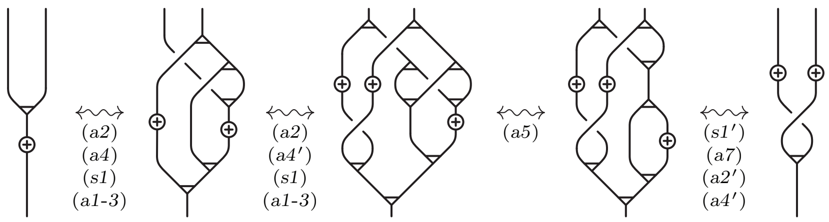

FIGURE B.1.1. Proof of (*s5*).

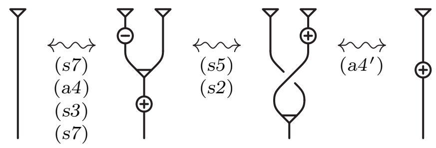

FIGURE B.1.2. Proof of (*s7*).

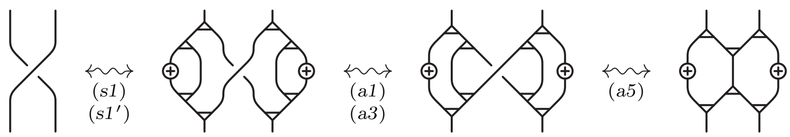

FIGURE B.1.3. Proof of (*s8*).

B.2. Consequences of the integral axioms in Table A.4

Proof of Proposition 2.4.5. The S-invariance of the integral form λ and of the integral element Λ imply that λ and Λ are respectively a two-sided integral form and a two-sided integral element (properties (*i1'*) and (*i2'*) in Table A.4). For (*i1'*), this is proved in Figure B.2.1, while the proof of (*i2'*) is obtained by rotating the diagram in Figures B.2.1 upside down. This implies that the braided monoidal category freely generated by a Hopf algebra with S-invariant integral form and element is invariant under the symmetry functor sym defined in Proposition 2.2.3. Therefore, the proofs of relations (*e3'*), (*e4'*), (*e5'*), and (*e8'*) can be obtained by symmetry from those of (*e3*), (*e4*), (*e5*), and (*e8*), respectively. The last relations and (*e6*) are proved in Figures B.2.2–B.2.6, while (*e7*) follows from (*e6*) and (*e3*-*3'*). □

[6]Kerler's axioms use ribbon elements instead of ribbon morphisms, but the two languages are equivalent.

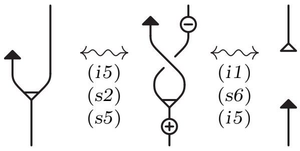

FIGURE B.2.1. Proof of (*i1′*).

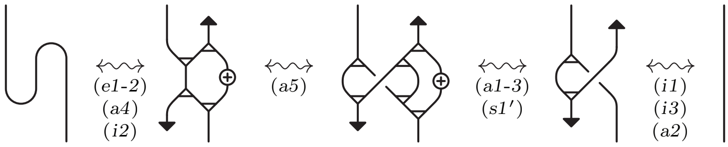

FIGURE B.2.2. Proof of (*e3*).

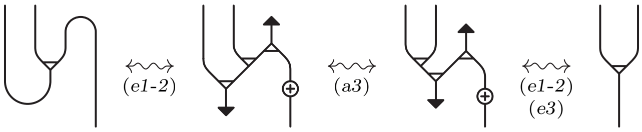

FIGURE B.2.3. Proof of (*e4*).

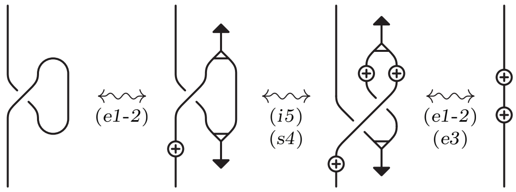

FIGURE B.2.4. Proof of (*e5*).

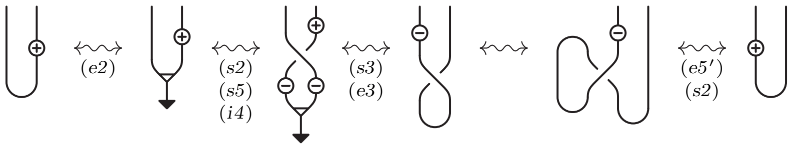

FIGURE B.2.5. Proof of (*e6*).

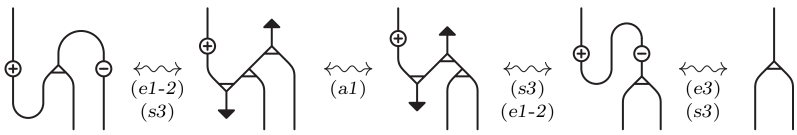

FIGURE B.2.6. Proof of (*e8*).

B.3. Properties of the ribbon structure of a BP Hopf algebra in Table A.5

Proof of Proposition 2.4.6. We will show that the properties in the first section of Table A.5 (coinciding with Table 2.4.4) are consequences of the rest of the ribbon axioms (*r1*)–(*r7*) together with the braided Hopf algebra axioms, but we will do this without using the existence of integrals.

Indeed, relation (*r5′*) follows from (*r5*), (*r3*), and (*s4*). In Figure B.3.1, we show that (*p3*) follows from (*r6*) and from the properties of the antipode. Moreover, as it is shown in Figure B.3.2, (*r6*) implies (*r7′*) as well. The same is true for (*p2*) (respectively (*p2′*)), which can be obtained by composing (*r6*) on the left (respectively on the right) with the counit, and by applying (*r4*) and (*a4*) (respectively (*a4′*)). Then, as it is shown in Figure B.3.3, property (*p5*) follows from (*r7*) and (*p2*), while the proof of (*p6*) is analogous, using (*s1*) in place of (*s1′*).

The symmetric relations (*p5′*) and (*p6′*), in which the antipode is placed on the left of the copairing, hold as well, and their proofs are obtained by applying the functor sym to the corresponding diagrams, and using (*p8′*) and (*p2*) instead of (*p8*) and (*p2′*). Then, relations (*p5-5′*) and (*p6-6′*) imply that both morphisms

$$\bar{\Omega} = (\mu \otimes \mu) \circ (\mathrm{id} \otimes ((\mathrm{id} \otimes S) \circ w) \otimes \mathrm{id}) : H \otimes H \to H \otimes H$$
$$\bar{\Omega}' = (\mu \otimes \mu) \circ (\mathrm{id} \otimes ((S \otimes \mathrm{id}) \circ w) \otimes \mathrm{id}) : H \otimes H \to H \otimes H$$

are two-sided inverses of the monodromy Ω. Therefore, they are the same, which implies (*p1*).

Notice that properties (*r5′*), (*r7′*), and (*p1*) imply that 4Alg is invariant under the functor sym (see Proposition 2.4.10).

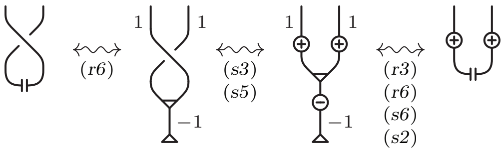

FIGURE B.3.1. Proof of (*p3*).

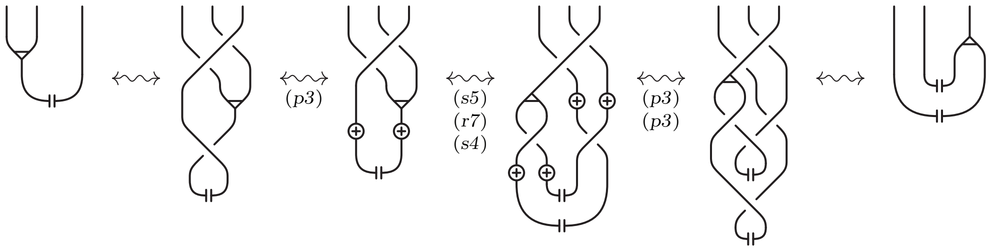

FIGURE B.3.2. Proof of (*r7′*).

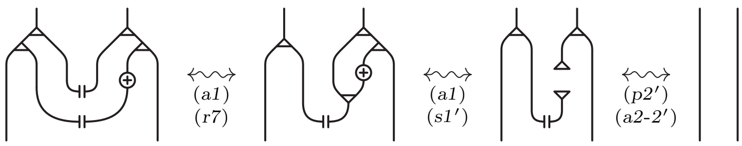

FIGURE B.3.3. Proof of (*p5*).

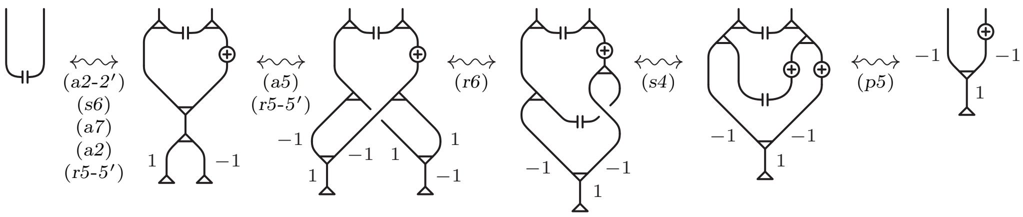

FIGURE B.3.4. Proof of (*p4*).

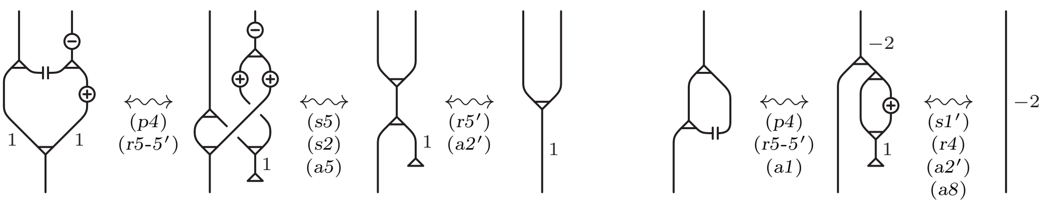

FIGURE B.3.5. Proofs of (*p7*) and (*p8*).

Relations (*p7*) and (*p8*) are proved in Figure B.3.5, while the proof of (*p9*) is analogous to the one of (*p8*), using (*r6*) instead of (*p4*) to express the copairing. Then, relations (*p7′*), (*p8′*), and (*p9′*) follow by symmetry. □

Proof of Proposition 2.4.7. We proceed now with the proof of the identities in the second section of Table A.5 (coinciding with Table 2.4.5), which concern the relationship between the ribbon structure and the integrals of the algebra.

Relation (*p10*) is derived by applying (*r4*) and (*r5*) to the product of the integral element Λ and the unit η. Relation (*e9*) immediately follows from (*r5*) and (*r5′*), while relations (*e11*) and (*e11′*) follow from (*p3*), (*p1*), and (*e5-5′*). The remaining relations (*p11*) and (*e10*) are proved correspondingly in Figures B.3.6 and B.3.7. $\square$

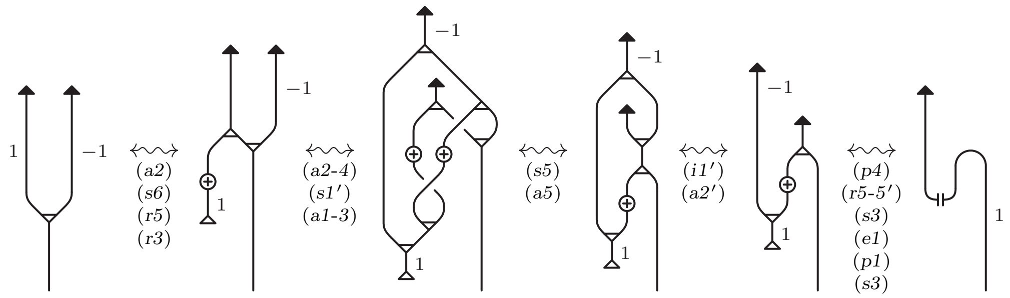

FIGURE B.3.6. Proof of (*p11*).

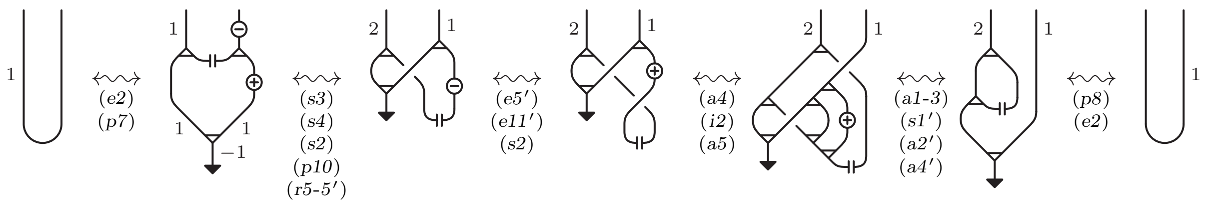

FIGURE B.3.7. Proof of (*e10*).

Proof of Proposition 2.4.8. Finally, we show that the properties in the last three sections of Table A.5 (coinciding with Table 2.4.6) hold in 4Alg. The equivalence between relation (*p12*) and axiom (*r8*) follows from the fact that (*p12*) can be obtained by composing both sides of (*r8*) with the invertible morphisms τ on the bottom and $c \circ \overline{\Omega} \circ (\tau \otimes \tau)$ on the top. Analogously, modulo the rest of the algebra axioms, relation (*p13*) is equivalent to axiom (*r9*). Indeed, to see that (*r9*) implies (*p13*), it is enough to observe that the diagram on the right-hand side of (*p13*) can be reduced to the single crossing on the left-hand side by applying (*r9*) at the crossing in the middle, and then using one move (*p1*) and four moves (*p5-6*) to cancel the corresponding copairings. The opposite argument shows that (*p13*) implies (*r9*) as well.

Relation (*p14*) is proved in Figure B.3.8, (*p14′*) follows by symmetry, while (*p15-15′*) follow from (*p14-14′*), (*r7*), and (*s1-1′*), and their proofs are left to the reader. $\square$

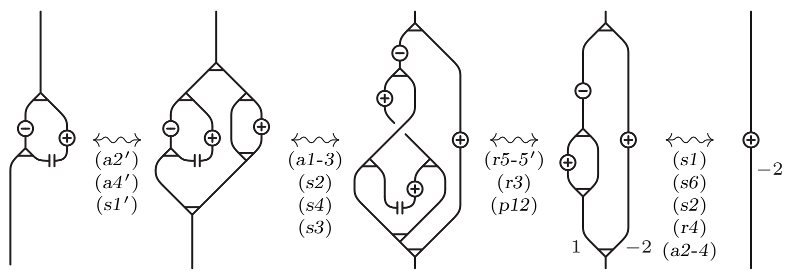

FIGURE B.3.8. Proof of (*p14*).

B.4. Properties of a factorizable anomaly free BP Hopf algebra in Table A.7

Relation (*f′*) is equivalent to (*f*) modulo (*i5*), (*e5*) and (*e11*). Identity (*f2*) is proved in Figure B.4.1, and then (*f2′*) follows by symmetry, while, using (*f2-2′*), one can easily derive (*f3-3′*) from (*r7*) and (*r7′*). Finally, relation ($\overline{n}$) is proved in Figure B.4.2.

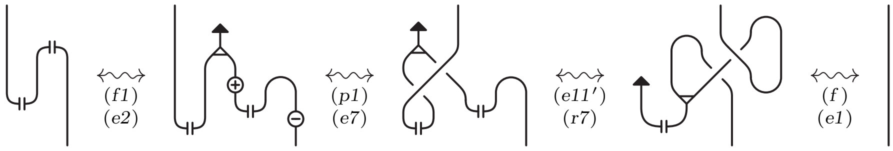

Figure B.4.1. Proof of (*f2*).

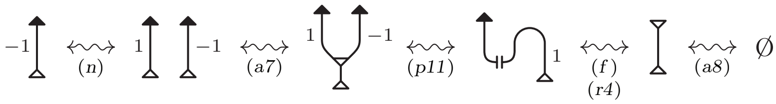

Figure B.4.2. Proof of ($\bar{n}$).

References

[Ak16] S. Akbulut, *4-Manifolds*, Oxf. Grad. Texts Math. 25 **25**, Oxford University Press, Oxford, 2016.

[As11] M. Asaeda, *Tensor Functors on a Certain Category Constructed From Spherical Categories*, J. Knot Theory Ramifications **20** (2011), no. 1, 1–46.

[BD22] A. Beliakova, M. De Renzi, *Refined Bobtcheva–Messia Invariants of 4-Dimensional 2-Handlebodies*, Essays in Geometry, 387–432, IRMA Lect. Math. Theor. Phys. **34**, Eur. Math. Soc., Zürich, 2023; arXiv:2205.11385 [math.GT].

[BD21] A. Beliakova, M. De Renzi, *Kerler–Lyubashenko Functors on* 4*-Dimensional* 2*-Handlebodies*, Int. Math. Res. Not. IMRN (2022), rnac039; arXiv:2105.02789 [math.GT].

[Bo23] I. Bobtcheva *Algebraic Characterisation of the Category of Cobordisms of 2-dimensional CW-complexes and the Andrews–Curtis Conjecture*; arXiv:2309.04830 [math.GT].

[Bo20] I. Bobtcheva *On the Algebraic Characterization of the Category of* 3*-Dimensional Cobordisms*; arXiv:2008.06706 [math.GT].

[BM02] I. Bobtcheva, M. Messia *HKR-Type Invariants of* 4*-Thickenings of* 2*-Dimensional CW Complexes*, Algebr. Geom. Topol. **3** (2003), no. 1, 33–87; arXiv:math/0206307 [math.QA].

[BP11] I. Bobtcheva, R. Piergallini, *On* 4*-Dimensional* 2*-Handlebodies and* 3*-Manifolds*, J. Knot Theory Ramifications **21** (2012), no. 12, 1250110, 230 pp; arXiv:1108.2717 [math.GT].

[CY94] L. Crane, D. Yetter, *On Algebraic Structures Implicit in Topological Quantum Field Theories*, J. Knot Theory Ramifications **8** (1999), no. 2, 125–163; arXiv:hep-th/9412025.

[EGNO15] P. Etingof, S. Gelaki, D. Nikshych, V. Ostrik, *Tensor Categories*, Math. Surveys Monogr. **205**, Amer. Math. Soc., Providence, RI, 2015.

[FS10] J. Fuchs, C. Schweigert, *Hopf Algebras and Finite Tensor Categories in Conformal Field Theory*, Rev. Un. Mat. Argentina **51** (2010), no. 2, 43–90; arXiv:1004.3405 [hep-th].

[FY89] P. Freyd , D. Yetter, *Braided Compact Closed Categories with Applications to Low Dimensional Topology*, Adv. Math. **77** (1989), no. 2, 156–182.

[Go91] R. Gompf, *Killing the Akbulut–Kirby 4-Sphere, With Relevance to the Andrews–Curtis and Schoenflies Problems*, Topology **30** (1991), no. 1, 97–115.

[GS99] R. Gompf, A. Stipsicz, *4-Manifolds and Kirby Calculus*, Grad. Stud. Math. **20**, American Mathematical Society, Providence, RI, 1999.

[Ha00] K. Habiro, *Claspers and Finite Type Invariants of Links*, Geom. Topol. **4** (2000), no. 1, 1–83; arXiv:math/0001185 [math.GT].

[Ha05] K. Habiro, *Bottom Tangles and Universal Invariants*, Algebr. Geom. Topol. **6** (2006), no. 3, 1113–1214; arXiv:math/0505219 [math.GT].

[Ha22] K. Habiro, private communication.

[Ju14] A. Juhász, *Defining and Classifying TQFTs via Surgery*, Quantum Topol. **9** (2018), no. 2, 229–321; arXiv:1408.0668 [math.GT].

[Ke98] T. Kerler, *Bridged Links and Tangle Presentations of Cobordism Categories*, Adv. Math. **141** (1999), no. 2, 207–281; arXiv:math/9806114 [math.GT].

[Ke01] T. Kerler, *Towards an Algebraic Characterization of* 3*-Dimensional Cobordisms*, Diagrammatic Morphisms and Applications (San Francisco, CA, 2000), 141–173, Contemp. Math. **318**, Amer. Math. Soc., Providence, RI, 2003; arXiv:math/0106253 [math.GT].

[KL01] T. Kerler, V. Lyubashenko, *Non-Semisimple Topological Quantum Field Theories for 3-Manifolds with Corners*, Lecture Notes in Math. **1765**, Springer-Verlag, Berlin, 2001.

[Ki89] R. Kirby, *The Topology of* 4*-Manifolds*, Lecture Notes in Math. **1374**, Springer-Verlag, Berlin, 1989.

[Li97] W.B.R. Lickorish, *Introduction to Knot Theory*, Graduate Texts in Mathematics **175**, Springer, New York, 1997.

[Ly94] V. Lyubashenko, *Invariants of* 3*-Manifolds and Projective Representations of Mapping Class Groups via Quantum Groups at Roots of Unity*, Comm. Math. Phys. **172** (1995), no. 3, 467–516; arXiv:hep-th/9405167.

[Ma71] S. Mac Lane, *Categories for the Working Mathematician*, Grad. Texts in Math. **5**, Springer-Verlag, New York-Berlin, 1971.

[Ma93] S. Majid, *Braided Groups and Algebraic Quantum Field Theories*, Lett. Math. Phys. **22** (1991), no. 3, 167–175.

[Ma94] S. Majid, *Algebras and Hopf Algebras in Braided Categories*, Lecture Notes in Pure and Appl. Math. **158**, Marcel Dekker, Inc., New York, NY, 1994, 55–105; arXiv:q-alg/9509023 [math.QA].

[Mo93] S. Montgomery, *Hopf Algebras and Their Actions on Rings*, CBMS Regional Conf. Ser. in Math. **82**, published for the Conference Board of the Mathematical Sciences, Washington, DC, by the American Mathematical Society, Providence, RI, 1993.

[MP92] S. Matveev, M. Polyak, *A Geometrical Presentation of the Surface Mapping Class Group and Surgery*, Comm. Math. Phys. **160** (1994), no. 3, 537–550.

[Oh02] T. Ohtsuki, *Problems on Invariants of Knots and* 3*-Manifolds*, Geom. Topol. Monogr. **4**, Geometry & Topology Publications, Coventry, 2002, 377–572; arXiv:math/0406190 [math.GT].

[RT90] N. Reshetikhin, V. Turaev, *Ribbon Graphs and Their Invariants Derived From Quantum Groups*, Comm. Math. Phys. **127** (1990), 1–26.

[RT91] N. Reshetikhin, V. Turaev, *Invariants of* 3*-Manifolds via Link Polynomials and Quantum Groups*, Invent. Math. **103** (1991), no. 1, 547–597.

[Sh94] M. Shum, *Tortile Tensor Categories*, J. Pure Appl. Algebra **93** (1994), no. 1, 57–110.

[Tu94] V. Turaev, *Quantum Invariants of Knots and 3-Manifolds*, De Gruyter Stud. Math. **18**, Walter de Gruyter & Co., Berlin, 1994.

Institute of Mathematics, University of Zurich, Winterthurerstrasse 190, CH-8057 Zurich, Switzerland
Email address: anna.beliakova@math.uzh.ch

IIS Savoia Benincasa, Italy
Email address: i.bobtchev@gmail.com

Institut Monpelliéran Alexander Grothendieck, Université de Montpellier, Place Eugène Bataillon, 34090 Montpellier, France
Email address: marco.de-renzi@umontpellier.fr

Scuola di Scienze e Tecnologie, Università di Camerino, Italy
Email address: riccardo.piergallini@unicam.it